

Itaconic acid can be used as a bio-based building block for the synthesis of a large number of chemicals and polymers. Since 1950, *Aspergillus terreus* is used for the industrial production of itaconic acid. However, despite the long history and experience, itaconic acid production in *A. terreus* remains challenging and above all the required control of the morphology leads to high production costs, which causes a relatively low market volume of itaconic acid despite its chemical potential. Ustilaginaceae are promising alternative hosts that offer new possibilities to achieve more efficient itaconic acid production.

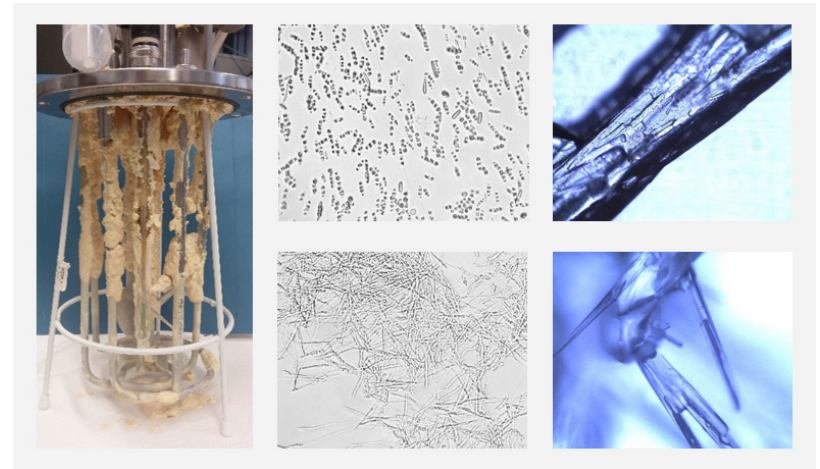
In this thesis, *Ustilago maydis* and *Ustilago cynodontis* were applied as microbial hosts to achieve efficient itaconic acid production from glucose. Itaconic acid production in *U. maydis* and *U. cynodontis* was improved by metabolic engineering. The itaconic acid titer was enhanced 4.2-fold in *U. maydis* and 6.5-fold in *U. cynodontis* compared to corresponding wildtype strains. In order to ensure robust and non-filamentous cells growing under certain relevant conditions for itaconic acid production, the gene *fuz7* was deleted in both strains. The gene *fuz7* is part of the Ras/mitogen-activated protein kinase pathway and plays an important role in conjugation tube formation and filamentous growth.

Thus, for the first time, itaconic acid production in a bioreactor with the otherwise strong filamentously growing *U. cynodontis* was realized. Further, by optimizing the pH value, using different feeding strategies and repeated-batch systems titer up to 83 g L⁻¹ could be reached in *U. cynodontis*. In *U. maydis*, fermentations in combination with *in situ* product removal using calcium carbonate precipitation resulted in a titer over 200 g L⁻¹ itaconic acid.

Altogether, by an integrated approach of metabolic and morphological engineering, coupled with process development, the efficiency of itaconic acid production with *U. maydis* and *U. cynodontis* could be significantly enhanced.

Hamed H. Tehrani

Engineering the morphology and metabolism of *Ustilago* to expand the process window for itaconic acid production



Engineering the morphology and metabolism of *Ustilago* to expand the process window for itaconic acid production

Hamed H. Tehrani



Engineering the morphology and metabolism of *Ustilago* to expand the process window for itaconic acid production

Von der Fakultät für Mathematik, Informatik und Naturwissenschaften der
RWTH Aachen University zur Erlangung des akademischen Grades eines
Doktors der Naturwissenschaften genehmigte Dissertation

vorgelegt von

Hamed Hosseinpour Tehrani

Master of Science

aus

Teheran, Iran

Berichter:

Univ.-Prof. Dr.-Ing. Lars M. Blank

Univ.-Prof. Dr. Nick Wierckx

Tag der mündlichen Prüfung: 19.06.2019

Diese Dissertation ist auf den Internetseiten der Universitätsbibliothek verfügbar.

Bibliografische Information der Deutschen Nationalbibliothek

Die Deutsche Nationalbibliothek verzeichnet diese Publikation in der Deutschen Nationalbibliografie; detaillierte bibliografische Daten sind im Internet über <https://portal.dnb.de> abrufbar.

Hamed H. Tehrani:

Engineering the morphology and metabolism of *Ustilago* to expand the process window for itaconic acid production

1. Auflage, 2019

Gedruckt auf holz- und säurefreiem Papier, 100% chlorfrei gebleicht.

Apprimus Verlag, Aachen, 2019
Wissenschaftsverlag des Instituts für Industriekommunikation und Fachmedien
an der RWTH Aachen
Steinbachstr. 25, 52074 Aachen
Internet: www.apprimus-verlag.de, E-Mail: info@apprimus-verlag.de

Printed in Germany

ISBN 978-3-86359-757-3

D 82 (Diss. RWTH Aachen University, 2019)

Eidesstattliche Erklärung

Hamed, Hosseinpour Tehrani

Erklärt hiermit, dass diese Dissertation und die darin dargestellten Inhalte die eigenen sind und selbstständig, als Ergebnis der eigenen originären Forschung, generiert wurden.

Hiermit erkläre ich an Eides statt

1. Diese Arbeit wurde vollständig oder größtenteils in der Phase als Doktorand dieser Fakultät und Universität angefertigt;
2. Sofern irgendein Bestandteil dieser Dissertation zuvor für einen akademischen Abschluss oder eine andere Qualifikation an dieser oder einer anderen Institution verwendet wurde, wurde dies klar angezeigt;
3. Wenn immer andere eigene- oder Veröffentlichungen Dritter herangezogen wurden, wurden diese klar benannt;
4. Wenn aus anderen eigenen- oder Veröffentlichungen Dritter herangezogen wurde, wurde stets die Quelle hierfür angegeben. Diese Dissertation ist vollständig meine eigene Arbeit, mit der Ausnahme solcher Zitate;
5. Alle wesentlichen Quellen von Unterstützung wurden benannt;
6. Wenn immer ein Teil dieser Dissertation auf der Zusammenarbeit mit anderen basiert, wurde von mir klar gekennzeichnet, was von anderen und was von mir selbst erarbeitet wurde;
7. Ein Teil oder Teile dieser Arbeit wurden zuvor veröffentlicht und zwar in

Hamed Hosseinpour Tehrani, Apilaasha Tharmasothirajan, Elia Track, Lars M. Blank and Nick Wierckx. Engineering the morphology and metabolism of pH tolerant *Ustilago cynodontis* for efficient itaconic acid production. *Metabolic Engineering* (2019) 54, 293-300, <https://doi.org/10.1016/j.ymben.2019.05.004>

Hamed Hosseinpour Tehrani, Elena Geiser, Meike Engel, Sandra K. Hartmann, Abeer H. Hossain, Peter J. Punt, Lars M. Blank, Nick Wierckx. (2019). The interplay between transport and metabolism in fungal itaconic acid production. *Fungal Genetics and Biology*, 125, 45-52, <https://doi.org/10.1016/j.fgb.2019.01.011>.

Elena Geiser, **Hamed Hosseinpour Tehrani**, Svenja Meyer, Lars M. Blank and Nick Wierckx. (2018). Evolutionary freedom in the regulation of the conserved itaconate cluster by Rial1 in related Ustilaginaceae. *Fungal Biology and Biotechnology*, 5, 14, <https://doi.org/10.1186/s40694-018-0058-1>

Hamed Hosseinpour Tehrani, Lars M. Blank and Nick Wierckx (2018). Morphologic engineering in basidiomycota. Patent Application: EP 18 176 325.1

Aachen, 11.07.2019

Hamed Hosseinpour Tehrani



Danksagung

Ich möchte mich ganz besonders bei meinem Doktorvater Prof. Dr. Lars M. Blank und bei meinem Gruppenleiter und Mentor Prof. Dr. Nick Wierckx bedanken. Vielen Dank an euch beide, dass Ihr es mir ermöglicht habt an so einem spannenden und interessanten Projekt zu arbeiten und mir dabei geholfen habt meine Ziele zu erreichen.

Lars ich möchte mich ganz herzlich bei dir für deine Unterstützung, Hilfestellungen, Ratschläge und für deine Motivation über all die Jahre bedanken. Weiterhin danke ich dir dafür, dass du es mir ermöglicht hast in einem so gut ausgestatteten und modernen Labor zu arbeiten. Vielen Dank für das Vertrauen und die vielen Möglichkeiten, die du mir neben meiner Promotion ermöglicht hast. Ganz besonders möchte ich dir dafür danken, dass du dir immer Zeit genommen hast und immer versuchst hast einem zu helfen. Ich werde die Zusammenarbeit mit dir sehr vermissen, und hoffe sehr, dass sich unsere Wege in der Zukunft noch mehrmals kreuzen werden.

Nick, dir möchte ich für deine intensive und hervorragende Betreuung, für deine Geduld, für deine beruhigende Art und für deine Hilfestellungen beim Schreiben danken. Du hast mich stets unterstützt und gefördert und mir sehr viel ermöglicht. Vor allem hast du mir gezeigt, was es heißt Wissenschaftler zu sein. Außerdem möchte ich dir für dein Vertrauen danken. Du hast mir sehr viele Freiräume in der Versuchsplanung gelassen und mir die Chance gegeben mich selbst zu entwickeln. Gleichzeitig war deine Tür immer offen, wenn man Hilfe benötigt hat. An dieser Stelle vielen lieben Dank für alle wissenschaftliche Diskussionen, die wir über die Jahre hatten. Mir werden die Meetings freitags um 10 Uhr fehlen. Ich werde mich immer gerne an diese Zeit zurückerinnern vor allem an all unsere Reisen quer durch Europa, wo wir auch die Möglichkeit hatten nicht nur über Wissenschaft zu reden, sondern auch über wichtigere Themen wie z.B. Essen. Danke, dass du so viel Energie in dieses Projekt gesteckt hast und mir die Möglichkeit gegeben hast mit dir zusammen nach Jülich zu gehen, um an unserer erfolgreichen Forschung mit *Ustilago* weiterzuschreiben.

Meiner Projektpartnerin Johanna möchte ich für Ihre Unterstützung und für die gute Zusammenarbeit in den letzten Jahren danken.

Auch meinen Studenten Isabel, Elia, Alexander, Svenja, Sinan, Devran, Sarah, Anne, Viviane, Ana, Apilaasha und Katharina möchte ich ganz herzlich danken. Vielen lieben dank für eure Zeit, Ausdauer, Motivation und euren Ehrgeiz. Ihr wart alle ein großer Bestandteil dieses Projektes und habt sehr zu seinem Erfolg beigetragen.

Ein großer Dank gilt dem gesamten iAMB. Ahmed, Andreas, Andrea, Annette, Benedikt, Bernd, Birgitta, Birthe, Brehmi, Carl, Carola, Christoph H., Christoph L., Christoph T., Dario, Deiziane, Desi, Dieter, Eda, Eik, Elena, Elke, Erick, Frank, Gisela, Hao, Hendrik, Henrik, Isabel, Ivan, Jan, Jan S., Jannis, Johanna, Julia S., Kalle, Kerstin, Kristina, Lars K., Liesa, Maike, Manja, Martin, Mathias, Miriam, Monika, Nilam, Nisha, Philipp, Rabea, Salome, Sandra, Sandra H., Sandra S., Sebastian Z., Sebastian K., Simone, Suresh, Thiemo, Thomas, Till, Tobias, Ulf, Ulrike, Ute, Valeria, Vanessa, Wie, Wing-Jin, Yulei. Es war eine wunderschöne, einzigartige und vor allem erlebnisreiche Zeit mit euch. Ich habe mich immer wohl gefühlt und ich hoffe das wir uns das ein oder andere Mal noch sehen.

Ein ganz spezieller Dank geht an Elena. Am Anfang hatte ich noch Angst vor dir, dann wurdest du eine sehr gute Betreuerin und Mentorin für mich und schließlich eine sehr gute Freundin. Vielen lieben Dank für alles Elena.

Meinen ehemaligen Betreuer Thiemo möchte ich für seine Unterstützung während und nach der Masterarbeit danken. Außerdem danke ich dir dafür, dass du dich immer für mich eingesetzt hast

und mich in meinen Plänen für ein Doktorstudium stets motiviert hast.

Ganz besonders möchte ich mich bei Peter, Thomas, Manfred, Ralf und Tim von der mechanischen und elektrischen Werkstatt bedanken. Danke Jungs, dass Ihr mir immer so gut wie alle Wünsche erfüllt habt und alles reparieren konntet. Ohne euch wären viele Versuche wahrscheinlich anders gelaufen.

Ein großer Dank geht auch an Benedikt, Maïke und Sebastian. Benedikt zum Glück weiß ich nicht mehr die Anzahl der Nächte und Wochenenden, die wir zusammen im Labor verbracht haben. Es waren eindeutig zu viele und ich bin froh, dass ich diese nicht alleine verbringen musste. Maïke, dir vielen Dank für alle Momente, in denen du mein Gejammer ertragen und mich aufgemuntert hast. Sebastian, mir werden eindeutig unsere Abende im Köpi fehlen, wo wir stets unseren Frust rauslassen konnten und eine warme Gulaschsuppe und ein Pils bekommen haben.

Meiner Freundin Vanessa möchte ich für Ihr Verständnis danken, dass ich nicht immer so viel Zeit hatte, dafür dass Sie immer ein offenes Ohr für mich hatte, mich in schlecht gelaunten Momenten aufmunterte und mir bewusst machte, dass man sich auch ab und zu ausruhen muss und dass meine *Ustilago's* auch ein Tag ohne mich auskommen.

Meinen Eltern, Maryam und Hamid, meinen Schwestern, Mahssa und Sanaz, meinen Schwägern, Peyman und Pedram, und meinen Nichten, Diba und Baanoo, gilt der größte Dank. Danke für eure Unterstützung über all die Jahre, ob finanziell oder emotional. Danke, dass ihr mir immer vorgelebt habt, dass man hart arbeiten muss und sich nicht zurücklehnen darf um seine Ziele und Träume verwirklichen zu können und das Aufgeben im Leben keine Option sein sollte.

Funding

This work was funded by the German Federal Ministry of Food and Agriculture (BMEL), through the Specialist agency renewable raw materials e. V. (FNR) as part of the ERA-IB project “TTRAFFIC” (FKZ 22030515). The laboratory of Lars M. Blank was partially funded by the Deutsche Forschungsgemeinschaft (DFG, German Research Foundation) under Germany’s Excellence Strategy within the Cluster of Excellence TMFB 236 and Exzellenzcluster 2186 „The Fuel Science Center“.



*“The most dangerous phrase
in the language is,
we’ve always done it this way”
-Grace Hopper-*

Summary	III
Zusammenfassung	V
List of abbreviations	VII
List of figures	XI
List of tables	XIII
1 General introduction	3
1.1 Transfer to a sustainable and environmentally friendly industry	3
1.2 Organic acids as platform chemicals	3
1.2.1 Citric acid	5
1.2.2 Succinic acid	6
1.2.3 Lactic acid	7
1.2.4 Malic acid	8
1.2.5 Itaconic acid	9
1.3 Scope and outline of this thesis	16
2 Material and Methods	19
2.1 Plasmid cloning- and strain engineering	19
2.2 Culture conditions	21
2.3 Analytical methods	22
2.4 Genome sequencing	23
2.5 Phylogenetic analyses	24
3 Results	29
3.1 Evolutionary freedom in the regulation of the conserved itaconate cluster Rial in related Ustilaginaceae	29
3.1.1 Abstract	29
3.1.2 Introduction	29
3.1.3 Results and discussion	32
3.1.4 Conclusion	46
3.1.5 Acknowledgements	46
3.2 The interplay between transport and metabolism in fungal itaconic acid production	49
3.2.1 Abstract	49
3.2.2 Introduction	49
3.2.3 Results and discussion	51
3.2.4 Conclusion	56
3.2.5 Acknowledgements	57

Table of contents

3.3	Engineering the morphology and metabolism of pH tolerant <i>Ustilago cynodontis</i> for efficient itaconic acid production.....	61
3.3.1	Abstract	61
3.3.2	Introduction	61
3.3.3	Results and discussion	62
3.3.4	Conclusion	72
3.3.5	Acknowledgements.....	72
3.4	Process engineering of pH tolerant <i>Ustilago cynodontis</i> for efficient itaconic acid production.....	75
3.4.1	Abstract	75
3.4.2	Introduction	75
3.4.3	Results and discussion	76
3.4.4	Outlook.....	85
3.4.5	Acknowledgements.....	85
3.5	Integrated strain- and process design enable production of 220 g L ⁻¹ itaconic acid with <i>Ustilago maydis</i>	88
3.5.1	Abstract	88
3.5.2	Introduction	88
3.5.3	Results and discussion	89
3.5.4	Outlook.....	96
3.5.5	Acknowledgements.....	97
4	General discussion and outlook	101
4.1	Organic acids and their potential to initiate change	101
4.2	Morphology.....	101
4.3	Metabolic Engineering	103
4.4	Process Engineering: A long journey with challenges.....	105
4.4.1	Conclusion	107
	Appendix.....	109
	Supplemental tables.....	111
	Supplemental figures.....	121
	Supplemental data	127
	References	133
	Curriculum vitae	155

Summary

Itaconic acid is a versatile building block in the polymer industry due to its two functional groups. Radical polymerization of the methylene group and/or esterification of the carboxylic acid with a wide range of co-monomers enable a rapidly expanding application range. Since 1950, *Aspergillus terreus* is used for industrial production of itaconate. However, despite the long history and experience, itaconate production in *A. terreus* remains challenging and above all the required control of the morphology leads to high production costs, which causes a relatively low market volume of itaconate despite its chemical potential. Due to good scientific fundamentals and robustness, Ustilaginaceae promises alternative hosts that offer new possibilities to achieve more efficient itaconate production.

The overall aim of this thesis was to achieve efficient itaconate production from glucose with Ustilaginaceae. In a screening of several Ustilaginaceae, genetic equipment for itaconate production could be determined for all tested strains. In addition to *Ustilago maydis*, which is well studied in the context of itaconate production, *Ustilago cynodontis* was chosen mainly due to its tolerance to low pH.

Comparative analysis of the mitochondrial and extracellular transporters involved in itaconate and (S)-2-hydroxyparaconate biosynthesis by *U. maydis*, and *A. terreus* elucidated that the mitochondrial transporter of *A. terreus* (MttA) enabled a more efficient itaconate production in *U. maydis* and *U. cynodontis*. Itaconate production could be further improved in both strains by metabolic engineering using CRISPR/Cas9 and FLP/FRT systems for marker-free deletion of the itaconate oxidase ($\Delta cyp3$), knock-in of the strong and constitutive promoter P_{ref} upstream of the regulator-encoding gene *ria* in *U. maydis* or by overexpression of this regulator in *U. cynodontis*. Thus, production could be enhanced 4.2-fold in *U. maydis* and 6.5-fold in *U. cynodontis* compared to corresponding wildtype strains.

In order to ensure robust and non-filamentous cells growing in a yeast-like manner under certain process-relevant conditions, both strains were modified in a morphological engineering approach. The gene *fuz7*, which is part of the Ras/mitogen-activated protein kinase (MAPK) pathway and plays an important role in conjugation tube formation and filamentous growth, was therefore deleted in both strains. The obtained yeast-like-growing strains open up a range of possibilities in the field of process development.

Thus, for the first time, itaconate production in a bioreactor with the otherwise strong filamentously growing *U. cynodontis* could be realized. By optimizing the pH value, different feeding strategies and repeated-batch systems titer up to 83 g L⁻¹, overall yields up to 0.45 g_{ITA} g_{GLC}⁻¹ and maximum productivities up to 1.4 g L⁻¹ h⁻¹ could be reached. In *U. maydis*, fermentations in combination with in situ product removal using calcium carbonate precipitation resulted in a titer of 220 g L⁻¹ itaconate, which is so far the highest reported value for microbially produced itaconate.

In conclusion, by an integrated approach of metabolic and morphological engineering, coupled with process development, the efficiency of itaconate production with *U. maydis* and *U. cynodontis* could be significantly enhanced. The production strains engineered in this thesis enable new process engineering strategies and ensure stable unicellular growth, thereby likely contributing to the future expansion of the fields of application of itaconate as an important bio-based building block in the near future.

Zusammenfassung

Itaconsäure ist aufgrund seiner beiden funktionellen Gruppen ein vielseitiger Baustein in der Polymerindustrie. Durch radikale Polymerisation der Methylengruppe und/oder durch Veresterung der Carboxylgruppen mit einer großen Anzahl an möglichen Co-Monomeren wird ein breites Anwendungsspektrum ermöglicht. Seit 1950 wird *Aspergillus terreus* zur Herstellung von Itaconsäure eingesetzt. Trotz der langen Historie und Erfahrung ist die Itaconsäure-Produktion in *A. terreus* eine anspruchsvolle Aufgabe und die Kontrolle der Morphologie führt zu hohen Kosten, die zu einem kleinen Marktanteil trotz seiner guten chemischen Eigenschaften führt. Aufgrund guter wissenschaftlicher Grundlagen und ihrer Robustheit sind Ustilaginaceae vielversprechende alternative Biokatalysatoren, die neue Möglichkeiten bieten um eine effizientere Itaconsäure-Produktion zu erreichen.

Das übergeordnete Ziel dieser Arbeit war eine effiziente Itaconsäure-Produktion aus Glukose mit Ustilaginaceae. In einem Screening mehrerer Ustilaginaceae konnten für alle getesteten Stämme genetische Grundlagen für die Itaconsäure-Produktion bestimmt werden. Neben *Ustilago maydis*, der ein gut untersuchter Wirt für die Itaconsäure-Produktion ist, wurde *Ustilago cynodontis* wegen seiner Toleranz gegenüber niedrigem pH-Werten gewählt. Die Untersuchung von an der Itaconat- und (S)-2-hydroxyparaconatbiosynthese beteiligten mitochondrialen und extrazellulären Transportern von *U. maydis* und *A. terreus* ergaben, dass der mitochondriale Transporter von *A. terreus* eine effizientere Itaconsäure-Produktion in *U. maydis* und in *U. cynodontis* ermöglicht. Die Itaconsäure-Produktion konnte in beiden Stämmen durch Deletion der Itaconat-Oxidase, tausch des nativen Promoter P_{ria1} durch P_{etef} in *U. maydis* oder durch eine Überexpression vom Regulator *ria1* in *U. cynodontis* weiter verbessert werden. So konnte die Produktion in *U. maydis* um das 4,2-fache und in *U. cynodontis* um das 6,5-fache gesteigert werden. Um diese genetischen Veränderungen umzusetzen, wurde CRISPR/Cas9 Technologie oder FLP/FRT-Systeme angewandt. Um ein robustes Zellwachstum unter prozessrelevanten Bedingungen zu gewährleisten, wurden beide Stämme in einem morphologischen Ansatz modifiziert. Dazu wurde das Gen *fuz7*, welches Teil der Ras/mitogen-aktivierten Proteinkinase (MAPK) Kaskade ist und eine wichtige Rolle beim filamentösen Wachstum einnimmt, deletiert. Die dadurch entstandenen hefeähnlichen Zellen eröffnen somit neue Möglichkeiten im Bereich der Prozessentwicklung.

Somit konnte erstmals die Itaconsäure-Produktion in einem Bioreaktor mit dem sonst stark filamentös wachsendem *U. cynodontis* realisiert werden. Durch Optimierung des pH-Wertes, der Fütterungsstrategien und durch Zellrückgewinnungssysteme konnten Titer bis zu 83 g L^{-1} mit einer Ausbeute von $0,45 \text{ g}_{\text{ITA}} \text{ g}_{\text{GLC}}^{-1}$ und einer maximalen Produktivität von $1,4 \text{ g L}^{-1} \text{ h}^{-1}$ erreicht werden. Für *U. maydis* wurden durch Fermentationen in Kombination mit der *in situ* Produktentfernung mittels Calciumcarbonatfällung Titer von 220 g L^{-1} Itaconsäure erreicht. Dieser Wert ist der bisher höchste erreichte Itaconsäure-Titer der Mikrobiell hergestellt wurde. Zusammenfassend lässt sich sagen, dass durch einen integrierten Ansatz durch Metabolic- und Morphological Engineering gekoppelt mit der Prozessentwicklung die Effizienz der Itaconsäure-Produktion mit *U. maydis* und *U. cynodontis* deutlich gesteigert werden konnte. Die in dieser Arbeit entwickelten Produktionsstämme ermöglichen aufgrund eines stabilen einzelligen Wachstums neue verfahrenstechnische Strategien. Die Umsetzung dieser trägt zur zukünftigen Erweiterung der Anwendungsgebiete von Itaconsäure als wichtigem biobasierten Baustein bei.

List of abbreviations

%	percentage
(c)	cytoplasmatic
°C	degree Celsius
<i>A. niger</i>	<i>Aspergillus niger</i>
<i>A. terreus</i>	<i>Aspergillus terreus</i>
Adi1/ <i>adi1</i>	cytosolic aconitate- δ -isomerase
ampR	ampicillin resistance cassette
antiSMASH	antibiotics and Secondary Metabolite Analysis SHell
ATCC	American Type Culture Collection
ATP	adenosin triphosphate
BLAST	Basic Local Alignment Search Tool
BMEL	Bundesministerium für Ernährung und Landwirtschaft
bp	basepairs
C	carbon
<i>C. krusei</i>	<i>Candida krusei</i>
Ca	calcium
Ca(OH) ₂	calcium hydroxide
CaCl ₂	calcium chloride
CaCO ₃	calcium carbonate
CadA/ <i>cadA</i>	<i>cis</i> -aconitate decarboxylase
CAS	Chemical Abstracts Service
Cas	CRISPR associated protein
cbx	carboxin
cbx ^R	carboxin resistance gene
CM-cellulose	carboxymethyl cellulose
Co.	Compagnie
CO ₂	carbon dioxide
CO ₃	carbon trioxide
CoA	coenzyme-A
CoCl ₂	cobalt (II) chloride
ColE1	origin of replication in <i>E. coli</i>
<i>crg1</i>	carbon source-regulated gene
CRISPR/Cas9	clustered regularly interspaced short palindromic repeats/CRISPR associated
CuSO ₄	cooper sulfate
<i>cyp1</i>	cytochrome P450 family gene
<i>Cyp3/cyp3</i>	itaconate P450 monooxygenase protein/gene
DNA	deoxyribonucleic acid
DO	dissolved oxygen
DOE	U.S. Department of Energy
DOT	dissolved oxygen tension
DSM	Deutsche Sammlung von Mikroorganismen
<i>E. coli</i>	<i>Escherichia coli</i>
e.g.	exempli gratia
EDTA	ethylenediaminetetraacetic acid
<i>em1</i>	elongator methionine-accepting tRNA gene
ERA-IB	European Research Area Industrial Biotechnology
<i>et al.</i>	et alii or et aliae
FeSO ₄	ferrous sulfate
FLP	flippase
FNR	Fachagentur Nachwachsender Rohstoffe
FRT	flippase recognition target
fwd	forward
g	gram
Gfp/ <i>gfp</i>	green fluorescent protein/gene
GLU	glucose
GLY	glycerol
h	hour
H ₂ O	water
H ₃ BO ₃	boric acid
HCl	hydrogen chloride
HP	(<i>S</i>)-2-hydroxyparaconate

List of abbreviation

hph	hygromycin resistance cassette
HPLC	high-performance liquid chromatography
hyg	hygromycin
hyg ^R	hygromycin resistance gene
iAMB	Institute of Applied Microbiology
ip	iron sulphur protein subunit of succinate dehydrogenase
ITA	itaconate
Itp1/ <i>itp1</i>	major facilitator superfamily transporter protein/gene
kg	kilogram
KH ₂ PO ₄	potassium dihydrogen phosphate
KI	potassium iodide
L	liter
LAB	lactic acid bacteria
M	molar
mal	malate
MEL	mannosylerythritol lipid
MES	2-(N-morpholino) ethanesulfonic acid
MfsA/ <i>mfsA</i>	major facilitator superfamily transporter protein/gene
MgSO ₄	magnesium sulfate
MIBiG	minimum information about a biosynthetic gene cluster
min	minute
Mio	million
mL	milliliter
mM	millimolar
MnCl ₂	manganese (II) chloride
mol	molar
mRNA	messenger ribonucleic acid
MTM	modified Tabuchi medium
Mtt1/ <i>mtt1</i>	mitochondrial trans-aconitate transporter protein/gene
MttA/ <i>mtt1</i>	mitochondrial trans-aconitate transporter protein/gene
N	nitrogen
n	number of samples
Na ₂ MoO ₄	sodium molybdate
NaOH	sodium hydroxide
<i>nar1</i>	nitrate reductase gene
nat	nourseothricin
NBRC	NITE Biological Resource Center
NH ₄ Cl	ammonium chloride
no.	number
O	oxygen
O ₂	molecular oxygen
OD	optical density
ORF	open reading frame
<i>P. antarctica</i>	<i>Pseudozyma antarctica</i>
<i>P. tsukubaensis</i>	<i>Pseudozyma tsukubaensis</i>
<i>P. hubeiensis</i>	<i>Pseudozyma hubeiensis</i>
PCR	polymerase chain reaction
pH	negative logarithm of the concentration of hydronium ions
phl	phleomycin
pKa	symbol for the acid dissociation constant at logarithmic scale
Poma	oma promotor
Potef	otef promotor
<i>prf1</i>	perforin gene
<i>Pt</i>	<i>Pseudozyma tsukubaensis</i>
<i>R. arrhizus</i>	<i>Rhizopus arrhizus</i>
Rdo1/ <i>rdo1</i>	putative ring cleaving dioxygenase
rev	reverse
RI	refractive index
Ria1/ <i>ria1</i>	transcriptional regulator
RNA	ribonucleic acid
rpm	revolutions per minute
rTCA-cycle	reductive tricarboxylic acid cycle
RWTH	Rheinisch-Westfälische Technische Hochschule

<i>S. cerevisiae</i>	<i>Saccharomyces cerevisiae</i>
<i>S. iseilematis-ciliati</i>	<i>Sporisorium iseilematis-ciliati</i>
<i>Si</i>	<i>Sporisorium iseilematis-ciliati</i>
SMURF	Secondary metabolite unique regions finder
ssp.	species
Tad1/ <i>tad1</i>	<i>trans</i> -aconitate decarboxylase protein/gene
tBLASTn	translated BLAST
TCA-cycle	tricarboxylic acid cycle
TMFB	Tailor-Made Fuels from Biomass
TTRAFFIC	Toxicity and Transport For Fungal production of Industrial Compounds
<i>U. cynodontis</i>	<i>Ustilago cynodontis</i>
<i>U. maydis</i>	<i>Ustilago maydis</i>
<i>U. rabenhorstina</i>	<i>Ustilago rabenhorstina</i>
<i>U. trichophora</i>	<i>Ustilago trichophora</i>
<i>U. vetiveriae</i>	<i>Ustilago vetiveriae</i>
<i>U. xerochloae</i>	<i>Ustilago xerochloae</i>
U.S.	United States
<i>Uc</i>	<i>Ustilago cynodontis</i>
USA	United States of America
USD	United states dollars
UV	ultraviolet
v/v	volume per volume
vvm	volume flow per unit of liquid volume per minute
VWR	Van Waters & Rogers
WT	wildtype
YEP	yeast extract peptone
ZeroCarbFP	ZeroCarbonFootprint
ZnSO ₄	zinc sulfate

List of figures

Figure 1. Chemical structure of citric acid	5
Figure 2. Chemical structure of succinic acid.....	6
Figure 3. Various substances that can be derived from succinic acid by chemical conversion	7
Figure 4. Chemical structure of lactic acid	7
Figure 5. Chemical structure of malic acid.....	8
Figure 6. Chemical structure of itaconic acid.....	9
Figure 7. Derivatives of itaconate.	10
Figure 8. Itaconate metabolism in <i>U. maydis</i> and <i>A. terreus</i>	13
Figure 9. Proposed intracellular organization of the (S)-2-hydroxyparaconate biosynthesis pathway in <i>U. maydis</i>	31
Figure 10. Itaconate and (S)-2-hydroxyparaconate production by various species in the Ustilaginaceae cultivated on glucose and glycerol.	33
Figure 11. Malate and itatartarate production by various Ustilaginaceae on glucose and glycerol.	34
Figure 12. Glucose and glycerol consumption by various Ustilaginaceae.....	36
Figure 13. Itaconate cluster composition of selected Ustilaginaceae and a phylogenetic tree of these genes.	38
Figure 14. Phylogenetic tree of the Rial1 transcriptional regulator of different Ustilaginaceae based on similarities and differences in their protein sequence.	39
Figure 15. Overview of the influence of overexpression of <i>Umag_rial1</i> , <i>Uc_rial1</i> , <i>Pt_rial1</i> and <i>Si_rial1</i> , on itaconate (ITA), (S)-2-hydroxyparaconate (HP), and malate (MAL) production.....	40
Figure 16. Schematic overview of the influence of overexpression of <i>Umag_rial1</i> , <i>Uc_rial1</i> , <i>Pt_rial1</i> and <i>Si_rial1</i> , on itatartarate (ITT) production.	41
Figure 17. Itaconate and (S)-2-hydroxyparaconate production by various Ustilaginaceae species and their mutants transformed with <i>Umag_rial1</i> , <i>Uc_rial1</i> , <i>Pt_rial1</i> , <i>Si_rial1</i>	42
Figure 18. Malate and itatartarate production by various Ustilaginaceae and their mutants transformed with <i>Umag_rial1</i> , <i>Uc_rial1</i> , <i>Pt_rial1</i> , <i>Si_rial1</i>	45
Figure 19. Common motif within the promoter regions of the itaconate cluster genes	46
Figure 20. Comparison of the itaconate and (S)-2-hydroxyparaconate biosynthesis pathways of <i>U. maydis</i> and <i>A. terreus</i>	50
Figure 21. Acid production and growth of various <i>U. maydis</i> strains expressing itaconate transport proteins.....	52
Figure 22. Acid production and growth of various <i>U. maydis</i> strains expressing mitochondrial transporters.	53
Figure 23. Controlled high-density pulsed fed-batch fermentation of <i>U. maydis</i> $\Delta Um_mtt1 + P_{actAT_mttA}$	55
Figure 24. Influence of buffer concentration on itaconate and (S)-2-hydroxyparaconate production by various <i>U. maydis</i> MB215 mutants.....	56
Figure 25. Acid production and growth of <i>U. maydis</i> MB215 (red) and <i>U. cynodontis</i> NBRC9727 (green).	63
Figure 26. Acid production and growth of <i>U. maydis</i> MB215 (red) and <i>U. cynodontis</i> NBRC9727 (green).	63
Figure 27. Controlled high-density pulsed fed-batch fermentations of <i>U. cynodontis</i> NBRC9727.....	64
Figure 28. Controlled high-density pulsed fed-batch fermentations of <i>U. cynodontis</i> NBRC9727.....	64
Figure 29. The cAMP and MAPK signaling pathways in <i>U. maydis</i>	65
Figure 30. Morphological engineering in <i>U. cynodontis</i> NBRC9727.....	66
Figure 31. Controlled high-cell density pulsed fed-batch fermentations of <i>U. cynodontis</i> $\Delta fuZ7$	69
Figure 32. Organic acid production of various <i>U. cynodontis</i> deletion strains.	70
Figure 33. Itaconate and erythritol production and growth of engineered <i>U. cynodontis</i> strains.....	71
Figure 34. Itaconate and erythritol production and growth of various engineered <i>U. cynodontis</i> strains.	71
Figure 36. Controlled high-density pulsed fed-batch fermentation of <i>U. cynodontis</i> $\Delta fuZ7$	79
Figure 37. Controlled high-density fed-batch fermentation of <i>U. cynodontis</i> NBRC 9727 $\Delta fuZ7^+$ $\Delta cyp3^+$ $P_{actMTTA}$ P_{ria1} P_{ria1}	81
Figure 38. Controlled high density fed-batch fermentation of <i>U. cynodontis</i> NBRC 9727 $\Delta fuZ7^+$ $\Delta cyp3^+$ $P_{actMTTA}$ P_{ria1} P_{ria1}	82
Figure 39. Controlled high density fed-batch fermentation of <i>U. cynodontis</i> NBRC 9727 $\Delta fuZ7^+$ $\Delta cyp3^+$ $P_{actMTTA}$ P_{ria1} P_{ria1}	83

List of figures

Figure 40. Glucose consumption of <i>U. cynodontis</i> NBRC 9727 Δ fuz7 Δ cyp3 ⁺ P _{etefmttA} P _{ria1ria1}	83
Figure 41. Controlled high density fed-batch fermentation of <i>U. cynodontis</i> NBRC 9727 Δ fuz7 Δ cyp3 ⁺ P _{etefmttA} P _{ria1ria1}	84
Figure 42. Repeated batch approach for itaconate production in <i>U. cynodontis</i>	85
Figure 43. Itaconate production and growth of engineered <i>U. maydis</i> strains.....	90
Figure 44. Itaconate production and growth of morphology-engineered <i>U. maydis</i> strains.....	92
Figure 45. Comparison of aqueous and total itaconate concentrations in culture of engineered <i>U. maydis</i> strains.....	93
Figure 46. Itaconate production and growth of engineered <i>U. maydis</i> strains on glycerol.....	94
Figure 47. Controlled pulsed fed-batch fermentation of <i>U. maydis</i> MB215 Δ cyp3 Δ P _{ria1::P_{etef} Δfuz7 P_{etefmttA}.....}	95
Figure 48. Controlled high-density pulsed fed-batch fermentation of <i>U. maydis</i> MB215 Δ cyp3 Δ P _{ria1::P_{etef} Δfuz7 P_{etefmttA} with NaOH titration.....}	95
Figure 49. Controlled high-density pulsed fed-batch fermentation of <i>U. maydis</i> MB215 Δ cyp3 Δ P _{ria1::P_{etef} Δfuz7 P_{etefmttA} in the presence of CaCO₃.....}	96
Figure 50. Life cycle of <i>U. maydis</i>	102
Figure 51. Plasmid maps of pETEF_CbxR_At_mttA and pETEF_CbxR_At_mfsA.....	121
Figure 52. Genetic tool development for <i>U. cynodontis</i> NBRC9727.....	121
Figure 53. Morphological engineering in <i>U. cynodontis</i> NBRC9727.....	122
Figure 54. Morphological engineering in <i>U. cynodontis</i> NBRC9727.....	123
Figure 55. Growth behavior of various <i>U. cynodontis</i> NBRC9727 strains.....	123
Figure 56. pH values of cultures of various <i>U. cynodontis</i> NBRC9727 strains.....	124
Figure 57. Erythritol production and growth of various <i>U. cynodontis</i> strains.....	124
Figure 58. Acid and erythritol production and growth of various <i>U. cynodontis</i> strains.....	125
Figure 59. Itaconate production of four individual P _{ria1ria1} transformants of <i>U. cynodontis</i> Δ fuz7 Δ cyp3 ⁺	125
Figure 60. Itaconate production of 63 individual P _{etefmttA} transformants of <i>U. cynodontis</i> Δ fuz7 Δ cyp3 ⁺ P _{ria1ria1}	126

List of tables

Table 1. World population and their development [2].....	3
Table 2. Building block chemicals.	4
Table 3. Itaconate production of wildtype strains generated by random mutagenesis.....	11
Table 4. Itaconate production of genetically modified organism.	12
Table 5. Ustilaginaceae used in this study.	20
Table 6. Production parameters of <i>U. maydis</i> MB215 and transporter mutants.....	54
Table 7. Production parameters of various <i>U. cynodontis</i> strains.....	68
Table 8. Protonation distribution of controlled high-density pulsed fed-batch fermentation.....	77
Table 9. Carbon distribution of various fermentation conditions	80
Table 10. Production parameter for itaconate of various fermentation conditions	80
Table 11. Feeding procedure during high-density pulsed fed-batch fermentation.....	111
Table 12. Feeding procedure during high-density pulsed fed-batch fermentation.....	112
Table 13. Oligonucleotides used for cloning, diagnostic PCRs and sequencing procedures.	113
Table 14. Plasmids.	117

Chapter 1

General introduction

Contributions:

This chapter was written by Hamed Hosseinpour Tehrani and reviewed by Lars M. Blank and Nick Wierckx.

1 General introduction

1.1 Transfer to a sustainable and environmentally friendly industry

Fossil resources have been used for more than a century to produce platform chemicals for energy production and transportations [1]. The increasing wealth and world population (Table 1) causes an higher demand for energy, food, and transportation fuels [1-4]. However, fossil resources are limited and unequally distributed on earth, which can easily lead to conflicts between countries. The main drawback of a fossil-based industry, however, is the high emission of greenhouse gases, which contribute to global warming [5, 6]. The environmental crisis associated with the exploitive use of fossil resources represents a prominent challenge for humanity. The much-needed shift from the linear fossil-based economy to a circular biobased economy requires renewable feedstocks based on biomass for the production of everyday commodities [7, 8]. In such a scenario, the emitted carbon dioxide would be fixed by plants or dedicated microbes to generate biomass that once again could be used as feedstock for bioproduction processes. Thereby a closed carbon cycle would be established on a short-term basis [9, 10].

Table 1. World population and their development [2].

Region	Population (millions)			
	2017	2030	2050	2100
World	7750	8551	9772	11184
Africa	1256	1704	2528	4468
Asia	4504	4947	5227	4780
Europe	742	739	716	653
Latin America and the Caribbean	646	718	780	712
Northern America	361	395	435	499
Oceania	41	48	57	72

1.2 Organic acids as platform chemicals

Platform chemicals are small molecules that can be utilized as building blocks for the production of chemicals and materials of higher value [11]. In 2004, the U.S. Department of Energy (DoE) tested more than 300 chemicals with great biotechnological potential and identified twelve building block chemicals that could potentially be produced competitively from biomass [12]. The evaluation was organized in several rounds with different characteristics of the compounds. The criteria for selection of the top 12 (Table 2A) was based on the potential markets for the building blocks and their derivatives and the technical complexity of their synthesis pathways. Further, the molecules should have multiple functional groups that possess the potential to be transformed into new families of useful molecules. Among the top 12 building blocks, nine organic acids including itaconate, fumarate, malate, and succinate were listed [12].

Table 2. Building block chemicals. A) Top 12 building block chemicals assigned in 2004 [12] and B) Top 10 building block chemicals assigned in 2010 [13].

A	B
1,4-succinic, fumaric and malic acid	ethanol
2,5-furan dicarboxylic acid	furans
3-hydroxy propionic acid	glycerol and derivatives
aspartic acid	biohydrocarbons
glucaric acid	lactic acid
glutamic acid	succinic acid
itaconic acid	hydroxypropionic acid/aldehyde
levulinic acid	levulinic acid
3-hydroxybutyrolactone	sorbitol
glycerol	xylitol
sorbitol	
xylitol/arabinitol	

In 2010 the list was revisited using following criteria: 1) the compound or technology has received significant attention in literature; 2) the compound illustrated a broad technology applicable to multiple products; 3) the technology provides direct substitutes for existing petrochemicals; 4) the technology is applicable to high-volume products; 5) a compound exhibits strong potential as a platform chemical; 6) scale-up of the product or a technology to pilot, demo, or full scale is underway; 7) The bio-based compound is an existing commercial product, prepared at intermediate or commodity levels; 8) the compound may serve as a primary building block of a biorefinery; 9) commercial production of the compound from renewable carbon is well established [13]. Thus, the new criteria resulted in a new list of the top 10 building blocks (Table 2B). The current market and technology will always influence the request on molecules and thus change the order of the top platform chemicals. Glycerol, for example, has lost attraction, since biodiesel production increased, and crude glycerol was flooding the markets. As a result, companies that produced glycerol chemically lost competitiveness and had to close [14]. But the general desire for low-cost monomers to compete with petroleum-derived molecules will not change [15].

One group of chemicals which is prominently represented in the lists are organic acids. Alone nine of them were among the top 12 building blocks in 2004 [12], while still, five were present in 2010 [13]. This clearly demonstrates the great importance and potential of this group, which is also reflected by its constant appearance in literature [8, 16-25]. The special character of organic acids is that they can be naturally produced by a high number of microorganisms and that their functional groups can be transformed into new families of usable compounds and used as a starting compound for a broad range of applications [8, 20]. However, despite the good basic properties organic acids bring with them, the market size for microbially produced organic acids is small. Only a very limited number of economic processes such as whole-cell biocatalytic citric acid [26], lactic acid [27], D-gluconic acid [28], itaconic acid [29], 2-keto-L-gluconic acid [30, 31] and succinic acid production [32] are established, whereby citric acid is with more than 1 million tons per year the

most prominent product.

An optimized fermentation process at lab-scale does not necessarily imply industrial applicability. While certain consumer markets allow a bio-premium in the final price, e.g., Lego, the chemical commodities most often not. Hence, to establish an industrial process, optimizations are needed, which allow production at a lower price compared to the petrochemical route. This is truly challenging as the petrochemical industry is optimized for the last 70 years. One requirement is low-cost substrates like it is common for lactic acid production [8, 33-39]. Even reported repeated fed-batch fermentations or cell retentions systems, enabling high-titer production, do not find application in the industry since they are too complex and too costly [8, 40, 41]. Further, the downstream process plays a significant role in how profitable a process can be. For example, the most produced commodity from lactic acid is polylactide, which is used as low-value packaging material. This automatically means that the production of lactic acid must also be cheap in order for the process to be profitable, especially because the quality of the polymerized product depends on the purity of the lactic acid [42-44]. Moreover, in order to lower production costs, it is required to reduce the use of complex media components such as yeast extract as they lead to high impurities in the fermentation broth and to reduce the production of by-products. In summary, many parameters must be optimized simultaneously to enable a profitable process. In this context, the selection of the microbial host, carbon source, reactor type, process conditions, purification methods, and many other parameters must be carefully considered. However, the market on which the product should be placed is a major determinant, because it specifies the price which ultimately determines allowed production cost and thus the path that can be taken. In the following sections, more detailed information on citric-, succinic-, lactic-, malic-, and itaconic acid are given, whereby the focus is on itaconic acid due to its prevalent significance for this thesis.

1.2.1 Citric acid

Citric acid (Figure 1) (3-carboxy-3-hydroxypentane-1,5-dioic acid, 3-carboxy-3-hydroxypentanedioic acid, 2-hydroxy-1,2,3-propanetricarboxylic acid) (CAS 77-92-9) is a saturated, non-toxic, organic C6-tricarboxylic acid with a molecular mass of 192.12 g mol⁻¹. Its solubility in water is 147.76 g L⁻¹ at 20 °C with pK_a-values of 3.13 (pK_{a1}), 4.76 (pK_{a2}), and 6.39 (pK_{a3}). Citric acid was discovered in 1784 by Carl Scheele and the first production was established by extraction from citrus fruits. Historically speaking, the production of citric acid by the filamentous fungus *Aspergillus niger* is the oldest known microbial process for high volume organic acid production [45-51].

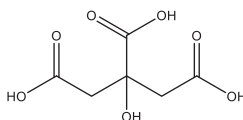


Figure 1. Chemical structure of citric acid.

The main use for citric acid is as a flavoring agent in the food industry. Other applications are as an acidifier and chelating agent in the chemical and pharma industry [17]. Since the demand was constantly increasing, the development was quickly pushed forward. In 1893 first accumulation of citric acid by microbes was observed and 1913 the first patent for citric acid production with *Aspergillus niger* was published [45, 51]. In 1917, a first fermentation process with *A. niger* was

established [46]. The rapid development leads that 90 % of the theoretical yield was reached [47-50]. Automatically, market size increased too. In 1998, the market volume was 879,000 tons [52] and increased further until 2007 to 1.6 million tons. In 2016, the citric acid market increased further and had a global market value of 2.5 billion USD and is estimated to reach 3.83 billion USD by 2025. [53, 54]. Thus, citric acid production is one of the largest biotechnological processes.

On the metabolic level, microbial production starts from pyruvate, which can be generated for example from glucose by glycolysis. Microbial production of citrate starts from pyruvate. In the mitochondrion, the pyruvate dehydrogenase complex converts one molecule pyruvate to one acetyl-CoA, and second pyruvate is carboxylated to oxaloacetate by the pyruvate carboxylase in the cytosol. Afterward, oxaloacetate is converted to malate and transported to the mitochondrion where it is converted by the citrate synthase together with acetyl-CoA to citrate, which is then transported out of the mitochondrion and subsequently out of the cell [55, 56].

1.2.2 Succinic acid

Succinic acid (Figure 2) (butanedioic acid, ethane-1,2-dicarboxylic acid) (CAS 110-15-6) is a saturated, non-toxic, organic, C4-dicarboxylic acid with a molecular mass of $118.09 \text{ g mol}^{-1}$. Its solubility in water is 58 g L^{-1} at $20 \text{ }^\circ\text{C}$ with pK_{a} -values of 4.2 ($\text{pK}_{\text{a}1}$) and 5.6 ($\text{pK}_{\text{a}2}$).

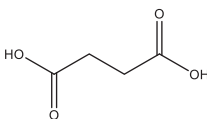


Figure 2. Chemical structure of succinic acid.

First isolation of succinic acid was reported by Georgius Agricola from amber [57]. In the beginning of industrial production, succinic acid was produced by fermentation but meanwhile, commercial production is via the petrochemical route [57, 58]. Especially because of its high production costs bio-based succinic acid could not assert itself so far [8]. Since it is part of the TCA-cycle, it was investigated in many different organisms like *Fusarium* [59] and *Aspergillus* [60] species, *Penicillium simplicissimum* [61], *Basfia succiniproducens* [62, 63] and yeasts, like *S. cerevisiae* [64] and *C. krusei* [65] and bacteria [57, 58, 66]. The current discussion is on succinate production from CO_2 [67]. Succinic acid is used for the synthesis of surfactant, detergent or foaming agent, as an ion chelator, in the food industry and for pharmaceuticals and antibiotics, and as a precursor for the production of different polymers, resins, and solvents [8, 20, 58]. Although a high number of various substances can be derived from succinic acid, the market size of approximately 131.73 million dollars in 2018 is very small [68]. This is mainly due to the high production costs that are incurred and impede its application although succinic acid would have the chemical potential to replace petroleum-derived maleic anhydride, which has a market size of 213,000 tons per year. Further substances that can be derived from succinic acid are depicted in Figure 3 [8].

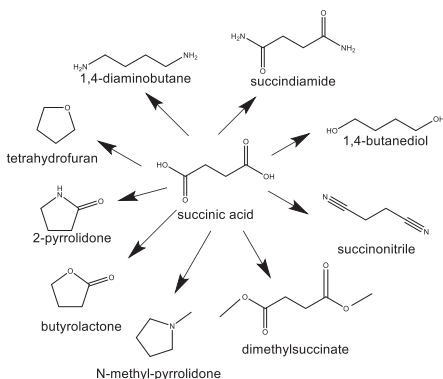


Figure 3. Various substances that can be derived from succinic acid by chemical conversion. The figure was adapted from Sauer *et al.* [8].

Metabolically, three different pathways for microbial production are known: Oxidative and reductive TCA-cycle and the glyoxylate bypass [17]. Advancing genetic tools and the ever-increasing gain of knowledge allow rational modifications within the metabolism to increase product formation in a metabolic engineering approach [69-72]. But also, applying non-rational methods like adaptive laboratory evolution, the production and tolerance could be further increased [73-75].

1.2.3 Lactic acid

Lactic acid (Figure 4) (2-hydroxypropanoic acid) (CAS 10326-41-7) is a non-toxic C3-organic acid with a molecular mass of 90.078 g mol⁻¹. Its solubility is so high that 1 part of lactic acid can dissolve 12 parts of water at 20 °C with pK_a-value of 3.86.

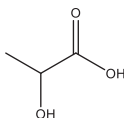


Figure 4. Chemical structure of lactic acid.

Lactic acid was discovered in 1780 by the Swedish chemist, Carl Wilhelm Scheele. He isolated it from sour milk. Up to 1857, it was assumed that lactic acid is a milk component until Pasteur discovered it as a microbial metabolite. Based on this discovery first fermentation and industrial production of lactic acid took place in 1881 in the United States of America [76]. Lactic acid finds many applications in food, pharmaceutical, cosmetic and chemical industry [44, 77]. The most important application is the polymerization of lactic acid to form polylactic acid, which is a polymer that can be produced from renewable resources and thus can replace petroleum-based consumables [78-80]. Lactic acid can be produced by chemical synthesis or by fermentation, whereby fermentation is preferred since it allows pure isomers and the use of renewable feedstocks [81]. In the last decades, lactic acid production increased continuously because more and more

new markets have been opened up. Alone in 2013, global lactic acid was estimated to be 714.2-kilo tons and it is expected to be 1,960-kilo tons by 2020 [82]. Further, global lactic acid production from microbial fermentation accounts for around 90% of total lactic acid production [81]. General lactic acid bacteria (LAB) such as *Lactobacilli* and *Carnobacterium* are used for the production. Further LAB are described in [81]. Depending on the final product, a distinction is made between homofermentative and heterofermentative. While homofermentative LAB convert glucose almost exclusively to lactic acid, heterofermentative LAB additionally form ethanol and CO₂ [81]. Furthermore, heterofermentative LAB can be subdivided in obligatory and facultative [81]. Further LAB have complex nutrient requirements especially because they are limited in synthesizing B vitamins and amino acids. Therefore, nutritionally rich media must be used in LAB fermentations [83]. But in literature also filamentous fungi such as *Rhizopus oryzae* and *R. arrhizus* are described as a natural producer. They utilize glucose aerobically to produce lactic acid and are well discussed in the literature [33, 84-89].

1.2.4 Malic acid

Malic acid (Figure 5) (hydroxybutanedioic acid or 2-hydroxysuccinic acid) (CAS 6915-15-7) has an asymmetric C-atom and thus occurs as L- (CAS 97-67-6) and as D-isomer (CAS 636-61-3). It is a saturated, non-toxic, organic, C₄-dicarboxylic acid with a molecular mass of 134.09 g mol⁻¹. Its solubility in water is 558 g L⁻¹ at 20 °C for DL-malic acid and 363.5 g L⁻¹ for D or L-malic acid; its pK_a-values are 3.46 (pK_{a1}) and 5.10 (pK_{a2}).

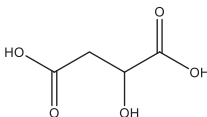


Figure 5. Chemical structure of malic acid.

In 1785, malic acid was isolated from apples, a source that was used for several decades [90]. It is mainly used in the beverage and food industry, but also in smaller amounts in metal cleaning, electroless plating, pharmaceuticals, infusions in hospitals, and in paints [18]. Due to high production costs, malic acid has a small market compared to other chemicals [8]. Approximately 40,000 tons malic acid were produced per year [18]. Yet until today, malic acid is mainly produced by hydration of maleic or fumaric acid resulting in a racemic mixture. Another option is the biotransformation of fumaric acid with immobilized cells expressing the enzyme fumarase. Depending on which organism is used yields for L-malic acid between 70 and nearly 100 % are possible [18, 91-94]. Since L-malic acid is an intermediate of the TCA-cycle, it is produced by all organisms. As is the case for many other organic acids, fungi are in focus of malic acid production, since they can naturally produce high titers [18, 91, 95-98]. Next to fungal production, also for some bacteria and *S. cerevisiae* strains malic acid production is reported [99-101]. Altogether there are four reported malic acid pathways: 1) TCA-cycle, 2) cytosolic rTCA-cycle, 3) cyclic glyoxylate pathway, and 4) non-cyclic glyoxylate pathway [99]. The biggest hurdle in microbial malic acid production is attaining sufficient product yields as yields are mostly far below theoretical, since always byproducts exist and the cumbersome purification from water, due to the high solubility [102].

1.2.5 Itaconic acid

Itaconic acid (Figure 6) (2-methylidenebutanedioic acid, 1-propene-2,3-dicarboxylic acid, methylenesuccinic acid) (CAS 97-65-4) is an unsaturated, non-toxic, organic, C₅-dicarboxylic acid with a molecular mass of 130.1 g mol⁻¹. Its solubility in water is 83 g L⁻¹ at 20 °C with pK_a-values of 3.84 (pK_{a1}) and 5.55 (pK_{a2}).

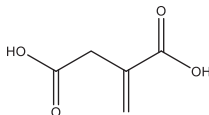


Figure 6. Chemical structure of itaconic acid.

First documentation about itaconate and its production was in the year 1837 [103]. The first production methods were based on chemical synthesis procedures [104-106]. Due to the high production costs involved in chemical synthesis, it was not possible to establish a foothold in the market [12, 107]. The first report about microbial production was published in 1931 with *Aspergillus itaconicus* [108] following by the first patent by Charles Pfizer Co. for the production with *A. terreus*. Over time, the fermentation process with *A. terreus* could be optimized, finally outcompeting the chemical process [109]. Thus since 1950 *A. terreus* is used for industrial itaconate production [110]. Due to its two functional groups, itaconate can be used versatile building block in the polymer industry. Radical polymerization and/or esterification with a wide range of co-monomers allow a rapidly expanding application range [25, 110]. Itaconate is mostly used as a co-monomer in the production of styrene-butadiene rubber and acrylate latexes, which are used in the paper and architectural industry [111]. Further polymerizations with acrylamide or methyl-methacrylate results in superabsorbent hydrogels for pharmaceutical applications [112-115]. Itaconate can be also polymerized with itself to obtain a polymer with high cation binding capacity, whereby the derivatives can be used as detergent additives, scale inhibitors, and dispersing agents [116]. Furthermore, itaconate is produced by mammalian macrophages where it plays a key role in the human immune response [117-119] against microbial pathogens, with possible applications as therapeutic agents for autoimmune diseases [120]. Further application can be found in Okabe *et al.* [110] or in Figure 7. Even though itaconate has so many potential applications, in 2011 its market size and value was only 41,400 t and \$74.5 million, respectively [23, 111]. This is caused by the high price with around two dollars per kilogram and is an exclusive criterion for further market penetration. To be competitive against petrol-based products, costs need to reduce to around \$0.5 per kg [121]. Assuming, that the price would decrease, itaconate has the possibility to replace polyacrylic acid whose production is petroleum-based and has a market worth of \$11 billion [23, 107, 110].

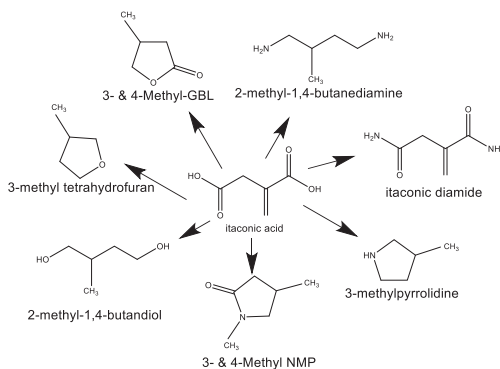


Figure 7. Derivatives of itaconate. The figure was adapted from Werpy [12].

To reduce the price of itaconate, more improvements are necessary. Certainly, fermentation conditions and especially the downstream process influence the price of the product [8]. But also used microorganism and C-sources influence the whole process, which in turn has an impact on the price. Unquestionably, many other factors such as location and energy costs play a role, in the following sections, only the influence of microorganism, fermentation, and downstream process is discussed.

1.2.5.1 Microbial hosts and metabolism for itaconate

Currently, *A. terreus* is used for industrial itaconic acid production. First, *A. terreus* strains producing itaconate were isolated in 1935 [122]. A screen of more than 300 strains in 1945 resulted in *A. terreus* NRRL 1960 as the best-producing strain, which was used for industrial itaconate production by Pfizer Co. in Brooklyn, NY, USA [106, 123]. Further factories were founded in England, Japan, and France. To reduce production costs facilities are nowadays located in the Asia-Pacific region [110, 111]. Next to *A. terreus*, also Ustilaginaceae such as *Pseudozyma* and *Ustilago* species, [95, 124-127] *Rhodotorula*, [128] *Candida* [127, 129], and *Helicobasidium* [130] species are known to produce itaconate. An overview of itaconate producing wildtype strains including titer, yield, and productivity is given in Table 3. Although the production parameters of the other strains such as *Ustilago* are so far apart, the search for new production organisms continues. Despite the long history and experience, itaconate production in *A. terreus* remains challenging and will be discussed in the next sections. Next, to the filamentous *A. terreus*, the yeast-like growing *U. maydis* is well studied and is a naturally itaconate producing organism.

Table 3. Itaconate production of wildtype strains generated by random mutagenesis [21].

Microorganism	Substrate	Itaconate (g L ⁻¹)	Yield (g _{ITA} g _{GLC} ⁻¹)	Productivity (g L ⁻¹ h ⁻¹)	Reference
<i>A. terreus</i> DSM 23081	glucose	129	0.58	1.15	[131]
<i>A. terreus</i> NRRL 1960	glucose	130	-	-	[22]
<i>A. terreus</i> DSM 23081	glucose	160	0.46	1	[132]
<i>A. terreus</i> SKR10 N45 ^a	hydrolyzed corn starch	50	0.42	0.35	[133]
<i>A. terreus</i> R104 ^a	glucose	52.7	0.72	0.55	[134]
<i>A. terreus</i> IFO-6365 TN-484 ^a	glucose	82.3	0.54	0.57	[135]
<i>Candidia sp. strain B-1</i> ^a	glucose	35	-	0.29	[129]
<i>Helicobasidium sp.</i>	-	-	-	-	[130]
<i>P. antarctica</i> NRRL Y-7808	glucose	30	0.38	-	[124]
<i>P. tsukubaensis</i> H488	glucose	74.7	0.49	0.36	[125]
<i>U. cynodontis</i> K470	glucose	28.4	-	-	[136]
<i>U. maydis</i> DSM 17144	glucose	44.5	0.24	0.31	[137]
<i>U. rabenhorstina</i> IFO 8995	glucose	15.7	-	-	[136]

^a Strains generated by random mutagenesis

In both organisms, the genes enabling itaconate biosynthesis are clustered and co-regulated [138, 139]. The biosynthetic pathway starts with the transport of *cis*-aconitate from the mitochondria to the cytosol by a mitochondrial tricarboxylate transporter, encoded by *Um_mtt1* or *At_mttA* [25, 139, 140]. Both transporters are assumed to do so by antiport exchange with cytosolic malate [141]. In *U. maydis*, this transport poses the rate-limiting step in itaconate production, since overexpression of *mtt1* leads to a strong increase in itaconate production [139]. In *A. terreus*, the cytoplasmic *cis*-aconitate is converted directly to itaconate by a cytosolic *cis*-aconitate decarboxylase (*cadA*) [142-144]. In contrast, *U. maydis* first isomerizes *cis*-aconitate to *trans*-aconitate by a cytosolic aconitate- δ -isomerase (Adi1). This *trans*-aconitate is subsequently decarboxylated to itaconate by a *trans*-aconitate decarboxylase (Tad1) [139]. *U. maydis* can further convert itaconate to (*S*)-2-hydroxyparaconate by an itaconate P450 monooxygenase (Cyp3). The latter is the lactone of L-itatartrate, which is also found in the supernatants of *U. maydis* [126, 136, 140]. This was also reported for some *A. terreus* strains [126, 145], likely through a similar P450 enzyme encoded by the *cypC* gene directly adjacent to the itaconate gene cluster [140, 146]. Interestingly (*S*)-2-hydroxyparaconate formation was not reported for *A. terreus* production strains [132, 147], maybe because these strains were selected by screening for high itaconate production leading to the selection of a defect *cypC* expression. Further in both organisms itaconate is transported out via a major facilitator superfamily transporter, encoded by *Um_itp1* and *At_mfsA*. Because both products (itaconate and (*S*)-2-hydroxyparaconate) are produced *via* the same pathway, and the gene clusters of both organisms only contain one gene encoding a cytosolic exporter, it is reasonable to assume that the same protein secretes both products. Metabolism and

cluster structure are depicted in Figure 8. This knowledge about metabolism allowed optimization by strain engineering in *Ustilago* and *Aspergillus* but also in other strains such as *E. coli*. Some examples are given in Table 4.

Table 4. Itaconate production of genetically modified organism. [21].

Microorganism	Substrate	Itaconate (g L ⁻¹)	Yield (g _{ITA} g _{GLC} ⁻¹)	Productivity (g L ⁻¹ h ⁻¹)	Reference
<i>A. niger</i> AB1.13 CitB#99	glucose	26.2	0.37 ^b	-	[148]
<i>A. terreus</i> A729	glucose	45.5	-	-	[149]
<i>C. glutamicum</i> AO-2/pEKEx2- malEcadapt	glucose	7.8	0.29	0.16	[150]
<i>E. coli</i> ita23	glucose	32	0.49 ^b	0.27	[151]
<i>S. cerevisiae</i>	glucose	0.168	-	-	[152]
<i>Synechocystis</i> sp. PCC6803	CO ₂	0.0145	-	-	[153]
<i>U. maydis</i> MB215 Δcyp3 P _{atg1} ria1	glucose	63.2	0.23 ^b	0.38	[140]
<i>Y. lipolytica</i>	glucose	4.6	0.058	0.045 ^a	[152]

^a Maximum productivity

^b Itaconate per consumed glucose

Despite the possibilities given by metabolic engineering, still *A. terreus* is a highly efficient filamentous fungus achieving nearly theoretical yields and titers over 100 g L⁻¹ at low pH values at suitable conditions [21, 131, 132].

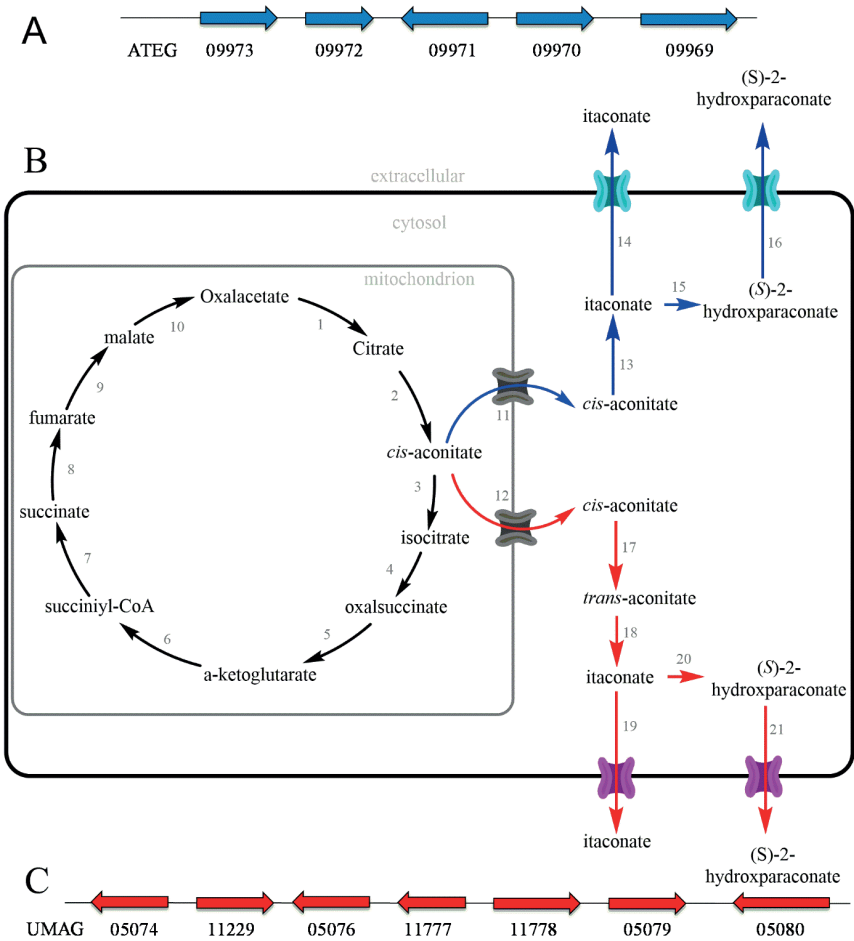


Figure 8. Itaconate metabolism in *U. maydis* and *A. terreus*. Itaconate cluster of *A. terreus* (blue) (A): ATEG_09973 (*cypC*), ATEG_09972 (*mfsA*), ATEG_09971 (*cadA*), ATEG_09970 (*mttA*) and ATEG_09969 (*iar*); TCA-cycle including metabolic steps for itaconate in *A. terreus* (blue) and *U. maydis* (red) (B): citrate synthase (1), aconitase(2, 3), isocitrate dehydrogenase (4, 5), a-ketoglutarate dehydrogenase (6), succinyl-CoA synthetase (7), succinate dehydrogenase (8), fumarase (9), malate dehydrogenase (10), citrate malate antiporter (11,12), *cis*-aconitate decarboxylase *cad* (13), major facilitator superfamily protein *mfsA* (14, 16), P450 monooxygenase *cypC* (15), aconitate- δ -isomerase *adi1* (17), *trans*-aconitate decarboxylase *tad1* (18), P450 monooxygenase *cyp3* (20) and itaconate transport protein *itp1* (19, 20); Itaconate cluster of *U. maydis* (red) (C): UMAG_05074 (*cyp3*), UMAG_11229 (*rdol*), UMAG_05076 (*tad1*), UMAG_11777 (*itp1*), UMAG_11778 (*adi1*), UMAG_05079 (*mtt1*) and UMAG_05080 (*rial*). Pathway of *A. terreus* was adapted from Steiger *et al.* [25].

1.2.5.2 Itaconate production

To be competitive, the productivity of itaconate production should be $2.5 \text{ g L}^{-1} \text{ h}^{-1}$ [12], this is far from best published values, since *A. terreus* has a long fermentation time of up to 45 days [21, 110]. The morphology of *A. terreus* ranges from branched to densely mycelium masses [154] and efficient itaconate production is only achieved in a pellet form with a diameter smaller $< 0.5 \text{ mm}$ [23, 155, 156]. Thus, itaconate production is morphology-dependent in *A. terreus*. Hence, the control of morphology plays a major role in *A. terreus*; especially it is influenced by many factors. In contrast, most Ustilaginaceae such as *U. maydis* produces itaconate with a stable yeast-like growth behavior [95, 107, 137]. For many medium components like iron, zinc, calcium, cobalt, nickel and especially manganese ions it is reported that they influence the morphology of *A. terreus* above a specific concentration or even inhibit key enzymes involved in itaconate production [22, 147, 156-160]. This represents a hurdle to decrease production costs with second generation feedstock, such as (hemi)cellulosic fraction of wood, which contains a mixture of these elements. This causes additional costs since the substrate has to be pretreated and if necessary, to purified from the fermentation medium [157, 161]. Further, low pH values are necessary for mycelium growth, otherwise, no itaconate is produced. It is assumed that low pH values induce relevant enzymes for itaconate production [162]. Meanwhile, different pH strategies are established, resulting in different titers, rates, and yields [131, 147]. Currently, highest titer with 160 g L^{-1} is achieved under pH control at 3.4 in the production phase [132]. For purification usually, itaconate is crystallized by evaporation-crystallization systems. Different strategies were established to achieve high quality and purity of itaconate [161, 163-169]. To reduce costs and purification steps coming from by-product formations and impurities from substrates, reactive extraction can be used. Since *A. terreus* react sensitively against solvents, this method is in their infancy [107, 170]. Despite the drawbacks associated to the morphology of *A. terreus*, *A. terreus* has been asserting itself for 60 years as itaconate producing strain. Especially the fact that morphology is a burden to improve itaconate production, new organisms should be established featuring a robust non-filamentous phenotype that is insensitive towards feedstock impurities and thus allows itaconate production in an efficient way. In the past, members of the Ustilaginaceae have particularly proven themselves to be good organic acid producers [95]. Mainly because of their versatile range of value-added chemicals, they became interesting for the biotechnology industry [126, 171, 172]. Since most of the members of Ustilaginaceae are plant pathogens, they were mostly investigated in terms of pathogenicity. They mainly infect crops, such as maize, barley, corn, wheat, oats, sorghum, and sugar cane [173]. They are responsible for high crop losses in the agricultural industry and cause a great deal of economic damage. The most prominent member in terms of itaconate production is *U. maydis* [171]. *U. maydis* is a well-established model organism for studies of biotrophic plant-pathogen interaction [171, 174-176], cell biology, DNA repair, mRNA transport and molecular methods and techniques [177-180]. In 2006, the genome sequence was fully annotated which was the basis for further developments applying genetic engineering [181, 182] such as, FLP/FRT system [183], Golden Gate Cloning [184] and CRISPR/Cas9 system [185]. Further, strong and constitutive promoters (*Potef*, *Poma*) [186-188] and inducible promoters (*crg1*, *nar1*, *mig*, *prf1*) [189-191] were established and antibiotics (carboxin, hygromycin, nourseothricin, phleomycin, geneticin) with their corresponding resistance cassettes are available [182, 192-196]. This development also made it possible to establish *U. maydis* as an itaconate producer. The highest published titer for itaconate of 63 g L^{-1} so far was published by Geiser *et al.* [140]. However, especially its yeast-like growth behavior, resistance against osmotic pressure,

hydromechanical stress, impurities, and its tolerance against high product concentrations, give *Ustilago* a few advantages over *Aspergillus* [107, 171, 197]. Further, it can utilize several carbon sources such as, glucose, glycerol, xylose, xylan, CM-cellulose, and homogenized plant tissue [137, 171, 197-200]. So far *U. maydis* has not yet been able to assert itself against *Aspergillus*. Although *U. maydis* has so many advantages, reached titers were still low compared to *Aspergillus* and production was limited to pH values above 5. Lower pH values enable reduced base consumption, easier downstream processing, and autosterility, which help to reduce the costs [8, 201]. But also members of Ustilaginaceae such as *U. cynodontis* are pH-tolerant organisms and able to produce itaconate under low-pH conditions. [95]. Thus, *U. cynodontis* can be used as a pH-tolerant production strain. It is also resistance against osmotic pressure, impurities, and is tolerance against high product concentrations. Additionally, experience from *U. maydis* such as medium composition and fermentation condition can be transferred from *U. maydis* to *U. cynodontis*. However also, further improvement in *U. maydis* is possible, concerning the yield and the fermentation process, especially its yeast-like growth makes it favorable in large-scale fermentations [24, 140].

1.3 Scope and outline of this thesis

The overall aim of this thesis was to establish efficient itaconate production hosts by strain engineering and optimization of the fermentation process in the yeast-like *Ustilago maydis* and pH-tolerant *Ustilago cynodontis* to enable a sustainable and bio-ecological process. This chapter 1 is a general introduction and provides the necessary information for a bio-based industry and the importance of building block chemicals, especially of the organic acids in terms of market potential and applications. This includes advantages and disadvantages of itaconate production in *A. terreus*, *U. maydis* and *U. cynodontis* and their importance as microbial catalysts.

To enhance itaconate production in other Ustilaginaceae such as *U. cynodontis*, *U. xerochloe*, and *U. vertiveriae* responsible gene cluster for itaconate biosynthesis were investigated in 13 strains from seven species in chapter 3.1. The sequences of the gene cluster for itaconate synthesis were analyzed and compared to the cluster of *U. maydis*, and the phylogenetic relationship of the itaconate cluster transcription factor of Rial was investigated. The itaconate gene cluster of *U. cynodontis* was further investigated in chapter 3.3.

Chapter 3.2 investigates the roles of the extracellular and mitochondrial transporters which are involved in itaconate production in *U. maydis* and *A. terreus*. In complementation studies and systematic cultivation, it could be shown that involved transporters had different product affinities. This knowledge enabled us to boost itaconate production remarkably in production strains generated in chapter 3.3 and 3.5.

In chapter 3.3, the strong filamentously growing and pH-tolerant *U. cynodontis* was established as itaconate production strain. Since no molecular tools were available, they were established based on *U. maydis* plasmids and methods. After that morphological engineering was applied to modify the strong filamentous growth into stable yeast-like growth. Responsible genes for filamentous growth were determined by BLAST and compared to *U. maydis*. The deletion of these genes resulted in stable yeast-like growth under process-relevant conditions. For further enhancement of itaconate production in *U. cynodontis* by metabolic engineering, the clarification of the genes belonging to the itaconate cluster, which was annotated in chapter 3.1 was necessary. These findings allowed to increase *U. cynodontis* itaconate production up to 6.5-fold compared to the wildtype. Furthermore, first fermentation experiments confirmed stable yeast-like behavior in bioreactor systems.

In chapter 3.4, production strains that were generated in chapter 3.3 were further investigated in bioreactors. Itaconate production with *U. cynodontis* could be further improved by determination of the optimal pH value combined with process optimizations and different feeding strategies. Thereby titer, rate, and yield could be increased drastically for itaconate. In chapter 3.5, we could combine recently published metabolic engineering strategies with discovered morphological improvements from chapter 3.2 and 3.3 in *U. maydis*. This powerful combination led to the highest produced itaconate titer achieved in a biotechnological process. This thesis clearly demonstrates the potential of the pH-tolerant *U. cynodontis* and yeast-like *U. maydis* as itaconate production organisms. Building on previous works, significant increases were achieved, and it was confirmed that *Ustilago* is on the right track to make the itaconate production process more sustainable and cost-effective. Based on the results, further optimizations should be continued in the future in order to achieve the primary goal of an environmentally friendly and sustainable process.

Chapter 2

Material and methods

Partially published as:

Hamed Hosseinpour Tehrani, Apilaasha Tharmasothirajan, Elia Track, Lars M. Blank and Nick Wierckx. Engineering the morphology and metabolism of pH tolerant *Ustilago cynodontis* for efficient itaconic acid production. *Metabolic Engineering* (2019) 54, 293-300, <https://doi.org/10.1016/j.ymben.2019.05.004>

Hamed Hosseinpour Tehrani, Elena Geiser, Meike Engel, Sandra K. Hartmann, Abeer H. Hossain, Peter J. Punt, Lars M. Blank and Nick Wierckx. The interplay between transport and metabolism in fungal itaconic acid production. *Fungal Genetics and Biology* (2019) 125:45-52, <https://doi.org/10.1016/j.fgb.2019.01.011>.

Elena Geiser, Hamed Hosseinpour Tehrani, Svenja Meyer, Lars M. Blank and Nick Wierckx. Evolutionary freedom in the regulation of the conserved itaconate cluster *Rial* in related *Ustilaginaceae*. *Fungal Biology and Biotechnology* (2018) 5.14, <https://doi.org/10.1186/s40694-018-0058-1>.

Contributions:

This chapter was written by Hamed Hosseinpour Tehrani and reviewed by Lars M. Blank and Nick Wierckx.

2 Material and Methods

2.1 Plasmid cloning- and strain engineering

All strains that were used and created in this thesis are listed with their genotypes, their origin, and the internal institute number in Table 5. All Plasmids (instead of pETEF_CbxR_*At_mttA* and pETEF_CbxR_*At_mfsA*) were assembled by Gibson assembly [202] using the NEBbuilder HiFi DNA Assembly kit (New England Biolabs, Ipswich, MA, USA). Primers were ordered as unmodified DNA oligonucleotides from Eurofins Genomics (Ebersberg, Germany). As polymerase Q5 High-Fidelity Polymerase was used. Detailed information about utilized primers and plasmids are listed in Table 13 and Table 14. All assembled or ordered plasmids were subcloned into *E. coli* 10B from New England Biolab or *E. coli* Dh5 α and confirmed by PCR, restriction or sequencing. Standard cloning techniques for *E. coli* were performed according to Sambrook *et al.* [203].

To constitutively express the transporter genes *mttA* (ATEG_09970) and *mfsA* (ATEG_09972) in *Ustilago maydis*, these genes were synthesized *in vitro* (GeneArt Life Technologies, Regensburg, Germany). Since *U. maydis* tends to pre-maturely polyadenylate heterologous mRNA [204], the sequence was di-codon optimized via the dicodon optimizer (<http://dicodon-optimization.appspot.com/>). Repeats of ≥ 8 bp lengths were manually edited. The full synthetic sequences are shown in the appendix (D1 and D2). The synthesized genes were subcloned into vector pETEF_GFP_CBX_Q018 [186, 188] using BamHI and NotI restriction sites resulting in the plasmids pETEF_CbxR_*At_mttA* and pETEF_CbxR_*At_mfsA* (Figure 51). The constructs were confirmed by sequencing by Life Technologies, Germany.

For the deletion of genes in Ustilaginaceae, homologous recombination with 1,000 bp flanking regions (F1, F2) and a hygromycin cassette were used. In some cases, constructs had FRT-sites additionally and were recycled afterward by Flp-Frt recombination with pFLPexpC [183] and are specified in the corresponding chapters. Marker recycled strains are indicated with a superscript ^r. For transformation, preparation of protoplasts and isolation of genomic DNA of *Ustilago maydis*, *U. cynodontis*, *U. vetiveriae*, *U. xerochloae*, *P. tsukubaensis*, *P. hubeiensis* and *S. iseilematis* protocols according to Brachmann *et al.* [182] were used. For random or site-specific integration of overexpression constructs into the genome of the different Ustilaginaceae, plasmids (P_{etef} *Pt_rial*, P_{etef} *Si_rial*, P_{etef} *Uc_rial*, P_{etef} *Umag_rial*-cbx, pETEF_CbxR_*At_mttA*, pETEF_CbxR_*At_mfsA*, pNATIV_*Uc_rial* and pUma43) were linearized by SspI except of P_{etef} *Pt_rial* which was linearized by BsrGI and pETEF_hyg_*mttA* which was linearized by XmnI. For exchange of the promoter of *rial* CRISPR/Cas9 system was used according to [185] and sgRNA has been selected online with [http://www.e-crisp.org/E-CRISP/\[205\]](http://www.e-crisp.org/E-CRISP/[205]). A donor-template was used to exchange the native promoter with the strong and constitutive P_{etef}. General integration was verified by PCR and sequencing, and single or multiple integrations by southern blot.

Table 5. Ustilaginaceae used in this study.

Strain designation	Resistance	Reference/GenBank/	iAMB
<i>Ustilago maydis</i> DSM17144 (<i>Ustilago maydis</i> MB215)	wild type	AACP00000000 [206]	2229
<i>Ustilago maydis</i> DSM17144 P _{etef} <i>Umag_rial</i>	cbx ^R	this study	2366
<i>Ustilago maydis</i> DSM17144 P _{etef} <i>Uc_rial</i>	cbx ^R	this study	4325
<i>Ustilago maydis</i> DSM17144 P _{etef} <i>Pt_rial</i>	cbx ^R	this study	4324
<i>Ustilago maydis</i> DSM17144 P _{etef} <i>Si_rial</i>	cbx ^R	this study	4327
<i>Ustilago maydis</i> DSM17144 Δ <i>Umag_rial</i>	hyg ^R	[207]	2112
<i>Ustilago maydis</i> DSM17144 Δ <i>Umag_rial</i> P _{etef} <i>Umag_rial</i>	hyg ^R , cbx ^R	[207]	2374
<i>Ustilago maydis</i> DSM17144 Δ <i>Umag_rial</i> P _{etef} <i>Uc_rial</i>	hyg ^R , cbx ^R	this study	4302
<i>Ustilago maydis</i> DSM17144 Δ <i>Umag_rial</i> P _{etef} <i>Pt_rial</i>	hyg ^R , cbx ^R	this study	4300
<i>Ustilago maydis</i> DSM17144 Δ <i>Umag_rial</i> P _{etef} <i>Si_rial</i>	hyg ^R , cbx ^R	this study	4305
<i>Ustilago maydis</i> ATCC22892	wild type	LYOO00000000	2162
<i>Ustilago maydis</i> ATCC22904	wild type	LZQT00000000	2172
<i>Ustilago maydis</i> ATCC22901	wild type	LZNJ00000000	2169
<i>Ustilago maydis</i> ATCCbA22899	wild type	LYZD00000000	2167
<i>Ustilago maydis</i> AB33P5Δ	wild type	[188]/ LZQU00000000	3260
<i>Ustilago maydis</i> AB33P5Δ P _{etef} <i>Umag_rial</i>	cbx ^R	this study	3562
<i>Ustilago maydis</i> AB33P5Δ P _{etef} <i>Uc_rial</i>	cbx ^R	this study	4350
<i>Ustilago maydis</i> AB33P5Δ P _{etef} <i>Pt_rial</i>	cbx ^R	this study	4348
<i>Ustilago maydis</i> AB33P5Δ P _{etef} <i>Si_rial</i>	cbx ^R	this study	4353
<i>Ustilago vetiveriae</i> CBS131474	wild type	MAIM00000000	2220
<i>Ustilago vetiveriae</i> CBS131474 P _{etef} <i>Umag_rial</i>	cbx ^R	[208]	3550
<i>Ustilago vetiveriae</i> CBS131474 P _{etef} <i>Uc_rial</i>	cbx ^R	this study	4314
<i>Ustilago vetiveriae</i> CBS131474 P _{etef} <i>Pt_rial</i>	cbx ^R	this study	4312
<i>Ustilago vetiveriae</i> CBS131474 P _{etef} <i>Si_rial</i>	cbx ^R	this study	4317
<i>Ustilago xerochloae</i> CBS131476	wild type	MAIN00000000	2210
<i>Ustilago xerochloae</i> CBS131476 P _{etef} <i>Umag_rial</i>	cbx ^R	this study	3556
<i>Ustilago xerochloae</i> CBS131476 P _{etef} <i>Uc_rial</i>	cbx ^R	this study	4321
<i>Ustilago xerochloae</i> CBS131476 P _{etef} <i>Pt_rial</i>	cbx ^R	this study	4319
<i>Ustilago xerochloae</i> CBS131476 P _{etef} <i>Si_rial</i>	cbx ^R	this study	4323
<i>Ustilago cynodontis</i> CBS131467	wild type	LZQV00000000	2217
<i>Ustilago cynodontis</i> CBS131467 P _{etef} <i>Umag_rial</i>	cbx ^R	this study	4166
<i>Ustilago cynodontis</i> CBS131467 P _{etef} <i>Uc_rial</i>	cbx ^R	this study	4308
<i>Ustilago cynodontis</i> CBS131467 P _{etef} <i>Pt_rial</i>	cbx ^R	this study	4306
<i>Ustilago cynodontis</i> CBS131467 P _{etef} <i>Si_rial</i>	cbx ^R	this study	4310
<i>Ustilago cynodontis</i> NBRC9727	wild type	LZZZ00000000	2706
<i>Ustilago cynodontis</i> NBRC9727 P _{etef} <i>Umag_rial</i>	cbx ^R	this study	4164
<i>Ustilago cynodontis</i> NBRC9727 P _{etef} <i>Uc_rial</i>	cbx ^R	this study	4338
<i>Ustilago cynodontis</i> NBRC9727 P _{etef} <i>Pt_rial</i>	cbx ^R	this study	4334
<i>Ustilago cynodontis</i> NBRC9727 P _{etef} <i>Si_rial</i>	cbx ^R	this study	4335
<i>Pseudozyma tsukubaensis</i> NBRC1940	wild type	MAIP00000000	2710
<i>Pseudozyma tsukubaensis</i> NBRC1940 P _{etef} <i>Umag_rial</i>	cbx ^R	this study	4169
<i>Pseudozyma tsukubaensis</i> NBRC1940 P _{etef} <i>Uc_rial</i>	cbx ^R	this study	4340
<i>Pseudozyma tsukubaensis</i> NBRC1940 P _{etef} <i>Pt_rial</i>	cbx ^R	this study	4339
<i>Pseudozyma hubetiensis</i> NBRC105055	wild type	MAIO00000000	2698
<i>Pseudozyma hubetiensis</i> NBRC105055 P _{etef} <i>Umag_rial</i>	cbx ^R	this study	4162
<i>Pseudozyma hubetiensis</i> NBRC105055 P _{etef} <i>Uc_rial</i>	cbx ^R	this study	4330
<i>Pseudozyma hubetiensis</i> NBRC105055 P _{etef} <i>Pt_rial</i>	cbx ^R	this study	4328
<i>Pseudozyma hubetiensis</i> NBRC105055 P _{etef} <i>Si_rial</i>	cbx ^R	this study	4332
<i>Sporisorium iselematis-ciliati</i> BRIP60887a	wild type	MJEU00000000	2838

<i>Sporisorium isilematis-ciliati</i> BRIP60887aP _{etef} Umag _{ria1}	cbx ^R	this study	4170
<i>Sporisorium isilematis-ciliati</i> BRIP60887a P _{etef} Uc _{ria1}	cbx ^R	this study	4344
<i>Sporisorium isilematis-ciliati</i> BRIP60887a P _{etef} Pt _{ria1}	cbx ^R	this study	4342
<i>Sporisorium isilematis-ciliati</i>	cbx ^R	this study	4347
<i>Ustilago maydis</i> DSM17144 ΔUm _{mtt1}	hyg ^R	[139]	2110
<i>Ustilago maydis</i> DSM17144 ΔUm _{mtt1} +P _{etef} Um _{mtt1}	hyg ^R , cbx ^R	[207]	2318
<i>Ustilago maydis</i> DSM17144+P _{etef} Um _{mtt1}	cbx ^R	this study	2364
<i>Ustilago maydis</i> DSM17144 ΔUm _{mtt1} +P _{etef} At _{mttA}	hyg ^R , cbx ^R	this study	3092
<i>Ustilago maydis</i> DSM17144+P _{etef} At _{mttA}	cbx ^R	this study	3223
<i>Ustilago maydis</i> DSM17144 ΔUm _{itp1}	hyg ^R ,	[139]	2329
<i>Ustilago maydis</i> DSM17144 ΔUm _{itp1} +P _{etef} Um _{itp1}	hyg ^R , cbx ^R	[207]	2312
<i>Ustilago maydis</i> DSM17144+P _{etef} Um _{itp1}	cbx ^R	[139]	2360
<i>Ustilago maydis</i> DSM17144 ΔUm _{itp1} +P _{etef} At _{mfsA}	hyg ^R , cbx ^R	this study	3150
<i>Ustilago maydis</i> DSM17144+P _{etef} At _{mfsA}	cbx ^R	this study	3153
<i>Ustilago cynodontis</i> NBRC9727 + pNEBUC	cbx ^R	this study	3709
<i>Ustilago cynodontis</i> NBRC9727 + pSMUT	cbx ^R	this study	3712
<i>Ustilago cynodontis</i> NBRC9727 + pNEBUN	cbx ^R	this study	3710
<i>Ustilago cynodontis</i> NBRC9727 + pNEBUP	cbx ^R	this study	3711
<i>Ustilago cynodontis</i> NBRC9727 + pUMA43	cbx ^R	this study	5240
<i>Ustilago cynodontis</i> NBRC9727 Δras2	hyg ^R	this study	4135
<i>Ustilago cynodontis</i> NBRC9727 Δfuz7	hyg ^R	this study	4136
<i>Ustilago cynodontis</i> NBRC9727 Δubc3	hyg ^R	this study	4137
<i>Ustilago cynodontis</i> NBRC9727 Δfuz7 ^r		this study	4228
<i>Ustilago cynodontis</i> NBRC9727 Δmtt1	hyg ^R	this study	4513
<i>Ustilago cynodontis</i> NBRC9727 Δitp1	hyg ^R	this study	4514
<i>Ustilago cynodontis</i> NBRC9727 Δfuz7 ^r Δcyp3	hyg ^R	this study	4470
<i>Ustilago cynodontis</i> NBRC9727 Δfuz7 ^r Δcyp3 ⁱ		this study	4595
<i>Ustilago cynodontis</i> NBRC9727 Δfuz7 ^r Δria1	hyg ^R	this study	4482
<i>Ustilago cynodontis</i> NBRC9727 Δfuz7 ^r Δria1 ⁱ		this study	4596
<i>Ustilago cynodontis</i> NBRC9727 Δfuz7 ^r Δcyp3 ⁱ P _{ria1ria1}	cbx ^R	this study	4852
<i>Ustilago cynodontis</i> NBRC9727 Δfuz7 ^r Δcyp3 ⁱ P _{etefmttA} P _{ria1ria1}	cbx ^R , hyg ^R	this study	4853
<i>Ustilago maydis</i> DSM17144 Δcyp3 P _{etefria1}	cbx ^R , hyg ^R	[140]	3025
<i>Ustilago maydis</i> DSM17144 Δcyp3		Joh. B. unpublished	3785
<i>Ustilago maydis</i> DSM17144 Δcyp3 ΔP _{ria1::P_{etef}#1}		this study	4174
<i>Ustilago maydis</i> DSM17144 Δcyp3 ΔP _{ria1::P_{etef}#2}		this study	4175
<i>Ustilago maydis</i> DSM17144 Δcyp3 Δfuz7 ΔP _{ria1::P_{etef}}	hyg ^R	this study	4186
<i>Ustilago maydis</i> DSM17144 Δcyp3 ΔP _{ria1::P_{etef}} Δfuz7 P _{etefmttA}	cbx ^R , hyg ^R	this study	4287

2.2 Culture conditions

E. coli strains were grown in medium containing 10 g L⁻¹ peptone, 5 g L⁻¹ sodium chloride, 5 g L⁻¹ glucose. Ustilaginaceae were grown in YEPS medium containing, 10 g L⁻¹ yeast extract, 10 g L⁻¹ peptone, and 10 g L⁻¹ sucrose.

Growth and production experiments of Ustilaginaceae were performed using screening medium according to Geiser *et al.* [95] with varying C-source concentrations, C-sources, supplements, buffer concentrations of 2-(N-morpholino) ethanesulfonic acid (MES), and CaCO₃ as indicated. This medium further contained various concentrations of NH₄Cl as indicated, 0.2 g L⁻¹ MgSO₄·7H₂O, 0.01 g L⁻¹ FeSO₄·7H₂O, 0.5 g L⁻¹ KH₂PO₄, 1 mL L⁻¹ vitamin solution, and 1 mL L⁻¹ trace element solution. The vitamin solution contained (per liter) 0.05 g D-biotin, 1 g D-calcium

pantothenate, 1g nicotinic acid, 25 g myo-inositol, 1g thiamine hydrochloride, 1g pyridoxol hydrochloride, and 0.2 g para-aminobenzoic acid. The trace element solution contained (per liter) 15 g EDTA, 0.45 g of $\text{ZnSO}_4 \cdot 7\text{H}_2\text{O}$, 0.10 g of $\text{MnCl}_2 \cdot 4\text{H}_2\text{O}$, 0.03g of $\text{CoCl}_2 \cdot 6\text{H}_2\text{O}$, 0.03 g of $\text{CuSO}_4 \cdot 5\text{H}_2\text{O}$, 0.04 g of $\text{Na}_2\text{MoO}_4 \cdot 2\text{H}_2\text{O}$, 0.45 g of $\text{CaCl}_2 \cdot 2\text{H}_2\text{O}$, 0.3 g of $\text{FeSO}_4 \cdot 7\text{H}_2\text{O}$, 0.10 g of H_3BO_3 , and 0.01 g of KI. Shaking cultures of Ustilaginaceae and mutants strains were performed in System Duetz[®] (24 well plates, Enzymscreen, Netherlands) with a filling volume of 1.5 mL ($d = 50$ mm, $n = 300$ rpm, $T = 30$ °C and $\Phi = 80$ %) or in 500 mL shaking flasks with a filling volume of 50 mL ($d = 25$ mm, $n = 200$ rpm, $T = 30$ °C and $\Phi = 80$ %) as indicated. Cultures were inoculated to a final OD_{600} of 0.5 with cells from an overnight culture in 50 mL screening medium containing 50 g L^{-1} glucose and 100 mM MES buffer. If System Duetz[®] was used [209], cultures were parallel inoculated into multiple plates, and for each sample point, a complete plate was taken as a sacrificial sample in order to ensure continuous oxygenation. For repeated batch cultivation in shake flask cultivation was performed in screening medium according to Geiser *et al.* [95] containing 33 g L^{-1} CaCO_3 and 50 g L^{-1} glucose. The cultures were centrifuged at $1,473 \text{ g}$ for 5 min at 30 °C with a Heraeus Megafuge 16R (Thermo Scientific) and a TX-400 rotor (Thermo Scientific). For subsequent cultivation, the cells were re-suspended in screening medium containing 25 g L^{-1} CaCO_3 without NH_4Cl and 50 g L^{-1} glucose.

Controlled batch cultivations in chapter 3.2 were performed in a New Brunswick BioFlo[®] 110 (Eppendorf, Germany). In chapter 3.3, 3.4, and 3.5. New Brunswick BioFlo[®]/CelliGen[®] 115 was used (Eppendorf, Germany). The Eppendorf BioFlo[®] 120 bioprocess control station (Eppendorf, Germany) was used in combination with the online glucose measurement system from Trace Analytics (Trace Analytics, Germany) in chapter 0 as indicated. A total volume of 1.3 L and a working volume of 0.5 L were used. For fermentations with CaCO_3 or if the glucose online measurement system of Trace Analytics was used a total volume of 2.0 L and a starting volume of 1.0 L was used. All cultivations were performed in batch medium according to Geiser *et al.* [140] containing 0.2 g L^{-1} $\text{MgSO}_4 \cdot 7\text{H}_2\text{O}$, 0.01 g L^{-1} $\text{FeSO}_4 \cdot 7\text{H}_2\text{O}$, 0.5 g L^{-1} KH_2PO_4 , 1 g L^{-1} yeast extract (Merck Millipore, Germany), 1 mL L^{-1} vitamin solution, 1 mL L^{-1} trace element solution and varying concentrations of glucose and NH_4Cl , as indicated. During cultivation, pH 6 was maintained by an automatic addition of 10 M NaOH or pH was kept above 6.2 by manual addition of CaCO_3 , as indicated. The dissolved oxygen tension (DOT) was kept constant at approximately 80 % air saturation by automatic adjustment of the stirring rate (700–1200 rpm), otherwise stirring rate was constant at 1000 or 1200 rpm, as indicated. The bioreactor was aerated with an aeration rate of 1 L min^{-1} (2 vvm) for a working volume of 0.5 L or 2 L min^{-1} (1 vvm) for total volume of 2 L, while evaporation was limited by sparging the air through a water bottle. The temperature was set at 30°C. The bioreactor was inoculated to a final OD_{600} of 0.75 with cells from an overnight culture in 50 mL screening medium containing 50 g L^{-1} glucose and 100 mM MES buffer.

For repeated-batch in a bioreactor chapter 3.4, the culture was centrifuged for 5 min to 20 min at 80 g and afterward re-suspended in 0.5 L batch medium without NH_4Cl and 0.5 g L^{-1} yeast extract.

2.3 Analytical methods

Cell densities were measured by determining the absorption at 600 nm with an Ultraspec 10 Cell Density Meter (Amersham Biosciences, Chalfont St Giles, UK).

To measure the cell density non-invasively the cell growth quantifier (CGQ) was used (Aquila biolabs GmbH, Germany) and every 15. measuring point is shown. For CDW determination 1 mL culture broth was centrifuged at maximum speed (Heraeus Megafuge 16R, TX-400 rotor, Thermo Scientific) and the pellet was dried (Scan Speed 40 lyophilizer, Labogene ApS) for 24 h at 38 °C

and weighed afterward.

For microscopy the OD_{600} of the culture was adjusted to 5 with 0.9 % NaCl. Differential interference contrast (DIC) microscopy was performed with a Leica DM500 light microscope (Leica Microsystems). Images were recorded with a Leica ICC50 digital microscope camera (Leica Microsystems). Images were taken at 100-, 630-, and 1000-fold magnification. The cell morphology was analyzed by microscopy at different time points in all cultivations.

The ammonium concentration in the culture supernatant was measured by a colorimetric method, according to Willis *et al.*[210] using salicylate and nitroprusside.

Products and substrates in the supernatants were analyzed in a DIONEX UltiMate 3000 High Performance Liquid Chromatography System (Thermo Scientific, Germany) with an ISERA Metab AAC column 300×7.8 mm column (ISERA, Germany) with a DIONEX UltiMate 3000 Variable Wavelength Detector set to 210 nm and a refractive index detector SHODEX RI-101 (Showa Denko Europe GmbH, Germany) or in a Beckmann Coulter System Gold High Performance Liquid Chromatography (Beckmann Coulter GmbH, Germany) with an Organic Acid Resin 300×8 mm column (CS-Chromatography, Germany), a differential refractometer LCD 201 (MELZ, Germany) and UV/VIS detector (Thermo Fischer, Germany). As solvent 5 mM H_2SO_4 with a flow rate of 0.6 mL min^{-1} and a temperature of 40°C was used. All samples prepared with HCl were filtered with Acrodisc® Syringe Filters (GHP, $0.20 \mu\text{m}$, \varnothing 13 mm) and the rest with Rotilabo® syringe filters (CA, $0.20 \mu\text{m}$, \varnothing 15 mm) and afterward diluted with 5 mM H_2SO_4 . All components were identified via retention time and UV/RI quotient compared to corresponding standards.

Synthesized (*S*)-2-hydroxyparaconate (purity $\sim 70\%$) was used as the HPLC standard for quantification and hence the indicated (*S*)-2-hydroxyparaconate values should be taken as rough estimates only [140]. Since no standards of itatartarate are commercially available, this compound was analyzed relatively based on HPLC peak area ($\text{mAU} \cdot \text{min}$) using the UV detector.

All experiments were performed in four replicates unless stated. Otherwise, occasional analytical outliers were excluded. Error indicates the deviation from the mean for $n = 2$, if $n > 2$ error indicates the standard error of the mean. In chapter 3.1 statistical analysis was performed using unequal variances t-test with unilateral distribution (P values: < 0.01 were considered significant and indicated in figures with *). In chapter 3.2, Statistical differences between batch cultures in System Duetz plates were determined by 1-way ANOVA with Turkey HSD for Post-Hoc analysis ($p < 0.05$). In chapter 3.3, 3.4, and 3.5 statistical significance was assessed by t-test (two-tailed distribution, heteroscedastic, $p \leq 0.05$).

2.4 Genome sequencing

Genomic DNA was isolated by standard phenol-chloroform extraction [211]. Eurofins Genomics (Ebersberg, Germany) created the library using the NEBNext® Ultra DNA Library Prep Kit for Illumina® (Art No E7370), and sequenced the library using an Illumina HiSeq2500 machine with TruSeq SBS kit v3 both according to manufacturer's instructions. The sequencing mode was 1x100, and the processing used the HiSeq Control software 2.0.12.0 RTA 1.17.21.3 bcl2fastq-1.8.4. A Quality check of the sequence data was performed with FastQC (Version 0.11.2). The SPAdes-3.7.0-Linux pipeline was used for *de novo* genome assembly of single-read libraries and read error or mismatch correction including BayesHammer, IOnHammer, SPAdes, MismatchCorrector, dipSPAdes, and truSPAdes. The k-mer size was determined to 55 using VelvetOptimiser Version 2.2.5. The Whole Genome Shotgun sequences have been deposited in DDBJ/ENA/GenBank. Their accession numbers are listed in Table 5.

2.5 Phylogenetic analyses

The evolutionary history of itaconate cluster DNA sequences was inferred using the Neighbor-Joining method [212] after alignment via ClustalW algorithm with the MEGA 7: Molecular Evolutionary Genetics Analysis version 7.0 for bigger datasets Alignment Explorer. The optimal tree with the sum of branch length = 1.88603985 is shown. The tree is drawn to scale, with branch lengths in the same units as those of the evolutionary distances used to infer the phylogenetic tree. The evolutionary distances were computed using the Maximum Composite Likelihood method [213] and are in the units of the number of base substitutions per site. The analysis involved 13 nucleotide sequences. All positions containing gaps and missing data were eliminated. There were a total of 10874 positions in the final dataset. Evolutionary analyses were conducted in MEGA7 [214].

For the phylogenetic tree of Ria1, protein sequences were aligned via ClustalW (codon) algorithm with MEGA 7 [214]. The evolutionary history was inferred using the Neighbor-Joining method [212]. The optimal tree with the sum of branch length = 2.49320505 is shown. The tree is drawn to scale, with branch lengths in the same units as those of the evolutionary distances used to infer the phylogenetic tree. The evolutionary distances were computed using the Poisson correction method [215] and are in the units of the number of amino acid substitutions per site. The analysis involved 13 amino acid sequences. All positions containing gaps and missing data were eliminated. There were a total of 269 positions in the final dataset. Evolutionary analyses were conducted in MEGA7 [214].

Chapter 3

Results

Chapter 3.1

Evolutionary freedom in the regulation of the conserved itaconate cluster Ria1 in related Ustilaginaceae

Partially published as:

Elena Geiser, Hamed Hosseinpour Tehrani, Svenja Meyer, Lars M. Blank and Nick Wierckx. Evolutionary freedom in the regulation of the conserved itaconate cluster Ria1 in related Ustilaginaceae. Fungal Biology and Biotechnology (2018) 5.14, <https://doi.org/10.1186/s40694-018-0058-1>.

Contributions

Elena Geiser and Hamed Hosseinpour Tehrani contributed equally to this manuscript. Nick Wierckx, Lars M. Blank conceived the project. Elena Geiser and Hamed Hosseinpour Tehrani designed experiments and analyzed results. Elena Geiser wrote the manuscript with the help of Hamed Hosseinpour Tehrani. Hamed Hosseinpour Tehrani and Svenja Meyer generated overexpression strains. Elena Geiser performed cultivation experiments and analytics.

3 Results

3.1 Evolutionary freedom in the regulation of the conserved itaconate cluster *Ria1* in related Ustilaginaceae

3.1.1 Abstract

Itaconate is getting growing biotechnological significance, due to its use as a platform compound for the production of bio-based polymers, chemicals, and novel fuels. Currently, *Aspergillus terreus* is used for its industrial production. The Ustilaginaceae family of smut fungi, especially *Ustilago maydis*, has gained biotechnological interest, due to its ability to naturally produce this dicarboxylic acid. The unicellular, non-filamentous growth form makes these fungi promising alternative candidates for itaconate production. Itaconate production was also observed in other Ustilaginaceae species such as *U. cynodontis*, *U. xerochloae*, and *U. vetiveriae*. The investigated species and strains varied in a range of 0 to 8 g L⁻¹ itaconate. The genes responsible for itaconate biosynthesis are not known for these strains and therefore not characterized to explain this variability. Itaconate production of 13 strains from 7 species known as itaconate producers among the family Ustilaginaceae were further characterized. The sequences of the gene cluster for itaconate synthesis were analyzed by a complete genome sequencing and comparison to the annotated itaconate cluster of *U. maydis*. Additionally, the phylogenetic relationship and inter-species transferability of the itaconate cluster transcription factor *Ria1* was investigated in detail. Doing so, itaconate production could be activated or enhanced by overexpression of *Ria1* originating from a related species, showing their narrow phylogenetic relatedness.

3.1.2 Introduction

Secondary metabolites are organic, naturally produced, bioactive compounds with low molecular weight, that are produced by fungi, bacteria, and plants via pathways not belonging to the primary metabolism of this organism [216, 217]. In 2000, a literature survey identified more than 23,000 already discovered secondary metabolites mainly from the fungal kingdom [217, 218]. Closely related species usually produce related compounds, and each compound is produced in a highly-narrowed taxonomy [216, 219]. Genes coding for the biosynthesis of secondary metabolites is usually co-localized in a gene cluster with a size of approximately over 10,000 bp depending on the complexity of the metabolite and regions of non-coding base pairs of up to 2000 bp between the coding genes [216, 220, 221]. In cases of polyketide synthases, these regions are more extended [222]. These clusters contain genes coding for corresponding biosynthesis enzymes and transporters, regulatory proteins like transcription factors, and optionally modifying enzymes. Secondary metabolite clusters are often controlled by a complex regulatory network [223]. Several levels of regulation exist, which allow the organism to respond to various environmental influences. Transcription of these clusters can be regulated either by specific/narrow-domain or by global/broad-domain transcription factors or regulators or a combination thereof. Alternatively, regulation can be chromatin-mediated by histone acetylation or methylation [223]. Itaconate and its lactone (*S*)-2-hydroxyparaconate are examples of secondary metabolites. Itaconate is produced by fungi like *Aspergillus terreus* and *Ustilago maydis*, but also by less well-known Ustilaginaceae species, such as *Ustilago cynodontis*, *Ustilago vetiveriae*, and *Ustilago xerochloae* [95, 108, 126, 208]. Itaconate has industrial applications as a co-monomer, for example, in the production of acrylonitrile-butadiene-styrene and acrylate latexes in the paper and architectural coating industries [110]. According to an independent evaluation report of the U.S. Department of Energy (DoE) in 2004 [12], itaconate was assigned to be among the top 12 building

blocks with a high biotechnological potential, enabling a conversion into a range of new interesting molecules such as 2-or 3-methyltetrahydrofuran with applications as novel biofuels [224, 225]. Recent studies showed that genes for the biosynthesis of itaconate are co-localized in the genome and co-regulated in *U. maydis* [139], and therefore fulfilling the main criteria to be a secondary metabolite. *U. maydis*' itaconate cluster (GenBank: KT852988.1) contains two itaconate biosynthesis genes *UMAG_tad1* and *UMAG_ad1* encoding a *trans*-aconitate decarboxylase (Tad1) and an aconitate- δ -isomerase (Adi1), and two transporter genes *UMAG_itp1* and *UMAG_mtt1* encoding an itaconate transport protein (Itp1) and a mitochondrial tricarboxylate transporter (Mtt1), respectively (Figure 9). Their expression is co-regulated by the transcriptional regulator Ria1, also encoded in this cluster, which is considered as an itaconate cluster specific/narrow domain transcription factor, triggering the transcription of the itaconate biosynthesis genes [139]. Overexpression of *UMAG_ria1* upregulated the expression of biosynthesis core-cluster genes and transporters [139]. Additionally, the (*S*)-2-hydroxyparaconate biosynthesis gene *UMAG_cyp3* encoding the cytochrome P450 family three monooxygenase Cyp3 and *UMAG_rdo1* encoding a putative ring-cleaving dioxygenase is adjacent to the itaconate gene cluster of *U. maydis*, the former of which converts itaconate to (*S*)-2-hydroxyparaconate [140]. Further, it was reported by Guevarra and Tabuchi that (*S*)-2-hydroxyparaconate is converted to itatartarate by a lactonase [126, 136]. *UMAG_cyp3* and *UMAG_rdo1* are not part of the core cluster and not directly upregulated by overexpression of *UMAG_ria1* [139]. However, all itaconate cluster genes, including the two adjacent to the core cluster, *UMAG_cyp3*, and *UMAG_rdo1*, are strongly upregulated during teliospore formation in the late biotrophic growth stage during plant colonization [226-228].

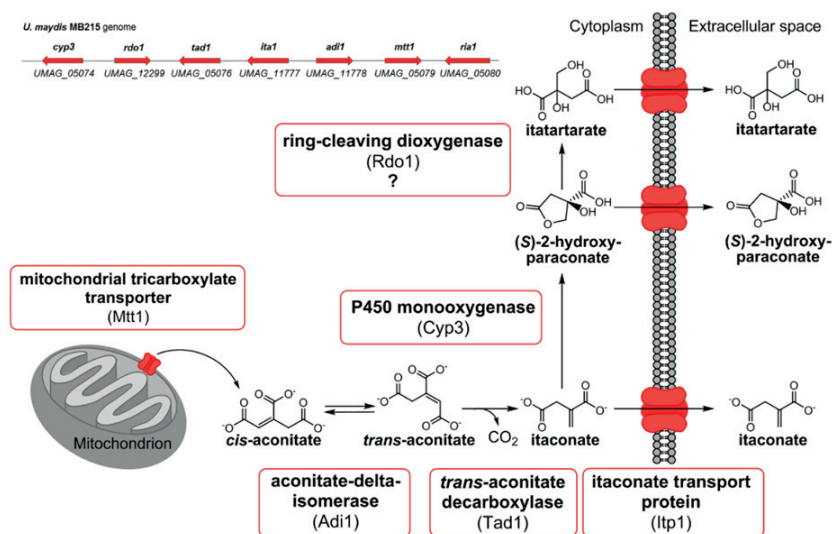


Figure 9. Proposed intracellular organization of the (S)-2-hydroxyparaconate biosynthesis pathway in *U. maydis*. *Cis*-aconitate is secreted by the mitochondrial tricarboxylate transporter Mtt1. In the cytosol *cis*-aconitate is converted into itaconate via the intermediate *trans*-aconitate. Itaconate can be further converted to (S)-2-hydroxyparaconate by Cyp3. (S)-2-hydroxyparaconate might be converted to itatartarate with the help of Rdo1. Secretion of itaconate and possibly (S)-2-hydroxyparaconate and itatartarate into the medium is mediated by the major facilitator Itp1. Updated pathway from Geiser *et al.*, 2016 [140].

The number of so far undiscovered secondary metabolites produced by enzymes encoded by cryptic or orphan gene clusters is innumerable high [229, 230]. However, the availability of numerous whole fungal genome sequences and *in silico* gene prediction by bioinformatic algorithms, such as SMURF [231], MiBiG [232], antiSMASH [233], and FungiFun [234], allow the identification of these cryptic gene clusters. These bioinformatic tools enable ‘genome mining’ via comparison of protein sequence and structure homology. Traditional ways of activating the expression of secondary metabolites clusters include the variation in the cultivation conditions, such as medium, pH, temperature, aeration, or light, or co-cultivation with other microbes to simulate the natural expression conditions [223]. Often these physiological or ecological triggers are not sufficient to activate these clusters, and therefore, several strategies have been developed to induce undiscovered silent secondary metabolite cluster [223]. The most prominent strategies are genetic engineering approaches: the overexpression of a cluster-specific transcription factor gene allowing the increased expression of the whole cluster [229]. In this case, the overexpression of the enzymes encoded within the cluster leads to various products, a potential challenge for natural product production [229]. Also besides, the endogenous promoters of secondary metabolism biosynthesis genes can be exchanged for strong inducible or constitutive promoters or global regulators can be overexpressed or deleted. A prominent example of the activation of a silent gene cluster is the overexpression of the transcriptional regulator gene *apdR* in *Aspergillus nidulans*, which induced the expression of all cluster genes, leading to the discovery of the cytotoxic aspyridones [229]. Itaconate production is naturally induced by nitrogen limitation in *U. maydis* and was also observed in other related Ustilaginaceae species such as *U. cynodontis*,

U. xerochloae, *U. vetiveriae* that show high potential to be promising and effective itaconate producers [95, 208, 235]. However, the investigated species and strains varied in their product spectra and the amount of secreted product. Among the species, individual strains of *U. maydis* differed profoundly in their itaconate and (S)-2-hydroxyparaconate production [95]. Some of the species investigated, for example *U. vetiveriae* strain CBS 131474, produced itaconate or (S)-2-hydroxyparaconate only with glycerol as carbon source. Also, itaconate production varied depending on extracellular pH. While in wild type *U. maydis* itaconate production is only possible in the pH-range of 5 to 7, *U. cynodontis* strains also produce itaconate at pH values below 3. The genes responsible for itaconate biosynthesis and how they are regulated to explain this variation in production levels and environmental inputs are not known for these specific strains.

In the current study, 13 itaconate producers of the Ustilaginaceae family were further characterized by their itaconate cluster sequence-function relationship. The itaconate gene clusters of these strains were identified by genome sequencing [235] and comparison to the annotated itaconate cluster of *U. maydis* strain MB215. To explore the evolutionary conservation of regulation of the itaconate cluster in respect to itaconate production by members of the Ustilaginaceae family, the phylogenetic relationship and inter-species transferability of the itaconate cluster transcription factor Rial1 was investigated. Itaconate production could be activated or enhanced by overexpression of Rial1 originating from related species. This is the first time that activation of silent itaconate clusters by overexpression of a cluster-specific transcription factor in Ustilaginaceae species other than *U. maydis* is shown.

3.1.3 Results and discussion

3.1.3.1 *Variation in itaconate and (S)-2-hydroxyparaconate production among Ustilaginaceae*

Previous studies showed a high variation in natural itaconate production among related Ustilaginaceae species cultured on glucose and glycerol as carbon sources [95, 208]. Besides their varying amounts of product and product spectrum, they also differed in their efficiency of carbon utilization. Some of the species produced itaconate only on a single carbon source like glycerol or glucose. These differences motivated us to investigate itaconate and derivatives production on glucose and glycerol in more detail (Figure 10 and Figure 11). *U. maydis* Δ *Umag_rial* was used as a negative control since the transcriptional regulator gene *rial* is deleted and therefore itaconate production abolished. In *U. maydis* strain AB33P5 Δ five extracellular proteases are deleted [188]. With these deletions, the strain is well suited for the secretion of heterologous or intrinsic extracellular biomass degrading CAZymes. This strain would be an optimal candidate for the synthesis of itaconate or other valuable chemicals directly from biomass-derived substrates[236]. However, it does not produce itaconate, and the lack of extracellular proteases significantly reduces the growth rate of this mutant.

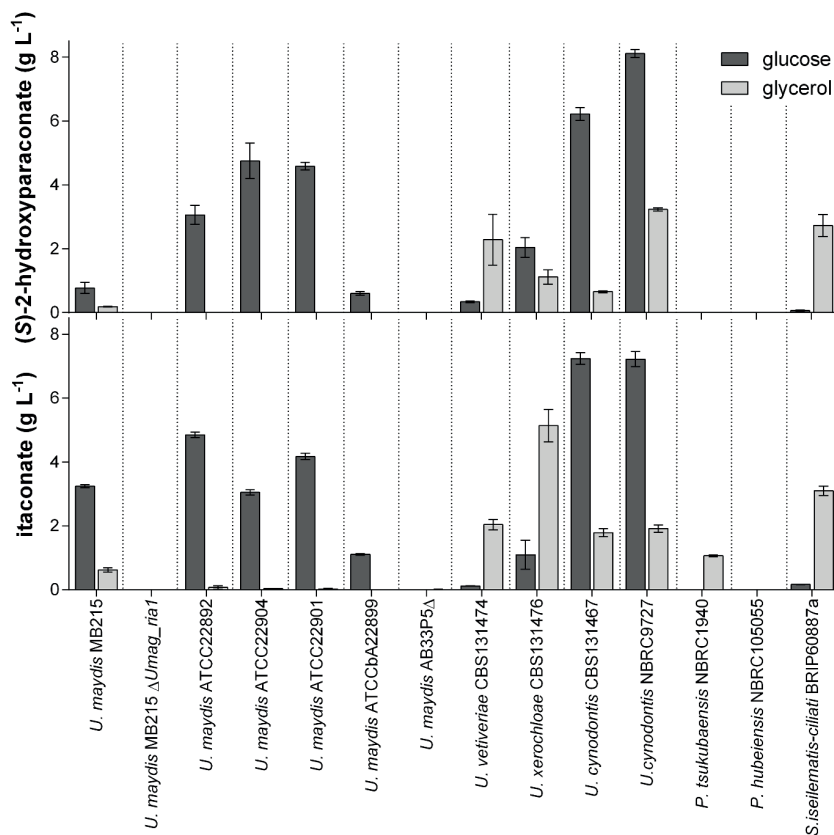


Figure 10. Itaconate and (S)-2-hydroxyparaconate production by various species in the Ustilaginaceae cultivated on glucose and glycerol. Itaconate and (S)-2-hydroxyparaconate concentrations after 120 h or 384 h System Duetz[®] cultivations in screening medium with glucose or glycerol, respectively. The *U. maydis* Δ *Umag_ria1* mutant derived from wild type strain MB215 was used as a negative control. Error bars indicate standard deviation from the mean (n=3).

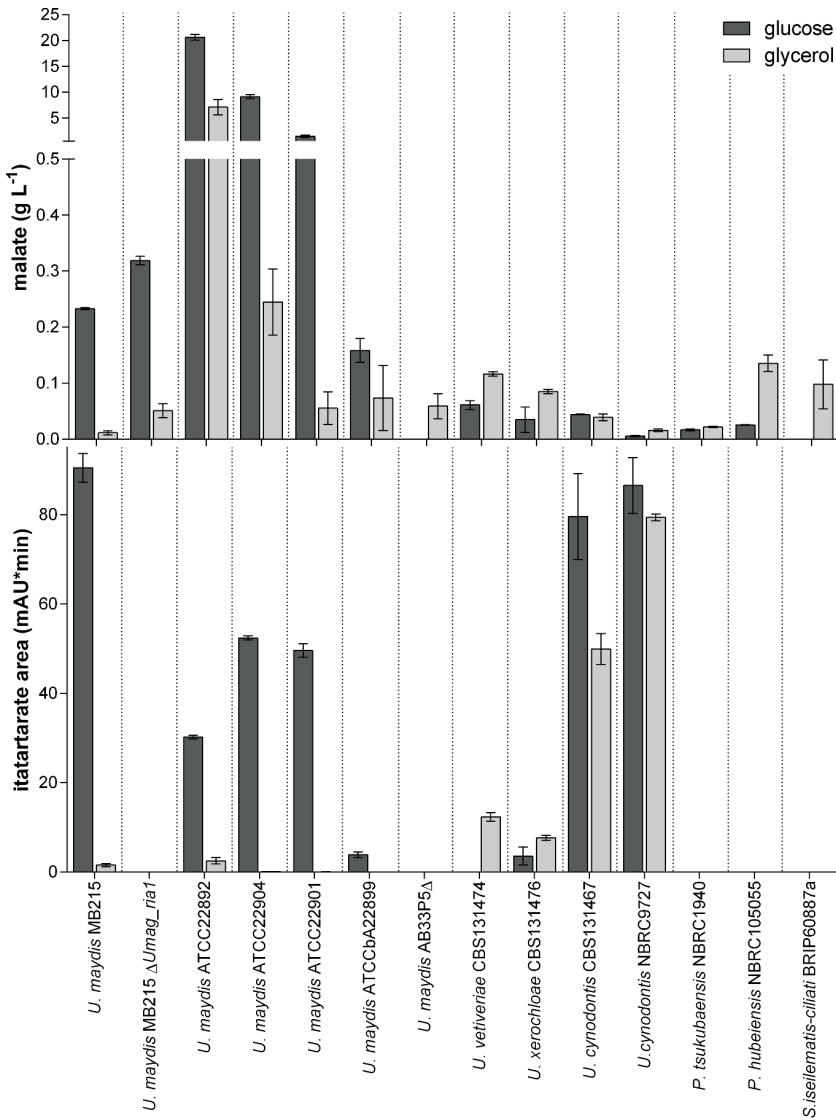


Figure 11. Malate and itatartarate production by various Ustilaginaceae on glucose and glycerol. Malate concentrations and itatartarate UV area after 120 h or 384 h System Duetz[®] cultivations in screening medium with glucose or glycerol, respectively. *U. maydis* MB215 Δ *Umag_ria1* was used as a negative control. Error bars indicate standard deviation from the mean (n=3).

All wild type strains consumed at least 50% of the glucose in the 120 h except *U. maydis* AB33P5 Δ , which utilized 40% (Figure 12). The growth on glycerol is slower in comparison to glucose. Therefore samples were taken after 384 h. At this time point, all strains consumed at least 30% of the glycerol, except of *U. maydis* AB33P5 Δ , which used 13% (Figure

12). Most *U. maydis* strains produced itaconate only on glucose as the carbon source, whereas *U. vetiveriae*, *P. tsukubaensis*, and *S. iseilematis-ciliati* did so only on glycerol. *U. cynodontis* and *U. xerochloae* produced itaconate on both carbon sources. *U. maydis* AB33P5 Δ , *U. maydis* Δ *Umag_ria1*, and *P. hubeiensis* did not produce itaconate at all. Since (*S*)-2-hydroxyparaconate and itatartarate are derivatives from itaconate [126], the production of these compounds was also investigated. (*S*)-2-hydroxyparaconate production of the tested strains on glucose and glycerol was similar to itaconate production (Figure 12), except of *P. tsukubaensis*, which only produced itaconate. Also, estimated itatartarate production levels showed a similar trend compared to (*S*)-2-hydroxyparaconate production except for *S. iseilematis-ciliati*, which did not to produce itatartarate (Figure 11). Previous studies showed a negative correlation between itaconate and malate production [97]. Therefore malate production was also determined. All strains produced malate on glucose and glycerol except for *U. maydis* AB33P5 Δ and *S. iseilematis-ciliati*, which produced malate only on glycerol (Figure 11). In general *U. maydis* strains showed the highest malate titers. These results are in accordance with our previous study [95].

A possible reason for these varying titers of itaconate and its derivatives could be differences in the sequences of the itaconate and (*S*)-2-hydroxyparaconate biosynthesis genes, or the genetic inventory of these genes. Furthermore, different regulation or relative expression levels of the biosynthesis genes could cause varying production [217, 223]. Due to the targeted disruption of the genes encoding its five proteases, *U. maydis* strain AB33P5 Δ is a slow-growing strain in comparison to wild type and other Ustilaginaceae strains, possibly caused by different timing of the strains concerning C- or N-source utilization or their growth rate [237]. To gain a deeper understanding of the sequence-function relationship between itaconate/(*S*)-2-hydroxyparaconate biosynthesis genes and production, the genomes of 13 Ustilaginaceae were analyzed and genes related to the synthesis of these secondary metabolites annotated and characterized.

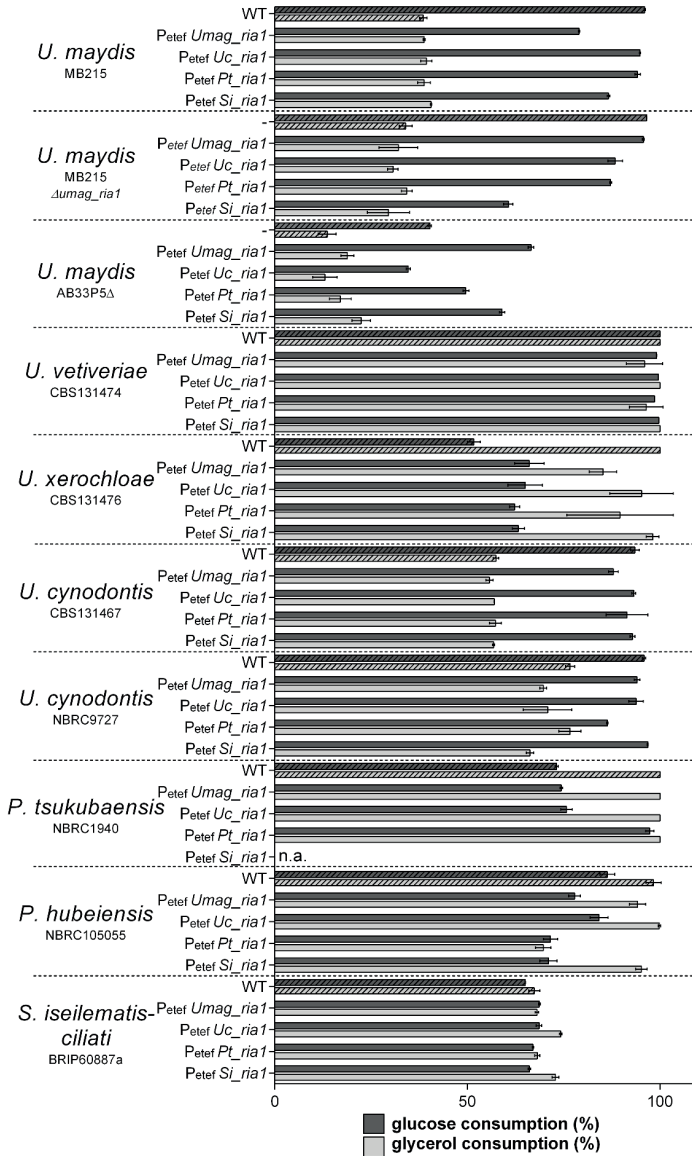


Figure 12. Glucose and glycerol consumption by various Ustilaginaceae. Glucose and glycerol consumption in % after 120 h or 384 h System Duetz® cultivations in screening medium with glucose or glycerol, respectively. Error bars indicate standard deviation from the mean (n=3).

3.1.3.2 Genetic differences in the itaconate biosynthesis cluster

The Whole Genome Shotgun sequences of *Ustilago maydis* MB215 (DSM17144), *Ustilago maydis* ATCC 22892, *Ustilago maydis* ATCC22904, *Ustilago maydis* ATCC22901, *Ustilago maydis* ATCCbA22899, *Ustilago maydis* AB33P5Δ, *Ustilago vetiveriae* CBS131474, *Ustilago xerochloae* CBS131476, *Ustilago cynodontis* CBS131467, *Ustilago cynodontis* NBRC9727, *Pseudozyma tsukubaensis* NBRC1940, *Pseudozyma hubeiensis* NBRC105055, and *Sporisorium isilematis-ciliati* BRIP60887a have been deposited in DDBJ/ENA/GenBank [235]. Their accession numbers are listed in Table 5. To find the genes responsible for itaconate and (S)-2-hydroxyparaconate biosynthesis in these sequenced strains, the protein sequences encoded in the *U. maydis* MB215 itaconate biosynthesis cluster (GenBank KT852988.1) were used as queries against the Whole Genome Shotgun sequences database using the tBLASTn algorithm [140, 238]. Multiple hits with neighboring genes were defined as putative itaconate clusters. For cluster annotation, the highest resulting homologous sequences were further analyzed using the online tool “Augustus gene prediction” to identify start/stop codons and exons [239], followed by manual curation. Furthermore, protein sequences of *U. maydis* MB215 were compared to the predicted proteins of the investigated Ustilaginaceae using the global protein sequence multiple alignment tool (BLOSUM 62) [240] in Clone Manager 9 Professional Edition. The protein sequence identity of the investigated Ustilaginaceae proteins compared to the itaconate cluster of reference strain *U. maydis* MB215 is presented in (Figure 13B). Additionally, the phylogenetic tree based on the DNA sequences of itaconate clusters of different Ustilaginaceae indicates the phylogenetic relationship among the chosen strains (Figure 13A).

Exact phylogenetic classification among Ustilaginaceae is challenging, with several species being renamed based on a new analysis of indicator genes such as nuclear ribosomal RNA genes [241-243]. Wang *et al.* especially mentioned that strains in the genus *Pseudozyma* have an uncertain phylogenetic position due to the taxonomic confusion between their teleomorphic genera [244]. Therefore, a phylogenetic relation is shown based on the DNA sequence of the itaconate cluster (Figure 13A).

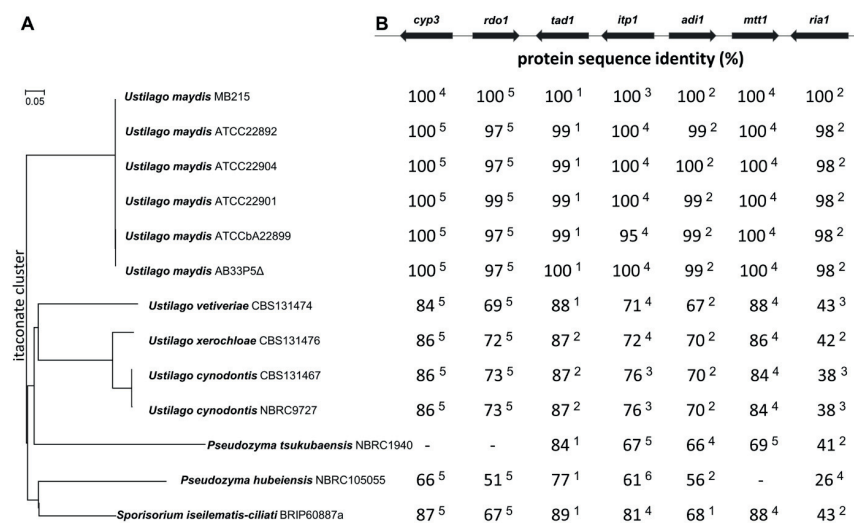


Figure 13. Itaconate cluster composition of selected Ustilaginaceae and a phylogenetic tree of these genes. A: Phylogenetic tree based on the DNA sequences of itaconate clusters of different Ustilaginaceae. The optimal tree with the sum of branch length = 1.88603985 is shown. The evolutionary distances are in the units of 0.05 base substitutions per site. B: Itaconate cluster comparison of selected Ustilaginaceae. Numbers given show sequence identity as percentage compared to the reference strain *U. maydis* MB215 using global protein sequence multiple alignment tool (BLOSUM 62). Superscript number indicate number of exons for each gene. Absent genes are indicated with a dash (-).

In all sequenced organisms, except *P. tsukubaensis* and *P. hubeiensis*, the complete gene cluster for itaconate synthesis and a conserved synteny of all genes (gene orientation and chromosome) were identified (Figure 13B). The cluster in *P. tsukubaensis* does not contain *rdo1* and *cyp3*. For these two genes, no likely homologous candidate was found elsewhere in the genome, explaining the lack of (*S*)-2-hydroxyparaconate and itatartarate production in this strain (Figure 10). In *P. hubeiensis*, *mtt1* is not present in the itaconate cluster or its direct surrounding DNA regions. In *U. maydis* MB215, the deletion of *UMAG_mtt1* led to a strong decrease in itaconate production [139]. This transporter, which putatively shuttles malate and *cis*-aconitate between the mitochondria and the cytoplasm, is the rate-limiting step in itaconate biosynthesis in *U. maydis* MB215 [245]. Since itaconate formation was not completely abolished by *Umag_mtt1* deletion in *U. maydis*, most likely other less specialized, and therefore less efficient, transport proteins substituted its function, as most eukaryotic mitochondrial transporters have a diverse substrate spectrum with different affinities [246]. At least one similar mitochondria tricarboxylate transporter gene is present in the genome of *P. hubeiensis*, which could take over the function of *Mtt1*. This gene showed 54% sequence similarity on protein level in comparison to *Umag_mtt1* and 98% to *Umag_02365* upon tBLASTn analysis [238]. The latter gene, *Umag_02365*, is known to be one of two related mitochondrial citrate transporters in *U. maydis*, with redundant function to *Umag_mtt1* [245]. This may explain why *P. hubeiensis* failed to produce itaconate. In general, the conservation of a protein sequence could point to its evolutionary origin. The comparison showed that among the tested *U. maydis* strains the itaconate cluster is conserved. At the DNA level, the clusters in different *U. maydis* strains are > 98% similar and the clusters of the two *U. cynodontis* strains have 99% sequence identity on DNA level. For the other species, the

sequence identity of proteins encoded by the itaconate and (*S*)-2-hydroxyparaconate biosynthesis (*cyp3*, *tad1*, and *adi1*) and transporters (*itp1* and *mtt1*) genes were mostly conserved in a range of 56 to 89% compared to the *U. maydis* MB215 sequence. The most divergent protein of the itaconate cluster is Rial1, a transcription factor of approximately 380 amino acids. The annotated *Uc_ria1* of both *U. cynodontis* strains encodes a transcription factor of 471 amino acids. A conserved helix-loop-helix structural motif could be found in all 13 regulators approximately in position 100-AA by SMART analysis, which is a characteristic DNA-binding motif for one of the largest families of dimerizing transcription factors [247, 248]. The phylogenetic tree of the predicted Rial1 transcriptional regulators is shown in Figure 14. Rial1 proteins of *U. maydis* species are very closely related. *U. cynodontis* and *U. xerochloae* are closely related [249], which is reflected in the relatedness of their Rial1 proteins. However, *U. maydis* and *U. vetiveriae* are phylogenetically closely related as well [249], even though their Rial1 proteins are only 43% identical. This may indicate that the amino acid sequence of Rial1 proteins is evolving faster than its actual function, for which just the DNA-binding motif is essential. The Rial1 sequence of *P. hubeiensis* is phylogenetically the most distant of the species compared. In general, no accurate subcategorization of the transcription factor according to the species is possible. A reason might be the difficulties mentioned above in the categorization of the Ustilaginaceae. In summary, all tested strains have the genetic inventory for itaconate biosynthesis, and the synteny of the itaconate cluster is preserved in most of the investigated Ustilaginaceae. *P. tsukubaensis* and *P. hubeiensis* do not possess the complete itaconate cluster, partly explaining the differences in the product spectrum. However, the variable itaconate and (*S*)-2-hydroxyparaconate titer, especially among different *U. maydis* strains with highly similar clusters, could not be explained. As different regulation or expression levels might be responsible for these production differences, the Rial1 transcriptional regulator of the tested Ustilaginaceae was investigated in more detail.

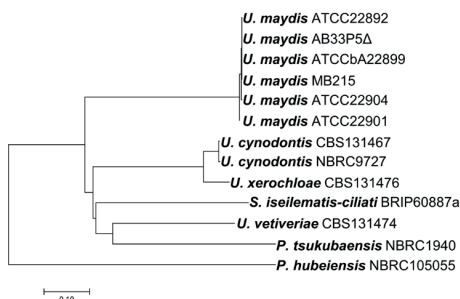


Figure 14. Phylogenetic tree of the Rial1 transcriptional regulator of different Ustilaginaceae based on similarities and differences in their protein sequence. The optimal tree with the sum of branch length = 2.49320505 is shown. The tree is drawn to scale, with branch lengths in the same units as those of the evolutionary distances used to infer the phylogenetic tree. The evolutionary distances are in the units of 0.1 amino acid substitutions per site.

3.1.3.3 Inter-species transferability of Rial1 regulator

The itaconate clusters of the tested strains are mostly conserved, while production levels of itaconate differ. As one example, the *U. maydis* AB33P5Δ gene cluster is 98% similar at the DNA level to that of *U. maydis* ATCCbA22899; however, strain AB33P5Δ does not produce itaconate or (*S*)-2-hydroxyparaconate while strain ATCCbA22899 does. Probably in some strains, like

U. maydis AB33P5 Δ , *ria1* is functional but not expressed. To test whether production differences are a result of different regulation, the inter-species transferability of *Ria1* was investigated by overexpression of various *ria1* genes to activate the production of itaconate. We chose the itaconate cluster regulator genes *Umag_ria1*, *Uc_ria1*, *Pt_ria1*, and *Si_ria1* of *U. maydis* MB215, *U. cynodontis* NBRC9727, *P. tsukubaensis*, and *S. isilematis-ciliati*, respectively, due to their considerable differences in the sequences of both the itaconate cluster and *Ria1*. These regulators were expressed under control of the constitutive promoter P_{etef} in *U. maydis* MB215, *U. maydis* AB33P5 Δ , *U. vetiveriae*, *U. xerochloae*, *U. cynodontis* CBS131467, *U. cynodontis* NBRC9727, *P. tsukubaensis*, *P. hubeiensis*, and *S. isilematis-ciliati*, as well as in the control strain *U. maydis* MB215 Δ *Umag_ria1*. Successful integration was verified by PCR.

	glucose												glycerol																							
	Um				Uc				Pt				Si				Um				Uc				Pt				Si							
	+	+	+	+	+	+	+	+	+	+	+	+	+	+	+	+	+	+	+	+	+	+	+	+	+	+	+	+	+	+	+	+	+	+	+	+
<i>U. maydis</i> MB215	+	+	+	+	+	+	+	+	+	+	+	+	+	+	+	+	+	+	+	+	+	+	+	+	+	+	+	+	+	+	+	+	+	+	+	+
<i>U. maydis</i> MB215 Δ <i>Umag_ria1</i>	+	+	+	+	+	+	+	+	+	+	+	+	+	+	+	+	+	+	+	+	+	+	+	+	+	+	+	+	+	+	+	+	+	+	+	+
<i>U. maydis</i> AB33P5 Δ	+	+	+	+	+	+	+	+	+	+	+	+	+	+	+	+	+	+	+	+	+	+	+	+	+	+	+	+	+	+	+	+	+	+	+	+
<i>U. vetiveriae</i> CBS131474	+	+	+	+	+	+	+	+	+	+	+	+	+	+	+	+	+	+	+	+	+	+	+	+	+	+	+	+	+	+	+	+	+	+	+	+
<i>U. xerochloae</i> CBS131476	+	+	+	+	+	+	+	+	+	+	+	+	+	+	+	+	+	+	+	+	+	+	+	+	+	+	+	+	+	+	+	+	+	+	+	+
<i>U. cynodontis</i> CBS131467	=	=	=	=	=	=	=	=	=	=	=	=	=	=	=	=	=	=	=	=	=	=	=	=	=	=	=	=	=	=	=	=	=	=	=	=
<i>U. cynodontis</i> NBRC9727	=	=	+	+	=	=	+	+	=	=	+	+	=	=	+	+	=	=	+	+	=	=	+	+	=	=	+	+	=	=	+	+	=	=	+	+
<i>P. tsukubaensis</i> NBRC1940	=	=	+	+	=	=	+	+	=	=	+	+	=	=	+	+	=	=	+	+	=	=	+	+	=	=	+	+	=	=	+	+	=	=	+	+
<i>P. hubeiensis</i> NBRC105055	+	+	+	+	+	+	+	+	+	+	+	+	+	+	+	+	+	+	+	+	+	+	+	+	+	+	+	+	+	+	+	+	+	+	+	+
<i>S. isilematis-ciliati</i> BRIP60887a	+	+	+	+	+	+	+	+	+	+	+	+	+	+	+	+	+	+	+	+	+	+	+	+	+	+	+	+	+	+	+	+	+	+	+	+
	ITA				HP				MAL				ITA				HP				MAL															

+ increased ($p < 0.01$)
 = wt level
 - decreased ($p < 0.01$)
 n.a.

Figure 15. Overview of the influence of overexpression of *Umag_ria1*, *Uc_ria1*, *Pt_ria1* and *Si_ria1*, on itaconate (ITA), (S)-2-hydroxyparaconate (HP), and malate (MAL) production. Differences in production were determined after 120 h or 384 h System Duetz[®] cultivations in screening medium containing either glucose or glycerol as the sole carbon source.

All strains tested consumed at least 35% of the applied glucose after 120 h and 30% of the applied glycerol after 384 h except *U. maydis* AB33P5 Δ , which used 13% glycerol (Figure 12). A summary of the activation experiments is shown in (Figure 15) and (Figure 16). The itaconate and (S)-2-hydroxyparaconate production yield (gram product per gram substrate) of the activated strains was determined on both glucose and glycerol (Figure 17) as well as the malate yield and the estimated relative itatartarate production (Figure 18). In *U. maydis* MB215 Δ *Umag_ria1*, itaconate production could be restored by expression of all tested regulators (*Umag_ria1*, *Uc_ria1*, *Pt_ria1*, and *Si_ria1*), demonstrating the functionality of this expression system, as well as their transferability of the genes between related species. It should be noted that quantitative differences in production level may be caused by different copy numbers, or by the random ectopic integration locus, of the integrated regulator, which were not determined in detail. Thus, these results should be viewed mostly in a qualitative manner. In strains that do not produce itaconate on glucose, such as *U. maydis* AB33P5 Δ (derivative of *U. maydis* FB1), *U. vetiveriae*, *P. tsukubaensis*, *P. hubeiensis*, and *S. isilematis-ciliati* itaconate production could be activated by expression of all tested regulators, except *Uc_ria1*. This suggests that in these wild type strains, the itaconate cluster genes are silent because the regulator gene *ria1* is silent and not transcribed. Constitutive

expression of the itaconate regulator *ria1*, even originating from different species, activated the expression of the itaconate cluster genes, which resulted in itaconate production.

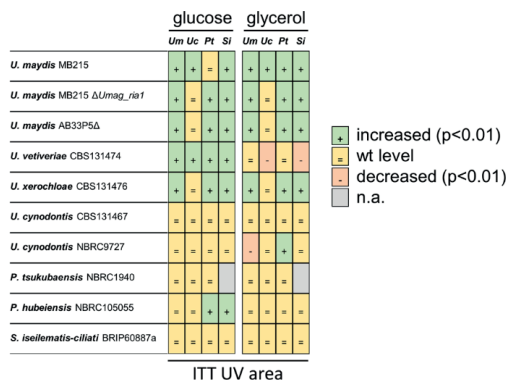


Figure 16. Schematic overview of the influence of overexpression of *Umag_ria1*, *Uc_ria1*, *Pt_ria1* and *Si_ria1*, on itatartarate (ITT) production. Differences in itatartarate production were determined after 120 h or 384 h System Duetz[®] cultivations in screening medium containing glucose or glycerol, respectively.

As already encountered for the wild type strains, (*S*)-2-hydroxyparaconate and itatartarate production correlated with itaconate production. In general, activation or enhancement of itaconate biosynthesis also activated or enhanced (*S*)-2-hydroxyparaconate and itatartarate biosynthesis (Figure 15, Figure 16 Figure 18). An exception is *P. tsukubaensis* that does not possess the (*S*)-2-hydroxyparaconate biosynthesis genes *rdol* and *cyp3*, and therefore (*S*)-2-hydroxyparaconate and itatartarate are not produced in the activated strains. Zambanini *et al.* showed a negative correlation of itaconate and malate biosynthesis after overexpression of *Umag_ria1* in *U. vetiveriae* CBS131474 on glycerol [97]. This is in line with our results. However, for the other tested Ustilaginaceae this negative correlation could not be shown, as in most activated strains, malate production resembled the wild type level (Figure 15 and Figure 18).

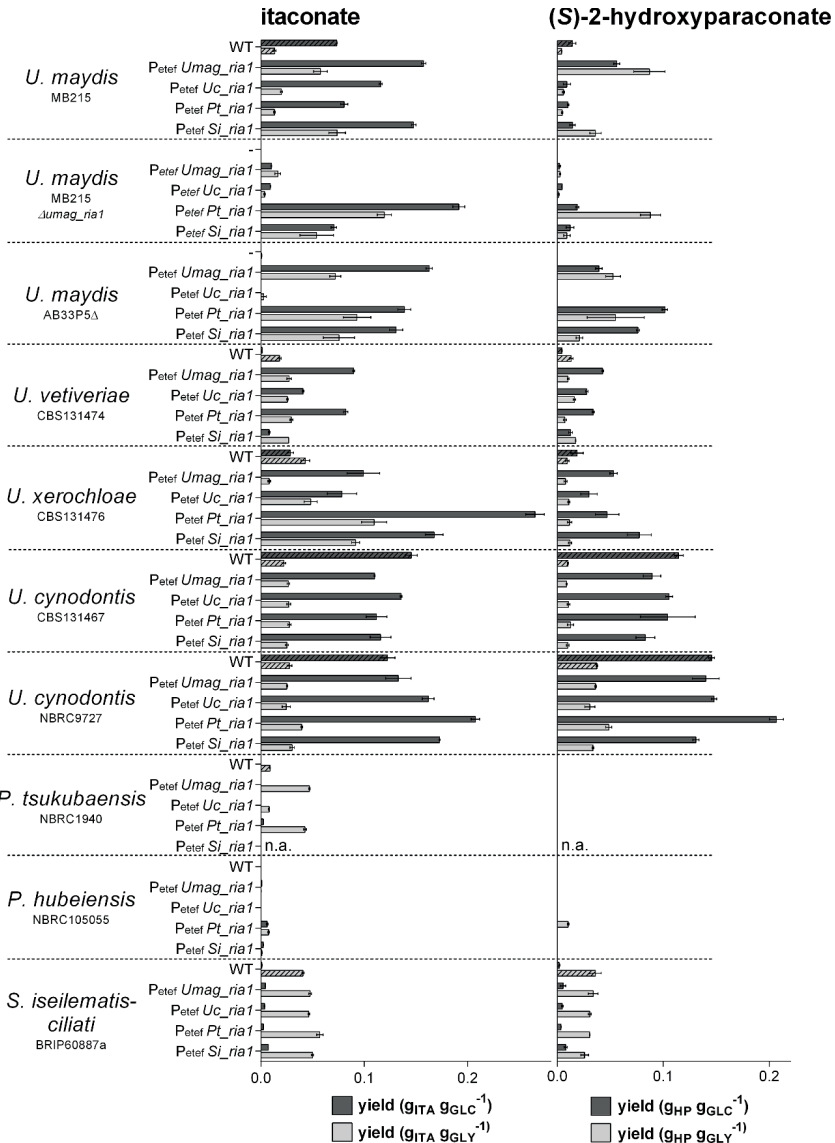


Figure 17. Itaconate and (S)-2-hydroxyparaconate production by various Ustilaginaceae species and their mutants transformed with *Umag_ria1*, *Uc_ria1*, *Pt_ria1*, *Si_ria1*. Itaconate ($g_{ITA} g_{GLC}^{-1}$, $g_{ITA} g_{GLY}^{-1}$) and (S)-2-hydroxyparaconate ($g_{HP} g_{GLC}^{-1}$, $g_{HP} g_{GLY}^{-1}$) yield after 120 h or 384 h System Duetz® cultivations in screening medium containing glucose (GLC) and glycerol (GLY), respectively. A dash (–) indicates the negative control without an overexpression construct. Error bars indicate standard deviation from the mean (n=3).

Comparing the successfully activated or improved strains, those expressing *Uc_ria1* perform considerably less well than strains expressing the other regulators. The deletion of *Uc_ria1* in *U. cynodontis* NBRC9727 completely abolished itaconate production (data not shown), indicating that *Uc_ria1* is essential for itaconate production. However, *U. cynodontis* NBRC9727 ΔUc_ria1 could not be complemented by *Uc_ria1* under control of the constitutive promoter P_{etef} , although complementation experiments under control of the native promoter P_{Uc_ria1} and terminator T_{Uc_ria1} and a random genome integration was successfully (data not shown). This indicates that the integration locus of genes under control of P_{etef} plays a crucial role in heterologous expression in *U. cynodontis* and that the chosen expression cassette design may have affected the outcome of *ria1* overexpression in different hosts. In *U. cynodontis* strains itaconate production could not be considerably enhanced, even by overexpression of the native regulator *Uc_ria1*. In contrast, strains more closely related phylogenetically with a lower wild type production level, such as *U. xerochloae*, could still enhance itaconate production by overexpression of *Uc_ria1*. Since the *U. cynodontis* strains were the best performing wild types, it might be possible that the natural expression level of the cluster genes is already at a high level, and the rate-limiting factor lies upstream of the itaconate production pathway. Alternatively, induction by Rial is in *U. cynodontis* already at its maximum.

Although the itaconate production of *P. tsukubaensis* and *S. iseilematis-ciliati* strains is comparatively low, the regulators *Pt_ria1* and *Si_ria1* seem to be the most universally applicable, since they improved itaconate production in 80% of the tested strains when cultured on glucose or glycerol. Therefore, *Pt_ria1* and *Si_ria1* might open new possibilities to activate itaconate production in other species through heterologous gene expression approaches.

In general, the differences in itaconate production in strains expressing the same regulator could have several explanations. The chosen constitutive promoter P_{etef} is a modified *tef* promoter controlling transcription of the gene for the translation elongation factor 2 of *U. maydis* [186]. It may be less efficient in other Ustilaginaceae than in *U. maydis*. However, its functionality was verified in *U. trichophora* [98] and *U. vetiveriae* [208]. As mentioned before, different copy numbers of the integrated regulators can cause differences in transcription levels and therefore, in production levels. Especially for results on glycerol showing a similar overall trend than on glucose, different growth kinetics, including, growth rates and substrate uptake rates can cause differences in itaconate production. The growth rate on glycerol of Ustilaginaceae is lower in comparison to that on glucose, hence less nitrogen for biomass synthesis per time is required, which subsequently influences nitrogen limitation during cultivation. Nitrogen limitation is necessary for the natural induction of itaconate production in *U. maydis* [137]. The maximum theoretical yield of itaconate production is directly related to the consumed C/N ratio, and thus, weak growth (low growth rate) could result in a lower yield given the chosen cultivation time. Altogether, itaconate production could be activated or enhanced by overexpression of Rial originating from a related species, even though the chosen Rial protein sequences are very dissimilar. This is the first time that activation of silent itaconate clusters by overexpression of a cluster-specific transcription factor across species and even genus boundaries was shown. Since overexpression of Rial upregulates all genes of the itaconate core cluster in *U. maydis* MB215 [139], promoter regions of the co-regulated genes will likely have a common conserved regulator binding domain. In this study, the phylogenetic relatedness and the feasible inter-species transferability of Rial regulator originating from related species could be shown. To identify potential common regulatory sequences, *in silico* analysis for conserved sequence motifs was performed using the MEME algorithm Version 4.12.0 under standard settings [250]. This analysis

revealed that promoters of Rial1-regulated genes share a putative conserved Rial1 binding domain with a short consensus sequence (CN[T/C]NNNN[G/A]TCACG[C/T]) (Figure 19). This sequence can be found in all tested Ustilaginaceae in either orientation in the promoter regions of all annotated cluster genes in at least one copy with an average E-value of 1.8×10^{-83} . Interestingly, none of the *rial* promoters themselves contain this element. Since most of the tested regulators do not seem to be very species-specific, this site likely binds regulators from multiple species. Although the role of this motif as the binding site for Rial1 needs to be confirmed by biochemical methods, its occurrence in the sequenced wild type strains (*U. maydis* MB215 (DSM17144), *U. vetiveriae* CBS131474, *U. xerochloae* CBS131476, *U. cynodontis* CBS131467, *P. tsukubaensis* NBRC1940 and *P. hubeiensis* NBRC105055, and *S. iseilematis-ciliati* BRIP60887a) strongly suggests that despite the relatively low amino acid sequence similarity of Rial1 in these species, the function of this regulator is the same.

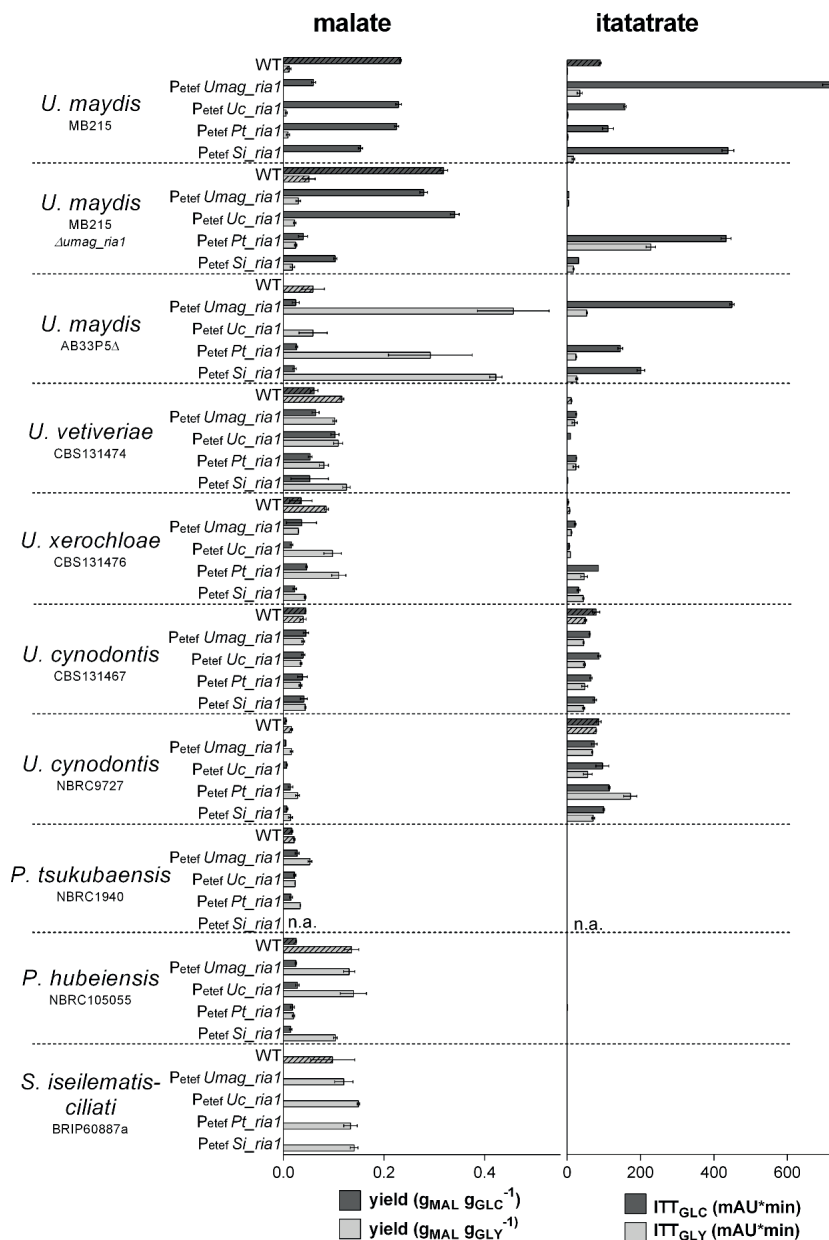


Figure 18. Malate and itatartate production by various Ustilaginaceae and their mutants transformed with *Umag_ria1*, *Uc_ria1*, *Pt_ria1*, *Si_ria1*. Malate ($g_{MAL} g_{GLC}^{-1}$, $g_{MAL} g_{GLY}^{-1}$) yield and itatartate titer after 120 h or 384 h System Duetz[®] cultivations in screening medium containing glucose (GLC) and glycerol (GLY), respectively. A dash (-) indicates the negative control without an overexpression construct. Error bars indicate standard deviation from the mean (n=3).



Figure 19. Common motif within the promoter regions of the itaconate cluster genes in all tested Ustilaginaceae was identified by MEME analysis [250].

3.1.4 Conclusion

This study indicates phenotypically that itaconate production differences among related Ustilaginaceae species are based on different transcriptional regulation of the itaconate cluster genes, governed in turn by the expression level of *Ria1*. All tested strains have genetic equipment for itaconate production; also, itaconate non-producers. However, in some strains, the itaconate clusters are silent because the itaconate regulator *ria1* is silent. By overexpression of itaconate cluster-specific transcription factors *Ria1* originating from related species, we could activate silent itaconate clusters, even though the amino acid sequences of *Ria1* regulators are relatively dissimilar. In addition to the silent itaconate clusters being activated, itaconate production in weak producers could be enhanced up to 4-fold. Notably, the activated form of *U. maydis* strain AB33P5 Δ might be a promising candidate for the combination of biomass degradation and itaconate production in one strain [236]. As such, this study contributes to demonstrating the industrial applicability of Ustilaginaceae for the biotechnological production of itaconate, and also suggests that activation of silent secondary metabolite clusters can be achieved in a range of related species with reduced genetic engineering efforts.

3.1.5 Acknowledgements

We thank Sandra Przybilla (Philipps-University Marburg, Germany) for the supply of *Ustilago maydis* DSM17144 Δ *Umag_ria1*, *Ustilago maydis* DSM17144 Δ *Umag_ria1* P_{tef} *Umag_ria1*, and *Escherichia coli* Top10 + P_{tef} *Umag_ria1-Cbx* and Kerstin Schipper (Heinrich-Heine-University Düsseldorf, Germany) for *Ustilago maydis* AB33P5 Δ .

Chapter 3.2

The interplay between transport and metabolism in fungal itaconic acid production

Partially published as:

Hamed Hosseinpour Tehrani, Elena Geiser, Meike Engel, Sandra K. Hartmann, Abeer H. Hossain, Peter J. Punt, Lars M. Blank and Nick Wierckx. *The interplay between transport and metabolism in fungal itaconic acid production. Fungal Genetics and Biology (2019) 125:45-52, <https://doi.org/10.1016/j.fgb.2019.01.011>.*

Contributions:

Elena Geiser and Hamed Hosseinpour Tehrani contributed equally to this work. Nick Wierckx and Peter Punt conceived the project. Elena Geiser and Hamed Hosseinpour Tehrani designed and performed experiments and analyzed results with the help of Nick Wierckx, Lars M. Blank and Peter Punt. Hamed Hosseinpour wrote the manuscript with the help of Elena Geiser, Nick Wierckx, Lars M. Blank and Peter Punt. Sandra K. Hartmann performed southern blots, Meike Meyer constructed *U. maydis* transformants and Abeer H. Hossain provides sequence information and discussion for *A. terreus* transporters.

3.2 The interplay between transport and metabolism in fungal itaconic acid production

3.2.1 Abstract

Besides enzymatic conversions, many eukaryotic metabolic pathways also involve transport proteins that shuttle molecules between subcellular compartments, or into the extracellular space. Fungal itaconate production involves two such transport steps, involving an itaconate transport protein (Itp), and a mitochondrial tricarboxylate transporter (Mtt). The filamentous ascomycete *Aspergillus terreus* and the unicellular basidiomycete *Ustilago maydis* both produce itaconate, but do so via very different molecular pathways, and under very different cultivation conditions. In contrast, the transport proteins of these two strains are assumed to have a similar function. This study aims to investigate the roles of both the extracellular and mitochondrial transporters from these two organisms by expressing them in the corresponding *U. maydis* knockouts and monitoring the extracellular product concentrations. Both transporters from *A. terreus* complemented their corresponding *U. maydis* knockouts in mediating itaconate production. Surprisingly, complementation with *A. terreus* *At_MfsA* from *A. terreus* led to a partial switch from itaconate to (*S*)-2-hydroxyparaconate secretion. Apparently, the export protein from *A. terreus* has a higher affinity for (*S*)-2-hydroxyparaconate than for itaconate, even though this species is classically regarded as an itaconate producer. Complementation with *At_MttA* increased itaconate production by 2.3-fold compared to complementation with *Um-Mtt1*, indicating that the mitochondrial carrier from *A. terreus* supports a higher metabolic flux of itaconic acid precursors than its *U. maydis* counterpart. The biochemical implications of these differences are discussed in the context of the biotechnological application in *U. maydis* and *A. terreus* for the production of itaconate and (*S*)-2-hydroxyparaconate.

3.2.2 Introduction

Itaconic acid can be used as a bio-based building block for the synthesis of a large number of chemicals and polymers. In 2004, the U.S. Department of Energy declared itaconic acid as one of the top 12 bio-based platform chemicals with high biotechnology potential [12]. Nowadays, it is mainly used in the production of synthetic fibers, for coatings, thickeners, anti-scaling agents in water treatments, and in the pharmaceutical sector [107, 110, 111, 225, 251]. It's role as central mammalian immunoregulator has recently been reported opening novel uses, e.g., in the treatment for autoimmune conditions [120]. Fungi can also convert itaconate into the chiral lactone (*S*)-2-hydroxyparaconate [140, 252]. The functional groups within this product can be further manipulated in many directions to access a multitude of high-value and different fine chiral chemicals with a wide range of potential applications ranging from medicine to pesticides to quantum computing [253, 254].

The unicellular basidiomycete *Ustilago maydis* and the filamentous ascomycete *Aspergillus terreus* both naturally produce itaconate (Figure 20). In both organisms, the genes enabling itaconate biosynthesis are clustered and co-regulated [139, 255]. The biosynthetic pathway starts with the transport of *cis*-aconitate from the mitochondria to the cytosol by a mitochondrial tricarboxylate transporter, encoded by *Um_mtt1* or *At_mttA* [139, 140, 256]. Both transporters are assumed to do so by antiport exchange with cytosolic malate [141]. In *U. maydis* MB215, this transport poses the rate-limiting step in itaconate production, since overexpression of *mtt1* leads to a strong increase in itaconate production [139]. In contrast, overexpression of *mttA* has no significant impact on itaconate production by *A. terreus* LYT10 [257], although heterologous overexpression of *mttA*, along with *cadA*, did have a positive impact on itaconate production in *Aspergillus niger* [255, 258]. In *A. terreus*, the cytoplasmic *cis*-aconitate is converted

directly to itaconate by a cytosolic *cis*-aconitate decarboxylase (*cadA*) [142-144]. In contrast, *U. maydis* first isomerizes *cis*-aconitate to *trans*-aconitate by a cytosolic aconitate- δ -isomerase (Adi1). This *trans*-aconitate is subsequently decarboxylated to itaconate by a *trans*-aconitate decarboxylase (Tad1) [139].

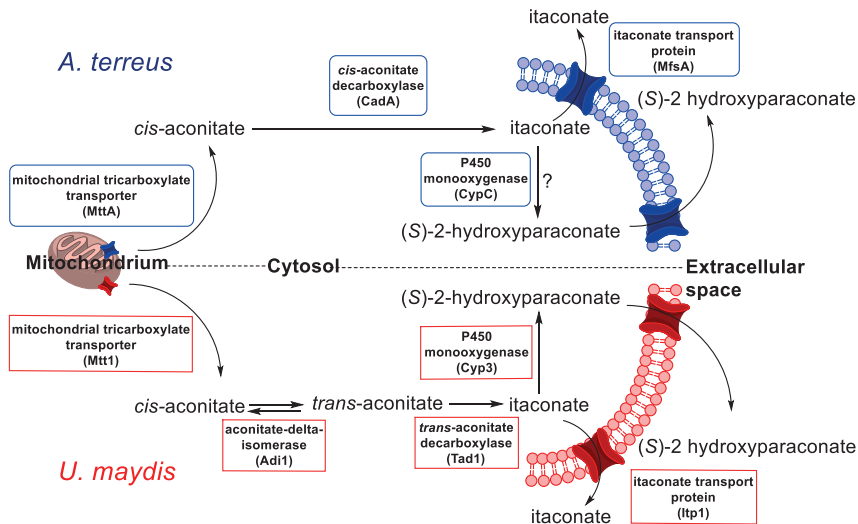


Figure 20. Comparison of the itaconate and (S)-2-hydroxyparaconate biosynthesis pathways of *U. maydis* and *A. terreu*.

Recently, Geiser *et al.* [140] demonstrated that in *U. maydis*, itaconate is further converted to (S)-2-hydroxyparaconate by an itaconate P450 monooxygenase (Cyp3). The latter is the lactone of L-itatartarate, which is also found in the supernatants of *U. maydis* [126, 136]. Some *A. terreu* strains have also been reported to produce these products [126, 259], likely through a similar P450 enzyme encoded by the *cypC* gene directly adjacent to the itaconate gene cluster [140, 146]. However, (S)-2-hydroxyparaconate production is not reported for strains such as *A. terreu* NRRL 1960 or *A. terreu* DSM 23081 [132, 147], possibly because these strains were selected by screening for high itaconate production leading to the selection of a defect in *cypC* expression. Both *U. maydis* and *A. terreu* possess a major facilitator superfamily transporter, encoded by *Um itp1* and *At mfsA*, which are assumed to be itaconate exporters [140, 148, 255]. Overexpression of *mfsA* in *A. terreu* and *A. niger* led to an increase in itaconate production [255, 257], while *itp1* overexpression in *U. maydis* did not increase production [140]. However, in light of the fact that both itaconate and (S)-2-hydroxyparaconate are produced via the same pathway, and that the gene clusters of both organisms only contain one gene encoding a cytosolic exporter, it is reasonable to assume that the same protein secretes both products. Although the functions of the transporters involved in the production of itaconate and its derivative (S)-2-hydroxyparaconate are likely similar in both *U. maydis* and *A. terreu*, the differences in their protein sequence, and their underlying biosynthetic pathways may affect their specific activity and/or substrate affinity. In addition, the mechanism of (S)-2-hydroxyparaconate transport

has thus far not been investigated. Thus, this study aims to characterize these transporter proteins in the unicellular fungus *U. maydis* and to investigate their influence on the production of itaconate and (S)-2-hydroxyparaconate.

3.2.3 Results and discussion

3.2.3.1 Comparing the role of *Itp1* from *U. maydis* and *MfsA* from *A. terreus* in itaconic acid production

Both *Ustilago maydis* and *Aspergillus terreus* can oxidize itaconate to (S)-2-hydroxyparaconate, but they each only carry one gene encoding a Mfs-type cytoplasmic membrane transporter in their itaconate gene clusters. In order to compare the exporters of these two genera in the same biological background, both *At_mfsA* from *A. terreus* and *Um_itp1* from *U. maydis* were expressed under control of the P_{etef} promoter in *U. maydis* MB215 ΔUm_itp1 . The *At_mfsA* gene was dicodon-optimized to enable expression in *U. maydis* [204]. To ensure comparability, the constructs were integrated into the *ip*-locus, and single copy insertions were selected by diagnostic PCR and Southern blot analysis. Subsequently, in targeted single copy transformants, itaconate and (S)-2-hydroxyparaconate production, glucose consumption, and OD₆₀₀ were analyzed in order to elucidate the role of the exporters encoded by *At_mfsA* from *A. terreus* and *Um_itp1* from *U. maydis* in the corresponding *U. maydis* deletion strain (MB215 ΔUm_itp1) (Figure 21A, D, C, F). Exponential growth takes place in the first 18-24 h, after which nitrogen is depleted from the medium, and further OD₆₀₀ changes are considered secondary growth as described previously [137, 197]. In the growth phase, determined through the OD₆₀₀ after 24 h, the engineered strains did not differ significantly from each other, except for *U. maydis* MB215 ΔUm_itp1 . This indicates that except for the latter strain, which likely grew worse due to intracellular product accumulation, volumetric production can be used as proxy for specific production. Surprisingly, although the expression of *At_mfsA* did lead to a slight itaconate production, it did not fully restore the production of *U. maydis* ΔUm_itp1 to the level of the wildtype (Figure 21). In contrast, the control strain *U. maydis* $\Delta Um_itp1 + P_{etef}Um_itp1$ produced 1.4-fold more itaconate than the wildtype (Figure 21A). Conversely, $\Delta Um_itp1 + P_{etef}Um_itp1$ produced less (S)-2-hydroxyparaconate than the wildtype, while $\Delta Um_itp1 + P_{etef}At_mfsA$ produced 1.7-fold more (S)-2-hydroxyparaconate than the wildtype (Figure 21D). The P450 monooxygenase encoded by *cyp3* converts itaconate to (S)-2-hydroxyparaconate in the cytoplasm [140]. The fact that complementation with both transporters significantly elevates the extracellular concentration of both products in comparison to the ΔUm_itp1 deletion strain indicates that *Um_Itp1* and *At_MfsA* can both transport itaconate as well as (S)-2-hydroxyparaconate. However, when both products are produced simultaneously, our data suggest that competitive inhibition between these metabolites takes place, with *Um_Itp1* having a higher affinity for itaconate, and *At_MfsA* favoring (S)-2-hydroxyparaconate (Figure 21B, E and Table 6).

An explanation for the low concentration of (S)-2-hydroxyparaconate produced by $\Delta Um_itp1 + P_{etef}Um_itp1$ compared to the wildtype could be that the overexpression of *Um_Itp1* with the strong and constitutive promoter P_{etef} enables a more efficient secretion of itaconate, thereby lowering its concentration in the cytoplasm. This would lower the substrate concentration of Cyp3, reducing the (S)-2-hydroxyparaconate production rate as long as the enzyme is not operating under substrate-saturating conditions. The reverse effect likely occurs in *U. maydis* $\Delta Um_itp1 + P_{etef}At_mfsA$, resulting in higher itaconate and lower (S)-2-hydroxyparaconate concentrations in the cytoplasm, thereby increasing Cyp3 activity. In this way, product export and the metabolic rates of the branched production pathway are inherently linked. Although this is

likely an essential driver for product specificity in the natural habitats of *U. maydis* and *A. terreus*, it may be less relevant in optimized itaconate production strains, which do not produce (*S*)-2-hydroxyparaconate. However, it does suggest that the K_m value of *At_MfsA* for itaconate is higher than that of *Um_Itp1*. If this is indeed the case, the resulting elevated cytosolic itaconate concentration could lead to product inhibition of CadA or Tad1, suggesting that *Um_Itp1* could be a better itaconate exporter even if (*S*)-2-hydroxyparaconate is not produced.

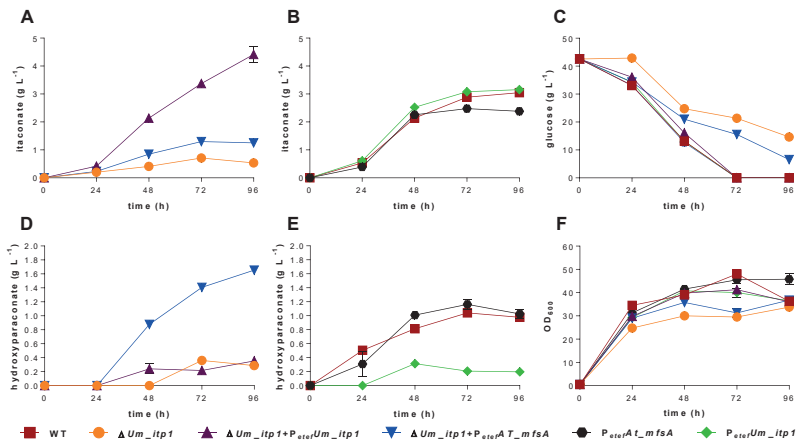


Figure 21. Acid production and growth of various *U. maydis* strains expressing itaconate transport proteins. Itaconate (A-B), (*S*)-2-hydroxyparaconate (D-E), and glucose concentration (C), as well as growth (OD₆₀₀) (F) of *itp1 / mfsA* expressing mutants in comparison to wildtype and ΔUm_itp1 controls during System Duetz[®] cultivation in screening medium. Error bars indicate the standard error of the mean (n=4).

3.2.3.2 Comparing the role of *Mtt1* from *U. maydis* and *MttA* from *A. terreus* in itaconic acid production

In order to quantitatively compare mitochondrial transporters in the same biological background, both *At_mttA* from *A. terreus* and *Um_mtt1* from *U. maydis* were expressed under control of the P_{etef} promoter in *U. maydis* MB215 ΔUm_mtt1 in the corresponding *U. maydis* deletion strain (MB215 ΔUm_mttA) as described above for *mfsA*. Both constructs complemented the itaconate producing phenotype of the ΔUm_mtt1 deletion strain, confirming that *At_MttA* and *Um_Mtt1* have a similar biochemical function. The complementation strains reached higher maximum titers than the wildtype (Figure 22A, D), likely due to the higher expression from the strong, constitutive P_{etef} promoter [140, 188, 260]. However, *U. maydis* $\Delta Um_mtt1 + P_{etef}At_mttA$ produced 1.3-fold more itaconate than *U. maydis* $\Delta Um_mtt1 + P_{etef}Um_mtt1$ (Figure 22A). The fact that the $\Delta Um_mtt1 + P_{etef}At_mttA$ strain also grew significantly worse indicates that its specific production rate is likely increased even further. The production rates of (*S*)-2-hydroxyparaconate in the complementation strains were also increased, although the maximum titer was not affected (Table 6). The fact that the strain expressing *At_mttA* produces more itaconate indicates that the mitochondrial transporter from *A. terreus* can sustain a higher *cis*-aconitate flux compared to *Mtt1* from *U. maydis*. An alternative explanation would be that the two mitochondrial carriers have

different antiport substrates. Circumstantial evidence suggests that *cis*-aconitate is mostly likely exchanged for malate by *At*_MttA [141, 256]. The fact that this protein can complement a ΔUm_mtt1 deletion suggests that the *U. maydis* protein transports the same substrates, while the improved itaconate production with *At*_MttA suggests that this protein either has a higher V_{max} or a lower K_m .

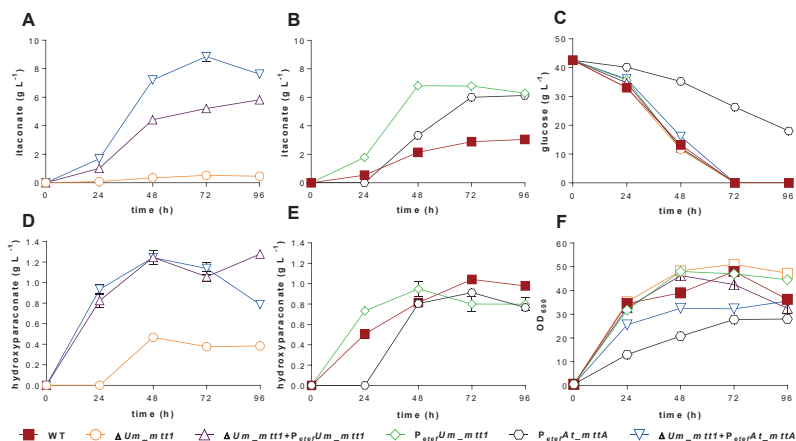


Figure 22. Acid production and growth of various *U. maydis* strains expressing mitochondrial transporters. Itaconate (A-B), (S)-2-hydroxyparaconate (D-E), and glucose concentration (C), as well as growth (OD₆₀₀) (F) of *mtt1* / *mttA* expressing mutants in comparison to wildtype and ΔUm_mtt1 controls during System Duetz[®] cultivation in screening medium is shown. Error bars indicate the standard error of the mean (n=4).

Given the already higher titers of these complementation strains, we sought to improve itaconate further and/or (S)-2-hydroxyparaconate production by selecting transformants with multicopy insertions of $P_{ete1}At_mttA$ in wildtype *U. maydis* MB215. However, this resulted in a decreased production of itaconate compared to the complementation strain $\Delta Um_mtt1+P_{ete1}At_mttA$ (Figure 22B). Biomass growth and glucose consumption were strongly decreased in the overexpression strain (Figure 22C, F). Similar growth defects were observed by Huang *et al.* [257] upon overexpression of *mttA* in *A. terreus*, even though itaconate production was not increased in this strain. A burden of membrane protein overexpression *per se* is unlikely since a control strain with multiple copies of $P_{ete1}Um_mtt1$ in wildtype *U. maydis* MB215 did not show this growth defect. This control strain still produces less itaconate than the single copy complementation strain $\Delta Um_mtt1+P_{ete1}At_mttA$ (Figure 22A, B), which indicates that a higher expression level doesn't cause the increased itaconate production of the *At*_mttA-expressing strain. In wildtype *U. maydis*, genes of the itaconate cluster are induced upon the depletion of nitrogen from the medium [137, 139, 261], thereby separating itaconate production from biomass growth. The use of the constitutive P_{ete1} promoter for expression of *At*_mttA leads to the production of MttA in the growth phase, thus posing a drain of the central metabolite *cis*-aconitate from the mitochondria, which is likely responsible for the growth defect. The fact that this was not observed upon overexpression of *Um*_Mtt1 is in line with the other indications that *At*_MttA is a more effective transporter of

cis-aconitate. To evaluate the potential of *U. maydis* $\Delta Um_mttI+P_{etef} At_mttA$ for itaconate production, this strain was cultured in pH-controlled high-density pulsed fed-batch fermentations with $4 \text{ g L}^{-1} \text{ NH}_4\text{Cl}$ and a starting concentration of $188 \pm 1.3 \text{ g L}^{-1}$ glucose (Figure 23).

Table 6. Production parameters of *U. maydis* MB215 and transporter mutants during System Duetz® cultivation in screening medium is shown. Errors indicate the standard error of the mean (n=4).

	titer _{max} (g L ⁻¹) ^a		Y _{P/S} ^b		r _P (g L ⁻¹ h ⁻¹) ^c	
	ITA ^d	2-HP ^e	ITA	2-HP	ITA	2-HP
WT	3.0 ± 0.1	1.0 ± 0.0	0.07 ± 0.00	0.02 ± 0.00	0.03 ± 0.00	0.003 ± 0.004
ΔUm_itp1	0.7 ± 0.1	0.4 ± 0.1	0.02 ± 0.00	0.01 ± 0.00	0.01 ± 0.00	0.003 ± 0.001
$\Delta Um_itp1+P_{etef}Um_itp1$	4.4 ± 0.5	0.4 ± 0.1	0.10 ± 0.01	0.01 ± 0.00	0.05 ± 0.00	0.004 ± 0.001
$P_{etef}Um_itp1$	3.2 ± 0.2	0.2 ± 0.0	0.07 ± 0.00	0.00 ± 0.00	0.03 ± 0.00	0.002 ± 0.000
$\Delta Um_itp1+P_{etef}AT_mfsA$	1.3 ± 0.1	1.7 ± 0.1	0.03 ± 0.00	0.05 ± 0.00	0.01 ± 0.00	0.02 ± 0.00
$P_{etef}AT_mfsA$	2.5 ± 0.1	1.2 ± 0.1	0.06 ± 0.00	0.02 ± 0.00	0.02 ± 0.00	0.01 ± 0.00
ΔUm_mttI	0.5 ± 0.0	0.5 ± 0.0	0.01 ± 0.00	0.01 ± 0.00	0.00 ± 0.00	0.00 ± 0.00
$\Delta Um_mttI+P_{etef}Um_mttI$	5.8 ± 0.2	1.3 ± 0.0	0.14 ± 0.00	0.03 ± 0.00	0.06 ± 0.00	0.01 ± 0.00
$P_{etef}Um_mttI$	6.8 ± 0.0	0.9 ± 0.1	0.15 ± 0.01	0.02 ± 0.00	0.07 ± 0.00	0.01 ± 0.00
$P_{etef}AT_mttA$	6.1 ± 0.2	0.9 ± 0.1	0.25 ± 0.01	0.03 ± 0.00	0.06 ± 0.00	0.01 ± 0.00
$\Delta Um_mttI+P_{etef}AT_mttA$	8.8 ± 0.6	1.2 ± 0.0	0.18 ± 0.00	0.02 ± 0.00	0.08 ± 0.00	0.01 ± 0.00

^a titer_{max}; maximum titer.

^b Y_{P/S}; overall yield product per consumed glucose.

^c r_P; overall production rate.

^d ITA; itaconate

^e 2-HP; (S)-2-hydroxyparaconate

Under these conditions, the engineered strain produced $33 \pm 3 \text{ g L}^{-1}$ itaconate and an estimated $24 \pm 2 \text{ g L}^{-1}$ (S)-2-hydroxyparaconate after 190 h. Under similar conditions wildtype, *U. maydis* MB215 produces $14.0 \pm 0.3 \text{ g L}^{-1}$ itaconate and $21.3 \pm 0.7 \text{ g L}^{-1}$ (S)-2-hydroxyparaconate with similar ammonium consumption and growth [140]. *U. maydis* $\Delta Um_mttI+P_{etef} At_mttA$ produced itaconate at an overall rate of $0.29 \pm 0.00 \text{ g L}^{-1} \text{ h}^{-1}$ and a yield of $0.15 \pm 0.00 \text{ g ita g}_{\text{glc}}^{-1}$, which is 2.1-fold, respectively 3.6-fold higher than the wildtype. It is interesting to note that both in shaken cultures and in controlled fed-batch, the engineered strains did not produce more (S)-2-hydroxyparaconate, even when itaconate production was increased. This indicates that the Cyp3 P450 monooxygenase that catalyzes the conversion of itaconate to (S)-2-hydroxyparaconate cannot support a higher flux. In total, *U. maydis* $\Delta Um_mttI+P_{etef} At_mttA$ produced $0.29 \text{ g L}^{-1} \text{ h}^{-1}$ acids (itaconate + (S)-2-hydroxyparaconate), which is comparable to itaconate production values achieved by Geiser *et al.* [140] after overexpression of *rial* and deletion of *cyp3*. Although these values are still relatively low, especially compared to *A. terreus* cultures, which can achieve itaconic acid titers up to 160 g L^{-1} with a maximum productivity of $1.9 \text{ g L}^{-1} \text{ h}^{-1}$, the combination of the abovementioned modifications with the tuned overexpression of *At_mttA* could further enhance itaconate production without (S)-2-hydroxyparaconate as a by-product.

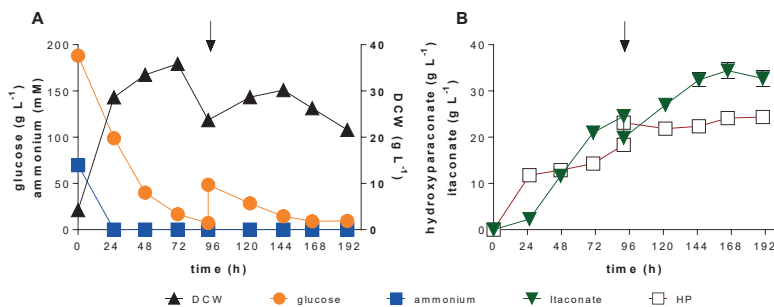


Figure 23. Controlled high-density pulsed fed-batch fermentation of *U. maydis* $\Delta Um_mtt1+P_{etf}AT_mttA$. A: DCW (▲), glucose (●) and ammonium concentration (■) and B: Concentration of itaconate (▼) and (S)-2-hydroxyitaconate (□) during fermentation in a bioreactor containing batch medium with 200 g L⁻¹ glucose, 4 g L⁻¹ NH₄Cl at pH 6.0 titrated with NaOH. Arrows indicate addition of 100mL of 50 % glucose. Error bars indicate the standard error of the mean (n=4).

3.2.3.3 Transporters involved in itaconate production do not affect pH optimum

The optimal extracellular pH for the itaconate production of *A. terreus* and *U. maydis* is very different. With *A. terreus*, itaconic acid is usually produced at a pH below 3.8, and limitations mostly govern the optimal pH range in cell morphology and pathway induction [22, 132, 147]. In contrast, wildtype *U. maydis* only produces itaconate at a pH above 5.5 [95]. One hypothesis could be that transporters involved in itaconate production, as crucial interaction points between cellular compartments and the intracellular and extracellular space, might be responsible for this difference. To test this hypothesis, the engineered complementation strains were cultivated in screening media with different buffers. The use of 33 g L⁻¹ CaCO₃ maintains pH values above 6 (Figure 24D). In contrast, by varying the concentration of a soluble MES buffer between 20 and 100 mM, the pH decreases to different extents during growth and itaconate production (Figure 24A, B, C). In wildtype *U. maydis* MB215, this results in the production of different final concentrations of itaconate, due to the difference in the concentration where pH drops below 5.5 and inhibits further production [95]. If the expression of the *A. terreus* transporters affects the pH optimum for itaconate production by *U. maydis*, the relative itaconate concentrations of these strains are expected to be higher than those of the controls expressing the native *U. maydis* transporters in the media with low buffer concentrations. However, this effect is not observed. Instead, the same trend of lower itaconate production with lower buffer capacity is observed for all strains (Figure 24B, E). However, strains that produce more itaconate in CaCO₃ buffer, such as *U. maydis* $\Delta Um_mtt1+P_{etf}At_mttA$, also consistently make more acids with limiting buffer concentrations (40, 70, and 100 mM MES). Such overproducing strains also reach a lower final pH, indicating that a low pH *per se* does not inhibit itaconate and (S)-2-hydroxyitaconate production in *U. maydis* (Figure 24B, C, E, F). One explanation for this could be that the inhibition of itaconate production at low pH values is the result of a dynamic equilibrium between uptake and secretion. Below pH 5.5, a significant fraction of fully protonated itaconic acid (pK_{a1} = 3.8) is formed. This protonated form, and not the dissociated form, can freely diffuse across the cytoplasmic membrane, facilitating itaconate reuptake into the cell [140]. Lower pH values will lead to higher extracellular concentrations of the protonated form, thus increasing the

diffusion-driven reuptake rate. This will reduce the net production of itaconate to zero when the reuptake rate equals the production rate, leading to an accumulation of intracellular itaconate, which would likely inhibit its production, and also places a burden on the maintenance of cytoplasmic pH homeostasis through weak acid uncoupling. This mechanism would explain why strains with a higher itaconate production rate can sustain a lower extracellular pH. In addition, the increase in intracellular itaconate would also enhance the rate of intracellular oxidation to (*S*)-2-hydroxyparaconate, while the reuptake of this oxidation product is lower than that of itaconate due to its lower pK_a value of 2.8 [126]. The fact that *A. terreus* can sustain efficient itaconate production at low pH values indicates that it has a higher specific production rate, likely supported by a higher intrinsic pH tolerance.

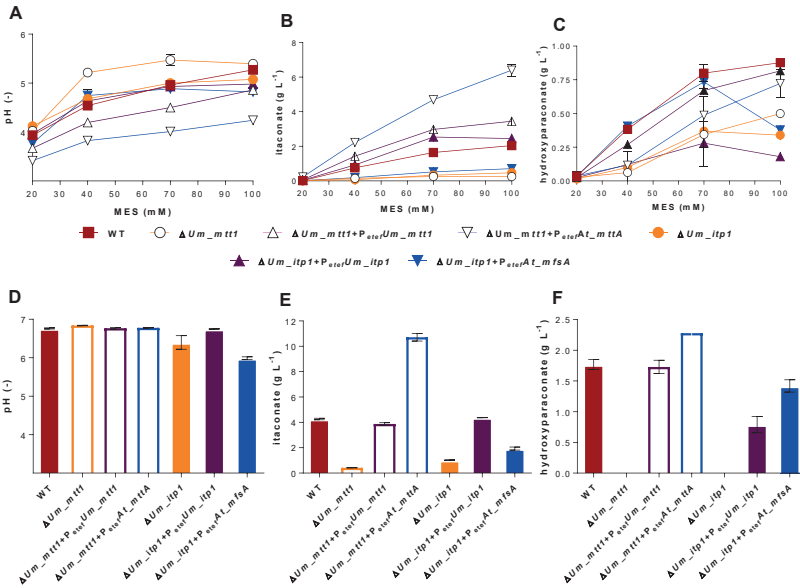


Figure 24. Influence of buffer concentration on itaconate and (*S*)-2-hydroxyparaconate production by various *U. maydis* MB215 mutants. pH values (A, D), itaconate (B, E), and (*S*)-2-hydroxyparaconate (C, F) concentrations after 72h cultivation in calcium carbonate (D, E, F) or different MES concentrations (A, B, C), respectively containing screening medium. Error bars indicate the deviation from the mean (n=2).

3.2.4 Conclusion

Comparative analysis of the mitochondrial and extracellular transporters involved in itaconate and (*S*)-2-hydroxyparaconate biosynthesis by *Ustilago maydis*, and *Aspergillus terreus* revealed striking differences, which strongly influence the absolute and relative production rates of these two secondary metabolites. This work suggests that fungal production of itaconate and (*S*)-2-hydroxyparaconate involves a complex interplay between metabolism, transport, and extracellular pH. It also provides valuable information for the rational design of efficient itaconate and (*S*)-2-hydroxyparaconate producing strains, which was demonstrated by the increased

production of *At_mttA*-expressing strains. However, further biochemical characterization of the investigated transporters is needed and will be the subject of a future study. The *At_MfsA* transporter is a promising target for the future metabolic engineering of an (*S*)-2-hydroxyparaconate producing strain since it will help to increase product specificity. In general, this study sheds light on the role of compartmentation, and the associated transporters, of the fungal biosynthesis pathway of itaconate and (*S*)-2-hydroxyparaconate. It also highlights the relevance of *U. maydis*, both as a model organism and as an industrial workhorse for the production of organic acids.

3.2.5 Acknowledgements

We thank Kylie L. Luska and Tim den Hartog (Institute for Technical and Macromolecular Chemistry, RWTH-Aachen) for contributions to (*S*)-2-hydroxyparaconate synthesis.

Chapter 3.3

Engineering the morphology and metabolism of pH tolerant *Ustilago cynodontis* for efficient itaconic acid production

Partially published as:

Hamed Hosseinpour Tehrani, Apilaasha Tharmasothirajan, Elia Track, Lars M. Blank and Nick Wierckx. Engineering the morphology and metabolism of pH tolerant *Ustilago cynodontis* for efficient itaconic acid production. *Metabolic Engineering* (2019) 54, 293-300, <https://doi.org/10.1016/j.ymben.2019.05.004>

Contributions:

Hamed Hosseinpour Tehrani performed most experiments. Nick Wierckx conceived the study. Hamed Hosseinpour Tehrani designed and performed experiments and analyzed results with the help of Nick Wierckx and Lars M. Blank. Hamed Hosseinpour Tehrani wrote the manuscript with help of Nick Wierckx and Lars M. Blank. Apilaasha Tharmasothirajan performed partially cultivation experiments for morphological studies and Elia Track partially contributed to tool development in *U. cynodontis*. Further Alexander Thielemann, Devran Gencoglu, and Sinan Cakar helped by strain engineering and Svenja Meyer support CGQ cultivation experiments.

3.3 Engineering the morphology and metabolism of pH tolerant *Ustilago cynodontis* for efficient itaconic acid production

3.3.1 Abstract

Besides *Aspergillus terreus* and *Ustilago maydis*, *Ustilago cynodontis* is also known as a natural itaconate producer. *U. cynodontis* was reported as one of the best itaconate producing species in the family of the Ustilaginaceae, featuring a relatively high pH tolerance in comparison to other smut fungi. However, in contrast to *U. maydis*, it readily displays filamentous growth under sub-optimal growth conditions. In this study, *U. cynodontis* is established as an efficient pH-tolerant itaconic acid producer through a combination of morphological and metabolic engineering. Deletions of the genes *ras2*, *fuz7*, and *ubc3* abolished the filamentous growth of *U. cynodontis*, leading to a stable yeast-like growth under a range of stress-inducing conditions. The yeast-like morphology was also maintained in a pulsed fed-batch production of 21 g L⁻¹ itaconic acid and 9.3 g L⁻¹ (S)-2-hydroxyparaconate at a pH of 3.8. The genetic and metabolic basis of itaconic acid production in *U. cynodontis* was characterized through comparative genomics and gene deletion studies. A hyper-producer strain was metabolically engineered using this knowledge resulting in a 6.5-fold improvement of titer.

3.3.2 Introduction

Itaconic acid is a versatile building block in the polymer industry due to its two functional groups. Radical polymerization of the methylene group and/or esterification of the carboxylic acid, with a wide range of co-monomers, allow for a rapidly expanding application range [25, 110]. Itaconate is most widely used as a co-monomer in the production of styrene-butadiene rubber and acrylate latexes, which are used in the paper and architectural industry [111]. Further polymerization with acrylamide or methyl-methacrylate results in superabsorbent hydrogels for pharmaceutical applications [112-115]. Itaconate can also be polymerized with itself to obtain a polymer with high cation binding capacity, whereby the derivatives can be used as detergent additives, scale inhibitors, and dispersing agents [116]. Due to these polymer applications, itaconic acid has been an established industrial bio-based chemical since the 1950s [110]. In addition, the U.S. Department of Energy identified it as a promising platform chemical, which can be converted into a range of useful derivatives [12]. More recently, itaconate has also been identified as a key metabolite in the human immune response [262], with possible applications of its membrane-permeable dimethyl ester as a therapeutic agents for autoimmune diseases [120]. Currently, *Aspergillus terreus* is used for industrial itaconic acid production. Given the right conditions, this highly efficient filamentous fungus achieves near theoretical yields and titers over 100 g L⁻¹ at low pH values [132, 263, 264]. *Ustilago maydis* is also a well-studied itaconic acid producer, its main differences to *A. terreus* being its yeast-like growth [139, 140]. In both organisms, the genes encoding the itaconate production pathway are clustered and co-regulated, and the metabolic pathway is well studied [136, 139, 142, 143, 146, 255, 256, 259]. Process optimization and strain engineering drastically enhanced the performance of both organisms, with *A. terreus* still being the better producing strain in terms of yield, titer, and rate [23, 264]. That said, the process-associated advantage of the yeast-like growth of *U. maydis*, although hard to express in numeric terms, may make this organism more favorable, especially at large scale [24]. Itaconate production is not uncommon in Ustilaginaceae, and this trait is also found in other *Ustilago* species like *Ustilago veitiveriae* [208], as well as in some *Pseudozyma* and *Sporisorium* species [95]. The itaconate gene cluster is conserved in almost all of these species and in many cases it can be activated through overexpression of the cluster-associated regulator Ria1, even across genus

boundaries [265]. One species of particular interest is *Ustilago cynodontis*, a relatively unknown pathogen of *Cynodon dactylon*, an invasive plant in parts of Europe [136, 266]. Geiser *et al.* reported in a screening that *U. cynodontis* is one of the best itaconate producing strains, especially at low pH [95]. Furthermore, this strain doesn't produce glycolipids [267]. These two traits will cause benefits later in process-engineering, such as reduced base consumption, easier downstream processing, and autosterility [201]. However, due to its strong filamentous growth, this species was thus far not intensively investigated [95]. In all known smut fungi, morphology is coupled to sexual development and pathogenesis, where haploid cells of different mating types fuse together to build up a dikaryotic filament, which penetrates the plant [175]. However, haploid cells can also grow filamentously under non-optimal growth conditions, like low pH values, nitrogen limitation, and in the presence of sunflower oil [137, 268-273]. In this study, we employ a combination of morphological and metabolic engineering to make *U. cynodontis* accessible as an efficient, yeast-like, alternative host for itaconic acid production at low pH. This is achieved by disrupting the signal transduction pathway involved in the sexual cycle of this species to avoid the morphological switch, and by overexpressing and/or deleting essential itaconate cluster genes to enhance itaconate production titer, rate, and yield.

3.3.3 Results and discussion

3.3.3.1 Comparing production behavior of *U. cynodontis* and *U. maydis*

Ustilago cynodontis was previously identified as a potent itaconate producer with a higher pH tolerance, but more distinct filamentous growth, than *Ustilago maydis* [95]. In order to confirm this, cultivation studies were performed in batch cultures with different buffers, leading to different pH values upon acid production. *U. maydis* MB215 and *U. cynodontis* NBRC9727 were cultured in System Duetz® 24-well plates, in screening medium buffered with 30 mM MES, 100 mM MES, and 33 g L⁻¹ CaCO₃ (Figure 25 and Figure 26). In all used buffers, *U. cynodontis* produced more itaconate than *U. maydis*. This difference was especially apparent in 30 mM MES, where *U. cynodontis* produced 2.6 ± 0.2 g L⁻¹ itaconate and an estimated 9.6 ± 0.2 g L⁻¹ (S)-2-hydroxyparaconate after 96 h, while *U. maydis* did not produce any detectable acid. The pH of the *U. cynodontis* culture decreased to 2.0 under these conditions, while that of the *U. maydis* culture did not drop below 4 (Figure 25D). The glucose consumption rate and growth of *U. maydis* were higher than that of *U. cynodontis*, indicating that the lack of acid production of the former can't be attributed to a general cellular inhibition (Figure 25E). A regulatory switch to other products is more likely, as it is known that *U. maydis* produces glycolipids at low pH conditions [206, 274]. Unfortunately, *U. cynodontis* grew strongly filamentously. Although this morphology did not affect itaconate production much in the well-aerated small-scale System Duetz® plates, scaling up to 1.3 L bioreactor was not successful as we encountered the same issues as described by Geiser *et al.* [95]. Only 5.1 ± 0.2 g L⁻¹ itaconate was produced at pH 6 and nearly none at pH 3.8 after 192 h (Figure 27 and Figure 28). Attempts to maintain yeast-like morphology in the bioreactor by changing culture condition as described by Zapata-Morin *et al.* [275] and Durieu-Trautmann *et al.* [276] were unsuccessful. Although challenging, a bioprocess with filamentous fungi is undoubtedly possible [19]. This would, however, negate the main benefit of *Ustilago* over *Aspergillus*, and we, therefore, opted for a genetic engineering approach to control the morphology of *U. cynodontis*.

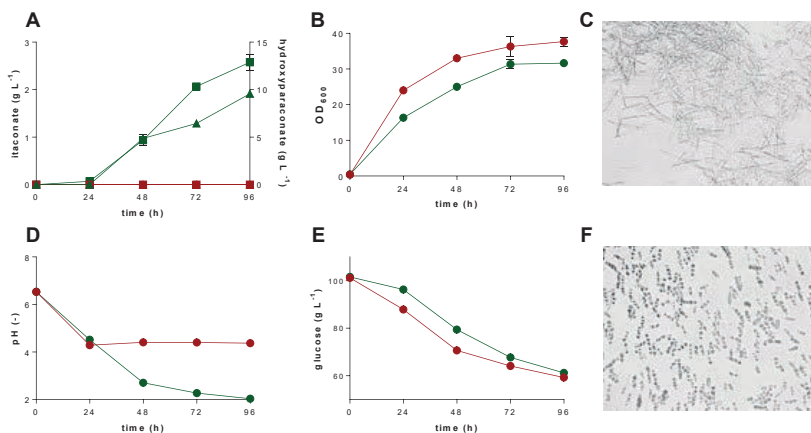


Figure 25. Acid production and growth of *U. maydis* MB215 (red) and *U. cynodontis* NBRC9727 (green). Itaconate (■) and (S)-2-hydroxyparaconate concentration (▲) (A), growth (OD₆₀₀) (B), pH values (D), glucoses consumption (E) DIC images of *U. cynodontis* (C) and from *U. maydis* (F) (magnification 630x), during System Duetz[®] cultivation in screening medium with 100 g L⁻¹ glucose buffered with 30 mM MES is shown. Errors indicate the standard error of the mean (n=3).

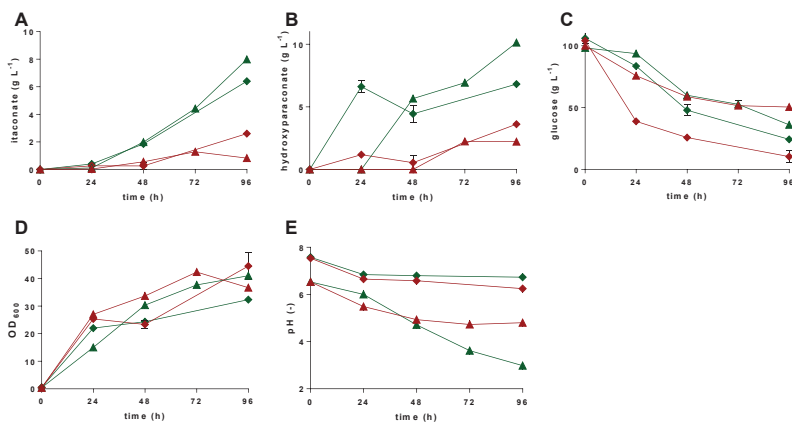


Figure 26. Acid production and growth of *U. maydis* MB215 (red) and *U. cynodontis* NBRC9727 (green). Itaconate (A) and (S)-2-hydroxyparaconate concentration (B), glucoses consumption (C), growth (OD₆₀₀) (D) and pH values (E) during System Duetz[®] cultivation in screening medium buffered with 100 mM MES (▲) or 33 g L⁻¹ CaCO₃ (◆) with 100 g L⁻¹ glucose is shown. Error bars indicate the standard error of the mean (n=3).

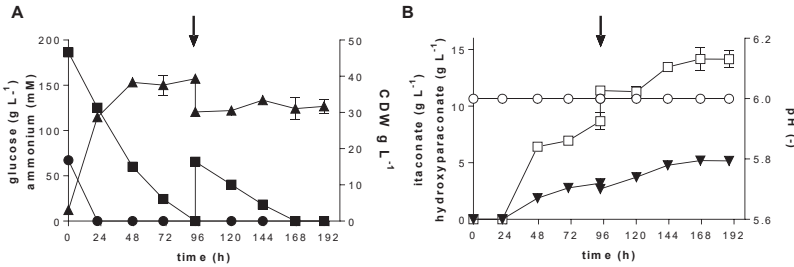


Figure 27. Controlled high-density pulsed fed-batch fermentations of *U. cynodontis* NBRC9727. A: CDW (▲), glucose (■) and ammonium concentration (●) and B: Concentration of itaconate (▼), (S)-2-hydroxyitaconate (□) and pH (○) in a bioreactor containing batch medium with 200 g L⁻¹ glucose, 4 g L⁻¹ NH₄Cl at pH 6.0 titrated with NaOH. Arrows indicate addition of 100mL of a 50 % glucose stock. Error bars indicate the deviation from the mean (n=2). The raw data originates from the Master Thesis of Apilaasha Tharmasothirajan [277].

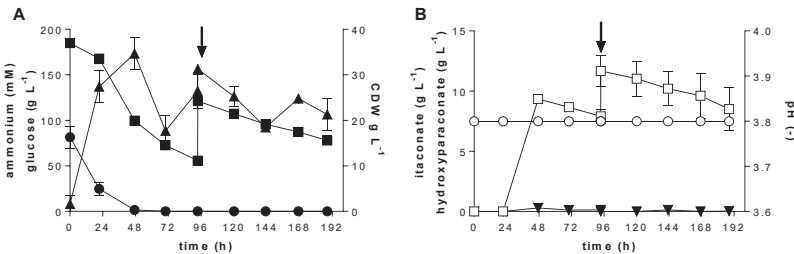


Figure 28. Controlled high-density pulsed fed-batch fermentations of *U. cynodontis* NBRC9727. A: CDW (▲), glucose (■) and ammonium concentration (●) and B: Concentration of itaconate (▼) and (S)-2-hydroxyitaconate (□) and pH (○) in a bioreactor containing batch medium with 200 g L⁻¹ glucose, 4 g L⁻¹ NH₄Cl at pH 3.8 titrated with NaOH. Arrows indicate addition of 100mL of a 50 % glucose stock. Error bars indicate the deviation from the mean (n=2). The raw data originates from the Master Thesis of Apilaasha Tharmasothirajan [277].

3.3.3.2 Morphological engineering in *Ustilago cynodontis* NBRC9727

Ustilago cynodontis belongs to the smut fungi, a group of biotrophic parasites. The process of plant colonization and infection is coupled with sexual development governed by a complex regulatory system, which is well studied in *Ustilago maydis*. Haploid cells with different mating types can recognize each other with a pheromone receptor system to fuse and build up a dikaryotic filament. The dikaryon is afterward able to invade the maize plant via an appressorium [228, 278, 279]. Two signal cascades, namely a cyclic AMP-dependent protein kinase A pathway and a Ras/mitogen-activated protein kinase (MAPK) pathway play a major role in plant-cell interaction in *U. maydis* and are involved in mating, pathogenicity, and morphology (Figure 29). The deletion of genes encoding components of these pathways causes *U. maydis* to lose the ability to induce filamentous growth and to colonize the maize plant [268, 280-282]. A tBLASTn analysis [238] of the proteins Ras2, Fuz7, and Ubc3, which are part of the *U. maydis* MAPK [175] signal cascades, against the genome sequence of *Ustilago cynodontis* NBRC9727 (GenBank accession number: LZZZ00000000; [235] identified putative orthologues with protein sequence identities between 89 and 99 %. Naming conventions of *U. maydis* genes will be adopted henceforth. In order to maintain the yeast-like growth of *U. cynodontis*, single deletions of *ras2*, *fuz7*, and *ubc3* were

constructed and characterized in terms of cell morphology, organic acid production, and fitness. Since no molecular tools were available for *U. cynodontis*, they were established based on *U. maydis* plasmids and methods (appendix; Figure 52 and D3). The resulting mutants were subjected to a variety of stresses typically encountered in biotechnological processes, including low pH (30 mM MES buffer), the presence of solids (33 g L⁻¹ CaCO₃), osmotic pressure (200 g L⁻¹ glucose), and growth on a non-preferred carbon source (100 g L⁻¹ glycerol). As a positive control for filamentous growth, the screening medium was supplemented with 7 % sunflower oil [268]. Morphology was analyzed macro- and microscopically at different time points of the cultivation, the pH course was documented, and samples were analyzed by HPLC for organic acid production.

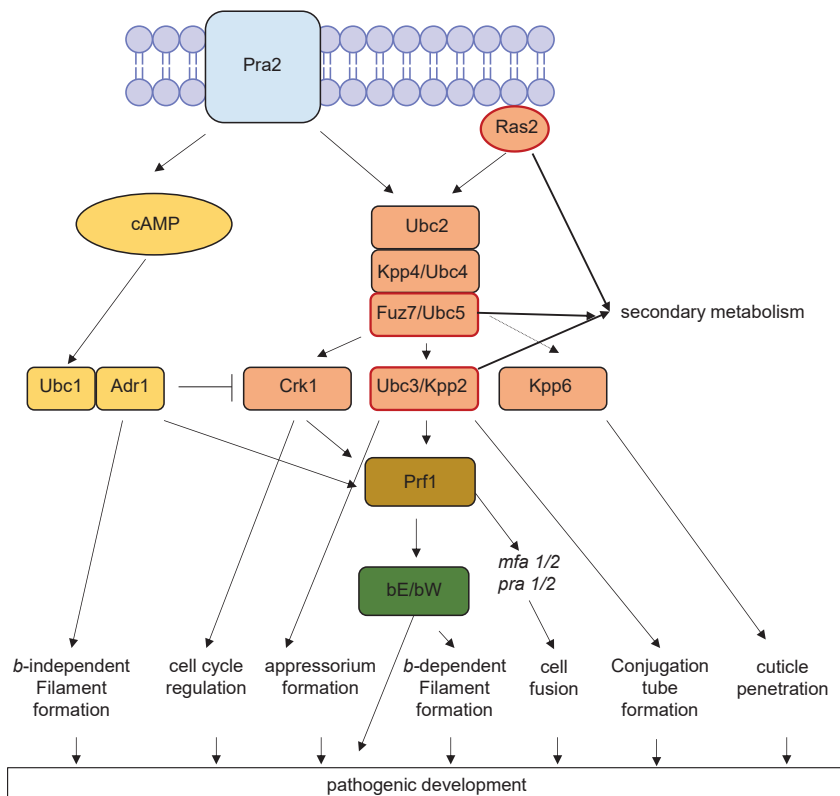


Figure 29. The cAMP and MAPK signaling pathways in *U. maydis* adapted with minor modifications from Kahman and Kämper [279], Brefort *et al.* [175] and Lanver *et al.* [278]. Deleted genes in the MAPK cascade are highlighted with red borders (*ras2*, *fuz7*, *ubc3*).

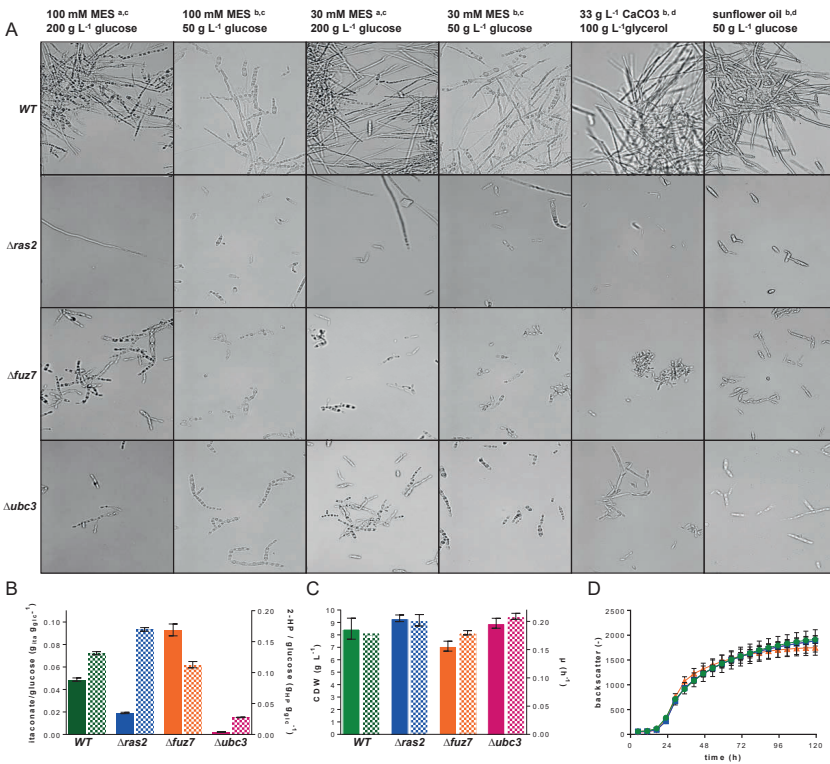


Figure 30. Morphological engineering in *U. cynodontis* NBRC9727. DIC images at a magnification of 1000 X after 48 h^(a) and 72 h^(b) cultivation (A), yields of itaconate (filled bars) and (S)-2-hydroxypropanoate (patterned bars) per consumed glucose (B), CDW (filled bars), growth rate (patterned bars) (C), and backscatter (D) during System Duetz[®] (A, B, ^(c)) or shake flask cultivation (C, D ^(d)) of *U. cynodontis* wildtype (green), $\Delta ras2$ (blue), $\Delta fuz7$ (orange), and $\Delta ubc3$ (pink) in screening medium with various carbon sources, carbon source concentrations, and buffer systems. Error bars indicate the standard error of the mean (n=3). Microscopy images were taken partially from the Master Thesis of Apilaasha Tharmasothirajan [277] and growth curve in D was taken from the Bachelor thesis of Svenja Meyer [283]

Exemplary DIC images after 48 h or 72 h with 100- and 1000-fold magnifications are shown in Figure 30A, and in the appendix in Figure 53 and Figure 54. Typically, a mixture of filamentous and yeast-like cells was observed for the wildtype, with high glucose concentration, sunflower oil, and glycerol causing more filamentous cells. In contrast, no filamentous growth was observed in the *fuz7* and *ubc3* knockout strains under all tested conditions, while *U. cynodontis* $\Delta ras2$ grew filamentously in the high glucose concentration and partially also in the other conditions. Macroscopic differences were also apparent, especially on glycerol, where *U. cynodontis* $\Delta fuz7$ had a yellowish color, while all other strains became highly pigmented and showed extensive clumping (appendix; Figure 55). However, this did not correlate with filamentous growth, which was only observed in the wildtype. Taken together, these results are in good accordance with the phenotypes observed in *ras2*, *fuz7*, and *ubc3* knockout strains of *U. maydis* [268], indicating that these genes have a similar function in *U. cynodontis*. While this will need to be confirmed in the context of plant-pathogen interaction with *C. dactylon*, for the purposes of this study it can be

concluded that the disruption of these genes, especially *fuz7*, is instrumental for morphology control under biotechnologically relevant conditions. Because the focus of this work was to optimize itaconate production in *U. cynodontis*, cultures were also analyzed by HPLC and pH was determined to ascertain the effect of the knockouts on organic acid secretion (Figure 30B, Table 7, and in the appendix Figure 56). While deletion of *ras2* and *ubc3* resulted in a strong decrease in itaconate production for all buffer conditions, the $\Delta fuz7$ strain reached a significantly higher titer in all tested conditions, except 100 mM MES buffer, in which the mutant produced significantly less than the wildtype. Especially large differences were observed in weakly buffered conditions, where the $\Delta fuz7$ strain produced 2.3-fold more itaconate than the wildtype and 8.3-fold more than the $\Delta ras2$ strain. In contrast, *U. cynodontis* $\Delta ras2$ produced more (*S*)-2-hydroxyparaconate than either the wildtype or the $\Delta fuz7$ strain, especially if stronger buffers were used with glucose as carbon source. These differences in production achieved by disruption of the same MAPK signal cascade at different entry points indicate an unexpected link between the regulation of *Ustilago*'s life cycle and the itaconate gene cluster. Partly, these differences may be attributed to cell morphology, like in *A. terreus* where itaconate is only efficiently produced in a specific pellet morphology [132, 284, 285]. That said, the differences between knockout strains displaying the same morphology indicates a more intricate regulatory network, which connects different levels of the MAPK signal cascade with secondary metabolite production like it is the case for several other fungi [286].

Table 7. Production parameters of various *U. cynodontis* strains during System Duetz® cultivation in screening medium with various carbon sources, carbon source concentrations, and buffers. Errors indicate the standard error of the mean (n=3).

conditions		<i>U. cynodontis</i>	$\Delta ras2$	$\Delta fuz7$	$\Delta ubc3$
30 mM MES 50 g L ⁻¹ GLC	$Y_{P/S}(g_{ITA}g_{GLC}^{-1})^a$	0.05 ± 0.00	0.02 ± 0.00	0.09 ± 0.01	0.00 ± 0.00
	$Y_{P/S}(g_{HP}g_{GLC}^{-1})^a$	0.13 ± 0.00	0.17 ± 0.00	0.11 ± 0.01	0.03 ± 0.00
	ITA ^b (g L ⁻¹) ^d	2.10 ± 0.05	0.57 ± 0.01	4.75 ± 0.20	0.08 ± 0.02
	HP ^c (g L ⁻¹) ^d	5.66 ± 0.10	5.07 ± 0.11	5.77 ± 0.18	1.07 ± 0.02
100 mM MES 50 g L ⁻¹ GLC	$Y_{P/S}(g_{ITA}g_{GLC}^{-1})^a$	0.13 ± 0.00	0.04 ± 0.00	0.12 ± 0.00	0.03 ± 0.00
	$Y_{P/S}(g_{HP}g_{GLC}^{-1})^a$	0.14 ± 0.00	0.25 ± 0.00	0.12 ± 0.00	0.06 ± 0.00
	ITA (g L ⁻¹) ^d	6.28 ± 0.08	1.20 ± 0.06	5.25 ± 0.07	1.11 ± 0.03
	HP (g L ⁻¹) ^d	6.95 ± 0.04	7.39 ± 0.13	5.14 ± 0.03	2.03 ± 0.03
33 g L ⁻¹ CaCO ₃ 50 g L ⁻¹ GLC	$Y_{P/S}(g_{ITA}g_{GLC}^{-1})^a$	0.09 ± 0.00	0.10 ± 0.00	0.13 ± 0.00	0.03 ± 0.00
	$Y_{P/S}(g_{HP}g_{GLC}^{-1})^a$	0.09 ± 0.01	0.19 ± 0.00	0.11 ± 0.00	0.06 ± 0.00
	ITA (g L ⁻¹) ^d	4.70 ± 0.12	3.62 ± 0.04	5.88 ± 0.05	1.08 ± 0.09
	HP (g L ⁻¹) ^d	4.35 ± 0.34	6.83 ± 0.06	4.80 ± 0.04	2.31 ± 0.04
33 g L ⁻¹ CaCO ₃ 100 g L ⁻¹ GLY	$Y_{P/S}(g_{ITA}g_{GLY}^{-1})^e$	0.06 ± 0.00	0.04 ± 0.01	0.07 ± 0.01	0.02 ± 0.00
	$Y_{P/S}(g_{HP}g_{GLY}^{-1})^e$	0.07 ± 0.00	0.05 ± 0.01	0.05 ± 0.00	0.03 ± 0.00
	ITA (g L ⁻¹) ^d	5.15 ± 0.13	1.83 ± 0.54	8.39 ± 0.80	1.61 ± 0.07
	HP (g L ⁻¹) ^d	6.00 ± 0.29	2.56 ± 0.69	5.30 ± 0.06	2.85 ± 0.11

^a $Y_{P/S}$: overall yield product per consumed glucose

^b ITA: itaconate

^c HP: (S)-2-hydroxyparaconate

^d maximum titer

^e $Y_{P/S}$: overall yield product per consumed glycerol

The abovementioned knockouts drastically impact the life cycle of *Ustilago* and may therefore, also affect the fitness of the cells. To determine whether this is the case, growth rates of the mutants were determined using the Cell Growth Quantifier® with screening medium including 50 g L⁻¹ glucose and 30 mM MES (Figure 30D). With exponential growth rates of 0.18 ± 0.01 h⁻¹ for the wildtype, 0.20 ± 0.02 h⁻¹ for the $\Delta ras2$ strain, 0.18 ± 0.01 h⁻¹ for $\Delta fuz7$, and 0.21 ± 0.01 h⁻¹ for $\Delta ubc3$, these deletions didn't negatively affect the growth rate of *U. cynodontis*, and the $\Delta ubc3$ strain even showed a minor but significant increased rate compared to the wildtype. Final OD₆₀₀ (33.67 ± 0.58 for the wildtype, 39.3 ± 1.15 for the $\Delta ras2$ strain, 32.33 ± 1.15 for $\Delta fuz7$, and 39.67 ± 1.53 for $\Delta ubc3$) and CDW (Figure 30C) were also determined to exclude any effects of morphology on the biomass analysis in later stages, where secondary growth is a significant factor [137, 197]. Also here there was no significant difference between the wildtype and the mutants. As a final test, *U. cynodontis* $\Delta fuz7$ was applied in pulsed-fed-batch cultures in a 1.3-L bioreactor stirred at 1,200 rpm. The culture was started at pH 6, and allowed to drop down to pH 2.1, after which it was further maintained at pH 3.8 through the addition of NaOH. This regime is similar to that described by Heverkerl *et al.* [263] for *A. terreus*. Also under these conditions, *U. cynodontis*

Δfuz7 showed stable yeast-like growth and a homogenous broth for the whole 284 h of fermentation, resulting in the production of $21.2 \pm 0.0 \text{ g L}^{-1}$ itaconate, with a yield of $0.22 \pm 0.01 \text{ gITA gGLC}^{-1}$ and a productivity of $0.07 \text{ g L}^{-1} \text{ h}^{-1}$. Further 9.25 g L^{-1} (*S*)-2-hydroxyparaconate was produced (Figure 31). In total $30.42 \pm 0.11 \text{ g L}^{-1}$ acid was produced, which corresponds to a yield of $0.32 \pm 0.01 \text{ g}_{\text{ACID}} \text{ g}_{\text{GLC}}^{-1}$. In all, these results show that deletions in the MAPK pathway, which governs the sexual cycle of *Ustilago* enable the control of cell morphology under biotechnologically relevant conditions, without significantly affecting cell fitness. The achieved stable yeast-like morphology will likely positively affect bioprocess parameters such as the oxygen transfer rate, viscosity, clogging, and reduced the sensitivity to hydro-mechanical stress [197]. *U. cynodontis Δfuz7* was chosen for further study since it was the goal of this study to increase itaconate production at low pH.

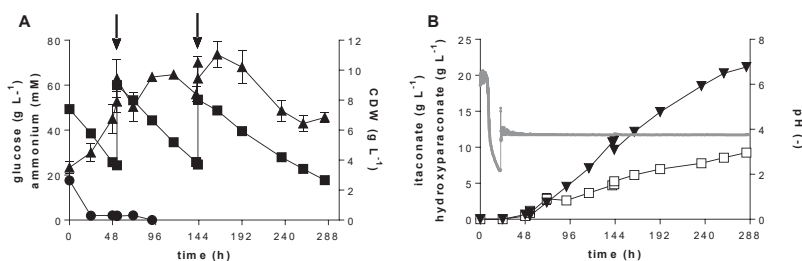


Figure 31. Controlled high-cell density pulsed fed-batch fermentations of *U. cynodontis Δfuz7*. A: CDW(▲), glucose (■) and ammonium concentration(●) and B: Concentration of itaconate (▼) and (*S*)-2-hydroxyparaconate (□) and pH (continuous line) in a bioreactor containing batch medium with 50 g L⁻¹ glucose, 0.8 g L⁻¹ NH₄Cl at an initial pH of 6, which was allowed to drop until 21.3 h, after which it was controlled at 3.8 with NaOH. The stirring rate was constant at 1200 rpm. Arrows indicate addition of 100 mL of 50 % glucose. Error bars indicate the deviation from the mean (n=2). Raw data were taken from the Master Thesis of Apilaasha Tharmasothirajan [277].

3.3.3.3 Metabolic engineering of *U. cynodontis* to improve itaconate production

In *Ustilago maydis*, the characterization of the itaconate production pathway and the associated gene cluster enabled significant enhancements in product yield, titer, and rate by metabolic engineering [139, 140]. Further, the itaconate cluster is conserved in several Ustilaginaceae, including *Ustilago cynodontis* NBRC9727 [265]. To confirm the putative functions of the most important genes in this cluster, deletion mutants of genes encoding the mitochondrial transporter (*Uc_mtt1*) and extracellular transporter (*Uc_itp1*) were constructed in the wildtype background. Further deletions of the regulator (*Uc_ria1*) and the P450 monooxygenase (*Uc_cyp3*) were constructed in *U. cynodontis Δfuz7^r* (r = recycled hygromycin cassette). To characterize these deletion mutants, cultivation studies in screening medium with 50 g L⁻¹ glucose buffered with 30 mM MES and 100 mM MES were performed, using *U. cynodontis* NBRC9727 and *U. cynodontis Δfuz7^r* as controls (Figure 32, and in the Appendix Figure 57, and Figure 58). Deletion of both transporters (*Uc_mtt1*, *Uc_itp1*) and the regulator *Uc_ria1* abolished or strongly reduced itaconate and (*S*)-2-hydroxyparaconate production. In *U. maydis* deletion of the transporters resulted in a decrease of itaconate production but not in a complete loss like observed here [139]. The deletion of *cyp3* led to a complete loss of (*S*)-2-hydroxyparaconate production and yielded three times more itaconate. This matches the results of Geiser *et al.* [139] for *U. maydis* with the exception that itaconate production was not increased to the same relative extent. The

characterization of these deletion strains demonstrates that the genes *ria1*, *cyp3*, *mtt1*, and *itp1*, and in addition to that also likely the rest of the gene cluster in *U. cynodontis*, are involved in the itaconate biochemical pathway, thereby providing the fundamental knowledge needed to optimize itaconate production through metabolic engineering.

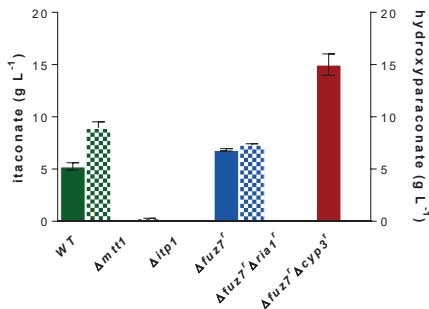


Figure 32. Organic acid production of various *U. cynodontis* deletion strains. Itaconate and (S)-2-hydroxyparaconate production by various *U. cynodontis* mutants in comparison to wildtype and $\Delta fuz7$ controls during System Duetz[®] cultivation in screening medium with 100 mM MES and 50 g L⁻¹ glucose. Error bars indicate the standard error of the mean (n=3).

In *U. maydis* a combination of *cyp3* deletion and *ria1* overexpression drastically improved itaconate production, with a 4-fold higher production compared to the wildtype [139, 140]. Also, overexpression of the mitochondrial transporter *mtt1* led to a similar increase of itaconate in the *ria1* overexpression mutant [139]. Recently we could show that the mitochondrial transporter *At_MttA* from *A. terreus* enables higher itaconate production in *U. maydis* [287]. These modifications were thus sequentially introduced into *U. cynodontis* $\Delta fuz7$. To overexpress *At_mttA*, the gene was controlled by the promoter P_{etef} and the terminator T_{nos} from *U. maydis*, while the overexpression construct was integrated randomly into the genome. Overexpression of the native *ria1* was also achieved by random genome integration, but in this case, *ria1* was controlled by its native promoter and terminator since previous complementation experiments with P_{etef} and T_{nos} were not successful for *ria1* [265]. Overexpression of this gene was thus achieved by an increase in copy number, maintaining its native regulation. To exclude locus-dependent negative effects of the random genomic insertion, four individual transformants of the *ria1* construct and 63 transformants of the *mttA* construct were evaluated and the best performing clone was selected for further study (appendix; Figure 59 and Figure 60 and Figure 60). The resulting strains were characterized in screening medium buffered with 30 mM MES (Figure 33) or with 100 mM MES (Figure 34). Overexpression of *ria1* led to a 1.7-fold increase in itaconate production compared to *U. cynodontis* $\Delta fuz7$ $\Delta cyp3$. Additional overexpression of the mitochondrial transporter encoding *At_mttA* in *U. cynodontis* $\Delta fuz7$ $\Delta cyp3$ $P_{etef}ria1$ increased production a further 49 %. Compared to the wildtype *U. cynodontis* $\Delta fuz7$ $\Delta cyp3$ $P_{etef}mttA$ $P_{ria1}ria1$ produced 6.5-fold more itaconate with a titer of 22.3 ± 0.2 g L⁻¹ and a yield of 0.42 ± 0.003 g_{ITA} g_{GLC}⁻¹. All engineered strains showed the same yeast-like morphology as previously observed for *U. cynodontis* $\Delta fuz7$, whereas the wildtype showed a mixture of yeast-like and filamentous cells. In contrast to *U. maydis*, no malate was observed, and instead low concentrations of erythritol were transiently produced as a byproduct. At least one unknown product was also detected by

HPLC as a peak with the RI-detector. Since no peak was observed with the UV detector, the compound might be an unknown polyol or glycolipid. When 100 mM MES was used as buffer, same patterns were observed with only marginally higher titers (Figure 34). With 30 mM MES, the optimized strain shows a linear itaconate production rate between 48 and 96 h, in spite of the fact that in this timespan, the pH was between 2.9 and 2.46. These two observations highlight the pH tolerance of *U. cyndontis* and the fact that the modifications did not significantly impact the fitness of the strain.

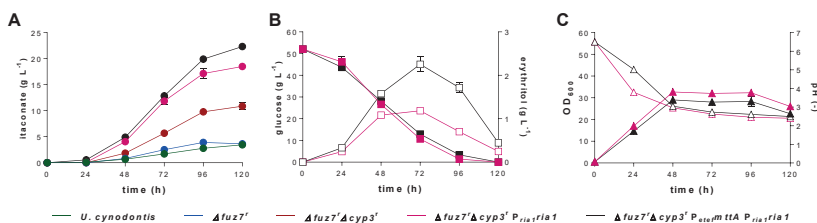


Figure 33. Itaconate and erythritol production and growth of engineered *U. cyndontis* strains. A: Itaconate production (●), B: glucose (■), and erythritol concentration (□) and C: OD₆₀₀ (▲), and pH (Δ) during System Duetz[®] cultivation in screening medium with 30 mM MES and 50 g L⁻¹ glucose. Error bars indicate the standard error of the mean (n=3).

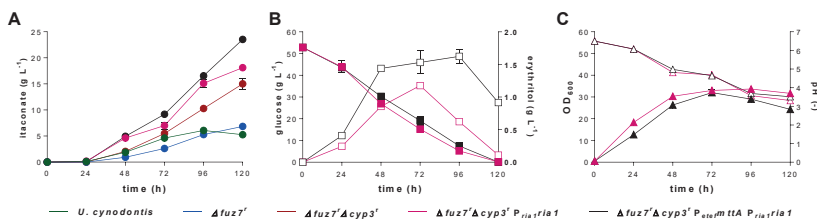


Figure 34. Itaconate and erythritol production and growth of various engineered *U. cyndontis* strains. A: Itaconate production, B: glucose (■), and erythritol concentration (□) and C: OD₆₀₀ (▲), and pH (Δ) during System Duetz[®] cultivation in screening medium with 100 mM MES and 50 g L⁻¹ glucose. Error bars indicate the standard error of the mean (n=3).

3.3.4 Conclusion

This study addressed one of the main drawbacks of *Ustilago* compared to *Aspergillus* in itaconic acid production, namely pH tolerance. We could transform the strong filamentous growth of the pH tolerant *U. cynodontis* NBRC9727 into a stable yeast-like growth by morphological engineering under process-relevant conditions. Combined with metabolic engineering, itaconate production was increased 6.5-fold with minimal impact on host fitness and pH tolerance. This powerful combination of stable yeast-like morphology and pH tolerance opens up a range of possibilities in the field of process development. Given its unstable morphology, basic operations like pumping or filtration of fermenter broth are complicated with *A. terreus*. Fermentation intensification is now becoming possible with the optimized *U. cynodontis*, enabling efficiency gains through the development of continuous processes, *in situ* product removal, or cell retention. Thus, the process window of itaconic acid production has been greatly expanded into new dimensions.

3.3.5 Acknowledgements

We thank Kerstin Schipper and Michael Feldbrügge (Institute for Microbiology, Heinrich Heine University Düsseldorf) for providing the plasmids pstorI_1rh_WT (pUMa1522), pstorI_1rh_M1 (pUMa1523), pMF1-h and pFLPexPC and Jan Schirawski (Institute of Applied Microbiology, RWTH-Aachen) for the plasmids pSMUT, pNEBUC, pNEBUN and pNEBUP and Kylie L. Luska and Tim den Hartog (Institute for Technical and Macromolecular Chemistry, RWTH-Aachen) for contributions to (S)-2-hydroxyparaconate synthesis.

Chapter 3.4

Process engineering of pH tolerant *Ustilago cynodontis* for efficient itaconic acid production

Will be submitted for publication as:

Hamed Hosseinpour Tehrani, Katharina Saur, Apilaasha Tharmasothirajan, Lars M. Blank and Nick Wierckx. Process engineering of pH tolerant Ustilago cynodontis for efficient itaconic acid production.

Authors' contributions:

Hamed Hosseinpour Tehrani performed most experiments. Nick Wierckx conceived and supervised the study. Hamed Hosseinpour Tehrani designed and performed experiments and analyzed results with the help of Nick Wierckx and Lars M. Blank. Hamed Hosseinpour Tehrani wrote the manuscript with help of Nick Wierckx and Lars M. Blank. Apilaasha Tharmasothirajan and Katharina Saur contributed to fermentation experiments.

3.4 Process engineering of pH tolerant *Ustilago cynodontis* for efficient itaconic acid production

3.4.1 Abstract

Ustilago cynodontis ranks among the relatively unknown itaconate production organisms. In comparison to the well-known and established organisms like *Aspergillus terreus* and *Ustilago maydis*, genetic engineering and first optimizations for itaconate production were only recently developed in this thesis for *U. cynodontis*, enabling this pH tolerant organism to produce itaconate efficiently. Its filamentous phenotype thus far hindered the effective application of this strain. This problem was recently solved by morphological engineering, which, combined with metabolic engineering, yielded new hyperproducing *U. cynodontis* strains. These strains were so far mostly characterized in small scale shaken cultures. Here, we characterize engineered *U. cynodontis* strain in controlled bioreactors and optimize the process for itaconate production. In pH-controlled fed-batch experiments, an optimal pH of 3.6 could be determined for itaconate production in *U. cynodontis* $\Delta fuz7$. With the optimized *U. \Delta fuz7 \Delta cyp3^r P_{efefmttA} P_{ria1}ria1*, titers up to $82.9 \pm 0.8 \text{ g L}^{-1}$ were reached in a high-density pulsed fed-batch fermentation at this pH. The use of a constant glucose feed controlled by in-line glucose analysis increased the yield in the production phase to $0.61 \text{ g}_{\text{ITA}} \text{ g}_{\text{GLC}}^{-1}$, which is 84 % of the theoretical maximum. Productivity could be improved to a maximum of $1.44 \text{ g L}^{-1} \text{ h}^{-1}$, and product toxicity could be prevented by a repeated-batch application. The results obtained are discussed in a biotechnological context and show the great potential of *U. cynodontis* as an itaconate producing host.

3.4.2 Introduction

Itaconic acid is an unsaturated dicarboxylic acid with two pK_a values at 3.84 and 5.55. Depending on the pH value, the undissociated form H_2ITA , the single dissociated form HITA^- and the double dissociated form ITA^{2-} can exist [107, 132]. Further it consists a methylene group, and its functional groups are especially interesting for the polymer industry. Depending on the groups chosen for polymerization, polymers with different properties can be synthesized and further used for different applications in the industry like in the pharmaceutical sector [110, 112, 114, 115, 288-291]. *Aspergillus terreus*, *Ustilago maydis* and *Ustilago cynodontis* are known as good itaconate producing organisms [21, 140, 292]. The biochemical pathways and underlying gene clusters responsible for itaconate production in these organisms are well-studied [139, 140, 255, 265] (chapter 0). Since over 60 years *A. terreus* is used for itaconate production by batch fermentation [110, 251]. What exactly triggers itaconate production in *A. terreus*, and especially why it produces itaconate, is still unknown [21]. In general production is initiated at low pH-values [23, 29, 293]. After initiating efficient itaconate production, it could be shown that increasing pH-value can enhance itaconate titers, whereby time point of increasing pH is important [131, 132]. By controlling the pH at 3.4 after the itaconate initiating phase, product titers up to 160 g L^{-1} could be achieved [132]. Further productivity could be increased by media optimization and pH-shift experiment to $1.15 \text{ g L}^{-1} \text{ h}^{-1}$ [131] and the highest known yield with $0.72 \text{ g}_{\text{ITA}} \text{ g}_{\text{GLC}}^{-1}$ was reached by optimizing oxygen transfer [134]. Following submerged fermentation with *A. terreus*, the itaconic acid is typically purified by repeated crystallization in industrial settings [294]. Although *A. terreus* is a highly efficient itaconate producer, some drawbacks exist for this host. One feature that causes high costs is the ability to grow as pellet or mycelia, respectively [285]. While pellet sizes between 0.1 to 0.5 mm resulted in the highest itaconate productivity [155], growing in mycelial form leads to a stop of itaconate production [132, 285]. This morphology is strongly influenced by media compositions. Currently molasses is used as carbon source to reduce costs.

Since impurities like manganese are known to induce mycelium formation, this impure substrate must be pretreated to remove impurities by ion exchange chromatography or ferrocyanide treatment [22]. This additionally steps make medium preparation costly. But also, pH- and shear stress can induce mycelial growth and abolish itaconate production in *A. terreus* [21].

Besides *A. terreus* many members of Ustilaginaceae are known to produce itaconate naturally [95]. The most well studied member of this family is *U. maydis*. In wildtype *U. maydis*, itaconate production is initiated by nitrogen limitation [261] and production takes place above pH-values of 5.5 [95]. While its yeast-like growth behavior is a benefit especially for production in a bioreactor, current values for titer, yield and productivity on glucose are far away from that what is published for *A. terreus* [140, 265]. *U. cynodontis* is another promising Ustilaginaceae which, however, displayed strong filamentous growth [95, 126]. Unlike *U. maydis*, *U. cynodontis* has a high pH tolerance, which poses major benefits for itaconate production. Recently we could overcome the strong filamentous growth behavior under biotechnologically relevant conditions through the deletion of *fuz7*, encoding a MAPK protein involved in the regulation of tube formation and filamentous growth. Further it was possible to increase itaconate production up to 6.5-fold compared to the wildtype by metabolic engineering, involving the deletion of P450 monooxygenase *cyp3* and the overexpression of the itaconate cluster regulator *Rial* and by heterologous expression of mitochondrial transporter *MttA* from *A. terreus* [292]. In this study, we apply this optimized *U. cynodontis* strain in controlled bioreactors. The optimal pH value for itaconate production is determined, followed by process optimization to enhance itaconate production by different glucose feeding strategies and by repeated batch. By this means, we demonstrate the potential of *U. cynodontis* as alternative pH-tolerant itaconate producer with a stable yeast-like morphology.

3.4.3 Results and discussion

3.4.3.1 *Influence of pH and yeast extract on itaconate production by engineered U. cynodontis*

Previously we reported that by deletion of *fuz7* the strong filamentous morphology of *Ustilago cynodontis* was switched to stable yeast-like growth, resulting in a better production of itaconate. Shaking flask experiments in different buffered media indicated that *U. cynodontis* has high pH tolerance, but the optimum for itaconate production could not be determined in this setup. Since it is known that the pH is a key factor in itaconate production with considerable influence on later downstream processes and that protonated itaconate leads to weak acid uncoupling [21, 107, 131, 132], we determine the optimal pH for itaconate production in *U. cynodontis* Δ *fuz7* by pH-controlled fed-batch fermentations (Figure 35). Cultures were performed at pH value of 1.9, 2.5, 3.2, 3.4, 3.6, 3.8, 5.5 and 6.0, these values were set from the beginning of inoculation by manual addition of HCl and controlled afterward with NaOH. The stirrer was set to 1000 rpm in batch medium without yeast extract, 0.8 g L⁻¹ NH₄Cl and 50 g L⁻¹ glucose at the beginning of fermentation. Corresponding titers, yields and OD₆₀₀ are depicted in Figure 35A, B. Strong growth inhibition was observed at pH 1.9 compared to the other cultures. However, *U. cynodontis* Δ *fuz7* both grew and produced itaconate at the second lowest pH of 2.5, although the yield was 1.9-fold lower than at the optimal pH of 3.6 where a titer of 24.7 g L⁻¹ and a yield of 0.27 g_{ITA} g_{GLC}⁻¹ were reached. This difference in production is likely related to the fact that itaconate has three protonation stages, as mentioned in the introduction. Below a pH value of 3.83 the undissociated form H₂ITA is predominant, above 3.83 the single dissociated form HITA⁻ and above 5.55 the

double dissociated ITA^{2-} is predominantly present. In the fully protonated form (H_2ITA) weak acids can diffuse through the plasma membrane and acidify the cytoplasm resulting in stress or growth inhibition for the cell. In contrast, HITA^- and ITA^{2-} cannot freely cross the membrane and stay in the fermentation broth [132, 295-297]. To determine the concentrations of each dissociation form of itaconic acid in this study, CurTiPot was used [298]. Between a pH value of 2.5 and 3.6, the concentration of protonated H_2ITA at the end of the cultures was $14.6 \pm 0.8 \text{ g L}^{-1}$ (Table 8). This concentration is relatively constant, especially considering the much larger differences in total titer, indicating that this protonated product level is inhibitory for the cells. Interestingly, with further increasing pH itaconic acid concentrations decrease, although the relatively harmless dissociated forms are predominant. This was also observed in itaconic acid production in *A. terreus*, where the optimum for production was determined at a pH of 3.4 [132]. However, with *A. terreus*, a morphological change was the main reason for this decrease. Such a morphological change was excluded with *U. cynodontis* Δfuz7 . Likely, the pH optimum for itaconate production is at least in part governed by regulatory mechanisms of the genes in the itaconate cluster.

Table 8. Protonation distribution of controlled high-density pulsed fed-batch fermentation of *U. cynodontis* Δfuz7 at different pH values. Titer, undissociated form H_2ITA , single dissociated form HITA^- and double dissociated ITA^{2-} during fermentation in a bioreactor containing batch medium without yeast extract with 50 g L^{-1} glucose and 0.8 g L^{-1} NH_4Cl controlled at different pH values titrated with NaOH. Error bars indicate the deviation from the mean (n=2) instead of fermentation at pH=3.6 (single representative bioreactor).

pH	Titer ^a (g L ⁻¹)	H ₂ ITA ^b (g L ⁻¹)	HITA ^{-c} (g L ⁻¹)	ITA ^{2-d} (g L ⁻¹)
1.9	0.0 ± 0.0	0.0 ± 0.0	0.0 ± 0.0	0.0 ± 0.0
2.5	15.0 ± 1.2	14.1 ± 1.2	0.9 ± 0.1	0.0 ± 0.0
3.2	20.9 ± 0.5	15.9 ± 0.4	5.0 ± 0.1	0.1 ± 0.0
3.4	22.0 ± 1.1	14.6 ± 0.7	7.2 ± 0.3	0.1 ± 0.0
3.6	24.7	13.7	10.7	0.3
3.8	24.6 ± 0.4	10.7 ± 0.2	13.3 ± 0.2	0.6 ± 0.0
5.5	20.1 ± 0.4	0.1 ± 0.0	6.2 ± 0.1	13.8 ± 0.2
6	17.0 ± 0.0	0.0 ± 0.0	2.1 ± 0.0	14.9 ± 0.0

^a titer: final titer

^b H₂ITA: undissociated

^c HITA⁻: single dissociated

^d ITA²⁻: double dissociated

For all used pH values, no filamentous growth was observed like in shaking cultures in Hosseinpour Tehrani *et al.* [292]. Differences in the color of the fermentation broth were observed. While at low pH-conditions the fermenter broth was yellowish or white, at higher pH-values it became more pigmented. Low amounts of erythritol as side product were measured, which did not show any particular trend. Another major side product was (S)-2-hydroxyparaconate. It has a lower pK_a-value than itaconate [136], and in *U. maydis*, low pH values stimulate the conversion of itaconate to (S)-2-hydroxyparaconate, likely by facilitating its uptake [140]. Hosseinpour Tehrani *et al.* [292] could show that by deletion of *cyp3*, (S)-2-hydroxyparaconate production could be abolished and simultaneously, itaconate production could be increased. A further major increase in itaconate production was achieved by overexpression of *ria1* and *mttA*. Possibly, these modifications affect the pH optimum at which *U. cynodontis* produces itaconate, which should be investigated in the future.

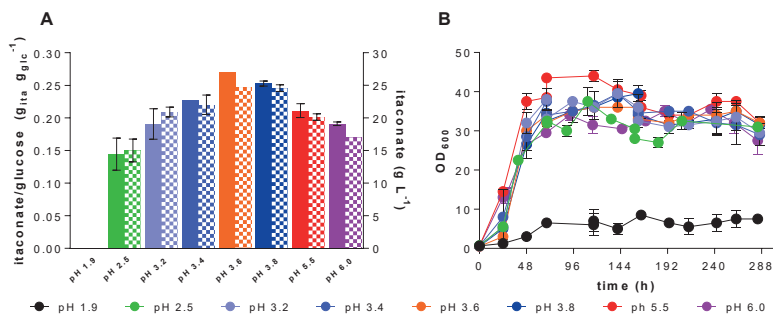


Figure 35. Controlled high-density pulsed fed-batch fermentation of *U. cynodontis* $\Delta fuz7$ at different pH values. A: yield in g_{ita} g_{glc}⁻¹ (filled bars) and itaconate concentration (patterned bars) and B: OD₆₀₀ during fermentation in a bioreactor containing batch medium without yeast extract with 50 g L⁻¹ glucose, and 0.8 g L⁻¹ NH₄Cl controlled at different pH values titrated with NaOH. Error bars indicate the deviation from the mean (n=2) instead of fermentation at pH=3.6 (single representative bioreactor). The figure is modified and partially adapted from the Master thesis of Apilaasha Thamasothirajan [277]

The above-mentioned determination of the pH optimum was performed in a fully mineral medium. Previous fermentations with *U. maydis* were often performed with 1 g L⁻¹ yeast extract added to the starting medium [95]. To see if this addition influences production behavior, the same fermentation with same settings was prepared with *U. cynodontis* $\Delta fuz7$, at determined optimal pH 3.6 with the exception that this time 1 g L⁻¹ yeast extract was not omitted from batch medium (Figure 36). The maximum titer of 25.5 ± 1.1 g L⁻¹ itaconate and yield of 0.25 ± 0.01 g_{ita} g_{glc}⁻¹ was similar to the determined production parameter during fermentation in batch medium without yeast extract. In contrast, maximum (*S*)-2hydroxyparaconate production was increased by 3.5-fold to 17.3 ± 1.1 g L⁻¹, and consequently the total acid concentration in batch medium with yeast extract was 1.4 fold higher. The key factor that could be improved in the case for itaconate was productivity (Figure 36B, D). Without yeast extract, 288 h was necessary, in contrast, addition of yeast extract reduced the time to 206 h and allowed a better and faster production of itaconate. Thus, we decided to following experiments to use batch medium (which includes 1 g L⁻¹ yeast extract) at a pH of 3.6.

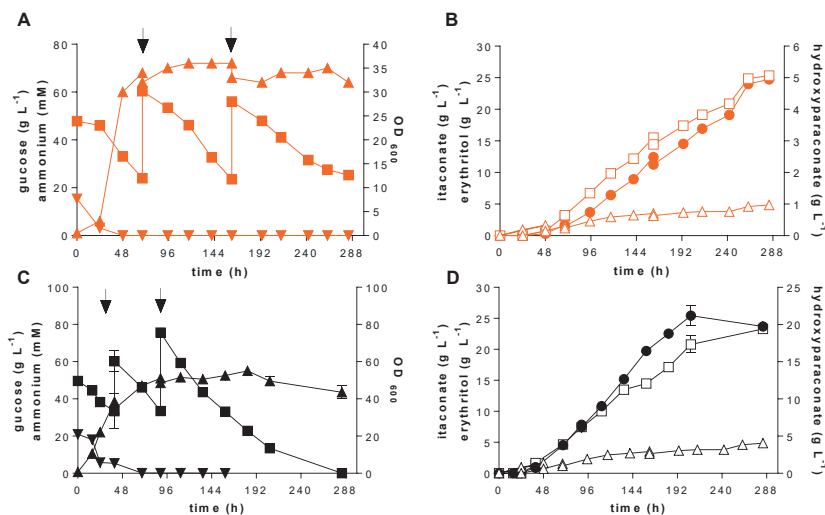


Figure 36. Controlled high-density pulsed fed-batch fermentation of *U. cyndodontis* $\Delta fuz7$. A, B: OD_{600} (\blacktriangle), glucose (\blacksquare) and ammonium concentration (\blacktriangledown), C, D: Concentration of itaconate (\bullet), (S)-2-hydroxyparaconate (\square) and erythritol (Δ) during fermentation in a bioreactor containing batch medium without (A,B) or with yeast extract (C, D) with 50 g L^{-1} glucose, 0.8 g L^{-1} NH_4Cl at pH 3.6 titrated with NaOH. Arrows indicate addition of 50 mL of 50 % glucose. Error bars indicate the deviation from the mean ($n=2$) instead of A and B (single representative bioreactor).

3.4.3.2 Enhanced itaconate production in a bioreactor

While pH optimum was determined with *U. cyndodontis* $\Delta fuz7$, the new hyperproducing strains described in Hosseinpour Tehrani *et al.* [292] were developed in parallel. With *U. cyndodontis* $\Delta fuz7^- \Delta cyp3^+ P_{etefmttA} P_{riarria1}$ a strain was engineered which produced 6.5-fold more itaconate compared to the wildtype. This fact led us to perform the following fermentations with this new strain. In order to assess the performance of this new strain in controlled fed-batch fermentation, it was cultured in batch medium at a constant pH of 3.6. Cultures of *A. terreus* are often started at a more neutral pH, letting the pH drop during growth after which pH control is switched on [131, 132]. This pH shift can have a positive impact on the growth phase by reducing pH stress, but it may also pose a higher risk of bacterial contamination. To test the effect of such a pH shift, another fermentation was started at pH 6.0, letting the pH drop to 3.6 during growth, after which it was controlled at pH 3.6 with NaOH for itaconate production (Figure 37 and Table 10). As expected, itaconate production could be increased in these fed-batch fermentations compared to in shaken batch cultures with the optimized $\Delta fuz7^- \Delta cyp3^+ P_{etefmttA} P_{riarria1}$ strain [292] and also compared to *U. cyndodontis* $\Delta fuz7$ in fed-batch cultures (Figure 36).

Starting directly at pH 3.6 had no negative impact on production compared to starting at pH 6.0. On the contrary, the maximum titer of $44.5 \pm 1.6 \text{ g L}^{-1}$ in the fermentation with a constant pH of 3.6 culture was slightly, but not significantly, higher than that of the fermentation with the pH shift with $41.8 \pm 0.3 \text{ g L}^{-1}$ (Figure 37C and Table 10). Also, similar values for biomass and CO_2 formation were observed for both settings (Table 9 and Figure 37B, D). Further, nitrogen limitation was achieved faster in fermentation with constant pH at 3.6 (Figure 37B). For both conditions, the same yield was observed (Table 10). Interestingly $1.59 \pm 0.07 \text{ mol mol}^{-1}$ NaOH was consumed per

mol itaconate in pH shifting fermentation, which is 2.1-fold more than fermentation with a constant pH of 3.6. Since the carbon balance is not closed (Table 9) for either condition, unidentified components have to be found in the future, especially because side product formation of further acids like ustilagic acid is known for Ustilaginaceae [95].

Table 9. Carbon distribution of various fermentation conditions with *U. cynodontis* NBRC 9727 $\Delta fus7^- \Delta cyp3^+$ $P_{citg}mttA$ $P_{ita1}trial$ in batch medium with various glucose and NH_4Cl concentrations. Errors indicate the standard error of the mean (n=3).

	constant pH 3.6	pH shift 6 - 3.6	high nitrogen
itaconate (%)	44.8 ± 0.2	45.1 ± 0.4	31.5 ± 1.1
CDW (%)	15.0 ± 1.8	16.2 ± 0.6	19 ± 1.1
erythritol (%)	0.9 ± 0.4	0.4 ± 0.1	1.8 ± 0.1
CO ₂ (%)	22.0 ± 2.0	23.0 ± 1.5	23.7 ± 0.9
unaccounted (%)	17.3 ± 2.4	15.7 ± 3.1	24.0 ± 3.1
C used (mol)	2.2 ± 0.1	2.1 ± 0.0	6.0 ± 0.1

Overall, the production parameters achieved here at pH 3.6 were similar to those achieved with *U. maydis* at pH > 6 where a maximum titer of $54.8 \pm 2.8 \text{ g L}^{-1}$, the productivity of $0.33 \pm 0.02 \text{ g L}^{-1} \text{ h}^{-1}$ and a yield of $0.48 \pm 0.02 \text{ g}_{ITA} \text{ g}_{GLC}^{-1}$ were reached [140]. Depending on the process setup, the low pH optimum of *U. cynodontis* can provide significant benefits such as lower consumption of titrating base and facilitated downstream processing [8, 201]. Also, the lower pH reduces the risk of contamination [107], possibly enabling auto-sterile conditions, although this is not given even for low pH processes [299]. Given these advantages and the fact that no differences in itaconate production were observed, further fermentations were performed at a constant pH of 3.6.

Table 10. Production parameter for itaconate of various fermentation conditions in different variants of batch medium with *U. cynodontis* NBRC 9727 $\Delta fus7^- \Delta cyp3^+$ $P_{citg}mttA$ $P_{ita1}trial$. Errors indicate the error from the mean (n=3) while fermentation with a constant glucose feed is a single representative approach.

	constant pH 3.6	pH shift 6-3.6	high nitrogen	constant glucose feed
titer ^M (g L ⁻¹) ^b	44.5 ± 1.6	41.8 ± 0.3	83.0 ± 0.8	78.6
Y _{P/S} (g _{ITA} g _{GLC} ⁻¹) ^c	0.4 ± 0.0	0.4 ± 0.0	0.3 ± 0.0	0.45
Y _{P/S} ^M (g _{ITA} g _{GLC} ⁻¹) ^d	0.5 ± 0.0	0.4 ± 0.0	0.4 ± 0.0	0.61
r _P (g L ⁻¹ h ⁻¹) ^e	0.2 ± 0.0	0.2 ± 0.0	0.6 ± 0.0	0.42
r _P ^M (g L ⁻¹ h ⁻¹) ^f	0.4 ± 0.0	0.3 ± 0.0	1.4 ± 0.0	0.85
NaOH ITA ⁻¹ (mol mol ⁻¹) ^g	0.7 ± 0.1	1.6 ± 0.1	0.8 ± 0.1	0.66

^a titer^M: maximum titer

^b Y_{P/S}: overall yield product per consumed glucose

^c Y_{P/S}^M: maximum yield product per consumed glucose during production phase

^d r_P: overall production rate

^e r_P^M: maximum production rate

^f NaOH ITA⁻¹: amount NaOH consumed per itaconate

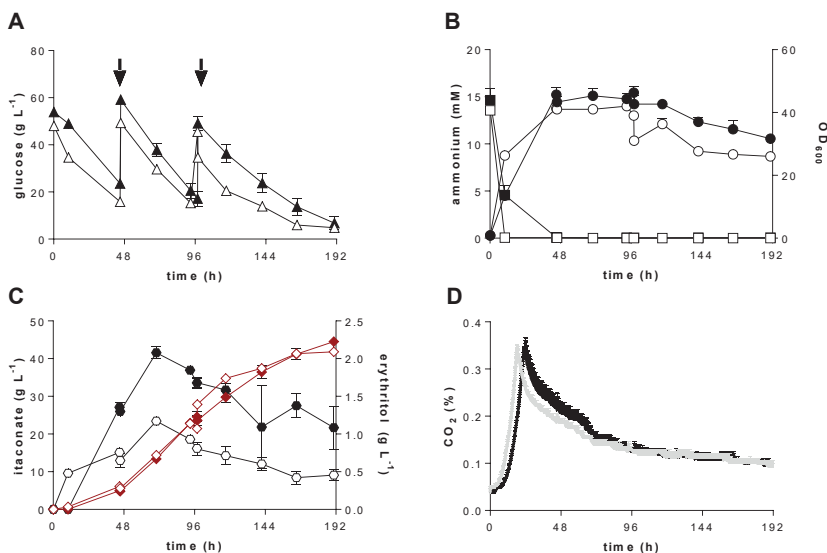


Figure 37. Controlled high-density fed-batch fermentation of *U. cynodontis* NBRC 9727 $\Delta fuz7 \Delta cyp3^P_{eregmttA} P_{ria1}ria1$. A: glucose concentration; B: OD_{600} and ammonium concentration; C: itaconate and erythritol concentration and D: CO_2 off-gas concentration during fermentation in a bioreactor containing batch medium with 50 g L^{-1} glucose, 0.8 g L^{-1} NH_4Cl with a natural pH shift from 6 to 3.6 (filled legends/ continuous grey line) or a constant pH at 3.6 (empty legends/continuous black line) controlled with NaOH. Arrows indicate addition of 100 mL of 50 % glucose. Error bars indicate the standard error of the mean ($n=3$). This figure is modified and adapted from the Master thesis of Katharina Saur [300]

Previous high-density fermentations with *U. maydis* have resulted in higher titers and productivities [137, 140], potentially reducing process and investment costs in an industrial context [301, 302]. However, they often come at the cost of lower yields, although the relation between cell density and production yield, titer, and rate and often non-linear [303]. In order to investigate the effect of higher cell densities of *U. cynodontis* $\Delta fuz7 \Delta cyp3^P_{eregmttA} P_{ria1}ria1$, fermentations with 200 g L^{-1} glucose and 4 g L^{-1} nitrogen were performed. For *U. maydis*, it is reported that higher titers are possible with these increased starting glucose and nitrogen concentrations [137, 140]. With this change, however, it must also be taken into account that problems can arise such as limitation and/or inhibition of substrates, high evolution rates of CO_2 and heat, and high oxygen demand with increasing viscosity of the medium [304].

The five-fold increase in ammonium as growth-limiting nutrient resulted in a maximum titer of $82.9 \pm 0.8 \text{ g L}^{-1}$ itaconate after 140 h. This maximum was followed by a gradual decrease of itaconate, even though glucose was still present (Figure 38). Simultaneously, CO_2 in exhaust gas dropped from 0.4 % to 0.04 %, and glucose consumption stopped (Figure 38A, B and Figure 39). Maximum productivity of $1.44 \pm 0.02 \text{ g L}^{-1} \text{ h}^{-1}$ was reached between 46 and 73 h, which is 3.8-fold more compared to fermentation with low nitrogen content (Table 10).

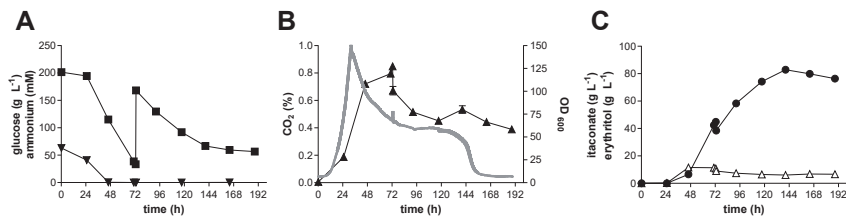


Figure 38. Controlled high density fed-batch fermentation of *U. cynodontis* NBRC 9727 $\Delta fus7^- \Delta cyp3^- P_{veg} mtA P_{ria} ria1$. glucose (●) and ammonium (▼) concentration; B: CO₂ concentration (continuous line) and OD₆₀₀ (▲); C: itaconate (●) and erythritol (Δ) concentration during fermentation in a bioreactor containing batch medium with 200 g L⁻¹ glucose, 4.0 g L⁻¹ NH₄Cl at pH 3.6 titrated with NaOH. Arrows indicate addition of 100 mL of 50 % glucose. Error bars indicate the standard error from the mean (n=3). This figure is modified and adapted from the Master thesis of Katharina Saur [300].

Interestingly, although five times more nitrogen was used, the OD₆₀₀ was only three times higher compared to fermentation with 0.8 g L⁻¹ NH₄Cl, suggesting a possible limitation in other medium components like in *U. maydis* [197]. Further, Klement *et al.* [197] and Zambanini *et al.* [208] could show that inhibition by high NH₄Cl concentrations can affect biomass growth, which might be avoided by pulse-feeding the nitrogen source. A gradual decrease in productivity, biomass formation, and drop in CO₂ production are visible after 72h indicating cell stress was initiated at this time point. The relatively sudden drop in the CO₂ evolution rate at 140h indicates that at this point a critical product concentration is reached, at which the cells are unable to maintain their viability, likely because at this point they are unable to counteract weak acids uncoupling due to the reduced substrate uptake rate. It is known that itaconate can inhibit the isocitrate-lyase, fructose 2,6-bisphosphate synthesis or substrate phosphorylation in mitochondria [118, 305, 306], which may further contribute to lowering the substrate uptake rate. However, in general, the high-cell-density cultures significantly increased the maximum titer and productivity compared to the low cell density cultures, at a relatively small cost to the product yield (Figure 38 and Table 10). The pulsed feed in the above-mentioned high-density culture significantly affected the production rate, likely due to cumulative osmotic and weak acid stress. In addition, it is known for *Ustilaginaceae* that high glucose concentration leads to slower growth and osmotic stress [140]. For these reasons, fermentation with a constant glucose concentration (20 g L⁻¹) was performed whereby other parameters were equivalent to the fermentation with high nitrogen. In order to ensure a constant substrate concentration, an in-line system for the analysis of glucose from Trace Analytics (Braunschweig/Germany) was used. The in-line sampling was enabled by a dialysis probe where the molecules diffused through a membrane into a transport buffer. The glucose measurement itself is based on an enzymatic reaction with glucose oxidase, which catalyzes β-D-Glucose to D-Glucono-δ-lactone and hydrogen peroxide in the presence of oxygen. The glucose content is then measured indirectly by the formed peroxide, which is oxidized to water and oxygen. The resulting current at the electrode is directly proportional to the amount of oxidized glucose [307]. The inline System of TraceAnalytics was further connected to the BioFlo 120[®] system from Eppendorf and was coupled to a pump which regulates the glucose feed, depending on the measured glucose concentration. Thus the glucose uptake rate could be determined by the rate of the pump. As an additional control, the consumption of the glucose stock solution was measured by means of a scale. Using this setup, nearly the same titer could be reached compared to the equivalent fermentation with pulsed glucose feeds, however, with a lower overall (0.42 g L⁻¹ h⁻¹) and

maximum ($0.84 \text{ g L}^{-1} \text{ h}^{-1}$) production rate (Figure 39 and Table 10). Interestingly, glucose consumption could be reduced by 30 % compared to the pulsed fed batch (Figure 40), leading to a much higher overall yield of $0.41 \text{ g}_{\text{ITA}} \text{ g}_{\text{GLC}}^{-1}$. During the production phase between 43 and 186 h, a yield of $0.61 \text{ g}_{\text{ITA}} \text{ g}_{\text{GLC}}^{-1}$ was achieved, which is 84% of the theoretical maximum. This much higher yield, along with the lower erythritol formation, strongly indicates that the cells suffer less from osmotic stress compared to the pulsed fed-batch. This is also corroborated by the decrease in productivity upon the pulse in the fermentation with high nitrogen, where the combined stress of substrate and product concentrations is about 4-fold higher. Despite the improvements achieved with the constant glucose concentration, the problem of product toxicity remains. This is confirmed by the decrease in productivity above 50 g L^{-1} itaconate, as also observed in the pulsed fed-batch, which is also reflected in the glucose uptake rate (Figure 40).

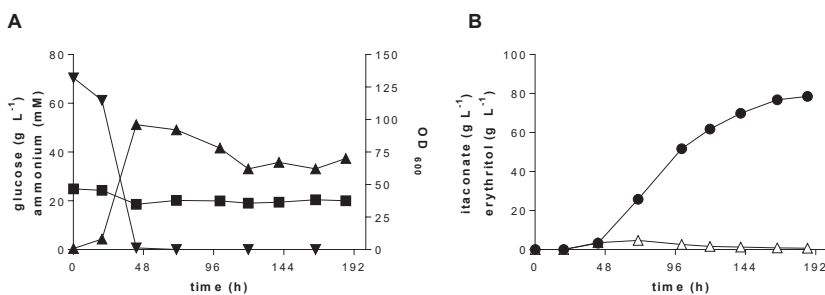


Figure 39. Controlled high density fed-batch fermentation of *U. cynodontis* NBRC 9727 $\Delta fuz7^{\Delta} \Delta cyp3^{\Delta} P_{etcmttA} P_{ria1ria1}$. A: glucose (■) and ammonium (▼) concentration and OD_{600} (▲); and B: itaconate (●) and erythritol (Δ) concentration during a single representative bioreactor cultivation in batch medium with constant glucose concentration, $4.0 \text{ g L}^{-1} \text{ NH}_4\text{Cl}$ at pH 3.6 titrated with NaOH.

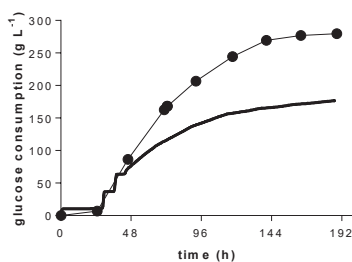


Figure 40. Glucose consumption of *U. cynodontis* NBRC 9727 $\Delta fuz7^{\Delta} \Delta cyp3^{\Delta} P_{etcmttA} P_{ria1ria1}$. Glucose consumption of fermentation in batch medium with pulsed-feed (●) or constant glucose concentration (continuous line), $4.0 \text{ g L}^{-1} \text{ NH}_4\text{Cl}$ at pH 3.6 titrated with NaOH. Error bars indicate the standard error of the mean ($n=3$) while fermentation with a constant glucose feed is a single representative approach.

Both fermentation approaches (pulsed fed-batch and constant glucose concentration) show clear signs of product toxicity at around 80 g L^{-1} itaconate at a pH of 3.6 (Figure 38, Figure 39, Figure 40 and Table 10). One way to overcome this would be *in situ* product removal by calcium salt

precipitation, as shown for *U. vetiveriae* [208] or by reactive extraction methods [308]. Alternatively, a continuous or semi-continuous process with cell recycling can help to overcome product toxicity as well [309].

3.4.3.3 Repeated batch to overcome Product-toxicity

In order to assess the stability of the biocatalyst under low pH, a repeated batch approach with cell recycling was applied to overcome product toxicity. The same conditions as in the fermentation with $4.0 \text{ g L}^{-1} \text{ NH}_4\text{Cl}$ were used. Above all, attention was paid to maintaining the productivity of $1.44 \pm 0.02 \text{ g L}^{-1} \text{ h}^{-1}$ observed in the early phase of the high-density cultures. After 120 h, cells were centrifuged and re-suspended in fresh batch medium without NH_4Cl . Yeast extract (0.5 g L^{-1}) was added to the medium because this addition greatly improved cell recovery in initial pilot experiments. In the initial batch phase, 77.6 g L^{-1} itaconate was produced which corresponds to a yield of $0.4 \text{ g}_{\text{ITA}} \text{ g}_{\text{GLC}}^{-1}$ (Figure 41). In the first repeated batch phase, 49 g L^{-1} itaconate with a yield of $0.5 \text{ g}_{\text{ITA}} \text{ g}_{\text{GLC}}^{-1}$ and in the second repeated batch 38 g L^{-1} with a yield of $0.5 \text{ g}_{\text{ITA}} \text{ g}_{\text{GLC}}^{-1}$ were produced. Base totalizer revealed that in the first 39 h of the first repeated batch and 28 h of the second batch, a lag phase occurred in which no itaconate was produced (Figure 41B). This lag phase can likely be attributed to the centrifugation steps used for the recycling, which deprive the cells of oxygen under low pH conditions. This lag phase was absent in shake flasks with CaCO_3 at neutral pH (Figure 42), and in addition no yeast extract was necessary for shake flask to recover the cells after the centrifuging step. The difference in the lag phases may be explained by different centrifugation times. While the first batch was centrifuged for 20 min, the second batch was only centrifuged for 5 min to minimize oxygen limitation. Cell density decreased with each repeated batch, which was reflected in the productivity. After the 3rd batch, subsequent batches failed to produce itaconate. Overall, cell recycling positively affected the product yield, which was stable across two repeated batches. However, significant lag phases and reductions in biomass and production rates indicate high stress imposed by the centrifugation steps applied here for cell recycling. To overcome these issues, a membrane-based cell retention system could be used [310].

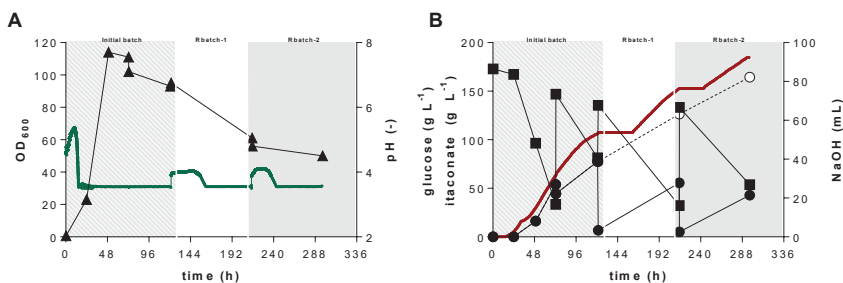


Figure 41. Controlled high density fed-batch fermentation of *U. cynodontis* NBRC 9727 $\Delta fuz7 \Delta cyp3^P_{entgMTA} P_{ric1ria1}$. A: OD₆₀₀ (▲) and pH (green line); B: glucose (■) itaconate (●) and total itaconate (dashed line) concentration, and used NaOH (red line) during single representative fermentation in a bioreactor containing batch medium with 200 g L^{-1} glucose, $4 \text{ g L}^{-1} \text{ NH}_4\text{Cl}$ at pH 3.6 titrated with 10 M NaOH . For repeated batch phase culture broth was centrifuged and subsequently re-suspended in 0.5 L batch medium without nitrogen, 170 g L^{-1} glucose and 0.5 g L^{-1} yeast extract.

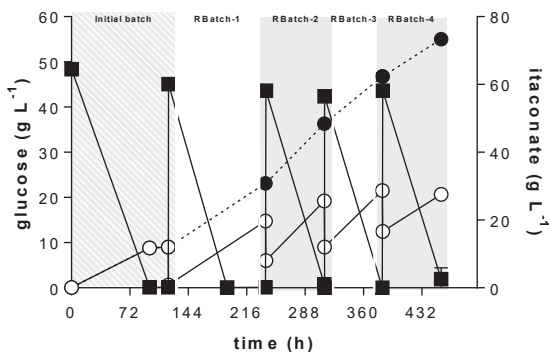


Figure 42. Repeated batch approach for itaconate production in *U. cynodontis* NBRC 9727 Δ fuz7⁻ Δ cyp3⁺ P_{itegmtA} P_{riat}riat1. Glucose (■), itaconate (○) and total itaconate (●, dashed line) concentration in screening medium containing 33 g L⁻¹ CaCO₃ and glucose during repeated batch cultivation in shaking flasks. For repeated batch phase culture broth was centrifuged for 5 min at 800 g and subsequently re-suspended in screening medium without nitrogen, 50 g L⁻¹ glucose and 25 g L⁻¹ CaCO₃. Error bars indicate the standard error from the mean (n=4).

3.4.4 Outlook

This study demonstrates the applicability of the pH tolerant *Ustilago cynodontis* in controlled batch cultivations, reaching high yield, titer, and rate at a low pH value. High-density fermentation, especially coupled with a continuous glucose feed, provided the overall best balance of production parameters, reaching high titers and yields with a minimal loss in productivity. Titrers of up to 82.9 g L⁻¹ were reached, which imposed significant product toxicity onto the cell, completely inhibiting the substrate uptake rate. Repeated-batch cultures indicated the potential to overcome product toxicity in a continuous itaconate production system with cell retention, especially if centrifugation steps can be avoided in the future. In all, this study demonstrates the possibilities enabled by the stable yeast-like morphology of the engineered *U. cynodontis* strain, while retaining the benefit of low pH fermentation.

3.4.5 Acknowledgements

We thank Dr. Wolfgang Künnecke and Dr. Michael Hartlep (TRACE Analytics GmbH, Braunschweig Germany) for the provision and instruction of the glucose sensor and also Christoph van Eickels (Eppendorf AG, Germany) to implement the system into the BioFlo®120. We thank the student Svenja Meyer (Institute of Applied Microbiology, RWTH Aachen University) for taking samples from the bioreactors.

Chapter 3.5

Integrated strain- and process design enable production of 220 g L⁻¹ itaconic acid with *Ustilago maydis*

Will be submitted for publication as:

Hamed Hosseinpour Tehrani, Johanna Becker, Isabel Bator, Katharina Saur, Svenja Meyer, Ana Catarina Rodrigues Lóia, Lars M. Blank and Nick Wierckx. Integrated strain- and process design enable production of 220 g L⁻¹ itaconic acid with *Ustilago maydis*.

Contributions:

Hamed Hosseinpour Tehrani performed most experiments. Nick Wierckx conceived and supervised the study. Hamed Hosseinpour Tehrani designed and performed experiments and analyzed results with the help of Nick Wierckx and Lars M. Blank. Hamed Hosseinpour Tehrani wrote the manuscript with help of Nick Wierckx and Lars M. Blank. Johanna Becker provided *U. maydis* Δcyp3, Isabel Bator engineered expression strain *U. maydis* Δcyp3 ΔPria1::P_{etef} and Ana Catarina Rodrigues Lóia helped to engineer *U. maydis* Δcyp3 ΔPria1::P_{etef} Δfuz7 and *U. maydis* Δcyp3 ΔPria1::P_{etef} Δfuz7 P_{etef}mttA. Svenja Meyer and Katharina Saur contributed to fermentation experiments.

3.5 Integrated strain- and process design enable production of 220 g L⁻¹ itaconic acid with *Ustilago maydis*

3.5.1 Abstract

Ustilago maydis is besides many other traits studied as an itaconate production host. Recently itaconate performance parameters could be increased significantly by metabolic- and bioprocess engineering. In this study, we could further increase itaconate production in *U. maydis* with an integrated approach of strain and process engineering. Next generation itaconate hyper-producing strains were generated using CRISPR/Cas9 and FLP/FRT genome editing tools for deletion, knock-in, and overexpression of genes. The strain performances in combination with *in situ* product crystallization with CaCO₃, resulted in a maximum titer of 220 g L⁻¹. This is a significant improvement compared to best-published itaconate titers reached with *U. maydis* and with *Aspergillus terreus*.

3.5.2 Introduction

More than 300 potential bio-based building blocks were selected from the U.S. Department of Energy according to criteria such as estimated processing costs, estimated selling price, and the technical complexity, in order to determine the most important chemicals that can be produced from biomass. In the top selection, nine belong to the group of organic acids [12], underlining the importance of this class of chemicals. One of these compounds is the unsaturated dicarboxylate itaconic acid. It was first described in 1837 [103] and primary reports about microbial production with *Aspergillus itaconicus* date back to 1931 [108]. Due to its two functional groups, radical polymerization of the methylene group and/or esterification of the carboxylic acid with different co-monomers is possible [25, 110, 311]. Thus, itaconate and its derivatives can be utilized in a variety of ways. This leads to a wide range of applications, like in the paper-, architectural-, pharmaceutical-, paint-, lacquer, and medical industry [21, 107, 111-115, 166]. It can also be used as an intermediate for biofuel production [225]. Further, itaconate production by mammalian macrophages is reported, where it plays a key role in the human immune response [117-119], with possible applications as therapeutic agents for autoimmune diseases [120].

In spite of this wide variety of potential applications, the market size of itaconic acid in 2011 was relatively small, with 41,400 tons and a market value of \$74.5 million [111]. This is caused by the relatively high price of approximately two dollars per kg and the availability of cheaper petrol-based alternatives such as acrylic acid. The reduction of this price is, therefore, an exclusive criterion for access to further markets. To be competitive against petrol-based products, costs need to reduce to around \$0.5 per kg [121]. Assuming that the price would decrease, itaconic acid can replace acrylic acid whose production is petroleum-based and has a market worth of \$11 billion [23, 107, 110]. Since 1950 *Aspergillus terreus* is used for the industrial production of itaconate [110]. Charles Pfizer Co. was granted the first patent for the production of itaconate with this filamentous fungus *A. terreus* by submerged cultivation [106]. During the last decades, the responsible metabolic pathways and regulatory mechanisms of itaconate production in *A. terreus* were studied in detail [25]. Above all, significant advances could be achieved through process optimizations. This long history of optimization has enabled titers above 100 g L⁻¹ and yields near the theoretical maximum at low pH, making *A. terreus* the current best production host for itaconate production [21, 131, 138, 141, 142, 146, 147]. However, despite the long history and experience, itaconate production in *A. terreus* remains challenging. A specific pellet growth form is required for high productivity [23, 284], and therefore, morphology has to be strictly controlled.

A. terreus reacts very sensitively to certain medium impurities, which can induce mycelium formation, stopping itaconate production [21, 132, 285]. Thus, the medium must be pretreated to remove impurities from production medium, especially when using less pure industrial substrates such as molasses [22, 110]. Consequently, morphological control influences the manufacturing process tremendously, leading to increased operational costs and failed batches.

Besides *A. terreus*, also *E. coli* [151] or Ustilaginaceae like the pH tolerant *Ustilago cynodontis* or the yeast-like *Ustilago maydis* are known as good itaconate producer [95, 126, 208, 292]. Among the Ustilaginaceae *U. maydis* is the most studied species in the fields of plant pathogenicity, cell biology, and biotechnology [140, 178, 265, 278, 312]. The Ustilaginaceae produce a broad spectrum of exciting products such as organic acids [95, 98, 126], glycolipids [171, 313], polyols [95, 314], and enzymes [171]. This, along with their yeast-like growth, makes them attractive for biotechnological applications [95].

That said, certain stresses can induce filamentous growth in *U. maydis* [268, 315] but efficient itaconate production with this species is, at least a small scale, not coupled to a specific morphology. In wildtype *U. maydis*, itaconate production is induced by nitrogen limitation [261] and requires pH values above five [95]. Like in *A. terreus*, the genes encoding the itaconate production pathway in *U. maydis* are clustered and co-regulated [138, 139]. Considerable progress has been made in increasing the yield, titer, and rate of itaconate production in *U. maydis* and related species by metabolic engineering and process development. Geiser *et al.* [139] characterized the itaconate production pathway and identified an itaconate oxidase Cyp3, which produces the downstream product (*S*)-2-hydroxyparaconate. The disruption of this oxidase, and overexpression of the cluster-associated regulator Ria1 led to a 4.5-fold increase in ITA production in *U. maydis* [140]. In *U. vetiveriae* itaconate production from glycerol could be increased 2.5-fold by overexpression of *ria1* or 1.5-fold by overexpression of the mitochondrial transporter *mtt1* [208].

In another study, we could show that the heterologous expression of the mitochondrial transporter MttA from *A. terreus* in *U. maydis* enables more efficient itaconate production than the native mitochondrial transporter [287]. Further, by deletion of *fuz7* in *U. cynodontis* a strong, stable yeast-like growth could be established for several relevant itaconic acid production conditions [292]. This is especially favorable for large scale fermentation [24]. Furthermore, with media optimization and optimization of the fermentation process such as pulsed fed-batch strategies product titers can be significantly increased [95, 236], especially when combined with *in situ* product removal approaches such as reactive extraction or calcium precipitation [107, 208, 308, 316].

These optimizations have individually made a significant impact on the efficiency of itaconate production in *Ustilago*. In this study, we consolidate several of these metabolic and bioprocess engineering strategies to achieve itaconate titers that surpass those currently achieved by any other host.

3.5.3 Results and discussion

3.5.3.1 *Engineering of a marker-free U. maydis MB215 for enhanced itaconate production*

Previously Geiser *et al.* reached titers up to $63.2 \pm 0.7 \text{ g L}^{-1}$ with production rates up to $0.38 \pm 0.00 \text{ g L}^{-1} \text{ h}^{-1}$ and a yield up to $0.48 \pm 0.02 \text{ g}_{\text{ITA}} \text{ g}_{\text{GLC}}^{-1}$ in bioreactor experiments by deletion of the itaconate oxidase encoding *cyp3* gene and overexpression of the transcriptional regulator Ria1

encoding gene ($\Delta cyp3 P_{etef} rial1$) [140]. Unfortunately, two out of five possible antibiotic resistance markers available for *U. maydis* were genomically incorporated in this design, which limited further modification steps. Recently Schuster *et al.* [185] established a CRISPR/Cas9 system for *U. maydis* enabling scarless and marker-free genome editing [317]. This technology, along with the FLP/FRT system for marker recycling already used in *U. maydis* [183] removes previous limitations of available antibiotic markers. For these reasons, we re-engineered the modifications described by Geiser *et al.* [140] using the CRISPR/Cas9 system from Schuster *et al.* [185]. To delete the oxidase encoding gene *cyp3* which produces the downstream product (*S*)-2-hydroxyparaconate, a repair template was used to delete the whole gene. It consisted of 1000 bp flanks homologous to sequences up- and downstream of *cyp3*. This strain was provided by Johanna Becker (data unpublished). The overexpression of *rial1* was not achieved by the *in trans* insertion of an expression cassette, but rather by a direct replacement of the native P_{rial1} promoter by the strong and constitutive P_{etef} promoter was implemented. Here the same strategy was chosen as for *cyp3*, including P_{etef} between the flanks of the repair templates. Promoter exchanges were previously shown to effectively upregulate native genes [236]. Two chosen transformants of the resulting strain ($\Delta cyp3 \Delta P_{rial1}::P_{etef}$ #1 and $\Delta cyp3 \Delta P_{rial1}::P_{etef}$ #2) were compared to the control strain from Geiser *et al.* [140] in System Duetz[®] 24-well plates [209], in screening medium with 50 g L⁻¹ glucose buffered either with 30 mM MES or 33 g L⁻¹ CaCO₃ (Figure 43). As expected, itaconate production was lower using 30 mM MES compared to 33 g L⁻¹ CaCO₃, since *U. maydis* prefers pH values above 5 [95]. In both tested conditions, the transformants showed no difference to the control except for one notable exception. Itaconate concentrations in the cultures with the $\Delta cyp3 P_{etef} rial1$ strain decreased markedly at 96 h with 30 mM MES (Figure 43A). This rapid decrease shows that *U. maydis* can degrade itaconate, likely through a similar pathway as described for *A. terreus* [71, 140]. Possibly, the expression of the genes encoding this degradation pathway is affected by the promoter replacement, which removed the native P_{rial1} promoter. For further investigations, we selected the strain *U. maydis* $\Delta cyp3 \Delta P_{rial1}::P_{etef}$ #2.

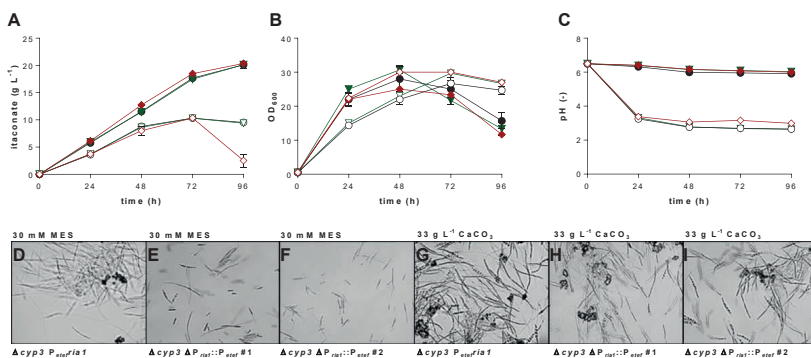


Figure 43. Itaconate production and growth of engineered *U. maydis* strains. Itaconate concentration (A), growth (OD₆₀₀, B), pH (C) and DIC images at a magnification of 630x (D-I) with $\Delta cyp3 \Delta P_{rial1}::P_{etef}$ #1 (green, ▼) and $\Delta cyp3 \Delta P_{rial1}::P_{etef}$ #2 (black, ●) in comparison to $\Delta cyp3 P_{etef} rial1$ (red, ◆) during shake flask cultivation in screening medium with 30 mM MES (open symbols) or 33 g L⁻¹ CaCO₃ (filled symbols) with 50 g L⁻¹ glucose. Error bars indicate the standard error of the mean (n=3). The raw data originates from the Master thesis of Isabel Bator [318].

In the cultures of these overproducing strains, we also observed a degree of filamentous growth. Although this is by far not as prominent as described for *U. cynodontis* 0[292], elongated cells and filaments were formed in all strains for all conditions, especially upon the addition of CaCO₃ (Figure 43G-I).

3.5.3.2 Morphological engineering in *U. maydis* $\Delta cyp3 \Delta P_{ria1}::P_{etef}$

Usually, filamentous growth in *U. maydis* is investigated in terms of pathogenicity. In its natural habitat, filamentous growth is indispensable to *U. maydis* for infection of *Zea mays*. This is strongly coupled with sexual development, including a complex regulatory system [228, 278, 279]. Filamentous growth can also occur in haploid cells when they encounter stresses such as low pH, nitrogen limitation, or the presence of sunflower oil [268, 272]. This ability to grow filamentously is rather an obstacle in a biotechnological context, as it strongly influences bioprocess parameters such as oxygen transfer, viscosity, and clogging, and it increases the sensitivity to hydro-mechanical stress [197]. In order to solve this problem and to restore robust yeast-like growth, the *fuz7* gene was deleted in the marker-free $\Delta cyp3 \Delta P_{ria1}::P_{etef}$ #2 strain by replacement with a hygromycin marker through homologous recombination, followed by FLP/FRT-mediated marker excision [183]. *Fuz7* is part of the Ras/mitogen activated protein kinase (MAPK) pathway, which plays an important role in conjugation tube formation and filamentous growth [280]. By deletion of *fuz7* in the strongly filamentous *U. cynodontis*, filamentous growth was repressed without influencing itaconate production and cell fitness under biotechnologically relevant conditions [292]. Deletion of *fuz7* in *U. maydis* is known to abolish filamentous growth, and it also renders the strain completely apathogenic [268, 280]. This inability to colonize the maize plant is an additional advantage in a biotechnological context, as it may alleviate possible regulatory hurdles for industrial applications.

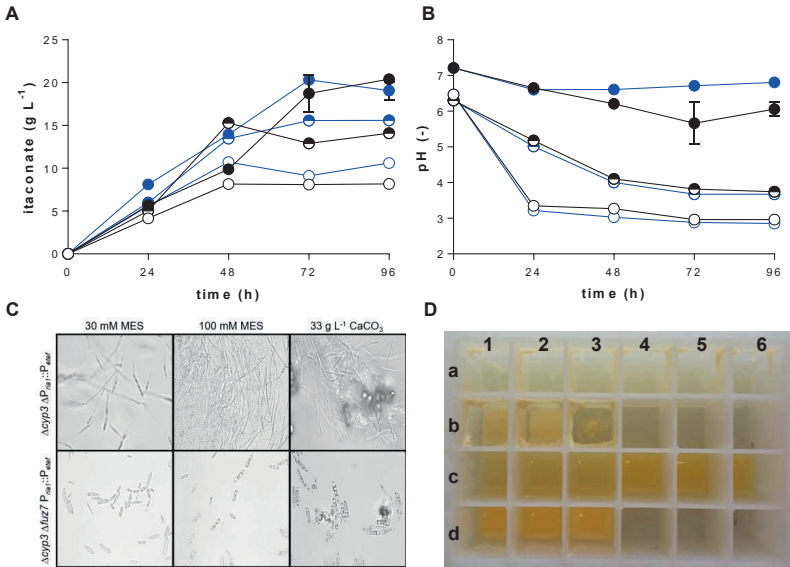


Figure 44. Itaconate production and growth of morphology-engineered *U. maydis* strains. *U. maydis* $\Delta cyp3 \Delta P_{ria1}::P_{eteF}$ (black, D_{a1-6, b1-3}) and *U. maydis* $\Delta cyp3 \Delta P_{ria1}::P_{eteF} \Delta fuz7$ (blue, D_{c1-6, d1-3}). Itaconate concentration (A), pH course (B), DIC images by an magnification of 630 (C) and 24 well plate during System Duetz[®] cultivation in screening medium with 30 mM MES (○, D_{a1-3+c1-3}), 100 mM MES (●, D_{a4-6+c4-6}) and 33 g L⁻¹ CaCO₃ (●, D_{b1-3+d1-3}) and 50 g L⁻¹ glucose. Error bars indicate the standard error of the mean (n=3).

In order to assess the effect of *fuz7* deletion, cultivation studies in screening medium with 30 mM and 100 mM MES, and 33 g L⁻¹ CaCO₃ were performed (Figure 44). As expected, *U. maydis* $\Delta cyp3 \Delta P_{ria1}::P_{eteF} \Delta fuz7$ grew completely yeast-like in all tested conditions. In contrast, *U. maydis* $\Delta cyp3 \Delta P_{ria1}::P_{eteF}$ grew filamentously (Figure 44C), resulting in extensive adherence to the walls of the culture plates (Figure 44D). This striking difference in morphology in the *fuz7* mutant greatly improves the handling of these cultures, while it did not negatively affect itaconate production. Rather, production was significantly better at the end of cultivation for 30 mM and 100 mM MES.

3.5.3.3 Mitochondrial transporter engineering in *U. maydis* $\Delta cyp3 \Delta P_{ria1}::P_{eteF} \Delta fuz7$

Recently we could show by complementation experiments that overexpression of the mitochondrial transporter encoded by *mttA* from *A. terreus* enables higher itaconate production in *U. maydis* than overexpressing the native *mtt1* [287]. Thus, in order to further increase itaconate production, we expressed *mttA* of *A. terreus* in *U. maydis* $\Delta cyp3 \Delta P_{ria1}::P_{eteF} \Delta fuz7$ using plasmid pETEF_CbxR_At *mttA* [287]. The best of three individual transformants were selected for further study. Upon the cultivation of this transformant with CaCO₃, a white precipitate was observed in samples of these cultures, indicating that the solubility limit of calcium itaconate was reached. As described for malic acid production with *U. trichophora*, and itaconate production with *U. vetiveriae*, calcium salts of these organic acids have a lower solubility, leading to *in situ* precipitation in cultures where high titers are reached, usually preceded by a transient supersaturation of the product [97, 208]. In order to assess the effect of *in situ* itaconate

precipitation in the engineered *U. maydis* strains, they were cultivated in System Duetz[®] plates in screening medium with 100 g L⁻¹ glucose and 66 g L⁻¹ CaCO₃. Samples were analyzed with, and without HCl treatment to re-solubilize the precipitated Ca-itaconate (Figure 45). With the higher glucose concentration, the difference between strains with and without *fuz7* deletion becomes more apparent, with the filamentous strains having a lower substrate uptake rate and a residual glucose concentration between 33.1 ± 2.6 g L⁻¹ and 38.2 ± 2.9 g L⁻¹. Consequently, the strain with *fuz7* deletion reached higher final titers, with *U. maydis* $\Delta cyp3 \Delta P_{ria1}::P_{etef} \Delta fuz7 P_{etef} mttA$ producing 33.6 ± 1.6 L⁻¹ itaconate,

An even more pronounced effect was observed with similar cultures using glycerol as C-source (Figure 46). Glycerol is a very poor substrate for wildtype *U. maydis* MB215 [97], and it invokes a high degree of filamentation and pigmentation in *U. cynodontis* (chapter 3.3). Especially the *fuz7* deletion had a very positive effect on the glycerol uptake rate and itaconate production, with the $\Delta cyp3 \Delta P_{ria1}::P_{etef} \Delta fuz7$ strain producing 13.1 ± 0.04 g L⁻¹, compared to 4.3 ± 0.4 g L⁻¹ produced by the $\Delta cyp3 \Delta P_{ria1}::P_{etef}$ control strain. Titers could be further increased with *U. maydis* $\Delta cyp3 \Delta P_{ria1}::P_{etef} \Delta fuz7 P_{etef} mttA$ to 16.1 ± 0.4 g L⁻¹ itaconate (Figure 46).

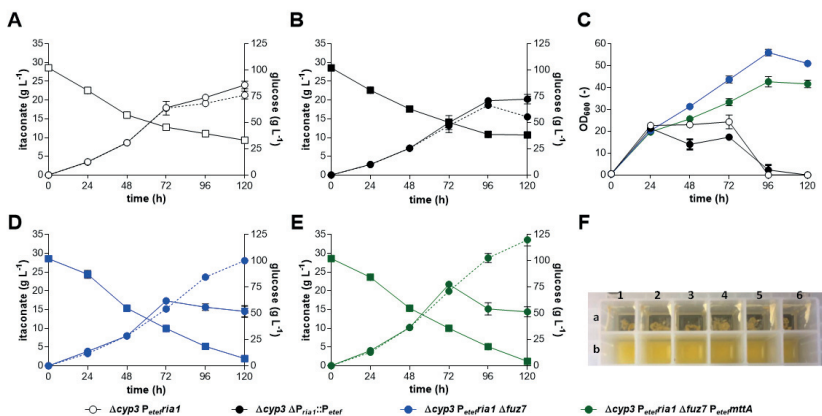


Figure 45. Comparison of aqueous and total itaconate concentrations in culture of engineered *U. maydis* strains. Itaconate production (●), glucose consumption (■) and macroscopic image of 24 well-plate after 96h (F) of *U. maydis* $\Delta cyp3 \Delta P_{ria1}$ (A, F_(a1-3)), $\Delta cyp3 \Delta P_{ria1}::P_{etef}$ (B, F_(b4-6)), $\Delta cyp3 \Delta P_{ria1}::P_{etef} \Delta fuz7$ (C, F_(c1-3)) and $\Delta cyp3 \Delta P_{ria1}::P_{etef} \Delta fuz7 P_{etef} mttA$ (D, F_(d4-6)) during System Duetz[®] cultivation in screening medium with 66 g L⁻¹ CaCO₃ and 100 g L⁻¹ glucose. Dotted lines represent samples treated with HCl and continuous lines represents untreated supernatant samples. Error bars indicate the standard error of the mean (n=3). Glucose values were combined for untreated and treated samples (n=6).

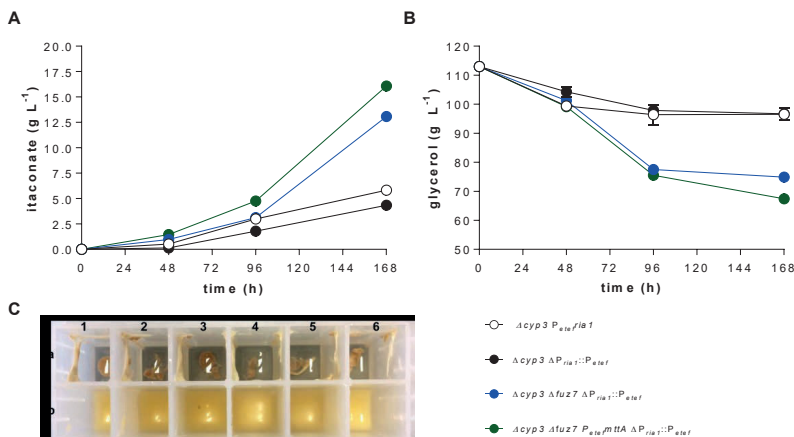


Figure 46. Itaconate production and growth of engineered *U. maydis* strains on glycerol. Itaconate concentration (A), growth (B) and macroscopic image of a 24 well-plate (C) of cultures of *U. maydis* Δcyp3 P_{ita1}/ItA1 (C_(a1-3)), Δcyp3 ΔP_{ita1}::P_{ita1} (C_(b1-3)), Δcyp3 ΔP_{ita1}::P_{ita1} Δfuz7 (C_(b1-3)) and Δcyp3 ΔP_{ita1}::P_{ita1} Δfuz7 P_{ita1}/mttA (C_(b4-6)) during System Duetz[®] cultivation in screening medium with 33 g L⁻¹ CaCO₃ and 112 g L⁻¹ glycerol. Error bars indicate the standard error of the mean (n=3).

3.5.3.4 Optimized itaconate production in a stirred bioreactor

In principle, the alleviation of product inhibition provided by the *in situ* precipitation of calcium itaconate enables much more extended cultures, in which productivity is only limited by the availability of the substrate and the stability of the biocatalyst. Therefore, in order to achieve high itaconate production, *U. maydis* MB215 Δcyp3 ΔP_{ita1}::P_{ita1} Δfuz7 P_{ita1}/mttA was cultivated in pulsed fed-batch fermentations with CaCO₃. The batch phase was started in screening medium containing 50 g L⁻¹ glucose and 1.6 g L⁻¹ NH₄Cl (Figure 47). The CaCO₃ was added manually whenever pH dropped below 6.2, in the first 313 h as a liquid suspension and after 313.5 h CaCO₃ as a powder. Glucose was also pulsed into the fermenter to keep the concentration above 20 g L⁻¹. The feeding schedule of CaCO₃ and glucose is given in (Table 11). The resulting titer of 140 g L⁻¹ itaconate was reached after 437 h. This is 2.2-fold more than the best published 63.2 ± 0.7 g L⁻¹ from Geiser *et al.* [140] with *U. maydis*. Biomass formation mainly occurred in the first 72 h and reached OD₆₀₀ values around 90, staying relatively constant for the rest of the fermentation. An overall yield of 0.39 g_{ITA} g_{GLC}⁻¹ was reached and the overall productivity was 0.32 g L⁻¹ h⁻¹, with maximum productivity between 24-120 h of 0.65 g L⁻¹ h⁻¹, after which it stayed relatively linear at 0.23 g L⁻¹ h⁻¹. This decrease in productivity might be caused by the high solids load of 10-15% CaCO₃ and Ca-itaconate in the fermentation broth, which could result in inhomogeneous mixing with pockets of low oxygen tension. For itaconate production, sufficient supply of oxygen is very important, with even transient oxygen limitations leading to a decrease of production [197, 319]. Future process development should thus focus on better mixing with these high solids loads, i.e., by changing stirrer geometry, which can promote better oxygen distribution in viscous media [320]. In addition to itaconate, the production of 31 g L⁻¹ malate was also observed, thereby increasing the total acid production to 170 g L⁻¹ and the total acid yield to 0.48 g_{ITA} g_{GLC}⁻¹. This could be the result of the additional supply of CO₂ by CaCO₃. The efficient microbial production

of malate via pyruvate relies on CO_2 as co-substrate [97], and the additional CO_2 provided by the CaCO_3 might imbalance the precursor supply of itaconate.

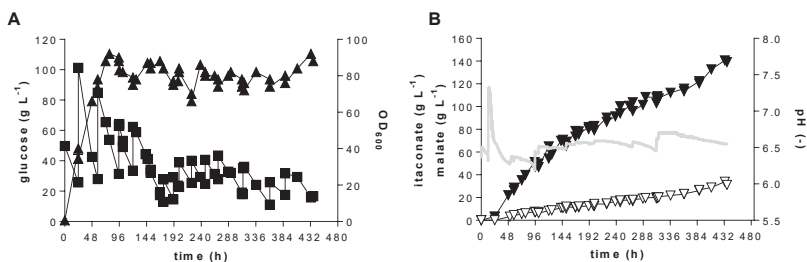


Figure 47. Controlled pulsed fed-batch fermentation of *U. maydis* MB215 $\Delta cyp3 \Delta Pral::P_{ete7} \Delta fuz7 P_{ete7} mttA$ in the presence of CaCO_3 . A: growth (▲), and glucose concentration (■) and B: Concentration of itaconate (▼), malate (▽), and pH (continuous line) during a single representative bioreactor cultivation in batch medium with a starting concentration of 50 g L^{-1} glucose and 1.6 g L^{-1} NH_4Cl . pH was kept above 6.2 by manual addition of CaCO_3 . Feeding schemes of glucose and CaCO_3 are listed in Table 11. The raw data originates from the Bachelor thesis of Svenja Meyer [283].

In a similar approach where pH was controlled by titration with NaOH, a drastic decrease in production was observed (Figure 48), reaching a maximum titer of only $35.9 \pm 1.5 \text{ g L}^{-1}$ with a yield of $0.2 \pm 0.01 \text{ g}_{\text{ITA}} \text{ g}_{\text{GLC}}^{-1}$ and overall productivity of $0.12 \pm 0.004 \text{ g L}^{-1} \text{ h}^{-1}$. In this titrated fermenter less than 1 g L^{-1} malate was produced, further indicating that the additional CO_2 from CaCO_3 increases malate production. The overall decrease of productivity in the titrated culture is likely caused by the overexpression of *mttA*, which significantly stresses the cells leading to reduced growth productivity as described previously [287]. The application of *in situ* itaconate crystallization with CaCO_3 thus greatly reduced product inhibition, which is especially relevant with this genuinely engineered strains, leading to almost threefold higher production rates.

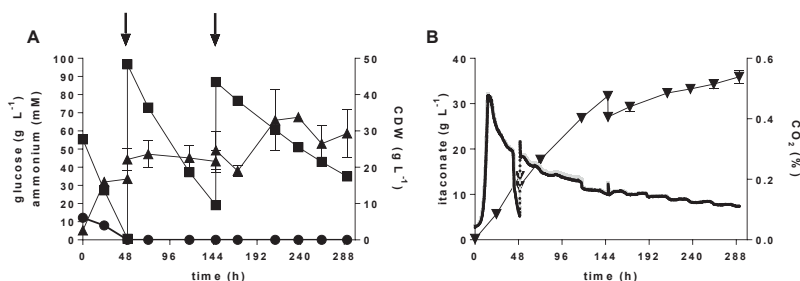


Figure 48. Controlled high-density pulsed fed-batch fermentation of *U. maydis* MB215 $\Delta cyp3 \Delta Pral::P_{ete7} \Delta fuz7 P_{ete7} mttA$ with NaOH titration. A: CDW (▲), glucose (■) and ammonium concentration (●) and B: Concentration of itaconate (▼) and offgas CO_2 (continuous line) during fermentation in a bioreactor containing batch medium with glucose, 0.8 g L^{-1} NH_4Cl at pH 6.0 titrated with NaOH. Arrows indicate addition of 100 mL of 50 % glucose. Error bars indicate the error from the mean ($n=3$).

To further improve the production rate, the cell density was increased by increasing the NH_4Cl concentration to 4 g L^{-1} and the starting glucose concentration to 200 g L^{-1} (Figure 49). A similar feeding strategy of glucose and CaCO_3 as above was applied (Table 12). As expected, higher biomass formation was observed with higher ammonium concentration, although the 2.5-fold higher nitrogen concentration only led to a moderate increase of the OD_{600} to around 110 g L^{-1} . A similar trend was observed with *A. terreus*, where a fourfold increase in phosphate as the growth-limiting nutrient only led to a twofold increase in biomass (Krull et al., 2017). In spite of this, the overall production rate was increased significantly to $0.45 \text{ g L}^{-1} \text{ h}^{-1}$. The higher overall production rate was also reflected in a higher maximum rate of $0.74 \text{ g L}^{-1} \text{ h}^{-1}$ between 24 h and 189 h followed by a fairly linear rate of $0.35 \text{ g L}^{-1} \text{ h}^{-1}$ for the rest of the fermentation. This higher rate enabled the production of 220 g L^{-1} itaconate in the same timeframe as the lower density culture. Occasional spikes in the measured itaconate concentration can be observed, likely due to the re-dispersion of Ca -itaconate clumps from the headspace into the broth. Indeed, extensive clumping could be observed owing to the very high solid loads of 20-25%. As expected, the higher rates come at the cost of a yield reduction to $0.33 \text{ g}_{\text{ITA}} \text{ g}_{\text{GLC}}$, as more glucose is consumed for biomass production and maintenance.

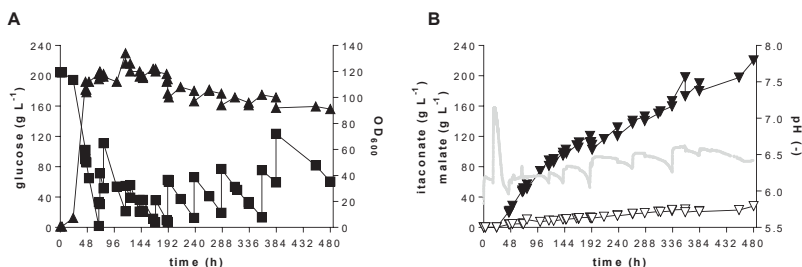


Figure 49. Controlled high-density pulsed fed-batch fermentation of *U. maydis* MB215 $\Delta\text{cyp3 } \Delta\text{Pnia1::Petef } \Delta\text{fuz7 PetefmttA}$ in the presence of CaCO_3 . A: growth (▲), and glucose concentration (■) and B: Concentration of itaconate (▼), malate (▽), and pH (continuous line) during a single representative bioreactor cultivation in batch medium with a starting concentration of 200 g L^{-1} glucose and $4 \text{ g L}^{-1} \text{ NH}_4\text{Cl}$. The pH was kept above 6.2 by manual addition of CaCO_3 . Feeding schemes of glucose and CaCO_3 are listed in Table 12. This figure is modified and adapted from the Bachelor thesis of Svenja Meyer [283].

3.5.4 Outlook

In this study, the combination of metabolic and morphological engineering together with *in situ* crystallization of itaconate yielded a titer of 220 g L^{-1} itaconate, which corresponds to 284 g L^{-1} calcium itaconate. This titer exceeds the 160 g L^{-1} achieved with *A. terreus* [132], although the yield and production rate achieved with *A. terreus* are still higher [21]. Especially the yield achieved with *U. maydis* could be further increased by the reduction of byproduct formation, as illustrated by the relatively high levels of malate production under these conditions. The strategy of *in situ* crystallization has not been reported in a biotechnological context with *A. terreus*, likely because the used pH values and the presence of solids strongly affect its morphology (Krull et al., 2017). In all, this study demonstrates the power of an integrated approach of strain and process engineering by steering *Ustilago*-based itaconate production into a quantitatively new dimension.

3.5.5 Acknowledgements

We thank Dr. Mariana Schuster and Prof. Dr. Regine Kahmann (Max Planck Institute for Terrestrial Microbiology, Department of Organismic Interactions, Marburg) for providing the plasmid pCas9_sgRNA_0 and Dr. Kerstin Schipper and Prof. Dr. Michael Feldbrügge (Institute for Microbiology, Heinrich Heine University Düsseldorf) for pstorI_1rh_WT (pUMa1522).

Chapter 4

General discussion and outlook

Authors' contributions:

This chapter was written by Hamed Hosseinpour Tehrani and reviewed by Lars M. Blank and Nick Wierckx.

4 General discussion and outlook

4.1 Organic acids and their potential to initiate change

The world's population is continuously increasing, which leads to an elevated demand for raw materials [3, 321]. To overcome challenges such as CO₂ emission, climate change, and pollution of the environment resulting from a petroleum-based industry, microbial production of bio-based products is required [8, 322]. The shift to a sustainable industry using renewable resources for the production of value-added compounds will be one of the main challenges of our society. One impressive group of compounds that have the potential to substitute petrochemical-derived chemicals and thus could decrease their production are the organic acids. Organic acids are a key group among the building block chemicals that can be produced in microbial processes [8, 20, 111, 323]. Above all, their functional groups make them an excellent starting material for the chemical industry [8, 23]. Organic acids possess many beneficial properties that make them promising molecules for industrial applications. For example, succinic, fumaric, and malic acid can replace the petroleum-derived commodity chemical maleic anhydride, and itaconic acid can substitute methyl methacrylate or polyacrylic acid, which all have large markets up to 3.2 billion t/a [8, 20, 25, 323]. This is the potential, while the current markets are small [8, 21, 23, 323]. The reason why organic acids have not been able to establish themselves so far is the enormous process costs compared to petroleum-based chemicals and the general challenges/requirements for industrial scale-up for microbial organic acid production [8, 21, 23]. High costs often result from low-performance microbial processes, costly downstream processing, or expensive feedstocks [8]. One prominent organic acid with a high potential for industrial applications is itaconate. Improving its microbial production using the smut fungi *Ustilago* as biocatalyst was the focus of this thesis.

4.2 Morphology

The morphology of fungi is a central criterion for efficient organic acid production, and in many cases, a defined and simple morphology is required for optimal production [156]. However, many parameters can negatively influence the morphology, including media components, bioreactor setups, and the pH. Therefore, stringent control of the process parameters for optimal morphology is required which considerably influences production costs [17, 324, 325]. In this thesis, one of the main challenges was the filamentous growth behavior of *U. cynodontis* and *U. maydis*. Both organisms belong to the Ustilaginaceae and are plant pathogens. Usually, *U. maydis* is described as a unicellular yeast-like growing organism while *U. cynodontis* is described as a strong filamentous fungus [95]. In this thesis filamentous growth was also for *U. maydis* production strains observed, thus the advantage of unicellular growth, especially for later bioprocessing was compromised strongly.

The filamentous growth in *U. maydis* is not unusual and rather normal or even necessary in its life cycle. The process of plant colonization and infection is coupled with sexual development governed by a complex regulatory system, which is well studied in *U. maydis*. In Figure 50, a simplified illustration of the life cycle is depicted. Haploid cells with different mating types can recognize each other with a pheromone receptor system to fuse and form a dikaryotic filament. The dikaryon is afterward able to invade the maize plant via an appressorium [228, 278, 279]. Two signal cascades, namely the cyclic AMP-dependent protein kinase A pathway and the Ras/mitogen-activated protein kinase (MAPK) pathway play a major role in plant-cell interaction in *U. maydis* and are involved in mating, pathogenicity, and morphology.

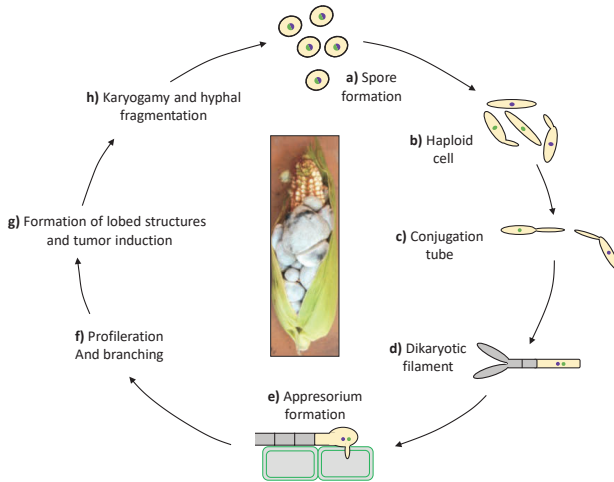


Figure 50. Life cycle of *U. maydis*. Simplified illustration of infestation process by *U. maydis* to infect the maize plant. Adapted from Feldbrügge *et al.* [326] with minor modifications.

The deletion of genes encoding components of these pathways causes *U. maydis* to lose the ability to induce filamentous growth and to colonize the maize plant [268, 280-282]. However also in haploid cells, filamentous growth is not unusual as mentioned in chapter 3.5. By deletion of *fuz7*, which is necessary for morphologic transition, filamentous growth was completely abolished in *U. maydis* and *U. cynodontis* under relevant itaconic acid production conditions. Strains featured stable yeast-like growth under several biotechnological conditions offering strong advantages during fermentation and general cell handling, as mentioned in chapter 3.3, 03.4, and 3.5. This newly acquired property in strain robustness / stress resistance is one key factor to reduce costs and open new possibilities for researchers working in this field. The deletion of different genes of the Ras/mitogen-activated protein kinase pathway resulted in different production abilities in this study. *Fuz7* deletion mutants showed the best itaconate production properties, while the *Ras2* deletion resulted in better (*S*)-2-hydroxyparaconate producing strains. Although all deletion strains showed comparable yeast-like growth under the microscope, the differences in production were enormous. That's not unusual for fungi. For example, itaconate production using *A. terreus* is also only efficient when the host shows specific pellet morphology [156, 284, 285]. A high number of genes are involved in the lifecycle of *U. maydis*. They were analyzed and characterized in terms of pathogenicity only, but this thesis demonstrates that strains modified regarding the MAPK signaling pathway can be promising hosts for biotechnological applications. The first attempts regarding this approach were also carried out in *T. reesei* where growth rate and cellulose production could be increased [156]. In future studies, involved genes from the cAMP and MAPK signaling pathway should be deleted in producing Ustilaginaceae to prepare a knock out library. Since the genes are highly conserved, this could be achieved, for example, applying CRISPR/Cas9 by choosing a common sgRNA in a way that it can be used for several strains in parallel to minimize the effort. The transformants could then be examined for their product diversity and their production performance to determine new hosts for new products

since Ustilaginaceae have a versatile metabolism [95]. For example, this approach could be used in *U. trichophora* for malic acid production [97] or in *U. vetiveriae* for itaconic acid production [208]. In this context, screening for strains with higher tolerance towards specific products or specific pH values would be also beneficial for organic acid production to overcome common challenges such as product toxicity and low-pH inhibition.

Since (S)-2-hydroxyparaconate can be advantageous for high-value application, such as the production of pheromones [254], *U. cynodontis* $\Delta ras2$ strain could be further optimized for the production of this compound as it was shown in chapter 3.3 that *U. cynodontis* is more efficient regarding the synthesis of (S)-2-hydroxyparaconate. Since Geiser *et al.* [139] demonstrated that overexpression of *cyp3* led to increased (S)-2-hydroxyparaconate production, this approach would be interesting in *U. cynodontis* $\Delta ras2$. Especially since it could be shown in chapter 3.3 that *cyp3* has the same function in *U. cynodontis* as in *U. maydis*. For further improvements of (S)-2-hydroxyparaconate production, the extracellular transporter *itp1* should be replaced by *mfsA* of *A. terreus*, as it could be shown in chapter 3.3 that heterologous expression of MfsA is beneficial for (S)-2-hydroxyparaconate production.

4.3 Metabolic Engineering

Metabolic engineering is a strategy to increase product to substrate yield, space-time yield, and titer. This can be achieved by deletion or overexpression of genes to improve the flux of a responsible pathway for a determined product. Further natural or synthetic pathways from other organisms can be introduced into the biotechnological host of choice to enable higher efficiency or unique functionality [327]. Since the itaconate cluster was identified and annotated for several Ustilaginaceae in chapter 3.1, the foundation was laid for the following steps. In this thesis, CRISPR/Cas9 and FLP/FRT were used for genome editing, including the deletion, insertion, and overexpression of genes, which dramatically increased itaconate production in *U. maydis* and *U. cynodontis*. In *U. maydis* production could be increased 4.2-fold, and a titer of 220 g L⁻¹ was reached. In *U. cynodontis* production could even be improved to 6.2-fold compared to wildtype. For further improvement, the own mitochondrial transporter should be deleted since it could be shown in chapter 3.1 that single integration of *mttA* from *A. terreus* boosts the production of itaconate.

Further up-regulation strategies of metabolic steps upstream from itaconate precursors, could help to increase itaconate production. In *A. niger* with this strategy, itaconate production could be enhanced drastically by nearly 50 %. This was achieved by the introduction of a truncated version of a 6-phosphofructo-1-kinase that showed reduced inhibition by citrate and ATP [58, 328]. To upregulate the metabolism also sufficient intracellular oxygen supply is necessary. Especially because itaconate production in *Ustilago* is highly dependent on continuous aeration and already short interruptions of oxygen supply led to a lower itaconate yield [146]. Thus, reducing oxygen sensitivity to oxygen limitation might be a benefit for itaconate production in *Ustilago*. In *A. terreus*, this was achieved by expressing hemoglobin from *Vitreoscilla* [329]. Possibly this strategy is also successful for *Ustilago*.

Since *cis*-aconitate decarboxylase (*cadA*) from *A. terreus* was successfully expressed heterologously in several organisms, such as *E. coli*, *S. cerevisiae*, *Yarrowia lipolytica*, *Candida lignohabitans* *Snechocystis* sp., and *Corynebacterium glutamicum* and could improve itaconate production [25], this approach could be used also in *Ustilago* to reduce the conversation steps in the cytosol. Additionally, the identification of the physiological role of itaconate in its natural producers such as *A. terreus* or *Ustilago* could help to understand cellular mechanisms that could

improve the process and find new targets for further improvements, especially on the regulation of its formation. It is assumed that itaconate is used as a defense strategy to combat competitors [23], but more research will be necessary for the future to understand the exact mechanisms in the natural habitats of *Ustilago* and *Aspergillus*.

To further increase especially the yield for itaconate, down-regulation or deletion of side products is a well-known strategy. For *U. maydis* glycolipids like ustilagic acid and mannosylerythritol lipids production is known, in contrast, *U. cynodontis* doesn't produce glycolipids [267, 330, 331]. Deletion of these compounds could help to drive the flux towards itaconate production and thus enhance the yield since more carbon would be available for itaconate anabolism. For *U. maydis* it was already shown that by deletions of *cyp1* (P₄₅₀ monooxygenase involved in ustilagic acid biosynthesis) or/and *eml1* (glycosyltransferase in the mannosylerythritol lipid biosynthesis) corresponding glycolipid production could completely be abolished [206], but unfortunately, itaconate production couldn't be improved [245]. In order to benefit from these modifications in the context of itaconate production as well, maybe simultaneous deletion of the whole gene cluster of ustilagic acid and mannosylerythritol lipids in one itaconate-hyperproducing strain would be advantageous. Since the production of glycolipids complicates sample handling and product recovery because of their hydrophobic droplet nature, with the abovementioned deletions sample preparation could be facilitated. Additionally, intracellular lipids could be deleted, especially because they are formed under nitrogen limiting conditions and thus under itaconate producing conditions [107] and are the reason why the pellet always floats on top and thus makes sample processing more difficult. Thus with the elimination of intracellular lipids not just the yield for itaconate could be improved but also for the further process.

Instead of preventing the formation of mannosylerythritol compounds, one could strive for their production as they are an interesting compound for biotechnological applications and can be used for different products [332]. *U. maydis* could be established in the future as a production host, especially due to the availability of a high number of molecular tools for this organism. In this context, *U. cynodontis* could also be established as a microbial cell factory for the synthesis of other organic acids such as malic acid, to exploit the advantage of pH tolerance. To further reduce by-product formation, the downregulation of other organic acids such as malic acid secretion in *U. maydis* could be taken into consideration. Since several organic acids are absolutely necessary as intermediates of the TCA cycle, deletions of associated reactions have to be considered with care. Therefore, the downregulation of respective enzymes using weak promoters could be a possibility.

Further, itaconate production could be increased by identifying associated degradation pathways like it was found recently for *A. niger*. By deletion of the key genes *ictA* and *ichA* Hossein *et al.* could increase itaconate production significantly. BLAST analysis with subsequent deletion of possible genes could possibly show the same effect in *U. maydis* or *U. cynodontis* [333]. Since in both strains, product toxicity was observed, adaptive laboratory engineering could be performed to generate more tolerant strains. The subsequent whole-genome sequencing could allow the identification of mutations in potential targets to further enhance the production in future with reverse engineering approaches.

Another critical factor is the screening procedure during the process of metabolic engineering. In order to reduce the required time, work and resources, pH Sensorspots technology from PreSens (PreSens, Germany) could be used. This would allow high-throughput screening for itaconate production strains by pH decreasing pH-values since better-producing strains lower the pH value more in the screening medium. However, also CRISPR/Cas9 technology should be improved in

the future, since the process lacked efficiency and the efforts to find the right transformants were very high in this study.

To exclude locus-dependent adverse effects of the random genomic insertion such as copy number effects, hot/cold spots on the genome, *ip*-locus site-specific integration like in *U. maydis* should be established for *U. cynodontis* to overcome this problem.

4.4 Process Engineering: A long journey with challenges

Other factors that increase production costs are the fermentation and downstream process. Parameters such as temperature, pH, media composition, and the used organism can have a significant influence on these two parameters.

The medium composition can have a significant influence on the physiology of microorganisms and influence in this way enormous production behavior. As mentioned in chapter 1, *A. terreus* is very sensitive towards medium impurities, and the medium must be purified. Otherwise *A. terreus* would undergo morphological changes that disturb itaconic acid production [21, 23, 156]. This leads to additional costs in the process. In contrast, *U. cynodontis* and *U. maydis* production strains engineered in this thesis showed stable yeast-like growth under several biotechnological relevant itaconate production conditions. This was achieved by rational modifications in lifecycle-associated proteins in both strains. Their robust morphological phenotype offers an enormous advantage for the fermentation process [25]. The fact that higher amounts of nitrogen did not yield in an equivalent increase of biomass indicates limitation by other medium components or toxic effects like Klement *et al.* reported for *U. maydis* [197]. High nitrogen concentration enables higher biomass formation, higher production rates but a decrease in the yield. To achieve this and avoid toxic effects, ammonium chloride could be added by a feeding profile. Additionally, the screening medium should be optimized to exclude a limitation by another component. These measures allow hopefully to reach more biomass resulting in better production behavior. Especially also, alternatives to yeast extract should be identified that are not as expensive as yeast extract but show the same effect. To achieve this and be able to test as many medium combinations as possible, automated robot techniques should be used to minimize the effort. Alternatively, also DOE software can be used to limit the selection of components. One component of the media which can drive up process costs is the carbon source. Refined sugar is an expensive carbon source, but due to its purity, it allows comparably cheap product purification [8]. However, the use of glucose as a substrate competes with human food production. Therefore alternative feedstock's such as agricultural wastes become more and more interesting since they are cheap and abundantly available [8]. Thus, the itaconate production costs could be further decreased and additionally in a bio-economy context.

For *U. maydis* pretreated cellulose in seawater and hydrolyzed hemicellulose fraction of pretreated beech wood were used successfully as substrate [197]. Also, for itaconate production by *A. terreus* pretreated wood hydrolysates [159, 334, 335] were established as a carbon source. However so far, none of the applications could assert itself due to strong growth deficits caused by inhibitory compounds [107, 197]. In this thesis itaconate production on glycerol was increased from nearly none to high amounts by deletion of *Fuz7* in *U. maydis* and *U. cynodontis*. In preliminary experiments, itaconate production from carrot extract as cheap carbon source was tested, with very comparable results to glucose. Further the deletion of *fuz7* in engineered *U. maydis* $\Delta cyp3 \Delta fuz7$ $P_{ete}mttA \Delta P_{ria1}::P_{ete}$ or *U. cynodontis* $\Delta fuz7 \Delta cyp3 P_{ete}mttA P_{ria1}ria1$ enabled the efficient itaconate production in a co-culture with cellulase-secreting *Trichoderma reesei* using cellulose as a carbon source for itaconate (personal communication Ivan Schlembach). In all these experiments, the

strains showed over the whole cultivation time a stable and yeast-like growth. *U. maydis* can grow on various substrates and expresses a set of lignocellulose-degrading enzymes which are necessary for plant invasion [137, 198-200, 336-338]. Based on these properties and on the results achieved in this work, especially the stable morphology on unwanted carbon sources, new experimental approaches with regard to lignocellulose as carbon source should be carried out. Many other processes also focus on cost reduction through alternative carbon sources like for instance lactic acid with red lentil flour in India [34, 35], kitchen waste in Japan [36], barley hydrolysates in the European Union [37] or liquefied cornstarch from cassava bagasse [38, 39]. Since organisms often cannot metabolize these sources directly a two-step utilization is a possibility. For succinic acid, wheat flour is first converted by a fungal bioprocess, and afterwards, it is fermented by *Actinobacillus succinogenes* to succinate [339]. However, these approaches are still in their initial stage and require further development since most organisms react sensitively to impurities that are often present in alternative feedstocks [8]. This underlines the importance of this thesis in which is clearly demonstrated that cell robustness and fitness and the possibility to handle several unlike conditions are essential factors that bring advantages for subsequent bioprocess optimization. The optimal carbon source must be chosen regarding the complete production process. Refined sugar is expensive but enables cheap downstream processing. Abovementioned carbon-providing waste streams are cheap, but they can comprise a large number of side products that interfere with bioprocess and thus lead to higher purification costs [8]. Ecologically speaking, alternative carbon sources are more sustainable because they are not in direct competition with the human food chain. Research is ongoing in this field, as mentioned above and will undoubtedly be one main criterion if microbial organic acid production can assert itself. Next to medium components also production parameters such as pH and temperature, among others have a high influence on the microbial physiology of the production costs.

For organic acid production, low pH values are preferred since this reduces base consumption, enhanced sterility, and benefits for later downstream processing [8, 201]. The possibility to execute low-pH fermentations depends strongly on the biocatalytic host organism, its tolerance towards low pH values, and its ability to produce the desired product under these conditions. In *A. terreus*, for example low pH values are necessary to induce itaconate production. After the initial induction, different pH shift experiments were performed to study the production behavior under multiple pH conditions. At a pH of 3.4, the best production was achieved [21]. Also, in some *Saccharomyces* and *Yarrowia* strains, organic acid production could be improved under low pH conditions. In contrast, most Ustilaginaceae are only able to produce sufficient amounts of organic acids above pH values of 5 [137]. Below a pH 5 itaconic acid and (*S*)-2-hydroxyparaconate production decreased drastically in *U. maydis*, and biomass formation was significantly decreased, which is depicted and discussed in chapter 3.3. However also, fermentations with high pH values have their advantages. Under this condition, organic acids are present in their double dissociated form and cause lower stress levels for the cell. Contrarily, under low pH value, organic acids are present in their undissociated form. In this form, the acid can diffuse freely across the membrane and cause weak organic acid stress. Product toxicity and weak organic acid stress are common challenges in organic acid fermentations [340, 341]. The option to produce organic acids at high pH values is beneficial due to the lowered acid stress. In this context, *U. maydis* is an ideal production host. In this thesis, high-pH fermentations were performed using CaCO₃ as a strong buffering agent. Itaconic acid was constantly removed from the media by complexation with CaCO₃. Thus the use of CaCO₃ as buffer integrated initial steps of the downstream process into the production process. This procedure was previously used for malic acid production with

U. trichophora [97]. The main drawback of this technique was the high viscosity and sedimentation during fermentation, which made the process in general quite difficult. To prevent sedimentation effects, guarantee a better homogenization and oxygen supply combination of Rushton impeller and pitched blade impeller could be used in the future. The pitched impeller helps to create a suction towards the bottom of the fermenter and thereby whirling up solid components and the Rushton impeller supports more efficient oxygen distribution in the fermentation broth (personal communication Lars Regestein). In the future, CaCO_3 should be replaced by CaCl_2 since in this case no solid medium components are present in the fermentation broth which facilitates product. Further, to prevent CaCO_3 and calcium-itaconate deposits, the cultivation of immobilized cells in an airlift reactor could be an option, since solids would sediment to the bottom and could then be removed periodically [342]. Moreover, airlift reactors are cheaper than stirred reactors. *U. cynodontis* is the exception under the Ustilaginaceae and produces organic acids for a wide range of pH values. Thereby best production was achieved at pH 3.6 in this thesis for itaconic acid production and enable the abovementioned advantages. Because product toxicity was observed for itaconate in *U. cynodontis*, in the future strategies must be developed to overcome this challenge. Since optimal production takes place at pH = 3.6 complexation with CaCO_3 as it was done for *U. maydis* is not possible. To further improve itaconic acid production in *U. cynodontis* in the future, *in situ* product removal by reactive extraction could be investigated. ISPR is an attractive option for product removal combined with the fermentation process. This would lead to reduced purification and downstream costs [343] and would further economize base for pH regulation since itaconate is constantly removed [344]. Reactive extraction is an efficient method for the recovery of carboxylic acids from fermentation broth. It is suitable for high substrate concentrations, and the reaction equilibrium can be adapted as required [344]. Trioctylamine is the most common reactive extractant for organic acid, and its high molecular weight and aliphatic tertiary amine combines high extraction efficiency with low water solubility [343, 345-347]. For extraction, the un-dissociated carboxyl groups of itaconate are complexed by TOA, thereby increasing the solubility in the organic phase. Since the dissociated form of the acid is not complexed by TOA, low pH values are necessary for efficient extraction and thus make this method possible for *U. cynodontis*. ISPR by reactive extraction of itaconate with TOA is already established for *A. terreus* [308]. In literature also further possibilities such as continuous cultures, repeated-batch cultures and, as mentioned above, genetic modifications are discussed to overcome product toxicity. [329, 341].

Another critical and significant parameter is temperature. Organic acid production can differ drastically depending on temperature [136, 170]. It could be shown in the past for *U. cynodontis* that the highest titers were reached at 25 °C [136]. In the future, temperature shift experiments could be performed to characterize the optimal temperature for the growth and production phase. This was also the case for malic acid production with *U. trichophora* with a temperature of 28°C for the growth phase and 37 °C during the production phase [102]. However, since cooling costs can decide about the success of a product and make up one major part of the overall costs, production at higher temperature is more useful.

4.4.1 Conclusion

In this thesis, itaconate production was immensely enhanced using *Ustilago* as a biocatalytic host. Thereby, it was achieved to close the gap in performance to the best itaconate producer *A. terreus*. Strong filamentous growth could be abolished in *U. maydis*, and *U. cynodontis* production strains by morphological engineering. This was achieved by the deletion of the *fuz7*

gene, which is involved in the lifecycle of Ustilaginaceae and plant infection. With this approach, stable and robust *U. maydis* and *U. cynodontis* strains were established for a high number of conditions which are relevant for itaconate production. This robustness enabled further media optimization, especially growth on not preferred C-sources, such as glycerol and carrot extract. Further, the engineered yeast-like growth of *U. cynodontis* enabled its first successful application in a bioreactor. Additionally the performance of *U. maydis* was enhanced by the deletion of *fuz7* what enhanced its performance in a fermenter. In both strains (*U. maydis* and *U. cynodontis*), itaconate production could be further increased drastically using metabolic engineering. In *U. cynodontis* production was increased to 6.5-fold and with *U. maydis* a titer of 220 g L⁻¹ was achieved, which is the highest value for itaconate with any microorganism. Further, this study solved one of the main drawbacks of *Ustilago* compared to *Aspergillus*, namely pH tolerance. With *U. cynodontis*, a pH-tolerant organic acid producer could be established, which has its pH optimum for itaconate at 3.6.

The powerful combination of stable yeast-like growth, pH tolerance in *U. cynodontis* and CaCO₃ precipitation with *U. maydis* open up a range of possibilities in the field of process development. While with CaCO₃ product toxicity could be prevented in *U. cynodontis* repeated-batch strategy could be developed to overcome product toxicity to continue itaconate production to a higher level and are the basis for future cell retention systems.

Especially the stable yeast-like morphology with the created strains generate a range of possibilities in the field of process development such as the transfer to larger systems and the investigation in retention systems and should be the basis for further research to achieve necessary production parameters to assert *Ustilago* as an industrial itaconate producer.

Appendix

Supplemental tables

Table 11. Feeding procedure during high-density pulsed fed-batch fermentation of *U. maydis* MB215 $\Delta cyp3 \Delta P_{ria1}::P_{atf7} \Delta fit7 P_{atf7}mtA$. CaCO₃ and glucose feed protocol during fermentation in a bioreactor containing batch medium with glucose, 1.6 g L⁻¹ NH₄Cl above pH 6.0 controlled with CaCO₃.

feed	hours (h)	glucose (mL)	CaCO ₃
1	24	100	
2	58	80	
3	95	50	
4	96		50 mL (L) ^a
5	102		50 mL (L) ^a
6	120	50	
7	151		50 mL (L) ^a
8	167.5		25 mL (L) ^a
9	173.5	25	
10	191	25	
11	201	30	30 mL (L) ^a
12	223	30	
13	247	30	
14	269.5	30	30 mL (L) ^a
15	311.5		50 mL (L) ^a
16	313.5	30	
17	315.5		50 g (S) ^b
18	360.5	30	
19	387.5	30	
Σ (g)		432	192.5

^aL: Liquid

^bS: Solid

Appendix

Table 12. Feeding procedure during high-density pulsed fed-batch fermentation of *U. maydis* MB215 $\Delta cyp3 \Delta P_{ria1}::P_{etef} \cdot \Delta fuiz7 P_{engmttA}$. CaCO₃ and glucose feed protocol during fermentation in a bioreactor containing batch medium with glucose, 4.0 g L⁻¹ NH₄Cl above pH 6.0 controlled with CaCO₃.

feed	hours (h)	glucose (mL)	CaCO ₃
1	45		50 mL (l) ^a
2	46.5		50 mL (l) ^a
3	68.5	50	
4	70.5	60	
5	77	100	
6	116	60	50 mL (l) ^a
7	124.5	30	
8	141		50 mL (l) ^a
9	147	30	30 mL (l) ^a
10	169.5	50	
11	189		50 mL (l) ^a
12	191	100	
13	193		50 g (s) ^b
14	238	100	
15	265		50 g (s) ^b
16	286.5	100	
17	335		50 g (s) ^b
18	358.5	100	
19	383.5	100	50 g (s) ^b
Σ (g)		704	340

^aL: Liquid

^bS: Solid

Table 13. Oligonucleotides used for cloning, diagnostic PCRs and sequencing procedures. Shown are the respective designations, description and sequence. Specific binding sequence are capitalized and lower case letters indicate overhangs.

Primer	Sequence (5' → 3')	description
HT-0	AGGATCTTACCCTGTTG	fwd. primer for verification of pSMUT integration
HT-0a	GAAAGGGCCTCGTGATAC	rev. primer for verification of pSMUT integration
HT-4a	ACAGACGTCGCGGTGAGTTC	fwd. primer for verification of <i>fuz7</i> deletion in <i>U. maydis</i>
HT-8a	GTCGAGCTCGGTACGGGT	fwd. primer for amplification of CRISPR_ <i>P_{etef}</i> target
HT-9	CCTTGCAATTCGCGCACACC	rev. primer for verification of right assembly of pCas9_ <i>P_{etef}_1</i>
HT-10	GCTCGGTACGGTACTAATG	rev. primer for verification of right assembly of pCas9_ <i>P_{etef}_1</i>
HT-12	CGTTGTAGAATGGAATTTTG	fwd. primer for amplification of pTARGET- <i>P_{riaI}</i>
HT-21a	CGAGACTCCTCGAGATTC	fwd. primer to amplify deletion construct for <i>mtt1</i> from pJet_ <i>UcN_mtt1</i> and to verify <i>mtt1</i> deletion in <i>U. cynodontis</i>
HT-22a	CAAACCCGTAGTACAGAC	rev. primer to amplify deletion construct for <i>mtt1</i> from pJet_ <i>UcN_mtt1</i> and to verify <i>mtt1</i> deletion in <i>U. cynodontis</i>
HT-27	TGGTGCCAGCTCTGTATATG	fwd. primer to amplify deletion construct for <i>itp1</i> from pJet_ <i>UcN_itp1</i> and to verify <i>itp1</i> deletion in <i>U. cynodontis</i>
HT-28	CCTATTGCGTCAGGCATTC	rev. primer to amplify deletion construct for <i>itp1</i> from pJet_ <i>UcN_itp1</i> and to verify <i>itp1</i> deletion in <i>U. cynodontis</i>
HT-42	CAA AATTCATTCTACAACG	rev. primer for amplification of CRISPR_ <i>P_{etef}</i> target
HT-43	AAAGTGTGCCGAGGTGAGG	for sequencing and verification of pCas9_ <i>P_{etef}_1</i>
HT-45	ctcgagtttttcagcaagatACTCTCCAATCTGATGG	fwd. primer for amplification of F2- <i>mtt1</i> to construct pJet_ <i>UcN_mtt1</i>
HT-46	acgccatggtTGCCCAACGACCTTTTTTC	rev. primer for amplification of F2- <i>mtt1</i> to construct pJet_ <i>UcN_mtt1</i>
HT-47	tcggtgggcaACCATGGCGTGACAATTG	fwd. primer for amplification of Hyg ^R - <i>mtt1</i> to construct pJet_ <i>UcN_mtt1</i>
HT-48	ctctcactttTATTAATGCGGCCGCACAG	rev. primer for amplification of Hyg ^R - <i>mtt1</i> to construct pJet_ <i>UcN_mtt1</i>
HT-49	cgcaataaAAAGTGAGAGGCGAGCGTCCCTAAAAAC	fwd. primer for amplification of F1- <i>mtt1</i> to construct pJet_ <i>UcN_mtt1</i>
HT-50	aggagatctctagaagatCCGCCACGCCCTGCGGACT	rev. primer for amplification of F1- <i>mtt1</i> to construct pJet_ <i>UcN_mtt1</i>
HT-51a	ctcgagtttttcagcaagatACAGTAGATTCCACACTTGC	fwd. primer for amplification of F2- <i>itp1</i> to construct pJet_ <i>UcN_itp1</i>
HT-52a	acgccatggtAGATTTTGCATCTGCG	rev. primer for amplification of F2- <i>itp1</i> to construct pJet_ <i>UcN_itp1</i>
HT-53a	cgcaaatctACCATGGCGTGACAATTG	fwd. primer for amplification of Hyg ^R - <i>itp1</i> to construct pJet_ <i>UcN_itp1</i>
HT-54a	ctggccagtTATTAATGCGGCCGCACAG	rev. primer for amplification of Hyg ^R - <i>itp1</i> to construct pJet_ <i>UcN_itp1</i>
HT-55a	cgcaataaCACTGGCCAGAAAGTACAGTC	fwd. primer for amplification of F1- <i>itp1</i> to construct pJet_ <i>UcN_itp1</i>
HT-56a	aggagatctctagaagatGGTCAGCTCGAGCTGGTATG	rev. primer for amplification of F1- <i>itp1</i> to construct pJet_ <i>UcN_itp1</i>
HT-82	gagcttcatgatcagctgctGTTTTAGAGCTAGAA	rev. primer for amplification of pTARGET- <i>P_{riaI}</i>
HT-83	ctcgagtttttcagcaagatTTTGGTGCGATCTCGTTC	fwd. primer for amplification of F1- <i>P_{oma}</i>
HT-84	atccccggccATGCGCTTTGCAGGGATG	rev. primer for amplification of F1- <i>P_{oma}</i>

Appendix

HT-85	caaagcgcacGGCCGGGATCTGATAG	Fwd. primer for amplification of P _{oma} from pUMa 2326
HT-86	ggccagatacACTTCTCGAGCAGGGGG ATTC	rev. primer for amplification of P _{oma} from pUMa 2326
HT-87	ctcgaagaagtGTATCTGGCCAGCCAGCC	fwd. primer for amplification of F2-P _{oma}
HT-88	aggagatctctagaagaatGGTCGAGCCAG GCGCATG	rev. primer for amplification of F2-P _{oma}
HT-89	TTTGGTGGCATCTCGTTC	fwd. primer for amplification on donor construct
HT-90	GGTCGAGCCAGGCGCATG	rev. primer for amplification on donor construct
HT-100	AAGGGTGGCATCGAGGAGAG	fwd. primer to amplify deletion construct of <i>ras2</i> from pFRT ^{WT} -UcN <i>ras2</i>
HT-101	CTCGAGCCACTTAGCCTTTC	rev. primer to amplify deletion construct of <i>ras2</i> from pFRT ^{WT} -UcN <i>ras2</i>
HT-109	TCCGCTTTGAGGTACAGTTG	fwd. primer to amplify deletion construct of <i>fuz7</i> from pFRT ^{WT} -UcN <i>fuz7</i>
HT-110	CCACATTAGCAGGTGGTATC	rev. primer to amplify deletion construct of <i>fuz7</i> from pFRT ^{WT} -UcN <i>fuz7</i>
HT-117	GACAAGCTCAGTGCCTCTC	fwd. primer to amplify deletion construct of <i>ubc3</i> from pFRT ^{WT} -UcN <i>ubc3</i>
HT-118	CACTTCCATCGGAACATGTG	rev. primer to amplify deletion construct of <i>ubc3</i> from pFRT ^{WT} -UcN <i>ubc3</i>
HT-119	CGATCCC GCGATTATCAC	fwd. primer for verification of <i>ras2</i> deletion in <i>U. cynodontis</i>
HT-120	CCAGTCACTCGCTCATTC	rev. primer for verification of <i>ras2</i> deletion in <i>U. cynodontis</i>
HT-121	ACGATTGTGCCAAGCTTC	fwd. primer for verification of <i>fuz7</i> deletion in <i>U. cynodontis</i>
HT-122	GCAGCTGATTGATGTTGG	rev. primer for verification of <i>fuz7</i> deletion in <i>U. cynodontis</i>
HT-123	CCATGTCTAGTCCCTTTC	fwd. primer for verification of <i>ubc3</i> deletion in <i>U. cynodontis</i>
HT-124	CGAGACAGGTTGACTTTC	rev. primer for verification of <i>ubc3</i> deletion in <i>U. cynodontis</i>
HT-147	ctcatcctgcaaaagcgcacTGGATGATGTTG TCTGTGTATGGTATG	fwd. primer for amplification P _{enef} from pETEF-05080 CbxR
HT-148	atggctggctggccagatacAGTTCGCATGC CTGCAGG	rev. primer for amplification P _{enef} from pETEF-05080 CbxR
HT-168	ctcgagttttcagcaagatCTTCTACAAGCG TGATTTACAAAGG	fwd. primer for amplification of F1- <i>ras2</i> to construct pFRT ^{WT} -UcN <i>ras2</i>
HT-169	acttctggccGTGGTCAGTCAGAGGGCG	rev. primer for amplification of F1- <i>ras2</i> to construct pFRT ^{WT} -UcN <i>ras2</i>
HT-170	gactgaccacGGCCAGAAGTTCCTATTC	fwd. primer for amplification of FRT ^{WT} +Hyg ^R - <i>ras2</i> to construct pFRT ^{WT} -UcN <i>ras2</i>
HT-171	gttgeccaacGGCCAGAAGTTCCTATAC	rev. primer for amplification of FRT ^{WT} +Hyg ^R - <i>ras2</i> to construct pFRT ^{WT} -UcN <i>ras2</i>
HT-172	acttctggccGTTGGGCAACTGTATT C	fwd. primer for amplification of F2- <i>ras2</i> to construct pFRT ^{WT} -UcN <i>ras2</i>
HT-173	aggagatctctagaagaatGTCTCTCTCTCA AGCACAC	rev. primer for amplification of F2- <i>ras2</i> to construct pFRT ^{WT} -UcN <i>ras2</i>
HT-174	ctcgagttttcagcaagatCCAAATCCGCCG TCGGAG	fwd. primer for amplification of F1- <i>ubc3</i> to construct pFRT ^{WT} -UcN <i>ubc3</i>
HT-175	acttctggccAAGTGAAGTGTGGAAG CATTTC	rev. primer for amplification of F1- <i>ubc3</i> to construct pFRT ^{WT} -UcN <i>ubc3</i>
HT-176	acttccacttGGCCAGAAGTTCCTATTC	fwd. primer for amplification of FRT ^{WT} +Hyg ^R - <i>ubc3</i> to construct pFRT ^{WT} -UcN <i>ubc3</i>
HT-177	cttctgctcaGGCCAGAAGTTCCTATAC	rev. primer for amplification of FRT ^{WT} +Hyg ^R - <i>ubc3</i> to construct pFRT ^{WT} -UcN <i>ubc3</i>
HT-178	acttctggccTGAGCAAGAGAGTGTGTT C	fwd. primer for amplification of F2- <i>ubc3</i> to construct pFRT ^{WT} -UcN <i>ubc3</i>

HT-179	aggagatctttetagaagaatCACGATCACACT TCCATC	rev. primer for amplification of F2- <i>ubc3</i> to construct pFRT ^{WT} - <i>UcN ubc3</i>
HT-180	ctcagagtttttcagcaagaatTCCGCTTTGAGGT ACAGTTG	fwd. primer for amplification of F1- <i>fuz7</i> to construct pFRT ^{WT} - <i>UcN fuz7</i>
HT-181	acttctggccGGTCGCCCTGTGATAGT G	rev. primer for amplification of F1- <i>fuz7</i> to construct pFRT ^{WT} - <i>UcN fuz7</i>
HT-182	aggggcgaccGGCCAGAAGTTCCTATT C	fwd. primer for amplification of FRT ^{WT} +Hyg ^R - <i>fuz7</i> to construct pFRT ^{WT} - <i>UcN fuz7</i>
HT-183	ggctgccatGGCCAGAAGTTCCTATAC	rev. primer for amplification of FRT ^{WT} +Hyg ^R - <i>fuz7</i> to construct pFRT ^{WT} - <i>UcN fuz7</i>
HT-184	acttctggccGATGGCAGCCCTAATGAG	fwd. primer for amplification of F2- <i>fuz7</i> to construct pFRT ^{WT} - <i>UcN fuz7</i>
HT-185	aggagatctttetagaagaatGCCCACATTAGC AGGTGG	rev. primer for amplification of F2- <i>fuz7</i> to construct pFRT ^{WT} - <i>UcN fuz7</i>
HT-204	ctcagagtttttcagcaagaatCCGATCGCTGTT AGGACAC	fwd. primer for amplification of F1- <i>fuz7</i> to construct pFRT ^{WT} - <i>Um fuz7</i>
HT-205	acttctggccCGTGAAACGTTGCAAAAC AG	rev. primer for amplification of F1- <i>fuz7</i> to construct pFRT ^{WT} - <i>Um fuz7</i>
HT-206	acgtttcaagGGCCAGAAGTTCCTATTC	fwd. primer for amplification of FRT ^{WT} +Hyg ^R - <i>fuz7</i> to construct pFRT ^{WT} - <i>Um fuz7</i>
HT-207	tctcagtcggGGCCAGAAGTTCCTATAC	rev. primer for amplification of FRT ^{WT} +Hyg ^R - <i>fuz7</i> to construct pFRT ^{WT} - <i>Um fuz7</i>
HT-208	acttctggccCCGACTGAGAGATTATGG TC	fwd. primer for amplification of F2- <i>fuz7</i> to construct pFRT ^{WT} - <i>Um fuz7</i>
HT-209	aggagatctttetagaagaatAATCGGAACCGT GTACCTG	rev. primer for amplification of F2- <i>fuz7</i> to construct pFRT ^{WT} - <i>Um fuz7</i>
HT-210	TCGCTGTTAGGACACAACCTG	fwd. primer to amplify deletion construct of <i>fuz7</i> from pFRT ^{WT} - <i>Um fuz7</i>
HT-211	CCGTGTACTGGCTGTGTAG	rev. primer to amplify deletion construct of <i>fuz7</i> from pFRT ^{WT} - <i>Um fuz7</i>
HT-212	GGATCCCGTGGATGATGTTG	fwd-primer for amplification the backbone to construct P _{eref} Uc <i>rial-cbx</i> , P _{eref} Pt <i>rial-cbx</i> and P _{eref} Si <i>rial-cbx</i> .
HT-212	GGATCCCGTGGATGATGTTG	rev. primer for verification of <i>fuz7</i> deletion in <i>U. maydis</i>
HT-213	TCTAGAGCGGCCGCCCGG	rev-primer for amplification the backbone to construct P _{eref} Uc <i>rial-cbx</i> , P _{eref} Pt <i>rial-cbx</i> and P _{eref} Si <i>rial-cbx</i> .
HT-214	CAACATCATCCACGGGATCCATGA GCCTCTCGAACAGCAATC	fwd-primer for amplification of <i>rial1</i> from <i>U. cynodontis</i> to construct P _{eref} Uc <i>rial-cbx</i> .
HT-215	AGCCGGGCGGCCGCTCTAGATCAT CGGTGCCGTCTCCTG	rev-primer for amplification of <i>rial1</i> from <i>U. cynodontis</i> to construct P _{eref} Uc <i>rial-cbx</i> .
HT-216	CAACATCATCCACGGGATCCATGA GCGTGTCAAACAGC	fwd-primer for amplification of <i>rial1</i> from <i>U. cynodontis</i> to construct P _{eref} Pt <i>rial-cbx</i> .
HT-217	AGCCGGGCGGCCGCTCTAGATCAT CGGTAACGCCTCTTG	rev-primer for amplification of <i>rial1</i> from <i>U. cynodontis</i> to construct P _{eref} Pt <i>rial-cbx</i> .
HT-218	CAACATCATCCACGGGATCCATGA AGATTCTCATCGACC	fwd-primer for amplification of <i>rial1</i> from <i>U. cynodontis</i> to construct P _{eref} Si <i>rial-cbx</i> .
HT-219	AGCCGGGCGGCCGCTCTAGATCAA CGATGACGTTTCTTTG	rev-primer for amplification of <i>rial1</i> from <i>U. cynodontis</i> to construct P _{eref} Si <i>rial-cbx</i> .
HT-228	ctcagagtttttcagcaagaatTTACAATTCTTTG CCTCTC	fwd. primer for amplification of F1- <i>cyp3</i> to construct pFRT ^{M1} - <i>UcN cyp3</i>
HT-229	acttctggccCTCGTATACTTGCAAAAT G	rev. primer for amplification of F1- <i>cyp3</i> to construct pFRT ^{M1} - <i>UcN cyp3</i>
HT-230	gtatagcgagGGCCAGAAGTTCCTATTC	fwd. primer for amplification of FRT ^{M1} +Hyg ^R - <i>cyp3</i> to construct pFRT ^{M1} - <i>UcN cyp3</i>
HT-231a	aaacatgtcCCCGGGAAGTTCCTATAC	rev. primer for amplification of FRT ^{M1} +Hyg ^R - <i>cyp3</i> to construct pFRT ^{M1} - <i>UcN cyp3</i>
HT-232a	ACTTCCCGGGGAACATGTTTCAGA ATGCTGC	fwd. primer for amplification of F2- <i>cyp3</i> to construct pFRT ^{M1} - <i>UcN cyp3</i>
HT-233	aggagatctttetagaagaatTCGGGATACCA TCACGAG	rev. primer for amplification of F2- <i>cyp3</i> to construct pFRT ^{M1} - <i>UcN cyp3</i>
HT-234	TGATCTTCTGCGAGCCGAAC	fwd. primer to amplify deletion construct of <i>cyp3</i> from pFRT ^{M1} - <i>UcN cyp3</i>

Appendix

HT-235	GCTTGGAGGAAGCCGATCTG	rev. primer to amplify deletion construct of <i>cyp3</i> from pFRT ^{M1} - <i>UcN cyp3</i>
HT-236	TTTGCCCTGCCGTCAACACTG	fwd. primer for verification of <i>cyp3</i> deletion in <i>U. cynodontis</i>
HT-237	TTGCCCCACACGATGATCGG	rev. primer for verification of <i>cyp3</i> deletion in <i>U. cynodontis</i>
HT-238	ctcgagttttcagcaagatGAAAGATTGGCACTACTG	fwd. primer for amplification of F1- <i>rial</i> to construct pFRT ^{M1} - <i>UcN rial</i>
HT-239	actcttgcccCACTCTCGATGCAAATTAATG	rev. primer for amplification of F1- <i>rial</i> to construct pFRT ^{M1} - <i>UcN rial</i>
HT-240	atcgagagtgGGCCAGAAGTTCCTATTC	fwd. primer for amplification of FRT ^{M1} +Hyg ^R - <i>rial</i> to construct pFRT ^{M1} - <i>UcN rial</i>
HT-241	ttacaactctCCCGGGGAGTTCCTATAC	rev. primer for amplification of FRT ^{M1} +Hyg ^R - <i>rial</i> to construct pFRT ^{M1} - <i>UcN rial</i>
HT-242	acttcccgggAGAGTTGTAAAGTTACCCTG	fwd. primer for amplification of F2- <i>rial</i> to construct pFRT ^{M1} - <i>UcN rial</i>
HT-243	aggagactctctagaagatACAATCAGTAA GTGCAGAC	rev. primer for amplification of F2- <i>cyp3</i> to construct pFRT ^{M1} - <i>UcN rial</i>
HT-244	TCTGGAAAGCGGGTACTG	fwd. primer to amplify deletion construct of <i>rial</i> from pFRT ^{M1} - <i>UcN rial</i>
HT-245	TCAAATGCAGCCAGGATG	rev. primer to amplify deletion construct of <i>rial</i> from pFRT ^{M1} - <i>UcN rial</i>
HT-246	GACACAGTTCATGCCTTGAG	fwd. primer for verification of <i>rial</i> deletion in <i>U. cynodontis</i>
HT-247	CAACTACATCGCTGGGATGG	rev. primer for verification of <i>rial</i> deletion in <i>U. cynodontis</i>
HT-292	CTCGAAATTGACGGTGGCTCGATTGATATTCTAG	fwd. primer for amplification backbone from <i>Petef_CBX_A_ter_mtt</i> to construct pETEF_hyg_mttA
HT-293	GAAAGCGAGACGAGTTGAG	rev. primer for amplification backbone from <i>Petef_CBX_A_ter_mtt</i> to construct pETEF_hyg_mttA
HT-294	gagccaccgtcaattcgagACCATGGCGTGACAATTG	fwd. primer for amplification hyg ^R from pMF1-h to construct pETEF_hyg_mttA
HT-295	gctcaactcgtctcgcttctTATTAATGCGGC CGCACAG	rev. primer for amplification hyg ^R from pMF1-h to construct pETEF_hyg_mttA
HT-296	CGGGTACCAGCTCGAATTC	fwd. primer for amplification of native <i>rial</i> to construct pNATIV- <i>UcN rial</i>
HT-297	ATTATACATTTAATACGCGATAGAAAC	rev. primer for amplification of native <i>rial</i> to construct pNATIV- <i>UcN rial</i>
HT-298	aaattcgagctcggtagccgGTACTGTACTGTACTGTACAAGAAGC	fwd. primer for amplification backbone from <i>Petef_CBX_A_ter_mtt</i> to construct pNATIV- <i>UcN rial</i>
HT-299	tcgcgtattaatgtataatCTCTGAAGGCGTCTCGGC	rev. primer for amplification backbone from <i>Petef_CBX_A_ter_mtt</i> to construct pNATIV- <i>UcN rial</i>
Potef-fwd	CCAATAAAGGGCGCTGTCTC	fwd-primer to verify genome-integration of P ^{etef} <i>Uc rial-cbx</i> , P ^{etef} <i>Pt rial-cbx</i> and P ^{etef} <i>Si rial-cbx</i>
Tnos-rev	CAAGACCGCAACAGGATTC	fwd-primer to verify genome-integration of P ^{etef} <i>Uc rial-cbx</i> , P ^{etef} <i>Pt rial-cbx</i> and P ^{etef} <i>Si rial-cbx</i>
pJET1.2-fwd _{URA}	CRACTACTATAGGGAGAGCGGC	for sequencing and verification of pTARGET-P _{URA}
pJET1.2-fwd _{URA}	AAGAACATCGATTTTCCATGGCAG	for sequencing and verification of pTARGET-P _{URA}
pJET1.2-fwd _{rial}	CRACTACTATAGGGAGAGCGGC	for sequencing and verification of pTARGET-P _{rial}
pJET1.2-fwd _{rial}	AAGAACATCGATTTTCCATGGCAG	for sequencing and verification of pTARGET-P _{rial}

Table 14. Plasmids. All plasmids used in this study are listed below with their relevant characteristics and references. If plasmid was cloned as part of this study a description of the assembly is listed.

Plasmid	Characteristics / description	Assembly description	Reference	iAMB
P_{etef} <i>Umag_rial-cbx</i>	amp ^R		[207]	3182
P_{etef} <i>Uc_rial-cbx</i>	amp ^R	Backbone was amplified with HT-212 and HT-213 form P_{etef} <i>Umag_rial-cbx</i> , <i>rial</i> was amplified from <i>U. cynodontis</i> NBRC 9727 genome with HT-218 and HT-219. Afterwards all fragments were assembled.	this thesis	4183
P_{etef} <i>Pt_rial-cbx</i>	amp ^R	Backbone was amplified with HT-212 and HT-213 form P_{etef} <i>Umag_rial-cbx</i> , <i>rial</i> was amplified from <i>U. cynodontis</i> NBRC 9727 genome with HT-214 and HT-215. Afterwards all fragments were assembled.	this thesis	4184
P_{etef} <i>St_rial-cbx</i>	amp ^R	Backbone was amplified with HT-212 and HT-213 form P_{etef} <i>Umag_rial-cbx</i> , <i>rial</i> was amplified from <i>U. cynodontis</i> NBRC 9727 genome with HT-216 and HT-217. Afterwards all fragments were assembled.	this thesis	4185
pETEF_CbxR_ <i>At_mttA</i>	ampR, di-codon optimized <i>mttA</i> from <i>A. terreus</i>	See chapter 2	this thesis	3010
pETEF_CbxR_ <i>At_mfsA</i>	ampR, di-codon optimized <i>mfsA</i> from <i>A. terreus</i>	See chapter 2	this thesis	3007
pNEBUC	Ori ColE1; ampR; UARS; cbx ^R		[348]	2951
pSMUT	Ori ColE1; ampR; <i>hph</i> , <i>hyg</i> ^R		[349]	3149
pNEBUN	Ori ColE1; ampR; UARS; nat ^R		[348]	2984
pNEBUP	Ori ColE1; ampR; UARS; <i>phi</i> ^R		[348]	2893
pUMa43	Ori ColE1; ampR; P_{etef} ; GFP, T_{ras} , cbx ^R		[350]	2484
pJET1.2/blunt	Rep(pMB1); ampR; <i>eco47IR</i> ; P_{IACUVS} ; T7 promoter		Thermo Fischer	
pstorI_1rh_WT (pUMa1522)	FRT_WT; Phsp70; Thsp70; <i>hyg</i> ^R		[184]	3261
pstorI_1rh_M1 (pUMa1523)	FRT_M1; Phsp70; Thsp70; <i>hyg</i> ^R		[188]	3262
pFLPexPC	Ori ColE1; ampR; UARS; FLP-Recombinase; <i>Pcrg1</i> ; cbx ^R		[183]	2898
pFRT ^{WT} - <i>UcN_ras2</i>	pJET1.2/blunt with FRT ^{WT} -sites, <i>hyg</i> ^R and 1000 bp flanking regions up and downstream from <i>ras2</i>	HIFI DNA assembly; F1- <i>ras2</i> and F2- <i>ras2</i> were amplified from <i>U. cynodontis</i> NBRC9727 genome, FRT ^{WT} sites including <i>hyg</i> ^R -cassette from <i>pstorI_1rh_WT</i>	this study	4127

Appendix

		(FRT+Hyg ^R <i>ras2</i>). Afterwards all fragments were assembled with pJET1.2/blunt as backbone		
pFRT ^{WT} - <i>UcN_fuz7</i>	pJET1.2/blunt with FRT ^{WT} -sites, hyg ^R and 1000 bp flanking regions up and downstream from <i>fuz7</i>	HIFI DNA assembly; F1- <i>fuz7</i> and F2- <i>fuz7</i> were amplified from <i>U. cynodontis</i> NBRC9727 genome, FRT ^{WT} sites including hyg ^R - cassette from pstor1_1rh_WT (FRT+Hyg ^R <i>fuz7</i>). Afterwards all fragments were assembled with pJET1.2/blunt as backbone	this study	4128
pFRT ^{WT} - <i>UcN_abc3</i>	pJET1.2/blunt with FRT ^{WT} -sites, hyg ^R and 1000 bp flanking regions up and downstream from <i>abc3</i>	HIFI DNA assembly; F1- <i>abc3</i> and F2- <i>abc3</i> were amplified from <i>U. cynodontis</i> NBRC9727 genome, FRT ^{WT} sites including hyg ^R - cassette from pstor1_1rh_WT (FRT+Hyg ^R <i>abc3</i>). Afterwards all fragments were assembled with pJET1.2/blunt as backbone	this study	4129
pMF1-h	Ori ColE1; ampR, hyg ^R		[182]	2053
pJet_ <i>UcN_mtt1</i>	pJET1.2/blunt, hyg ^R and 1000 bp flanking regions up and downstream from <i>mtt1</i>	HIFI DNA assembly; F1- <i>mtt1</i> and F2- <i>mtt1</i> were amplified from <i>U. cynodontis</i> NBRC9727 genome, hyg ^R -cassette from pMF1-h. Afterwards all fragments were assembled with pJET1.2/blunt as backbone	this study	3909
pJet_ <i>UcN_itp1</i>	pJET1.2/blunt, hyg ^R and 1000 bp flanking regions up and downstream from <i>itp1</i>	HIFI DNA assembly; F1- <i>itp1</i> and F2- <i>itp1</i> were amplified from <i>U. cynodontis</i> NBRC9727 genome, hyg ^R -cassette from pMF1-h. Afterwards all fragments were assembled with pJET1.2/blunt as backbone	this study	3718
pFRT ^{M1} - <i>UcN_cyp3</i>	pJET1.2/blunt with FRT ^{M1} -sites, hyg ^R and 1000 bp flanking regions up and downstream from <i>cyp3</i>	HIFI DNA assembly; F1- <i>cyp3</i> and F2- <i>cyp3</i> were amplified from <i>U. cynodontis</i> NBRC9727 genome, FRT ^{M1} sites including hyg ^R - cassette from pstor1_1rh_WT (FRT ^{M1} +Hyg ^R <i>cyp3</i>). Afterwards all fragments were assembled with pJET1.2/blunt as backbone	this study	4447
pFRT ^{M1} - <i>UcN_rial</i>	pJET1.2/blunt with FRT ^{M1} -sites, hyg ^R and 1000 bp flanking regions up and downstream from <i>rial</i>	HIFI DNA assembly; F1- <i>rial</i> and F2- <i>rial</i> were amplified from <i>U. cynodontis</i> NBRC9727 genome, FRT ^{M1} sites including hyg ^R - cassette from pstor1_1rh_WT (FRT ^{M1} +Hyg ^R <i>rial</i>). Afterwards all fragments were assembled with pJET1.2/blunt as backbone	this study	4471

pNATIV- <i>Ucn_ria1</i>	cbx ^R , <i>ria1</i> controlled by native promoter and terminator	HIFI DNA assembly; NATIV- <i>ria1</i> including promoter and terminator region was amplified from <i>U. cynodontis</i> NBRC9727 genome. Backbone was amplified from <i>Petef_CBX_A_ter_mtt</i> . Afterwards all fragments were assembled.	this study	4727
pETEF_hyg_mttA	hyg ^R , <i>mttA</i> controlled by constitutive promoter <i>Petef</i>	HIFI DNA assembly; hyg ^R cassette was amplified from pMF1-h and Backbone including <i>mttA</i> and <i>P_{etef}</i> from <i>Petef_CBX_A_ter_mtt</i>	this study	4726
pCas9_sgRNA_0	ori: origin of replication, bla: b-lactamase gene, ARS: autonomously replicating, cbx ^R , <i>U. maydis</i> U6 promoter, <i>P_{etef}</i> : strong constitutive promoter, <i>T_{nos}</i> : nos terminator		[185]	3595
pTARGET-P _{URA}	CRISPR_P _{URA} target (20 bp region upstream of the Acc65I site in pCas9_sgRNA_0, respective sgRNA sequence, the guide RNA scaffold, the U6 terminator, a 34 nucleotide stuffer sequence and the 20 bp region downstream of Acc65I site in pCas9_sgRNA_0) [185].	CRISPR_P _{URA} target was synthesized by Thermo Fischer and subcloned in pJET1.2/blunt vector.	this study	3669
pTARGET-P _{ria1}	CRISPR_P _{etef} target (20 bp region upstream of the Acc65I site in pCas9_sgRNA_0, respective sgRNA sequence, the guide RNA scaffold, the U6 terminator, a 34 nucleotide stuffer sequence and the 20 bp region downstream of Acc65I site in pCas9_sgRNA_0) [185].	Self-ligation; pTARGET-P _{URA} was amplified with phosphorylated primer HT-12 and HT-82 following by a self-liagtion.	this study	3975
pCas9_P _{etef} _1	pCas9_sgRNA_0 + sgRNA_P _{ria1}	HIFI DNA assembly; CRISPR_P _{etef} target was amplified from pTARGET-P _{ria1} and pCas9_sgRNA_0 was linearized with Acc65I. Afterwards both Fragments were assembled.	this study	4019
pDONOR_P _{oma} <i>ria1</i>	pJET1.2/blunt with constitutive promoter <i>P_{oma}</i> and 1000 bp flanking regions. F1 is in Chr04 at 37427-38426	HIFI DNA assembly; F1 and F2 was amplified from <i>U. maydis</i> genome and <i>P_{oma}</i> from pUMa 2326. Afterwards all Fragments were assembled.	this study	4020

Appendix

	and F2 is in Chr04 at 39761-40760			
pDONOR_P _{eteffria1}	pJET1.2/blunt with constitutive promoter P _{eteff} and 1000 bp flanking regions. F1 is in Chr04 at 37427-38426 and F2 is in Chr04 at 39761-40760	HIFI DNA assembly; Backbone was amplified from pDONOR_P _{omaria1} , P _{eteff} was amplified from		4072
pETEF-05080_CbxR	UMAG_05080 (regulator of itaconate, Rial)		[140]	3182
pJET1.2/blunt	Rep(pMB1); ampR; <i>eco471R</i> ; P _{IACUVS} ; T7 promoter		Thermo Fischer	
pFRT ^{WT} -Um_Δ <i>fuiz7</i>	pJET1.2/blunt with FRT ^{WT} -sites, <i>hyg^R</i> and 1000 bp flanking regions up and downstream from <i>fuiz7</i>	HIFI DNA assembly; F1- <i>fuiz7</i> and F2- <i>fuiz7</i> were amplified from <i>U. maydis</i> MB215 genome, FRT ^{WT} sites including <i>hyg^R</i> -cassette from pstorl_1rh_WT (FRT+ <i>Hyg^R_ras2</i>). Afterwards all fragments were assembled with pJET1.2/blunt as backbone	this study	4182

Supplemental figures

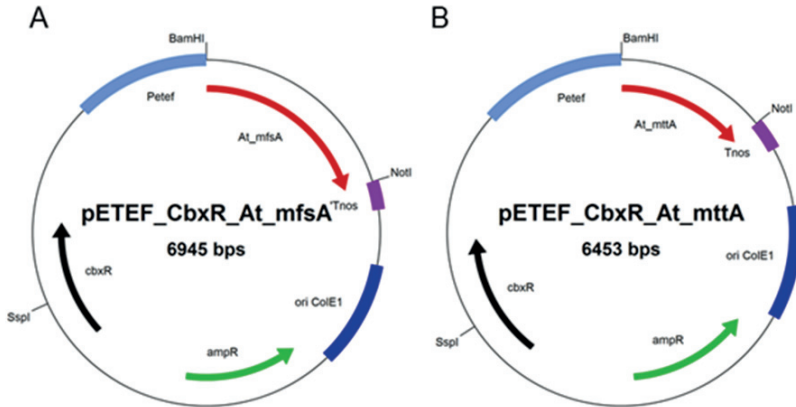


Figure 51. Plasmid maps of pETEF_CbxR_At_mttA and pETEF_CbxR_At_mfsA. Both plasmids contain, *cbxR*: carboxin resistance, *ampR*: ampicillin resistance, *ori ColE1*: origin of replication *E. coli*, *Petef*: constitutive promoter, *SspI*, *BamHI* and *NotI* as restriction sites, A: dicodon-optimized *mfsA* and B: dicodon-optimized *mttA*.

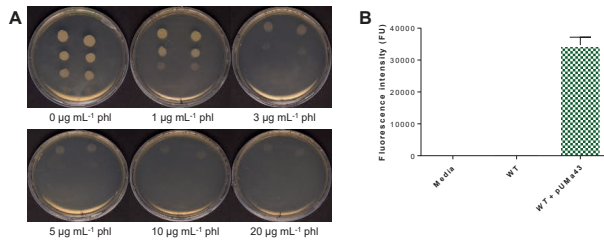


Figure 52. Genetic tool development for *U. cynodontis* NBRC9727. A: drop test of *U. cynodontis* NBRC9727 culture with different OD₆₀₀ (1, 0.1, 0.01, and 0.001) from top to the bottom on YEP plates containing different concentrations of phleomycin. B: fluorescence intensity of *U. cynodontis* NBRC9727 and a pUMa43 transformant in screening medium with 50 g L⁻¹ glucose and 100 mM MES is shown. As negative control pure media was used. Error bars indicate standard deviation from the mean (n=3).

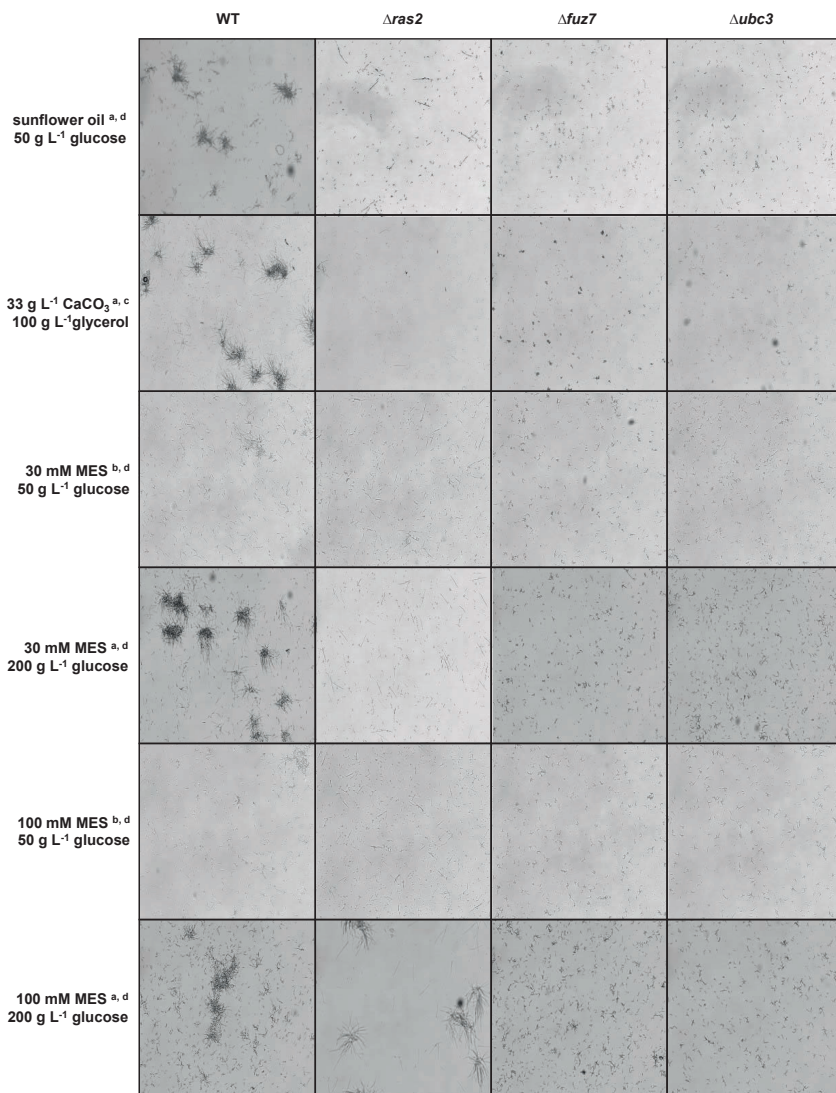


Figure 53. Morphological engineering in *U. cynodontis* NBRC9727. DIC images at a magnification of 100X during System Duetz[®] ^(c) or shaking flask ^(d) after 48 h ^(a) or 72 h ^(b) cultivation of *U. cynodontis* WT, $\Delta ras2$, $\Delta fuz7$, and $\Delta ubc3$ in screening medium with various carbon sources, carbon source concentrations, and buffer systems as indicated.

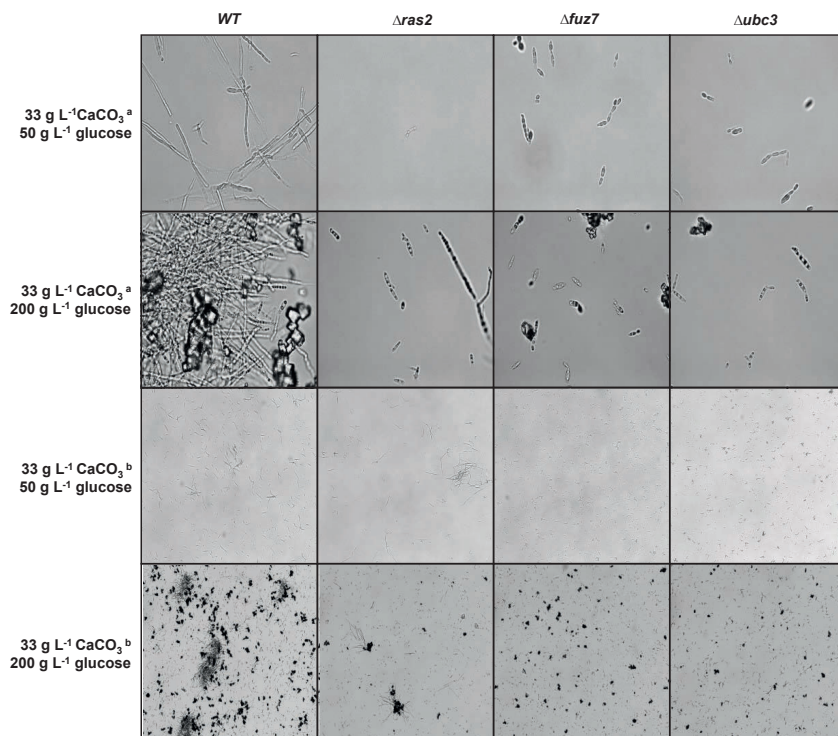


Figure 54. Morphological engineering in *U. cynodontis* NBRC9727. DIC images at a magnification of 100X during System Duetz[®] (c) or shaking flask (d) after 48 h (a) or 72 h (b) cultivation of *U. cynodontis* WT, $\Delta ras2$, $\Delta fuz7$, and $\Delta ubc3$ in screening medium with various carbon sources, carbon source concentrations, and buffer systems as indicated.

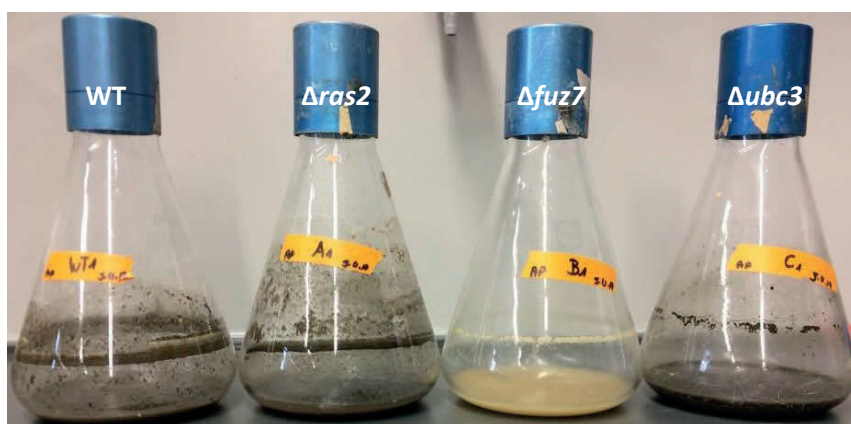


Figure 55. Growth behavior of various *U. cynodontis* NBRC9727 strains. Macroscopic images of *U. cynodontis*, $\Delta ras2$, $\Delta fuz7$, and $\Delta ubc3$ after 384h cultivation in screening medium with 100 g L⁻¹ glycerol and 33 g L⁻¹ CaCO₃.

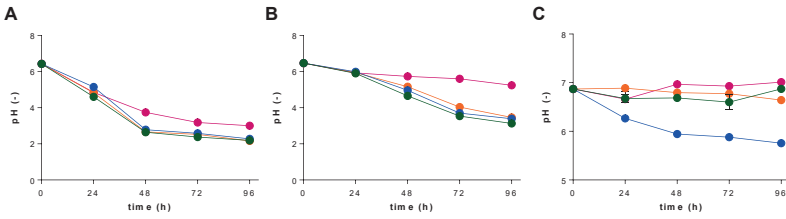


Figure 56. pH values of cultures of various *U. cynodontis* NBRC9727 strains. pH course of *U. cynodontis* WT (green), $\Delta ras2$ (blue), $\Delta fuz7$ (orange), and $\Delta ubc3$ (pink) during System Duetz[®] cultivation in screening medium with 50 g L⁻¹ glucose, 30 mM MES (A), 100 mM MES (B) and 33 g L⁻¹ CaCO₃. Error bars indicate the standard error of the mean (n=3).

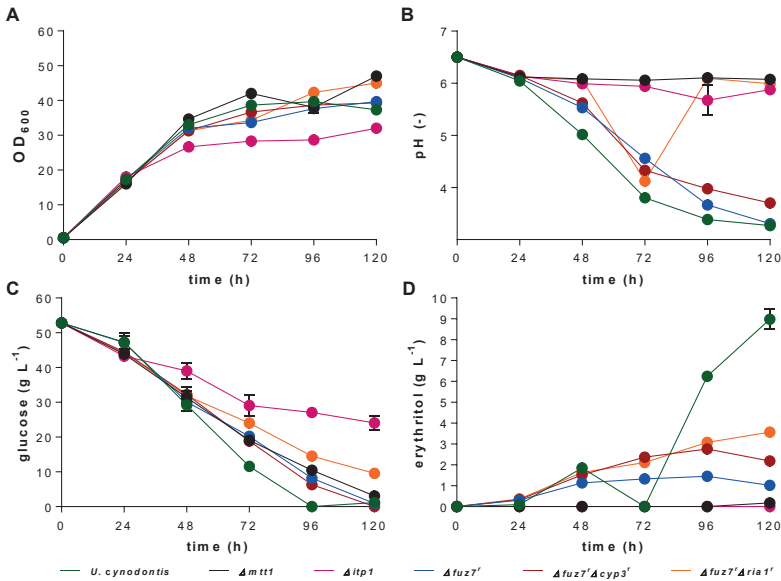


Figure 57. Erythritol production and growth of various *U. cynodontis* strains. Growth (OD₆₀₀) (A), pH course (B), glucose consumption (C), and erythritol production in various *U. cynodontis* mutants in comparison to wildtype and $\Delta fuz7^-$ controls during System Duetz[®] cultivation in screening medium with 100 mM MES and 50 g L⁻¹ glucose. Error bars indicate the standard error of the mean (n=3).

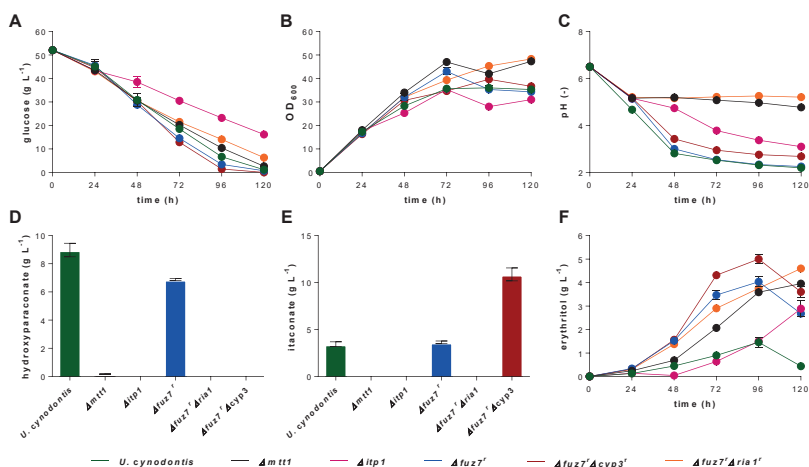


Figure 58. Acid and erythritol production and growth of various *U. cynodontis* strains. Glucose consumption (A), growth (OD₆₀₀) (B), pH course (C), (S)-2hydroxyparaconate (D), itaconate (E), and erythritol production (F) in various *U. cynodontis* mutants in comparison to wildtype and $\Delta fuz7$ controls during System Duetz[®] cultivation in screening medium with 30 mM MES and 50 g L⁻¹ glucose. Error bars indicate the standard error of the mean (n=3).

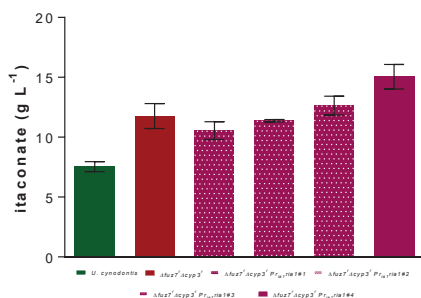


Figure 59. Itaconate production of four individual P_{ria1} transfectants of *U. cynodontis* $\Delta fuz7 \Delta cyp3$ and the respective controls during System Duetz[®] cultivation in screening medium with 100 mM MES and 50 g L⁻¹ glucose after 96 h. Error bars indicate the standard error of the mean (n=3). Transfectant #4 was selected for further study.

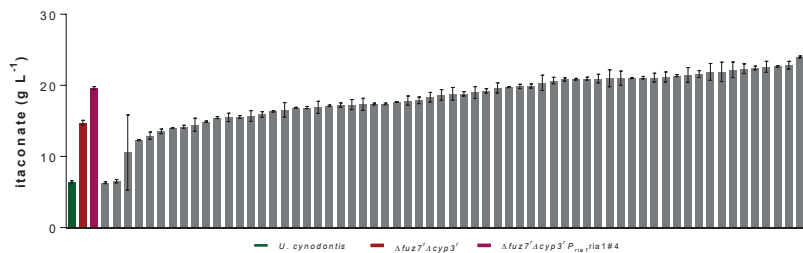


Figure 60. Itaconate production of 63 individual *P_{itaM1A}* transformants of *U. cynodontis* $\Delta fuz7^- \Delta cyp3^- P_{ita1\#4}$ (grey bars) and the respective controls during System Duetz[®] cultivation in screening medium with 100 mM MES and 50 g L⁻¹ glucose after 116 h. Error bars indicate the standard error of the mean (n=3). The strain indicated with the green dot was selected for further study.

Supplemental data**D1.** Annotated sequence of *mttA* dicodon-optimized for *U. maydis*.

BamHI
-+-----

```

1  cactataggg cgaattgaag gaaggccgtc aagccgcgat gtcggatcca tgggtcacgg
    dicodon-optimized MttA >>.....>
    m g h

61  cgacaccgag tcgccaacc ccacgaccac caccgagggc tcgggtcaaaa acgagcccga
    >.....dicodon-optimized MttA.....>
    g d t e s p n p t t t t e g s g q n e p

121  gaagaagggt cgtgacatcc cgctctggcg caagtgcgtc atcacctttg tcgtctcgtg
    >.....dicodon-optimized MttA.....>
    e k k g r d i p l w r k c v i t f v v s

181  gatgacgctc tgggtcactt tctcgtcgac ctgtctcgtg cccgccgctc ccgagatcgc
    >.....dicodon-optimized MttA.....>
    w m t l v v t f s s t c l l p a a p e i

241  caacgagttt gacatgaccg tcgagaccat caacatctcg aacgccggtg tcctcgtcgc
    >.....dicodon-optimized MttA.....>
    a n e f d m t v e t i n i s n a g v l v

301  catgggctac tcgtcgttta tctggggctc catgaacaag ctcgttggcc gtcgcactc
    >.....dicodon-optimized MttA.....>
    a m g y s s l i w g p m n k l v g r r t

361  gtacaacctc gctatctcga tgctctgcgc ttgctcggcg ggcacggccg ctgccatcaa
    >.....dicodon-optimized MttA.....>
    s y n l a i s m l c a c s a g t a a a i

421  cgaggagatg ttcatcgctt tcccgctgct ctcoggtctg accggtacct cgttcatggt
    >.....dicodon-optimized MttA.....>
    n e e m f i a f r v l s g l t g t s f m

481  ctcgggtcag acggtgctcg ccgacatctt cgagcccgcg taccgeggca ccgcccgtcg
    >.....dicodon-optimized MttA.....>
    v s g q t v l a d i f e p v y r g t a v

541  cttcttcatg gccggtaccc tctcgggtcc cgctatcggt ccgtgcgtcg gttggtcat
    >.....dicodon-optimized MttA.....>
    g f f m a g t l s g p a i g p c v g g v

601  cgtcacctc acctcgtggc gtgtcatctt ctggctccag ctcggcatgt cgggtctcgg
    >.....dicodon-optimized MttA.....>
    i v t f t s w r v i f w l q l g m s g l

661  tctcgtctc tcgtctctct tcttcccaa gatcgagggc aactcggaaa aggtctcgac
    >.....dicodon-optimized MttA.....>
    g l v l s l l f f p k i e g n s e k v s

721  cgccttaag cccaccacgc tcgtcaccat catcagcaag ttctcgccca ccgacgtgct
    >.....dicodon-optimized MttA.....>
    t a f k p t t l v t i i s k f s p t d v

781  caagcagtg gttaccacca acgtctctcc cgctgacctc tgctgtggtc tgctcgccat

```

Appendix

```
>.....dicodon-optimized MttA.....>
l k q w v y p n v f l a d l c c g l l a

841 caccagtac tegatcctca cctcggecg tgccatcttc aactegecgt tccacctcac
>.....dicodon-optimized MttA.....>
i t q y s i l t s a r a i f n s r f h l

901 cactgctctc gtctctggtc tcttctacct cgtcaccggt gccggtctcc teatcgctc
>.....dicodon-optimized MttA.....>
t t a l v s g l f y l a p g a g f l i g

961 gctcgttggt ggcaagctct cggaccgcac cgtccgccgc tacatcgta agcgcgctt
>.....dicodon-optimized MttA.....>
s l v g g k l s d r t v r r y i v k r g

1021 ccgtctgccc caggaccgtc tccactcggg tctgatcacg ctggttcggc tctcccgcg
>.....dicodon-optimized MttA.....>
f r l p q d r l h s g l i t l f a v l p

1081 cggtagctc atctacggct ggacgtcca ggaggacaag ggcgacatgg tggtgccat
>.....dicodon-optimized MttA.....>
a g t l i y g w t l q e d k g d m v v p

1141 catcgccgc ttcttcggc gctgggtct catggctcg tcaactgcc tcaaacgta
>.....dicodon-optimized MttA.....>
i i a a f f a g w g l m g s f n c l n t

1201 cgtcgccgag gcgtgccgc gcaaccgttc cgcgctcatt gccggcaagt acatgatcca
>.....dicodon-optimized MttA.....>
y v a e a l p r n r s a v i a g k y m i

1261 gtacacctt teggcggct cgtcggecgt cgtcgtccc gtcacgatg cgtcggcgt
>.....dicodon-optimized MttA.....>
q y t f s a g s s a l v v p v i d a l g

1321 cggcgagacc ttcacgtct gcgtcgtcgc etcgaccate gccggtctca tcaccgccg
>.....dicodon-optimized MttA.....>
v g e t f t l c v v a s t i a g l i t a

1381 catcgtcgc tggggtatca acatgcagcg atgggccgag cgtgccttca acatgccac
>.....dicodon-optimized MttA.....>
a i a r w g i n m q r w a e r a f n m p

      NotI
      --+-----
1441 ccagtgagcg gccgcccgt gggcctcatg ggccttcctt tcactgcccg ctttcacg
>....> dicodon-optimized MttA
t q -
```

D2. Annotated sequence of *mfsA* dicodon-optimized for *U. maydis*.

```

                                                                    BamHI
                                                                    -+----
1  cgaattgaag gaagccgcgc aagccacgt gtctgtgcca ggcgcgccag tcggatccat
                                                                    dicodon-optimized MfsA >>

61  ggactcgaag atccagacca acgtgccgct cccaaggct ccgctcatcc agaagcgcg
>.....dicodon-optimized MfsA.....>
m d s k i q t n v p l p k a p l i q k a

121  cggcaagcgc accaagggca tcctcgcgct ggtcgtggt gcctgcgccg gtcgcctcga
>.....dicodon-optimized MfsA.....>
r g k r t k g i p a l v a g a c a g a v

181  gatctcgatc acctaccocct tcgagtcggc caagaccocgt gctcagctca agcgtcgcaa
>.....dicodon-optimized MfsA.....>
e i s i t y p f e s a k t r a q l k r r

241  ccacgacgtc gcgcgcatca agcccgggat ccgcggtggt tacgcgggct acggtgccac
>.....dicodon-optimized MfsA.....>
n h d v a a i k p g i r g w y a g y g a

301  gctcgtcggc accaccgtca agcgtcgggt gcagttcgcc tcgttcaaca tctaccgatc
>.....dicodon-optimized MfsA.....>
t l v g t t v k a s v q f a s f n i y r

361  ggcgctctcg ggtcccaacg gtgagctctc gaccggtgcc tcggtgctcg ccggtcttgg
>.....dicodon-optimized MfsA.....>
s a l s g p n g e l s t g a s v l a g f

421  tgccggtgtc accgaggcgg tcctcgcgct caccgccgcc gaggccatca aaaccaagat
>.....dicodon-optimized MfsA.....>
g a g v t e a v l a v t p a e a i k t k

481  catcgatgct cgcaaggtcg gcaacgcca gctgtcgacc acctcgggtg ccatcgccgg
>.....dicodon-optimized MfsA.....>
i i d a r k v g n a e l s t t f g a i a

541  catctcgcgc gaccgtggtc cgctcgggtt cttctcggcc gtcggtocca ccactcgcgc
>.....dicodon-optimized MfsA.....>
g i l r d r g p l g f f s a v g p t i l

601  tcagtcgtcc aacgccgccg tcaagttcac cgtctacaac gagctcatcg gtctcgtcgc
>.....dicodon-optimized MfsA.....>
r q s s n a a v k f t v y n e l i g l a

661  taagtacagc aagaacggcg aggacgtcca cccgctcgcc tcgacgctgg tcggctcggt
>.....dicodon-optimized MfsA.....>
r k y s k n g e d v h p l a s t l v g s

721  caccggtgtc tgctgtgcct ggtcgcgcga gccgctcgac gtcataaaga cgcgcatgca
>.....dicodon-optimized MfsA.....>
v t g v c c a w s t q p l d v i k t r m

781  gtcgctccag gcgcgtcagc tctacggcaa cacgttcaac tgcgtcaaga cgtcgtcgcg
>.....dicodon-optimized MfsA.....>
q s l q a r q l y g n t f n c v k t l l

```



```
841 ctccgagggc atcgggtgtct tctggtcggg tgtctggttc cgcaccggtc gtcctcgcct
>.....dicodon-optimized MfsA.....>
r s e g i g v f w s g v w f r t g r l s
```

```
901 cacctcggcc atcatgttcc ccgtctacga gaaggtctac aagttcctca cecagcccaa
>.....dicodon-optimized MfsA.....>
l t s a i m f p v y e k v y k f l t q p
```

NotI

--+-----

```
961 ctgagcggcc gcccgattaa ttaatggagc acaagactgg cctcatgggc cttcctttca
>.>> dicodon-optimized MfsA
n -
```

```
1021 ctgc
```

D3. Tool adapting for genetic modification in *Ustilago cynodontis*

In order to enable the genetic modification of the filamentous character of *Ustilago cynodontis* to a stable yeast-like growth behavior and further to enhance itaconate production with metabolic engineering, tools for *Ustilago maydis* were adapted to work in *U. cynodontis*. In a first approach antibiotics and their corresponding resistance cassettes were tested. Different concentrations for carboxin (cbx), hygromycin (hyg), nourseothricin (nat) and phleomycin (phl), the most common used antibiotics in *U. maydis* [139, 182, 192, 194], were tested by drop test on YEP plates. Most used concentrations in *U. maydis* for this antibiotics are 2 mg L⁻¹ for cbx, 200 mg L⁻¹ hyg, 150 mg L⁻¹ nat and 40 mg L⁻¹ phl [351]. We used for cbx concentrations in a range from 1 – 15 mg L⁻¹, for hyg 100 – 500 mg L⁻¹, for nat 1 – 300 mg L⁻¹ and for phl 1 – 150 mg L⁻¹. Every 24 h growth was determined by visual analysis. Exemplary the results for phl are shown in Fig. S4A. No growth was observed after 48 h if at least 2 mg L⁻¹ cbx, mg L⁻¹ hyg, 10 mg L⁻¹ nat and 10 mg L⁻¹ phl were used. Subsequently, *U. cynodontis* protoplasts were transformed with pNEBUC, pSMUT, pNEBUN and pNEBUP, which contain cbx, hyg, nat, and phl resistance cassettes, respectively. Visible transformants were selected on plates with the corresponding antibiotics, followed by plasmid isolation from the protoplasts and re-transformation into *E. coli*. Re-isolated plasmids from *E. coli* resulted in plasmids with the correct sizes for pNEBUN, pNEBUP and pNEBUC. Because pSMUT is not a self-replicating plasmid like pNEBUN, pNEBUP and pNEBUC, it was integrated into the genome of *U. cynodontis* NBRC9727 and its presence was verified by PCR. For later overexpression of genes to improve itaconate production also a functional promoter and terminator were needed. Based on other Ustilaginaceae [98, 265], plasmid pUMa43 [350], which contains a cbx marker and a GFP-encoding gene controlled by the Promoter P_{etef} and the terminator T_{nos} was used for integration into the genome of *U. cynodontis* to verify their functionality. After integration, transformants were cultivated in screening medium for 96 h and fluorescence intensity was measured with a well plate reader. As depicted in Fig. S4B, the *U. cynodontis* strain transformed with pUMa43 showed significantly higher fluorescence than the wildtype, proving that this species is now genetically accessible.

References

1. Ragauskas, A.J., Williams, C.K., Davison, B.H., Britovsek, G., Cairney, J., Eckert, C.A., Frederick, W.J., Hallett, J.P., Leak, D.J., Liotta, C.L., Mielenz, J.R., Murphy, R., Templer, R. and Tschaplinski, T. (2006). The path forward for biofuels and biomaterials. *Science*, 311, 484-489.
2. United Nations, Department of Economic and Social Affairs. World population prospects the 2017 revision. Accessible: 10.04.2019. Available from: https://esa.un.org/unpd/wpp/publications/Files/WPP2017_KeyFindings.pdf.
3. Fedoroff, N.V. and Cohen, J.E. (1999). Plants and population: Is there time? *Proc. Natl. Acad. Sci.*, 96, 5903-5907.
4. U.S. Energy Information Administration. International Energy Outlook 2017. Accessible: 11.03.2019. Available from: [https://www.eia.gov/outlooks/ieo/pdf/0484\(2017\).pdf](https://www.eia.gov/outlooks/ieo/pdf/0484(2017).pdf).
5. Yu, K.M.K., Curcic, I., Gabriel, J. and Tsang, S.C.E. (2008). Recent Advances in CO₂ Capture and Utilization. *ChemSusChem*, 1, 893-899.
6. Barros, V. and Field, C. (2014). Climate change 2014 impacts, adaptation, and vulnerability part a: Global and sectoral aspects working group II contribution to the fifth assessment report of the intergovernmental panel on climate change preface. *Climate change 2014: Impacts, adaptation, and vulnerability, Pt A: Global and sectoral aspects*, Ix-Xi.
7. Straathof, A.J. (2014). Transformation of biomass into commodity chemicals using enzymes or cells. *Chem. Rev.*, 114, 1871-908.
8. Sauer, M., Porro, D., Mattanovich, D. and Branduardi, P. (2008). Microbial production of organic acids: expanding the markets. *Trends Biotechnol.*, 26, 100-108.
9. van Maris, A.J.A., Abbott, D.A., Bellissimi, E., van den Brink, J., Kuyper, M., Luttik, M.A.H., Wisselink, H.W., Scheffers, W.A., van Dijken, J.P. and Pronk, J.T. (2006). Alcoholic fermentation of carbon sources in biomass hydrolysates by *Saccharomyces cerevisiae*: current status. *Antonie van Leeuwenhoek*, 90, 391-418.
10. Restmac. Bioethanol production and use. Accessible: 05.03.2019. Available from: http://s3.amazonaws.com/zanran_storage/www.erec.org/ContentPages/52475800.pdf.
11. Farmer, T.J. and Mascal, M. (2015). Platform Molecules. in: *Introduction to chemicals from biomass*. John Wiley & Sons, Ltd. 89-155. ISBN-Nr: 9781118714485.
12. Werpy, T., Peterson, G. (2004). Top value added chemicals from biomass. Volume 1 - results of screening for potential candidates from sugars and synthesis gas. US-DoE.
13. Bozell, J.J. and Petersen, G.R. (2010). Technology development for the production of biobased products from biorefinery carbohydrates—the US Department of Energy’s “Top 10” revisited. *Green Chem.*, 12, 539-554.
14. Dharmadi, Y., Murarka, A., and Gonzalez, R. (2006). Anaerobic fermentation of glycerol by *Escherichia coli*: a new platform for metabolic engineering. *Biotechnol. Bioeng.*, 94, 821-9.
15. Nikolau, B.J., Perera, M.A., Brachova, L. and Shanks, B. (2008). Platform biochemicals for a biorenewable chemical industry. *Plant J.*, 54, 536-45.
16. Dobson, R., Gray, V., and Rumbold, K. (2012). Microbial utilization of crude glycerol for the production of value-added products. *J. Ind. Microbiol. Biot.*, 39, 217-26.
17. Magnuson, J.K. and Lasure, L.L. (2004). Organic acid production by filamentous fungi. in: *Advances in fungal biotechnology for industry, agriculture, and medicine*. Springer US. Boston, MA. 307-340. ISBN-Nr: 978-1-4419-8859-1.
18. Goldberg, I., Rokem, J.S., and Pines, O. (2006). Organic acids: old metabolites, new themes. *J. Chem. Technol. Biot.*, 81, 1601-1611.
19. Kubicek, C.P., Punt, P., and Visser, J. (2011). Production of organic acids by filamentous fungi. *Industrial Applications*, 215-234.
20. Becker, J., Lange, A., Fabarius, J. and Wittmann, C. (2015). Top value platform chemicals: bio-based production of organic acids. *Curr. Opin. Biotechnol.*, 36, 168-75.

References

21. Kuenz, A. and Krull, S. (2018). Biotechnological production of itaconic acid-things you have to know. *Appl. Microbiol. Biotechnol.*, 102, 3901-3914.
22. Karaffa, L., Diaz, R., Papp, B., Fekete, E., Sandor, E. and Kubicek, C.P. (2015). A deficiency of manganese ions in the presence of high sugar concentrations is the critical parameter for achieving high yields of itaconic acid by *Aspergillus terreus*. *Appl. Microbiol. Biotechnol.*, 99, 7937-44.
23. Karaffa, L. and Kubicek, C.P. (2019). Citric acid and itaconic acid accumulation: variations of the same story? *Appl. Microbiol. Biotechnol.*, 103, 2889-2902.
24. Regestein, L., Klement, T., Grande, P., Kreyenschulte, D., Heyman, B., Maßmann, T., Eggert, A., Sengpiel, R., Wang, Y., Wierckx, N., Blank, L.M., Spiess, A., Leitner, W., Bolm, C., Wessling, M., Jupke, A., Rosenbaum, M. and Büchs, J. (2018). From beech wood to itaconic acid: case study on biorefinery process integration. *Biotechnol. Biofuels*, 11, 279.
25. Steiger, M.G., Wierckx, N., Blank, L.M., Mattanovich, D. and Sauer, M. (2016). Itaconic acid - An emerging building block. in: Wiley-VCH Verlag GmbH & Co. KGaA. *Industrial Biotechnology: Products and processes*. Chapter 15. ISBN-Nr. 9783527807833.
26. Raymond L Snell and Leonard B Schweiger. (1947). Production of citric acid by fermentation. US2492667A.
27. Ting Liu Carlson and Eugene Max Peters, J. (1997). Low pH lactic acid fermentation. US08949420.
28. James N Currie, Jasper H Kane, and Alexander, F. (1931). Process for producing gluconic acid by fungi. US1893819A.
29. Robert C Nubel and Ratajak, E.J. (1962). Process for producing itaconic acid.
30. Jean-Claude Marie-Pierre Gh. De Troostembergh, Ignace André Debonne, Willy Richard Obyn, Catherine Gwena and Peuzet, M. (2002). Process for the manufacture of 2-keto-l-gulonic acid. EP20020767304.
31. Guanglin, Y., Yin, Z.T., Zizheng, Y., Wenzhu, N., Changhui, W. and Shuiding, W. (1988). Fermentation process. US4935359A.
32. Shmorhun.M., BER-myriant succinic acid biorefinery. Accessible: 20.04.2019. Available from: <https://www.osti.gov/biblio/1333678>.
33. Koutinas, A.A., Malbrancque, F., Wang, R., Campbell, G.M. and Webb, C. (2007). Development of an oat-based biorefinery for the production of L(+)-lactic acid by *Rhizopus oryzae* and various value-added coproducts. *J. Agric. Food Chem.*, 55, 1755-61.
34. Altaf, M., Naveena, B.J., and Reddy, G. (2007). Use of inexpensive nitrogen sources and starch for L(+) lactic acid production in anaerobic submerged fermentation. *Bioresour. Technol.*, 98, 498-503.
35. Altaf, M., Venkateshwar, M., Srijana, M. and Reddy, G. (2007). An economic approach for L-(+) lactic acid fermentation by *Lactobacillus amylophilus* GV6 using inexpensive carbon and nitrogen sources. *J. Appl. Microbiol.*, 103, 372-80.
36. Ohkouchi, Y. and Inoue, Y. (2007). Impact of chemical components of organic wastes on L(+)-lactic acid production. *Bioresour. Technol.*, 98, 546-553.
37. Venus, J. (2006). Utilization of renewables for lactic acid fermentation. *Biotechnol. J.*, 1, 1428-32.
38. John, R.P., Nampoothiri, K.M., and Pandey, A. (2007). Fermentative production of lactic acid from biomass: an overview on process developments and future perspectives. *Appl. Microbiol. Biotechnol.*, 74, 524-34.
39. John, R.P., Nampoothiri, K.M., and Pandey, A. (2007). Production of L(+) lactic acid from cassava starch hydrolyzate by immobilized *Lactobacillus delbrueckii*. *J. Basic Microbiol.*, 47, 25-30.

40. Sirisansaneeyakul, S., Luangpipat, T., Vanichsriratana, W., Srinophakun, T., Chen, H.H. and Chisti, Y. (2007). Optimization of lactic acid production by immobilized *Lactococcus lactis* IO-1. *J. Ind. Microbiol. Biot.*, 34, 381-91.
41. Meynial-Salles, I., Dorotyn, S., and Soucaille, P. (2008). A new process for the continuous production of succinic acid from glucose at high yield, titer, and productivity. *Biotechnol. Bioeng.*, 99, 129-35.
42. Auras, R., Harte, B., and Selke, S. (2004). An overview of polylactides as packaging materials. *Macromol. Biosci.*, 4, 835-64.
43. Young-Jung Wee, Kim, J.-N., and Ryu, H.-W. (2006). Biotechnological production of lactic acid and its recent applications. *Food Technol. Biotech.*, 44, 163-172.
44. Narayanan, N., Roychoudhury, P.K., and Srivastava, A. (2004). L (+) lactic acid fermentation and its product polymerization. *Electron. J. Biotechnol.*, 7, 167-U2.
45. Zahorski, B. (1913). Method of producing citric acid. US1066358.
46. Currie, J.N. (1917). The citric acid fermentation of *Aspergillus niger*. *J. Biol. Chem.*, 31, 15-37.
47. Shu, P. and Johnson, M.J. (1948). The interdependence of medium constituents in citric acid production by submerged fermentation. *J. Bacteriol.*, 56, 577-585.
48. Shu, P. and Johnson, M.J. (1948). Citric acid - production by submerged fermentation with *Aspergillus niger*. *Ind. Eng. Chem.*, 40, 1202-1205.
49. Xie, G. and West, T.P. (2009). Citric acid production by *Aspergillus niger* ATCC 9142 from a treated ethanol fermentation co-product using solid-state fermentation. *Lett. Appl. Microbiol.*, 48, 639-44.
50. Shu, P. and Johnson, M.J. (1947). Effect of the composition of the sporulation medium on citric acid production by *Aspergillus niger* in submerged culture. *J. Bacteriol.*, 54, 161-7.
51. Wehmer, C. (1893). Zur Charakteristik des citronensauren Kalkes und einige Bemerkungen über die Stellung der Citronensäure im Stoffwechsel. *Berichte der Deutschen Botanischen Gesellschaft*, 11, 333-343.
52. Lopez-Garcia, R. (2010). Citric Acid. in: Kirk-Othmer Encyclopedia of Chemical Technology, (ED). ISBN-Nr. 9780471484943.
53. Grand view Research. Citric acid market size worth \$3.83 billion by 2025 Accessible: 09.04.2019. Available from: <https://www.grandviewresearch.com/press-release/global-citric-acid-market>.
54. Grand view Research. Citric acid market size, share & trends analysis report by form (liquid powder), by application (pharmaceutical, F&B), by region, competitive landscape, and segment forecasts, 2018-2025. Accessible: 12.03.2019. Available from: <https://www.grandviewresearch.com/industry-analysis/citric-acid-market>.
55. Kubicek, C.P. and Rohr, M. (1986). Citric-Acid Fermentation. *Crit. Rev. Biotechnol.*, 3, 331-373.
56. Matthey, M. (1992). The Production of Organic-Acids. *Crit. Rev. Biotechnol.*, 12, 87-132.
57. Song, H. and Lee, S.Y. (2006). Production of succinic acid by bacterial fermentation. *Enzyme. Microb. Tech.*, 39, 352-361.
58. Zeikus, J.G., Jain, M.K., and Elankovan, P. (1999). Biotechnology of succinic acid production and markets for derived industrial products. *Appl. Microbiol. Biotechnol.*, 51, 545-552.
59. Bernhauer, K. (1950). Chemical activities of fungi, von J. W. Foster. Academic Press, Inc., New York 1949. 1. Aufl., 648 S., \$ 9.50. *Angewandte Chemie*, 62, 489-489.
60. Bercovitz, A., Peleg, Y., Battat, E., Rokem, J.S. and Goldberg, I. (1990). Localization of pyruvate-carboxylase in organic acid-producing *Aspergillus* Strains. *Appl. Environ. Microb.*, 56, 1594-1597.

References

61. Gallmetzer, M., Meraner, J., and Burgstaller, W. (2002). Succinate synthesis and excretion by *Penicillium simplicissimum* under aerobic and anaerobic conditions. *FEMS Microbiol. Lett.*, 210, 221-5.
62. Scholten, E. and Dagele, D. (2008). Succinic acid production by a newly isolated bacterium. *Biotechnol. Lett.*, 30, 2143-6.
63. Stellmacher, R., Hangebrauk, J., Wittmann, C., Scholten, E. and von Abendroth, G. (2010). Fermentative Herstellung von Bernsteinsäure mit *Basfia succiniciproducens* DD1 in Serumflaschen. *Chem. Ing. Tech.*, 82, 1223-1229.
64. Raab, A.M., Gebhardt, G., Bolotina, N., Weuster-Botz, D. and Lang, C. (2010). Metabolic engineering of *Saccharomyces cerevisiae* for the biotechnological production of succinic acid. *Metab. Eng.*, 12, 518-25.
65. Ahn, J.H., Jang, Y.-S., and Lee, S.Y. (2016). Production of succinic acid by metabolically engineered microorganisms. *Curr. Opin. Biotechnol.*, 42, 54-66.
66. Chatterjee, R., Millard, C.S., Champion, K., Clark, D.P. and Donnelly, M.I. (2001). Mutation of the *ptsG* gene results in increased production of succinate in fermentation of glucose by *Escherichia coli*. *Appl. Environ. Microb.*, 67, 148-154.
67. Liebal, U.W., Blank, L.M., and Ebert, B.E. (2018). CO₂ to succinic acid – estimating the potential of biocatalytic routes. *Metab. Eng. Commun.*, 7, e00075.
68. Global succinic acid market forecast to 2023: Increased use in industrial and coating & food & beverage industries driving demand Accessible: 11.03.2019. Available from: <https://www.prnewswire.com/news-releases/global-succinic-acid-market-forecast-to-2023-increased-use-in-industrial-and-coating--food--beverage-industries-driving-demand-300772445.html>.
69. Becker, J., Reinefeld, J., Stellmacher, R., Schafer, R., Lange, A., Meyer, H., Lalk, M., Zelder, O., von Abendroth, G., Schroder, H., Haefner, S. and Wittmann, C. (2013). Systems-wide analysis and engineering of metabolic pathway fluxes in bio-succinate producing *Basfia succiniciproducens*. *Biotechnol. Bioeng.*, 110, 3013-23.
70. Tsuge, Y., Hasunuma, T., and Kondo, A. (2015). Recent advances in the metabolic engineering of *Corynebacterium glutamicum* for the production of lactate and succinate from renewable resources. *J. Ind. Microbiol. Biot.*, 42, 375-89.
71. Chen, M., Huang, X., Zhong, C., Li, J. and Lu, X. (2016). Identification of an itaconic acid degrading pathway in itaconic acid producing *Aspergillus terreus*. *Appl. Microbiol. Biotechnol.*, 100, 7541-7548.
72. Akhtar, J., Idris, A., and Abd. Aziz, R. (2014). Recent advances in production of succinic acid from lignocellulosic biomass. *Appl. Microbiol. Biotechnol.*, 98, 987-1000.
73. Kwon, Y.D., Kim, S., Lee, S.Y. and Kim, P. (2011). Long-term continuous adaptation of *Escherichia coli* to high succinate stress and transcriptome analysis of the tolerant strain. *J. Biosci. Bioeng.*, 111, 26-30.
74. Li, N., Zhang, B., Chen, T., Wang, Z., Tang, Y.J. and Zhao, X. (2013). Directed pathway evolution of the glyoxylate shunt in *Escherichia coli* for improved aerobic succinate production from glycerol. *J. Ind. Microbiol. Biot.*, 40, 1461-75.
75. Jiang, M., Wan, Q., Liu, R., Liang, L., Chen, X., Wu, M., Zhang, H., Chen, K., Ma, J., Wei, P. and Ouyang, P. (2014). Succinic acid production from corn stalk hydrolysate in an *E. coli* mutant generated by atmospheric and room-temperature plasmas and metabolic evolution strategies. *J. Ind. Microbiol. Biot.*, 41, 115-23.
76. Ghaffar, T., Irshad, M., Anwar, Z., Aqil, T., Zulifqar, Z., Tariq, A., Kamran, M., Ehsan, N. and Mehmood, S. (2014). Recent trends in lactic acid biotechnology: A brief review on production to purification. *J. Radiat. Res. Appl. Sci.*, 7, 222-229.

77. Ouyang, J., Ma, R., Zheng, Z., Cai, C., Zhang, M. and Jiang, T. (2013). Open fermentative production of L-lactic acid by *Bacillus* sp. strain NL01 using lignocellulosic hydrolyzates as low-cost raw material. *Bioresour. Technol.*, 135, 475-80.
78. Abdel-Rahman, M.A., Tashiro, Y., and Sonomoto, K. (2013). Recent advances in lactic acid production by microbial fermentation processes. *Biotechnol. Adv.*, 31, 877-902.
79. Shi, D.J., Hua, J.T., Zhang, L. and Chen, M.Q. (2015). Synthesis of Bio-Based Poly(lactic acid-co-10-hydroxy decanoate) Copolymers with High Thermal Stability and Ductility. *Polymers*, 7, 468-483.
80. Ilmén, M., Koivuranta, K., Ruohonen, L., Suominen, P. and Penttilä, M. (2007). Efficient Production of Lactic Acid from Xylose by *Pichia stipitis*. *Appl. Environ. Microb.*, 73, 117-123.
81. Komesu, A., de Oliveira, J.A.R., Martins, L.H.D., Maciel, M.R.W. and Maciel, R. (2017). Lactic Acid Production to Purification: A Review. *Bioresources*, 12, 4364-4383.
82. Abdel-Rahman, M.A. and Sonomoto, K. (2016). Opportunities to overcome the current limitations and challenges for efficient microbial production of optically pure lactic acid. *J. Biotechnol.*, 236, 176-92.
83. Hofvendahl, K. and Hahn-Hägerdal, B. (2000). Factors affecting the fermentative lactic acid production from renewable resources1. *Enzyme. Microb. Tech.*, 26, 87-107.
84. Maas, R.H.W., Bakker, R.R., Eggink, G. and Weusthuis, R.A. (2006). Lactic acid production from xylose by the fungus *Rhizopus oryzae*. *Appl. Microbiol. Biotechnol.*, 72, 861-868.
85. Yin, P., Yahiro, K., Ishigaki, T., Park, Y. and Okabe, M. (1998). l(+)-lactic acid production by repeated batch culture of *Rhizopus oryzae* in air-lift bioreactor. *J. Ferment. Bioeng.*, 85, 96-100.
86. Liu, T., Miura, S., Yaguchi, M., Arimura, T., Park, E.Y. and Okabe, M. (2006). Scale-up of L-lactic acid production by mutant strain *Rhizopus* sp. MK-96-1196 from 0.003 m³ to 5 m³ in airlift bioreactors. *J. Biosci. Bioeng.*, 101, 9-12.
87. Yu, M.-C., Wang, R.-C., Wang, C.-Y., Duan, K.-J. and Sheu, D.-C. (2007). Enhanced production of L(+)-lactic acid by floc-form culture of *Rhizopus oryzae*. *Journal of the Chinese Institute of Chemical Engineers*, 38, 223-228.
88. Wu, X., Jiang, S., Liu, M., Pan, L., Zheng, Z. and Luo, S. (2011). Production of L-lactic acid by *Rhizopus oryzae* using semicontinuous fermentation in bioreactor. *J. Ind. Microbiol. Biot.*, 38, 565-71.
89. Guo, Y., Yan, Q., Jiang, Z., Teng, C. and Wang, X. (2010). Efficient production of lactic acid from sucrose and corncob hydrolysate by a newly isolated *Rhizopus oryzae* GY18. *J. Ind. Microbiol. Biot.*, 37, 1137-43.
90. Meek, J.S. (1975). The determination of a mechanism of isomerization of maleic acid to fumaric acid. *J. Chem. Educ.*, 52, 541.
91. Battat, E., Peleg, Y., Bercovitz, A., Rokem, J.S. and Goldberg, I. (1991). Optimization of L-malic acid production by *Aspergillus flavus* in a stirred fermentor. *Biotechnol. Bioeng.*, 37, 1108-16.
92. Roehr, M. and Kubicek, C.P. (2008). *Further Organic acids*. ed. In: *Biotechnology Set*. Wiley-VCH Verlag GmbH. p. 363-379. ISBN-Nr. 9783527620883
93. Peleg, Y., Rokem, J.S., Goldberg, I. and Pines, O. (1990). Inducible overexpression of the *fumI* gene in *Saccharomyces cerevisiae*: localization of fumarase and efficient fumaric acid bioconversion to L-malic acid. *Appl. Environ. Microb.*, 56, 2777-83.
94. Neufeld, R.J., Peleg, Y., Rokem, J.S., Pines, O. and Goldberg, I. (1991). L-Malic acid formation by immobilized *Saccharomyces cerevisiae* amplified for fumarase. *Enzyme. Microb. Tech.*, 13, 991-996.

References

95. Geiser, E., Wiebach, V., Wierckx, N. and Blank, L.M. (2014). Prospecting the biodiversity of the fungal family Ustilaginaceae for the production of value-added chemicals. *Fungal Biol. Biotechnol.*, 1, 2.
96. Brown, S.H., Bashkirova, L., Berka, R., Chandler, T., Doty, T., McCall, K., McCulloch, M., McFarland, S., Thompson, S., Yaver, D. and Berry, A. (2013). Metabolic engineering of *Aspergillus oryzae* NRRL 3488 for increased production of L-malic acid. *Appl. Microbiol. Biotechnol.*, 97, 8903-12.
97. Zambanini, T., Sarikaya, E., Kleineberg, W., Buescher, J.M., Meurer, G., Wierckx, N. and Blank, L.M. (2016). Efficient malic acid production from glycerol with *Ustilago trichophora* TZ1. *Biotechnol. Biofuels*, 9, 67.
98. Zambanini, T., Hosseinpour Tehrani, H., Geiser, E., Sonntag, C.K., Buesche, J.M.r., Meurer, G., Wierckx, N. and Blank, L.M. (2017). Metabolic engineering of *Ustilago trichophora* TZ1 for improved malic acid production. *Metab. Eng. Commun.*, 4, 12-21.
99. Zelle, R.M., de Hulster, E., van Winden, W.A., de Waard, P., Dijkema, C., Winkler, A.A., Geertman, J.-M.A., van Dijken, J.P., Pronk, J.T. and van Maris, A.J.A. (2008). Malic acid production by *Saccharomyces cerevisiae*: Engineering of pyruvate carboxylation, oxaloacetate reduction, and malate export. *Appl. Environ. Microb.*, 74, 2766-2777.
100. Takata, I., Yamamoto, K., Tosa, T. and Chibata, I. (1980). Immobilization of *Brevibacterium flavum* with carrageenan and its application for continuous production of L-malic acid. *Enzyme. Microb. Tech.*, 2, 30-36.
101. Zhou, Y.J., Yang, W., Wang, L., Zhu, Z., Zhang, S. and Zhao, Z.K. (2013). Engineering NAD⁺ availability for *Escherichia coli* whole-cell biocatalysis: a case study for dihydroxyacetone production. *Microb. Cell Fact.*, 12, 103.
102. Zambanini, T. (2016). What can we do with smut? Organic acid production from glycerol with Ustilaginaceae. Dissertation. RWTH-Aachen. Institute for Applied Microbiology.
103. Baup, S. (1837). Über eine neue Pyrogen-Citronensäure, und über Benennung der Pyrogen Säure überhaupt. *Annales de Chimie et de Physique*, 19, 29-38.
104. Shriner, R.L., Ford, C., and Roll, L.J. (1943). Itaconic anhydride and itaconic acid. in: *Organic Syntheses Collection Vol.2*. 368.
105. Shriner, R.L., Ford, C., and Roll, L.J. (1931). Itaconic anhydride and itaconic acid. in: *Organic Syntheses Collection Vol. 11*. 70.
106. Kane, J.H., Finlay, A.C., and Amann, P.F. (1945). Production of itaconic acid. US2385283A.
107. Klement, T. and Büchs, J. (2013). Itaconic acid - A biotechnological process in change. *Bioresource Technol.*, 135, 422-431.
108. Kinoshita, K. (1932). Über die Produktion von Itaconsäure und Mannit durch einen neuen Schimmelpilz. *Acta Phytochimica*, 5, 271-287.
109. Tate, B.E. (1981). Itaconic acid and derivatives, in Kirk-Othmer encyclopedia of chemical technology. ed. John Wiley&Sons. ISBN-Nr. 9780471238966.
110. Okabe, M., Lies, D., Kanamasa, S. and Park, E.Y. (2009). Biotechnological production of itaconic acid and its biosynthesis in *Aspergillus terreus*. *Appl. Microbiol. Biotechnol.*, 84, 597-606.
111. Weastra. (2013). Wp 8.1, determination of market potential for selected platform chemicals: itaconic acid, succinic acid, 2,5-furandicarboxylic acid. Technical report, Bioconcept. ed.
112. Bera, R., Dey, A., and Chakrabarty, D. (2015). Synthesis, characterization, and drug release study of acrylamide-co-itaconic acid based smart hydrogel. *Polym. Eng. Sci.*, 55, 113-122.
113. Betancourt, T., Pardo, J., Soo, K. and Peppas, N.A. (2010). Characterization of pH-responsive hydrogels of poly(itaconic acid-g-ethylene glycol) prepared by UV-initiated free radical polymerization as biomaterials for oral delivery of bioactive agents. *J. Biomed. Mater. Res.*, 93, 175-88.

114. Khalid, S.H., Qadir, M.I., Massud, A., Ali, M. and Rasool, M.H. (2009). Effect of degree of cross-linking on swelling and drug release behaviour of poly(methyl methacrylate-co-itaconic acid) [P(MMA/IA)] hydrogels for site specific drug delivery. *Journal of Drug Delivery Science and Technology*, 19, 413-418.
115. Ranjha, N.M., Mudassir, J., and Akhtar, N. (2008). Methyl methacrylate-co-itaconic acid (MMA-co-IA) hydrogels for controlled drug delivery. *J. Solgel Sci. Technol.*, 47, 23-30.
116. Huges, K.A. and Swift, G. (1991). Process for polymerization of itaconic acid. US5223592A.
117. Cordes, T., Michelucci, A., and Hiller, K. (2015). Itaconic acid: The surprising role of an industrial compound as a mammalian antimicrobial metabolite. *Annu. Rev. Nutr.*, 35, 451-73.
118. Michelucci, A., Cordes, T., Ghelfi, J., Pailot, A., Reiling, N., Goldmann, O., Binz, T., Wegner, A., Tallam, A., Rausell, A., Buttini, M., Linster, C.L., Medina, E., Balling, R. and Hiller, K. (2013). Immune-responsive gene 1 protein links metabolism to immunity by catalyzing itaconic acid production. *Proceedings of the National Academy of Sciences*, 110, 7820-7825.
119. Sugimoto, M., Sakagami, H., Yokote, Y., Onuma, H., Kaneko, M., Mori, M., Sakaguchi, Y., Soga, T. and Tomita, M. (2012). Non-targeted metabolite profiling in activated macrophage secretion. *Metabolomics*, 8, 624-633.
120. Bambouskova, M., Gorvel, L., Lampropoulou, V., Sergushichev, A., Loginicheva, E., Johnson, K., Korenfeld, D., Mathyer, M.E., Kim, H., Huang, L.H., Duncan, D., Bregman, H., Keskin, A., Santeford, A., Apte, R.S., Sehgal, R., Johnson, B., Amarasinghe, G.K., Soares, M.P., Satoh, T., Akira, S., Hai, T., de Guzman Strong, C., Auclair, K., Roddy, T.P., Biller, S.A., Jovanovic, M., Klechevsky, E., Stewart, K.M., Randolph, G.J. and Artyomov, M.N. (2018). Electrophilic properties of itaconate and derivatives regulate the $\text{I}\kappa\text{B}\zeta$ -ATF3 inflammatory axis. *Nature*, 556, 501-504.
121. Bafana, R. and Pandey, R.A. (2018). New approaches for itaconic acid production: bottlenecks and possible remedies. *Crit. Rev. Biotechnol.*, 38, 68-82.
122. Calam, C.T., Oxford, A.E., and Raistrick, H. (1939). Studies in the biochemistry of microorganisms: Itaconic acid, a metabolic product of a strain of *Aspergillus terreus* Thom. *Biochem. J.*, 33, 1488-95.
123. Pfeifer, V.F., Vojnovich, C., and Heger, E.N. (1952). Itaconic acid by fermentation with *Aspergillus terreus*. *Ind Eng. Chem.*, 44, 2975-2980.
124. Levinson, W.E., Kurtzman, C.P., and Kuo, T.M. (2006). Production of itaconic acid by *Pseudozyma antarctica* NRRL Y-7808 under nitrogen-limited growth conditions. *Enzyme. Microb. Tech.*, 39, 824-827.
125. Specht, R., Aurich, A., Kreyß, E., Barth, G. and Bodinus, C. (2014). Verfahren zur biotechnologischen Herstellung von Itaconsäure. DE 102008011854B4.
126. Guevarra, E.D. and Tabuchi, T. (1990). Accumulation of itaconic, 2-hydroxyparaconic, itatartaric, and malic-acids by strains of the genus *Ustilago*. *Agric. Biol. Chem.*, 54, 2353-2358.
127. Haskins, R.H. (1950). Biochemistry of the ustilaginales: I. Preliminary cultural studies of *Ustilago zaeae*. *Can. J. Microbiol.*, 28c, 213-223.
128. Kawamura, D., Furuhashi, M., Saito, O. and Matsui, H. (1981). Production of itaconic acid by fermentation. Japan Patent 56137893.
129. Tabuchi, T., Sugisawa, T., Ishidori, T., Nakahara, T. and Sugiyama, J. (1981). Itaconic acid fermentation by a yeast belonging to the genus *Candida*. *Agric. Biol. Chem.*, 45, 475-479.
130. Sayama, A., Kobayashi, K., and Ogoshi, A. (1994). Morphological and physiological comparisons of *Helicobasidium mompa* and *H. purpureum*. *Mycoscience*, 35, 15-20.

References

131. Hevekerl, A., Kuenz, A., and Vorlop, K.D. (2014). Influence of the pH on the itaconic acid production with *Aspergillus terreus*. Appl. Microbiol. Biotechnol., 98, 10005-12.
132. Krull, S., Hevekerl, A., Kuenz, A. and Pruss, U. (2017). Process development of itaconic acid production by a natural wild type strain of *Aspergillus terreus* to reach industrially relevant final titers. Appl. Microbiol. Biot., 101, 4063-4072.
133. Reddy, C.S. and Singh, R.P. (2002). Enhanced production of itaconic acid from corn starch and market refuse fruits by genetically manipulated *Aspergillus terreus* SKR10. Bioresour. Technol., 85, 69-71.
134. Shin, W.S., Lee, D., Kim, S., Jeong, Y.S. and Chun, G.T. (2013). Application of scale-up criterion of constant oxygen mass transfer coefficient (kLa) for production of itaconic acid in a 50 L pilot-scale fermentor by fungal cells of *Aspergillus terreus*. J Microbiol. Biotechn., 23, 1445-53.
135. Yahiro, K., Takahama, T., Park, Y.S. and Okabe, M. (1995). Breeding of *Aspergillus terreus* mutant TN-484 for itaconic acid production with high yield. J. Ferment. Bioeng., 79, 506-508.
136. Guevarra, E.D. and Tabuchi, T. (1990). Production of 2-hydroxyparaconic and itatartaric acids by *Ustilago cynodontis* and simple recovery process of the acids. Agric. Biol. Chem., 54, 2359-2365.
137. Maassen, N., Panakova, M., Wierckx, N., Geiser, E., Zimmermann, M., Bölker, M., Kliner, U. and Blank, L.M. (2014). Influence of carbon and nitrogen concentration on itaconic acid production by the smut fungus *Ustilago maydis*. Eng. Life Sci., 14, 129-134.
138. Li, A., van Luijk, N., ter Beek, M., Caspers, M., Punt, P. and van der Werf, M. (2011). A clone-based transcriptomics approach for the identification of genes relevant for itaconic acid production in *Aspergillus*. Fungal Genet. Biol., 48, 602-11.
139. Geiser, E., Przybilla, S.K., Friedrich, A., Buckel, W., Wierckx, N., Blank, L.M. and Bölker, M. (2015). *Ustilago maydis* produces itaconic acid via the unusual intermediate *trans*-aconitate. Microb. Biotechnol., 9, 116-126.
140. Geiser, E., Przybilla, S.K., Engel, M., Kleineberg, W., Buttner, L., Sarikaya, E., Den Hartog, T., Klankermayer, J., Leitner, W., Bölker, M., Blank, L.M. and Wierckx, N. (2016). Genetic and biochemical insights into the itaconate pathway of *Ustilago maydis* enable enhanced production. Metab. Eng., 38, 427-435.
141. Jaklitsch, W.M., Kubicek, C.P., and Scrutton, M.C. (1991). The subcellular organization of itaconate biosynthesis in *Aspergillus terreus*. J. Gen. Microbiol., 137, 533-539.
142. Bonnarne, P., Gillet, B., Sepulchre, A.M., Role, C., Beloeil, J.C. and Ducrocq, C. (1995). Itaconate biosynthesis in *Aspergillus terreus*. J. Bacteriol., 177, 3573-3578.
143. Dwiarti, L., Yamane, K., Yamatani, H., Kahar, P. and Okabe, M. (2002). Purification and characterization of *cis*-aconitic acid decarboxylase from *Aspergillus terreus* TN484-M1. J. Biosci. Bioeng., 94, 29-33.
144. Kanamasa, S., Dwiarti, L., Okabe, M. and Park, E.Y. (2008). Cloning and functional characterization of the *cis*-aconitic acid decarboxylase (CAD) gene from *Aspergillus terreus*. Appl. Microbiol. Biotechnol., 80, 223-9.
145. Jadwiga, J. and Diana, M. (1974). Studies on the metabolic pathway for itartaric acid formation by *Aspergillus terreus*. Acta Microbiologica Polonica Ser. B, 6, 51-61.
146. Steiger, M.G., Blumhoff, M.L., Mattanovich, D. and Sauer, M. (2013). Biochemistry of microbial itaconic acid production. Front. Microbiol., 4,
147. Kuenz, A., Gallenmuller, Y., Willke, T. and Vorlop, K.D. (2012). Microbial production of itaconic acid: developing a stable platform for high product concentrations. Appl. Microbiol. Biotechnol., 96, 1209-1216.

148. Hossain, A.H., Li, A., Brickwedde, A., Wilms, L., Caspers, M., Overkamp, K. and Punt, P.J. (2016). Rewiring a secondary metabolite pathway towards itaconic acid production in *Aspergillus niger*. *Microb. Cell Fact.*, 15, 130.
149. Tevz, G., Bencina, M., and Legisa, M. (2010). Enhancing itaconic acid production by *Aspergillus terreus*. *Appl. Microbiol. Biotechnol.*, 87, 1657-64.
150. Otten, A., Brocker, M., and Bott, M. (2015). Metabolic engineering of *Corynebacterium glutamicum* for the production of itaconate. *Metab. Eng.*, 30, 156-165.
151. Harder, B.J., Bettenbrock, K., and Klamt, S. (2016). Model-based metabolic engineering enables high yield itaconic acid production by *Escherichia coli*. *Metab. Eng.*, 38, 29-37.
152. Blazcek, J., Hill, A., Jamoussi, M., Pan, A., Miller, J. and Alper, H.S. (2015). Metabolic engineering of *Yarrowia lipolytica* for itaconic acid production. *Metab. Eng.*, 32, 66-73.
153. Chin, T., Sano, M., Takahashi, T., Ohara, H. and Aso, Y. (2015). Photosynthetic production of itaconic acid in *Synechocystis* sp. PCC6803. *J. Biotechnol.*, 195, 43-5.
154. Papagianni, M. (2004). Fungal morphology and metabolite production in submerged mycelial processes. *Biotechnol. Adv.*, 22, 189-259.
155. Gyamerah, M.H. (1995). Oxygen requirement and energy relations of itaconic acid fermentation by *Aspergillus terreus* NRRL 1960. *Appl. Microbiol. Biot.*, 44, 20-26.
156. Cairns, T.C., Zheng, X., Zheng, P., Sun, J. and Meyer, V. (2019). Moulding the mould: understanding and reprogramming filamentous fungal growth and morphogenesis for next generation cell factories. *Biotechnol. Biofuels*, 12, 77.
157. Batti, M. and Schweiger, L. (1963). Process for the production of itaconic acid. US3078217.
158. Gyamerah, M. (1995). Factors affecting the growth form of *Aspergillus terreus* NRRL 1960 in relation to itaconic acid fermentation. *Appl. Microbiol. Biotechnol.*, 44, 356-361.
159. Kobayashi, T. (1978). Production of Itaconic Acid from Wood Waste. *Process Biochemistry*, 13, 15-22.
160. Lockwood, L.B. and Nelson, G.E. (1946). Some factors affecting the production of itaconic acid by *Aspergillus terreus* in agitated cultures. *Archives of biochemistry*, 10, 365-74.
161. Kobayashi, T. (1971). Process for recovering itaconic acid and salts thereof from fermented broth. Japan Patent 3621 053.
162. Eimhjellen, K.E. and Larsen, H. (1955). The mechanism of itaconic acid formation by *Aspergillus terreus*. 2. The effect of substrates and inhibitors. *Biochem. J.*, 60, 139-47.
163. Lockwood, L. (1975). Production of organic acids by fermentation. In: Pepler HJ, Perlman D (eds) *Microbial technology*, vol2, Academic Press, New York, pp 356-386.
164. Anjum, S., Tripathi, S., Singh, N. and KS, G. (2016). Reactive extraction a boom for itaconic acid; a review. *Int. J. Recent. Sci. Res.*, 5,
165. López-Garzón, C.S. and Straathof, A.J.J. (2014). Recovery of carboxylic acids produced by fermentation. *Biotechnol. Adv.*, 32, 873-904.
166. Magalhaes, A.I., de Carvalho, J.C., Medina, J.D.C. and Soccol, C.R. (2017). Downstream process development in biotechnological itaconic acid manufacturing. *Appl. Microbiol. Biotechnol.*, 101, 1-12.
167. Magalhães, A.I., de Carvalho, J.C., Ramírez, E.N.M., Medina, J.D.C. and Soccol, C.R. (2016). Separation of Itaconic Acid from Aqueous Solution onto Ion-Exchange Resins. *J. Chem. Eng. Data*, 61, 430-437.
168. Holzhäuser, F.J., Artz, J., Palkovits, S., Kreyenschulte, D., Büchs, J. and Palkovits, R. (2017). Electrocatalytic upgrading of itaconic acid to methylsuccinic acid using fermentation broth as a substrate solution. *Green Chem.*, 19, 2390-2397.
169. Schute, K., Detoni, C., Kann, A., Jung, O., Palkovits, R. and Rose, M. (2016). Separation in biorefineries by liquid phase adsorption: Itaconic acid as case study. *Acs. Sustain. Chem. Eng.*, 4, 5921-5928.

References

170. Willke, T. and Kuenz, A. (2007). Itaconsäureherstellung aus nachwachsenden Rohstoffen als Ersatz für petrochemisch hergestellte Acrylsäure. . Bundesforschungsanstalt für Landwirtschaft - Institut für Technology,
171. Feldbrügge, M., Kellner, R., and Schipper, K. (2013). The biotechnological use and potential of plant pathogenic smut fungi. *Appl. Microbiol. Biotechnol.*, 97, 3253-3265.
172. Kirk, P.M., Cannon, P.F., David, J.C. and Stalpers, J.A. (2001). *Ainsworth and Bisby's dictionary of the fungi*: 9th edition. ed. Wallingford. 085199377X.
173. Bakkeren, G., Kamper, J., and Schirawski, J. (2008). Sex in smut fungi: Structure, function and evolution of mating-type complexes. *Fungal Genet. Biol.*, 45 Suppl 1, 15-21.
174. Bölker, M. (2001). *Ustilago maydis*-a valuable model system for the study of fungal dimorphism and virulence. *Microbiology*, 147, 1395-401.
175. Brefort, T., Doehlemann, G., Mendoza-Mendoza, A., Reissmann, S., Djamei, A. and Kahmann, R. (2009). *Ustilago maydis* as a pathogen. *annual review of phytopathology*, 47, 423-45.
176. Schirawski, J., Mannhaupt, G., Munch, K., Brefort, T., Schipper, K., Doehlemann, G., Di Stasio, M., Rossel, N., Mendoza-Mendoza, A., Pester, D., Muller, O., Winterberg, B., Meyer, E., Ghareeb, H., Wollenberg, T., Munsterkotter, M., Wong, P., Walter, M., Stukenbrock, E., Guldener, U. and Kahmann, R. (2010). Pathogenicity determinants in smut fungi revealed by genome comparison. *Science*, 330, 1546-8.
177. Holliday, R. (2004). Early studies on recombination and DNA repair in *Ustilago maydis*. *DNA Repair (Amst)*, 3, 671-82.
178. Steinberg, G. and Perez-Martin, J. (2008). *Ustilago maydis*, a new fungal model system for cell biology. *Trends Cell Biol.*, 18, 61-7.
179. Vollmeister, E., Schipper, K., and Feldbrügge, M. (2012). Microtubule-dependent mRNA transport in the model microorganism *Ustilago maydis*. *Rna Biol.*, 9, 261-268.
180. Dean, R., Van Kan, J.A.L., Pretorius, Z.A., Hammond-Kosack, K.E., Di Pietro, A., Spanu, P.D., Rudd, J.J., Dickman, M., Kahmann, R., Ellis, J. and Foster, G.D. (2012). The Top 10 fungal pathogens in molecular plant pathology. *Mol. Plant Pathol.*, 13, 804-804.
181. Kämper, J., Kahmann, R., Bolker, M., Ma, L.J., Brefort, T., Saville, B.J., Banuett, F., Kronstad, J.W., Gold, S.E., Muller, O., Perlin, M.H., Wosten, H.A.B., de Vries, R., Ruiz-Herrera, J., Reynaga-Pena, C.G., Snetselaar, K., McCann, M., Perez-Martin, J., Feldbrugge, M., Basse, C.W., Steinberg, G., Ibeas, J.I., Holloman, W., Guzman, P., Farman, M., Stajich, J.E., Sentandreu, R., Gonzalez-Prieto, J.M., Kennell, J.C., Molina, L., Schirawski, J., Mendoza-Mendoza, A., Greilinger, D., Munch, K., Rossel, N., Scherer, M., Vranes, M., Ladendorf, O., Vincon, V., Fuchs, U., Sandrock, B., Meng, S., Ho, E.C.H., Cahill, M.J., Boyce, K.J., Klose, J., Klosterman, S.J., Deelstra, H.J., Ortiz-Castellanos, L., Li, W.X., Sanchez-Alonso, P., Schreier, P.H., Hauser-Hahn, I., Vaupel, M., Koopmann, E., Friedrich, G., Voss, H., Schluter, T., Margolis, J., Platt, D., Swimmer, C., Gnirke, A., Chen, F., Vysotskaia, V., Mannhaupt, G., Guldener, U., Munsterkotter, M., Haase, D., Oesterheld, M., Mewes, H.W., Mauceli, E.W., DeCaprio, D., Wade, C.M., Butler, J., Young, S., Jaffe, D.B., Calvo, S., Nusbaum, C., Galagan, J. and Birren, B.W. (2006). Insights from the genome of the biotrophic fungal plant pathogen *Ustilago maydis*. *Nature*, 444, 97-101.
182. Brachmann, A., König, J., Julius, C. and Feldbrügge, M. (2004). A reverse genetic approach for generating gene replacement mutants in *Ustilago maydis*. *Mol. Genet. Genomics*, 272, 216-226.
183. Khrunyk, Y., Munch, K., Schipper, K., Lupas, A.N. and Kahmann, R. (2010). The use of FLP-mediated recombination for the functional analysis of an effector gene family in the biotrophic smut fungus *Ustilago maydis*. *New Phytol.*, 187, 957-968.

184. Terfrüchte, M., Joehnk, B., Fajardo-Somera, R., Braus, G.H., Riquelme, M., Schipper, K. and Feldbrügge, M. (2014). Establishing a versatile Golden Gate cloning system for genetic engineering in fungi. *Fungal Genet. Biol.*, 62, 1-10.
185. Schuster, M., Schweizer, G., Reissmann, S. and Kahmann, R. (2016). Genome editing in *Ustilago maydis* using the CRISPR-Cas system. *Fungal Genet. Biol.*, 89, 3-9.
186. Spellig, T., Bottin, A., and Kahmann, R. (1996). Green fluorescent protein (GFP) as a new vital marker in the phytopathogenic fungus *Ustilago maydis*. *Mol. Gen. Genet.*, 252, 503-509.
187. Flor-Parra, I., Vranes, M., Kämper, J. and Pérez-Martín, J. (2006). Biz1, a zinc finger protein required for plant invasion by *Ustilago maydis*, regulates the levels of a mitotic cyclin. *Plant Cell*, 18, 2369-2387.
188. Sarkari, P., Reindl, M., Stock, J., Muller, O., Kahmann, R., Feldbrügge, M. and Schipper, K. (2014). Improved expression of single-chain antibodies in *Ustilago maydis*. *J. Biotechnol.*, 191, 165-175.
189. Basse, C.W. (2005). Dissecting defense-related and developmental transcriptional responses of maize during *Ustilago maydis* infection and subsequent tumor formation. *Plant Physiol.*, 138, 1774-1784.
190. Brachmann, A., Weinzierl, G., Kämper, J. and Kahmann, R. (2001). Identification of genes in the bW/bE regulatory cascade in *Ustilago maydis*. *Mol. Microbiol.*, 42, 1047-1063.
191. Bottin, A., Kämper, J., and Kahmann, R. (1996). Isolation of a carbon source-regulated gene from *Ustilago maydis*. *Mol. Gen. Genet.*, 253, 342-352.
192. Keon, J.P.R., White, G.A., and Hargreaves, J.A. (1991). Isolation, characterization and sequence of a gene conferring resistance to the systemic fungicide carboxin from the maize smut pathogen, *Ustilago maydis*. *Curr. Genet.*, 19, 475-481.
193. Broomfield, P.L.E. and Hargreaves, J.A. (1992). A single amino-acid change in the iron-sulphur protein subunit of succinate dehydrogenase confers resistance to carboxin in *Ustilago maydis*. *Curr. Genet.*, 22, 117-121.
194. Mahlert, M., Leveleki, L., Hlubek, A., Sandrock, B. and Bölker, M. (2006). Rac1 and Cdc42 regulate hyphal growth and cytokinesis in the dimorphic fungus *Ustilago maydis*. *Mol. Microbiol.*, 59, 567-578.
195. Tsukuda, T., Carleton, S., Fotheringham, S. and Holloman, W.K. (1988). Isolation and characterization of an autonomously replicating sequence from *Ustilago maydis*. *Mol. Cell. Biol.*, 8, 3703-3709.
196. Gold, S.E., Bakkeren, G., Davies, J.E. and Kronstad, J.W. (1994). Three selectable markers for transformation of *Ustilago maydis*. *Gene*, 142, 225-30.
197. Klement, T., Milker, S., Jager, G., Grande, P.M., Dominguez de Maria, P. and Büchs, J. (2012). Biomass pretreatment affects *Ustilago maydis* in producing itaconic acid. *Microb. Cell Fact.*, 11, 43.
198. Geiser, E., Wierckx, N., Zimmermann, M. and Blank, L.M. (2013). Identification of an endo-1,4-beta-xylanase of *Ustilago maydis*. *Bmc Biotechnology*, 13,
199. Spoeckner, S., Wray, V., Nimtz, M. and Lang, S. (1999). Glycolipids of the smut fungus *Ustilago maydis* from cultivation on renewable resources. *Appl. Microbiol. Biotechnol.*, 51, 33-39.
200. Cano-Canchola, C., Acevedo, L., Ponce-Noyola, P., Flores-Martínez, A., Flores-Carreón, A. and Leal-Morales, C.A. (2000). Induction of lytic enzymes by the interaction of *Ustilago maydis* with *Zea mays* tissues. *Fungal Genet. Biol.*, 29, 145-151.
201. Roa Engel, C.A., van Gulik, W.M., Marang, L., van der Wielen, L.A. and Straathof, A.J. (2011). Development of a low pH fermentation strategy for fumaric acid production by *Rhizopus oryzae*. *Enzyme. Microb. Tech.*, 48, 39-47.

References

202. Gibson, D.G., Young, L., Chuang, R.Y., Venter, J.C., Hutchison, C.A. and Smith, H.O. (2009). Enzymatic assembly of DNA molecules up to several hundred kilobases. *Nat. Methods*, 6, 343.
203. Sambrook, J. and Russell, D.W. (2001). *Molecular cloning: A laboratory manual*. 3 ed. Cold Spring Harbor Laboratory Press, New York. ISBN-Nr. 978-1936113422.
204. Zarnack, K., Maurer, S., Kaffarnik, F., Ladendorf, O., Brachmann, A., Kamper, J. and Feldbrügge, M. (2006). Tetracycline-regulated gene expression in the pathogen *Ustilago maydis*. *Fungal Genet. Biol.*, 43, 727-738.
205. Heigwer, F., Kerr, G., and Boutros, M. (2014). E-CRISP: fast CRISPR target site identification. *Nat. Methods*, 11, 122.
206. Hewald, S., Josephs, K., and Bölker, M. (2005). Genetic analysis of biosurfactant production in *Ustilago maydis*. *Appl. Environ. Microb.*, 71, 3033-3040.
207. Przybilla, S.K. (2014). Genetische und biochemische Charakterisierung der Itaconsäure-Biosynthese in *Ustilago maydis*. Dissertation. Philipps-Universität Marburg. Biologie,
208. Zambanini, T., Hosseinpour Tehrani, H., Geiser, E., Merker, D., Schleese, S., Krabbe, J., Buescher, J.M., Meurer, G., Wierckx, N. and Blank, L.M. (2017). Efficient itaconic acid production from glycerol with *Ustilago vetiveriae* TZ1. *Biotechnol. Biofuels*, 10, 131.
209. Duetz, W.A., Ruedi, L., Hermann, R., O'Connor, K., Büchs, J. and Witholt, B. (2000). Methods for intense aeration, growth, storage, and replication of bacterial strains in microtiter plates. *Appl. Environ. Microb.*, 66, 2641-2646.
210. Willis, R.B., Montgomery, M.E., and Allen, P.R. (1996). Improved method for manual, colorimetric determination of total kjeldahl nitrogen using salicylate. *J. Agric. Food Chem.*, 44, 1804-1807.
211. Chomczynski, P. and Sacchi, N. (1987). Single-Step method of RNA isolation by acid guanidinium thiocyanate phenol chloroform extraction. *Anal. Biochem.*, 162, 156-159.
212. Saitou, N. and Nei, M. (1987). The neighbor-joining method - a new method for reconstructing phylogenetic trees. *Mol. Biol. Evol.*, 4, 406-425.
213. Tamura, K., Nei, M., and Kumar, S. (2004). Prospects for inferring very large phylogenies by using the neighbor-joining method. *P. Natl. Acad. Sci. USA*, 101, 11030-11035.
214. Kumar, S., Stecher, G., and Tamura, K. (2016). MEGA7: Molecular evolutionary genetics analysis version 7.0 for bigger datasets. *Mol. Biol. Evol.*, 33, 1870-1874.
215. Zuckerkandl, E. and Pauling, L. (1965). Evolutionary divergence and convergence in proteins. in: *Evolving Genes and Proteins*. Academic Press. 97-166. 978-1-4832-2734-4.
216. Keller, N.P., Turner, G., and Bennett, J.W. (2005). Fungal secondary metabolism - From biochemistry to genomics. *Nat. Rev. Microbiol.*, 3, 937-947.
217. Brakhage, A.A. and Schroeckh, V. (2011). Fungal secondary metabolites - Strategies to activate silent gene clusters. *Fungal Genet. Biol.*, 48, 15-22.
218. Lazzarini, A., Cavaletti, L., Toppo, G. and Marinelli, F. (2000). Rare genera of actinomycetes as potential producers of new antibiotics. *Anton. Leeuw. Int. J. G.*, 78, 399-405.
219. Verpoorte, R. and Alfermann, A. (2000). *Metabolic engineering of plant secondary metabolism*. ed. Springer, Dordrecht. ISBN-Nr. 978-94-015-9423-3.
220. Smith, D.J., Burnham, M.K.R., Bull, J.H., Hodgson, J.E., Ward, J.M., Browne, P., Brown, J., Barton, B., Earl, A.J. and Turner, G. (1990). Beta-lactam antibiotic biosynthetic genes have been conserved in clusters in prokaryotes and eukaryotes. *Embo Journal*, 9, 741-747.
221. Trail, F., Mahanti, N., Rarick, M., Mehig, R., Liang, S.H., Zhou, R. and Linz, J.E. (1995). Physical and transcriptional map of an aflatoxin gene cluster in *Aspergillus parasiticus* and functional disruption of a gene involved early in the aflatoxin pathway. *Appl. Environ. Microb.*, 61, 2665-73.

222. Blazic, M., Starcevic, A., Lisfi, M., Baranasic, D., Goranovic, D., Fujs, S., Kuscer, E., Kosec, G., Petkovic, H., Cullum, J., Hranueli, D. and Zucko, J. (2012). Annotation of the modular polyketide synthase and nonribosomal peptide synthetase gene clusters in the genome of *Streptomyces tsukubaensis* NRRL18488. *Appl. Environ. Microb.*, 78, 8183-8190.
223. Brakhage, A.A. (2013). Regulation of fungal secondary metabolism. *Nat. Rev. Microbiol.*, 11, 21-32.
224. Leitner, W., Klankermayer, J., Pischinger, S., Pitsch, H. and Kohse-Hoinghaus, K. (2017). Advanced biofuels and beyond: Chemistry solutions for propulsion and production. *Angew. Chem. Int. Edit.*, 56, 5412-5452.
225. Geilen, F.M.A., Engendahl, B., Harwardt, A., Marquardt, W., Klankermayer, J. and Leitner, W. (2010). Selective and flexible transformation of biomass-derived platform chemicals by a multifunctional catalytic system. *Angew. Chem. Int. Edit.*, 49, 5510-5514.
226. Tollot, M., Assmann, D., Becker, C., Altmüller, J., Duthel, J.Y., Wegner, C.E. and Kahmann, R. (2016). The WOPR protein Ros1 is a master regulator of sporogenesis and late effector gene expression in the maize pathogen *Ustilago maydis*. *PLoS Pathog.*, 12, e1005697.
227. Zheng, Y., Kief, J., Auffarth, K., Farfsing, J.W., Mahlert, M., Nieto, F. and Basse, C.W. (2008). The *Ustilago maydis* Cys2His2-type zinc finger transcription factor Mzr1 regulates fungal gene expression during the biotrophic growth stage. *Mol. Microbiol.*, 68, 1450-70.
228. Lanver, D., Müller, A.N., Happel, P., Schweizer, G., Haas, F.B., Franitz, M., Pellegrin, C., Reissmann, S., Altmüller, J., Rensing, S.A. and Kahmann, R. (2018). The biotrophic development of *Ustilago maydis* studied by RNA-seq analysis. *Plant Cell*, 30, 300-323.
229. Bergmann, S., Schumann, J., Scherlach, K., Lange, C., Brakhage, A.A. and Hertweck, C. (2007). Genomics-driven discovery of PKS-NRPS hybrid metabolites from *Aspergillus nidulans*. *Nat. Chem. Biol.*, 3, 213-217.
230. Hertweck, C. (2009). Hidden biosynthetic treasures brought to light. *Nat. Chem. Biol.*, 5, 450-452.
231. Khaldi, N., Seifuddin, F.T., Turner, G., Haft, D., Nierman, W.C., Wolfe, K.H. and Fedorova, N.D. (2010). SMURF: Genomic mapping of fungal secondary metabolite clusters. *Fungal Genet. Biol.*, 47, 736-741.
232. Medema, M.H., Kottmann, R., Yilmaz, P., Cummings, M., Biggins, J.B., Blin, K., de Bruijn, I., Chooi, Y.H., Claesen, J., Coates, R.C., Cruz-Morales, P., Duddela, S., Dusterhus, S., Edwards, D.J., Fewer, D.P., Garg, N., Geiger, C., Gomez-Escribano, J.P., Greule, A., Hadjithomas, M., Haines, A.S., Helfrich, E.J.N., Hillwig, M.L., Ishida, K., Jones, A.C., Jones, C.S., Jungmann, K., Kegler, C., Kim, H.U., Kotter, P., Krug, D., Masschelein, J., Melnik, A.V., Mantovani, S.M., Monroe, E.A., Moore, M., Moss, N., Nutzmann, H.W., Pan, G.H., Pati, A., Petras, D., Reen, F.J., Rosconi, F., Rui, Z., Tian, Z.H., Tobias, N.J., Tsunematsu, Y., Wiemann, P., Wyckoff, E., Yan, X.H., Yim, G., Yu, F.G., Xie, Y.C., Aigle, B., Apel, A.K., Balibar, C.J., Balskus, E.P., Barona-Gomez, F., Bechthold, A., Bode, H.B., Borriss, R., Brady, S.F., Brakhage, A.A., Caffrey, P., Cheng, Y.Q., Clardy, J., Cox, R.J., De Mot, R., Donadio, S., Donia, M.S., van der Donk, W.A., Dorrestein, P.C., Doyle, S., Driessen, A.J.M., Ehling-Schulz, M., Entian, K.D., Fischbach, M.A., Gerwick, L., Gerwick, W.H., Gross, H., Gust, B., Hertweck, C., Hofte, M., Jensen, S.E., Ju, J.H., Katz, L., Kaysser, L., Klassen, J.L., Keller, N.P., Kormanec, J., Kuipers, O.P., Kuzuyama, T., Kyrpidis, N.C., Kwon, H.J., Lautru, S., Lavigne, R., Lee, C.Y., Linguan, B., Liu, X.Y., Liu, W., Luzhetskyy, A., Mahmud, T., Mast, Y., Mendez, C., Metsa-Ketela, M., Micklefield, J., Mitchell, D.A., Moore, B.S., Moreira, L.M., Muller, R., Neilan, B.A., Nett, M., Nielsen, J., O'Gara, F., Oikawa, H., Osbourn, A., Osburne, M.S., Ostash, B., Payne, S.M., Pernodet, J.L., Petricek, M., Piel, J., Ploux, O., Raaijmakers, J.M., Salas, J.A., Schmitt, E.K., Scott, B., Seipke, R.F., Shen, B., Sherman, D.H., Sivonen, K., Smanski, M.J., Sosio, M.,

- Stegmann, E., Sussmuth, R.D., Tahlan, K., Thomas, C.M., Tang, Y., Truman, A.W., Viaud, M., Walton, J.D., Walsh, C.T., Weber, T., van Wezel, G.P., Wilkinson, B., Willey, J.M., Wohlleben, W., Wright, G.D., Ziemert, N., Zhang, C.S., Zotchev, S.B., Breitling, R., Takano, E. and Glockner, F.O. (2015). Minimum Information about a Biosynthetic Gene cluster. *Nat. Chem. Biol.*, 11, 625-631.
233. Medema, M.H., Blin, K., Cimermancic, P., de Jager, V., Zakrzewski, P., Fischbach, M.A., Weber, T., Takano, E. and Breitling, R. (2011). antiSMASH: rapid identification, annotation and analysis of secondary metabolite biosynthesis gene clusters in bacterial and fungal genome sequences. *Nucleic Acids Res.*, 39, W339-W346.
234. Priebe, S., Linde, J., Albrecht, D., Guthke, R. and Brakhage, A.A. (2011). FungiFun: A web-based application for functional categorization of fungal genes and proteins. *Fungal Genet. Biol.*, 48, 353-358.
235. Geiser, E., Ludwig, F., Zambanini, T., Wierckx, N. and Blank, L.M. (2016). Draft genome sequences of itaconate-producing *Ustilaginaceae*. *Genome Announc.*, 4, e01291-16.
236. Geiser, E., Reindl, M., Blank, L.M., Feldbrügge, M., Wierckx, N. and Schipper, K. (2016). Activating intrinsic carbohydrate-active enzymes of the smut fungus *Ustilago maydis* for the degradation of plant cell wall components. *Appl. Environ. Microb.*, 82, 5174-5185.
237. Sanchez, S., Chavez, A., Forero, A., Garcia-Huante, Y., Romero, A., Sanchez, M., Rocha, D., Sanchez, B., Avalos, M., Guzman-Trampe, S., Rodriguez-Sanoja, R., Langley, E. and Ruiz, B. (2010). Carbon source regulation of antibiotic production. *J. Antibiot.*, 63, 442-459.
238. Altschul, S.F., Madden, T.L., Schaffer, A.A., Zhang, J., Zhang, Z., Miller, W. and Lipman, D.J. (1997). Gapped BLAST and PSI-BLAST: a new generation of protein database search programs. *Nucleic Acids Res.*, 25, 3389-402.
239. Stanke, M., Steinkamp, R., Waack, S. and Morgenstern, B. (2004). AUGUSTUS: a web server for gene finding in eukaryotes. *Nucleic Acids Res.*, 32, W309-W312.
240. Henikoff, S. and Henikoff, J.G. (1992). Amino-acid substitution matrices from protein blocks. *P. Natl. Acad. Sci. USA*, 89, 10915-10919.
241. Wang, Q.M., Begerow, D., Groenewald, M., Liu, X.Z., Theelen, B., Bai, F.Y. and Boekhout, T. (2015). Multigene phylogeny and taxonomic revision of yeasts and related fungi in the *Ustilaginomycotina*. *Stud. Mycol.*, 81, 55-83.
242. McTaggart, A.R., Shivas, R.G., Boekhout, T., Oberwinkler, F., Vanky, K., Pennycook, S.R. and Begerow, D. (2016). *Mycosarcoma* (*Ustilaginaceae*), a resurrected generic name for corn smut (*Ustilago maydis*) and its close relatives with hypertrophied, tubular sori. *IMA Fungus*, 7, 309-315.
243. McLaughlin, D. and Spatafora, J. (2014). *Systematics and Evolution*. ed. Springer Berlin Heidelberg. ISBN-Nr. 978-3-642-55318-9.
244. Wang, L.P., Ridgway, D., Gu, T.Y. and Moo-Young, M. (2005). Bioprocessing strategies to improve heterologous protein production in filamentous fungal fermentations. *Biotechnol. Adv.*, 23, 115-129.
245. Geiser, E. (2015). Itaconic acid production by *Ustilago maydis*. Dissertation. RWTH-Aachen. Institute for Applied Technology.
246. Palmieri, F. (2004). The mitochondrial transporter family (SLC25): physiological and pathological implications. *Pflug. Arch. Eur. J. Phy.*, 447, 689-709.
247. Murre, C., Bain, G., Vandijk, M.A., Engel, I., Furnari, B.A., Massari, M.E., Matthews, J.R., Quong, M.W., Rivera, R.R. and Stuver, M.H. (1994). Structure and function of helix-loop-helix proteins. *Bba-Gene. Struct. Expr.*, 1218, 129-135.
248. Letunic, I., Doerks, T., and Bork, P. (2015). SMART: recent updates, new developments and status in 2015. *Nucleic Acids Res.*, 43, D257-D260.

249. Stoll, M., Piepenbring, M., Begerow, D. and Oberwinkler, F. (2003). Molecular phylogeny of *Ustilago* and *Sporisorium* species (Basidiomycota, Ustilaginales) based on internal transcribed spacer (ITS) sequences. *Can. J. Bot.*, 81, 976-984.
250. Bailey, T.L., Boden, M., Buske, F.A., Frith, M., Grant, C.E., Clementi, L., Ren, J.Y., Li, W.W. and Noble, W.S. (2009). MEME SUITE: tools for motif discovery and searching. *Nucleic Acids Res.*, 37, W202-W208.
251. Willke, T. and Vorlop, K.D. (2001). Biotechnological production of itaconic acid. *Appl. Microbiol. Biot.*, 56, 289-295.
252. Stodola, F.H., Friedkin, M., Moyer, A.J. and Coghill, R.D. (1945). Itartaric acid, a metabolic product of an ultraviolet-induced mutant of *Aspergillus terreus*. *J. Biol. Chem.*, 161, 739-742.
253. Brandt, J.R., Salerno, F., and Fuchter, M.J. (2017). The added value of small-molecule chirality in technological applications. *Nat. Rev. Chem.*, 1,
254. Mori, K. and Fukamatsu, K. (1992). Pheromone Synthesis .164. A synthesis of (1r,5s)-(+)-frontalin from (S)-2-hydroxyparaconic acid. *Liebigs Annalen Der Chemie*, 1191-1193.
255. Li, A., van Luijk, N., ter Beek, M., Caspers, M., Punt, P. and van der Werf, M. (2011). A clone-based transcriptomics approach for the identification of genes relevant for itaconic acid production in *Aspergillus*. *Fungal. Genet. Biol.*, 48, 602-11.
256. Steiger, M.G., Punt, P.J., Ram, A.F.J., Mattanovich, D. and Sauer, M. (2016). Characterizing MttA as a mitochondrial *cis*-aconitic acid transporter by metabolic engineering. *Metab. Eng.*, 35, 95-104.
257. Huang, X.N., Lu, X.F., Li, Y.M., Li, X. and Li, J.J. (2014). Improving itaconic acid production through genetic engineering of an industrial *Aspergillus terreus* strain. *Microb. Cell Fact.*, 13, 119.
258. van der Straat, L., Vernooij, M., Lammers, M., van den Berg, W., Schonewille, T., Cordewener, J., van der Meer, I., Koops, A. and de Graaff, L.H. (2014). Expression of the *Aspergillus terreus* itaconic acid biosynthesis cluster in *Aspergillus niger*. *Microb. Cell Fact.*, 13,
259. Jadwiga, J. and Diana, M. (1974). Studies on the metabolic pathway for itartaric acid formation by *Aspergillus terreus*. *Acta Microbiologica Polonica Ser. B*, 6, 51-61.
260. Zambanini, T., Hosseinpour Tehrani, H., Geiser, E., Sonntag, C.K., Buesche, J.M.r., Meurer, G., Nick, W. and Blank, L.M. (2017). Metabolic engineering of *Ustilago trichophora* TZ1 for improved malic acid production. *Metab. Eng. Commun.*, 4, 12-21.
261. Zambanini, T., Hartmann, S.K., Schmitz, L.M., Büttner, L., Hosseinpour Tehrani, H., Geiser, E., Beudels, M., Venc, D., Wandrey, G., Büchs, J., Schwarzländer, M., Blank, L.M. and Wierckx, N. (2017). Promoters from the itaconate cluster of *Ustilago maydis* are induced by nitrogen depletion. *Fungal Biol. Biotechnol.*, 4, 11.
262. Cordes, T., Michelucci, A., and Hiller, K. (2015). Itaconic acid: The surprising role of an industrial compound as a mammalian antimicrobial metabolite. *Annu. Rev. Nutr.*, 35, 451-73.
263. Hevekerl, A., Kuenz, A., and Vorlop, K.D. (2014). Influence of the pH on the itaconic acid production with *Aspergillus terreus*. *Appl. Microbiol. Biotechnol.*, 98, 10005-12.
264. Kuenz, A. and Krull, S. (2018). Biotechnological production of itaconic acid-things you have to know. *Appl. Microbiol. Biotechnol.*, 102, 3901-3914.
265. Geiser, E., Hosseinpour Tehrani, H., Meyer, S., Blank, L.M. and Wierckx, N. (2018). Evolutionary freedom in the regulation of the conserved itaconate cluster by Rial in related Ustilaginaceae. *Fungal Biol. Biotechnol.*, 5, 14.
266. GarciaGuzman, G. and Burdon, J.J. (1997). Impact of the flower smut *Ustilago cynodontis* (Ustilaginaceae) on the performance of the clonal grass *cynodon dactylon* (gramineae). *Am. J. Bot.*, 84, 1565-1571.

References

267. Morita, T., Konishi, M., Fukuoka, T., Imura, T. and Kitamoto, D. (2008). Identification of *Ustilago cynodontis* as a new producer of glycolipid biosurfactants, mannosylerythritol lipids, based on ribosomal DNA sequences. *J. Oleo. Sci.*, 57, 549-556.
268. Klose, J., de Sa, M.M., and Kronstad, J.W. (2004). Lipid-induced filamentous growth in *Ustilago maydis*. *Mol. Microbiol.*, 52, 823-835.
269. Klose, J. and Kronstad, J.W. (2006). The multifunctional beta-oxidation enzyme is required for full symptom development by the biotrophic maize pathogen *Ustilago maydis*. *Eukaryot. Cell*, 5, 2047-61.
270. Lovely, C.B. and Perlin, M.H. (2011). Cla4, but not Rac1, regulates the filamentous response of *Ustilago maydis* to low ammonium conditions. *Commun. Integr. Biol.*, 4, 670-3.
271. Ruiz-Herrera, J., León, C.G., Guevara-Olvera, L. and Cárabez-Trejo, A. (1995). Yeast-mycelial dimorphism of haploid and diploid strains of *Ustilago maydis*. *Microbiology*, 141, 695-703.
272. Martinez-Espinoza, A.D., Ruiz-Herrera, J., Leon-Ramirez, C.G. and Gold, S.E. (2004). MAP kinase and CAMP signaling pathways modulate the pH-induced yeast-to-mycelium dimorphic transition in the corn smut fungus *Ustilago maydis*. *Curr. Microbiol.*, 49, 274-281.
273. Smith, D.G., Garcia-Pedrajas, M.D., Gold, S.E. and Perlin, M.H. (2003). Isolation and characterization from pathogenic fungi of genes encoding ammonium permeases and their roles in dimorphism. *Mol. Microbiol.*, 50, 259-75.
274. Gunther, M., Grumaz, C., Lorenz, S., Stevens, P., Lindemann, E., Hirth, T., Sohn, K., Zibek, S. and Rupp, S. (2015). The transcriptomic profile of *Pseudozyma aphidis* during production of mannosylerythritol lipids. *Appl. Microbiol. Biotechnol.*, 99, 1375-88.
275. Zapata-Morín, P.A., Fuentes-Dávila, G., Adame-Rodríguez, J.M. and Aréchiga-Carvajal. (2010). Effect of pH and carbon source on the vegetative growth of *Ustilago cynodontis* (Pass.) Henn. in a solid and liquid culture medium. *Rev. Mex. Fitopatol.*, 28, 159-161.
276. Durieu-Trautmann, O. and Tavlitzki, J. (1975). Reversible and permanent effects of the carbon sources and various antibiotics on the morphology and metabolic properties of *Ustilago cynodontis* cells. *J. Cell Biol.*, 66, 102-113.
277. Tharmasothirajan, A. (2017). Master-thesis. Prozessoptimierung der biotechnologischen Produktion von organischen Säuren in *Ustilago*. Institute of Applied Microbiology, RWTH-Aachen.
278. Lanver, D., Tollot, M., Schweizer, G., Lo Presti, L., Reissmann, S., Ma, L.S., Schuster, M., Tanaka, S., Liang, L., Ludwig, N. and Kahmann, R. (2017). *Ustilago maydis* effectors and their impact on virulence. *Nat. Rev. Microbiol.*, 15, 409-421.
279. Kahmann, R. and Kämper, J. (2004). *Ustilago maydis*: how its biology relates to pathogenic development. *New Phytol.*, 164, 31-42.
280. Banuett, F. and Herskowitz, I. (1994). Identification of Fuz7, a *Ustilago maydis* MEK/MAPKK homolog required for *a*-locus-dependent and-independent steps in the fungal life-cycle. *Gene. Dev.*, 8, 1367-1378.
281. Mayorga, M.E. and Gold, S.E. (1999). A MAP kinase encoded by the *ubc3* gene of *Ustilago maydis* is required for filamentous growth and full virulence. *Mol. Microbiol.*, 34, 485-497.
282. Lee, N. and Kronstad, J.W. (2002). *ras2* controls morphogenesis, pheromone response, and pathogenicity in the fungal pathogen *Ustilago maydis*. *Eukaryot. Cell*, 1, 954-966.
283. Meyer, S. (2018). Master-thesis. Characterization of physiological parameters related to the production of itaconic acid with *Ustilago*. Institute of Applied Microbiology, RWTH-Aachen.
284. Gyamerah, M. (1995). Factors affecting the growth form of *Aspergillus terreus* NRRL 1960 in relation to itaconic acid fermentation. *Appl. Microbiol. Biot.*, 44, 356-361.

285. Gao, Q., Liu, J., and Liu, L.M. (2014). Relationship between morphology and itaconic acid production by *Aspergillus terreus*. J. Microbiol. Biotechnol., 24, 168-176.
286. Calvo, A.M., Wilson, R.A., Bok, J.W. and Keller, N.P. (2002). Relationship between secondary metabolism and fungal development. Microbiol. Mol. Biol. Rev., 66, 447-459.
287. Hosseinpour Tehrani, H., Geiser, E., Engel, M., Hartmann, S.K., Hossain, A.H., Punt, P.J., Blank, L.M. and Wierckx, N. (2019). The interplay between transport and metabolism in fungal itaconic acid production. Fungal Genet. Biol., 125, 45-52.
288. Bednarz, S., Fluder, M., Galica, M., Bogdal, D. and Maciejaszek, I. (2014). Synthesis of hydrogels by polymerization of itaconic acid–choline chloride deep eutectic solvent. Journal of Applied Polymer Science, 131,
289. Marvel, C.S. and Shepherd, T.H. (1959). Polymerization Reactions of Itaconic Acid and Some of Its Derivatives. The Journal of Organic Chemistry, 24, 599-605.
290. Veličković, J., Filipović, J., and Djakov, D.P. (1994). The synthesis and characterization of poly(itaconic) acid. Polymer Bulletin, 32, 169-172.
291. Betancourt, T., Pardo, J., Soo, K. and Peppas, N.A. (2010). Characterization of pH-responsive hydrogels of poly(itaconic acid-g-ethylene glycol) prepared by UV-initiated free radical polymerization as biomaterials for oral delivery of bioactive agents. J Biomed Mater Res A, 93, 175-88.
292. Hosseinpour Tehrani, H., Tharmasothirajan, A., Track, E., Blank, L.M. and Wierckx, N. (2019). Engineering the morphology and metabolism of pH tolerant *Ustilago cynodontis* for efficient itaconic acid production. Metab. Eng., 54, 293-300.
293. Eimhjellen, K.E. and Larsen, H. (1955). The mechanism of itaconic acid formation by *Aspergillus terreus*. 2. The effect of substrates and inhibitors. Biochem J, 60, 139-47.
294. Magalhaes, A.I., Jr., de Carvalho, J.C., Medina, J.D.C. and Soccol, C.R. (2017). Downstream process development in biotechnological itaconic acid manufacturing. Appl. Microbiol. Biotechnol., 101, 1-12.
295. Casal, M., Paiva, S., Queiros, O. and Soares-Silva, I. (2008). Transport of carboxylic acids in yeasts. FEMS Microbiol Rev, 32, 974-94.
296. Plumridge, A., Hesse, S.J., Watson, A.J., Lowe, K.C., Stratford, M. and Archer, D.B. (2004). The weak acid preservative sorbic acid inhibits conidial germination and mycelial growth of *Aspergillus niger* through intracellular acidification. Appl Environ Microbiol, 70, 3506-11.
297. Lambert, R.J. and Stratford, M. (1999). Weak-acid preservatives: modelling microbial inhibition and response. J Appl Microbiol, 86, 157-64.
298. CurTiPot-pH and acid-base titration curves: analysis and simulation freeware, version 4.2 CurTiPot-pH and acid-base titration curves: analysis and simulation freeware, version 4.2 Accessible: Available from: http://www.iq.usp.br/gutz/Curtipot_.html.
299. Straathof, A.J.J., Wahl, S.A., Benjamin, K.R., Takors, R., Wierckx, N. and Noorman, H.J. (2019). Grand research challenges for sustainable industrial biotechnology. Trends Biotechnol.,
300. Saur, K. (2018). Master thesis. Strain evaluation and new fermentation strategies to overcome product toxicity in *U. maydis* and the pH tolerant *U. cynodontis* for efficient itaconate production. Institute of Applied Microbiology. RWTH-Aachen.
301. Werpy, T., Peterson, G. (2004). Top value added chemicals from biomass. 2004 US-DoE report PNNL-16983.
302. Roffler, S.R., Blanch, H.W., and Wilke, C.R. (1988). In situ extractive fermentation of acetone and butanol. Biotechnol Bioeng, 31, 135-43.
303. Zambanini, T., Kleineberg, W., Sarikaya, E., Buescher, J.M., Meurer, G., Wierckx, N. and Blank, L.M. (2016). Enhanced malic acid production from glycerol with high-cell density *Ustilago trichophora* TZ1 cultivations. Biotechnol. Biofuels, 9,

References

304. Riesenberg, D. and Guthke, R. (1999). High-cell-density cultivation of microorganisms. *Appl. Microbiol. Biotechnol.*, 51, 422-430.
305. Nemeth, B., Doczi, J., Csete, D., Kacso, G., Ravasz, D., Adams, D., Kiss, G., Nagy, A.M., Horvath, G., Tretter, L., Mocsai, A., Csepanyi-Komi, R., Iordanov, I., Adam-Vizi, V. and Chinopoulos, C. (2016). Abolition of mitochondrial substrate-level phosphorylation by itaconic acid produced by LPS-induced Irg1 expression in cells of murine macrophage lineage. *Faseb j*, 30, 286-300.
306. Sakai, A., Kusumoto, A., Kiso, Y. and Furuya, E. (2004). Itaconate reduces visceral fat by inhibiting fructose 2,6-bisphosphate synthesis in rat liver. *Nutrition*, 20, 997-1002.
307. Application report: Glucose / Lactate. Accessible: Available from: https://www.trace.de/fileadmin/secureDownload/Applikationsbeispiele/Application_report_Glucose_Lactate_Dialysis.pdf.
308. Kreyenschulte, D., Heyman, B., Eggert, A., Maßmann, T., Kalvelage, C., Kossack, R., Regestein, L., Jupke, A. and Büchs, J. (2018). *In situ* reactive extraction of itaconic acid during fermentation of *Aspergillus terreus*. *Biochem. Eng. J.*, 135, 133-141.
309. Dashti, M.G. and Abdeshahian, P. (2016). Batch culture and repeated-batch culture of *Cunninghamella bainieri* 2A1 for lipid production as a comparative study. *Saudi Journal of Biological Sciences*, 23, 172-180.
310. Burgé, G., Chemarin, F., Moussa, M., Saulou-Bérion, C., Allais, F., Spinnler, H.-É. and Athès, V. (2016). Reactive extraction of bio-based 3-hydroxypropionic acid assisted by hollow-fiber membrane contactor using TOA and Aliquat 336 in n-decanol. *J. Chem. Technol. Biot.*, 91, 2705-2712.
311. Robert, T. and Friebel, S. (2016). Itaconic acid – a versatile building block for renewable polyesters with enhanced functionality. *Green Chem.*, 18, 2922-2934.
312. Vollmeister, E., Schipper, K., and Feldbrügge, M. (2012). Microtubule-dependent mRNA transport in the model microorganism *Ustilago maydis*. *Rna Biol.*, 9, 261-8.
313. Morita, T., Fukuoka, T., Imura, T. and Kitamoto, D. (2009). Production of glycolipid biosurfactants by basidiomycetous yeasts. *Biotechnol. Appl. Biochem.*, 53, 39-49.
314. Jeya, M., Lee, K.-M., Tiwari, M.K., Kim, J.-S., Gunasekaran, P., Kim, S.-Y., Kim, I.-W. and Lee, J.-K. (2009). Isolation of a novel high erythritol-producing *Pseudozyma tsukubaensis* and scale-up of erythritol fermentation to industrial level. *Appl. Microbiol. Biotechnol.*, 83, 225-231.
315. Lovely, C.B. and Perlin, M.H. (2011). Cla4, but not Rac1, regulates the filamentous response of *Ustilago maydis* to low ammonium conditions. *Commun. Integr. Biol.*, 4, 670-3.
316. Gorden, J., Geiser, E., Wierckx, N., Blank, L.M., Zeiner, T. and Brandenbusch, C. (2017). Integrated process development of a reactive extraction concept for itaconic acid and application to a real fermentation broth. *Eng. Life Sci.*, 17, 809-816.
317. Donohoue, P.D., Barrangou, R., and May, A.P. (2018). Advances in industrial biotechnology using CRISPR-Cas systems. *Trends Biotechnol.*, 36, 134-146.
318. Bator, I. (2017). Master-thesis. Enhancement of itaconic acid production in *Ustilago maydis* by metabolic engineering. Institute of Applied Microbiology, RWTH-Aachen.
319. Hartmann, S.K., Stockdreher, Y., Wandrey, G., Hosseinpour Tehrani, H., Zambanini, T., Meyer, A.J., Büchs, J., Blank, L.M., Schwarzländer, M. and Wierckx, N. (2018). Online in vivo monitoring of cytosolic NAD redox dynamics in *Ustilago maydis*. *Biochim. Biophys. Acta Bioenerg.*
320. Buckland, B.C., Gbewonyo, K., Dimasi, D., Hunt, G., Westerfield, G. and Nienow, A.W. (1988). Improved performance in viscous mycelial fermentations by agitator retrofitting. *Biotechnol. Bioeng.*, 31, 737-742.

321. Department of economic and social affairs. World population prospects the 2015 revision. Accessible: 10.04.2019. Available from: https://population.un.org/wpp/Publications/Files/Key_Findings_WPP_2015.pdf.
322. de Lorenzo, V., Prather, K.L.J., Chen, G.Q., O'Day, E., von Kameke, C., Oyarzun, D.A., Hosta-Rigau, L., Alsafar, H., Cao, C., Ji, W.Z., Okano, H., Roberts, R.J., Ronaghi, M., Yeung, K., Zhang, F. and Lee, S.Y. (2018). The power of synthetic biology for bioproduction, remediation and pollution control: The UN's Sustainable Development Goals will inevitably require the application of molecular biology and biotechnology on a global scale. *Embo Reports*, 19, e45658.
323. Choi, S., Song, C.W., Shin, J.H. and Lee, S.Y. (2015). Biorefineries for the production of top building block chemicals and their derivatives. *Metab. Eng.*, 28, 223-239.
324. Berovic, M. and Legisa, M. (2007). Citric acid production. *Biotechnology annual review*, 13, 303-43.
325. Grimm, L.H., Kelly, S., Krull, R. and Hempel, D.C. (2005). Morphology and productivity of filamentous fungi. *Appl. Microbiol. Biotechnol.*, 69, 375-84.
326. Feldbrügge, M., Kämper, J., Steinberg, G. and Kahmann, R. (2004). Regulation of mating and pathogenic development in *Ustilago maydis*. *Curr. Opin. Microbiol.*, 7, 666-672.
327. Erb, T.J., Jones, P.R., and Bar-Even, A. (2017). Synthetic metabolism: metabolic engineering meets enzyme design. *Curr. Opin. Chem. Biol.*, 37, 56-62.
328. Karaffà, L. and Kubicek, C.P. (2003). *Aspergillus niger* citric acid accumulation: do we understand this well working black box? *Appl. Microbiol. Biotechnol.*, 61, 189-96.
329. Lin, Y.H., Li, Y.F., Huang, M.C. and Tsai, Y.C. (2004). Intracellular expression of *Vitreoscilla* hemoglobin in *Aspergillus terreus* to alleviate the effect of a short break in aeration during culture. *Biotechnol. Lett.*, 26, 1067-72.
330. Hewald, S., Linne, U., Scherer, M., Marahiel, M.A., Kamper, J. and Bölker, M. (2006). Identification of a gene cluster for biosynthesis of mannosylerythritol lipids in the basidiomycetous fungus *Ustilago maydis*. *Appl. Environ. Microb.*, 72, 5469-77.
331. Teichmann, B., Linne, U., Hewald, S., Marahiel, M.A. and Bölker, M. (2007). A biosynthetic gene cluster for a secreted cellobiose lipid with antifungal activity from *Ustilago maydis*. *Mol. Microbiol.*, 66, 525-533.
332. Desai, J.D. and Banat, I.M. (1997). Microbial production of surfactants and their commercial potential. *Microbiology and molecular biology reviews* : MMBR, 61, 47-64.
333. Hossain, A.H., Ter Beek, A., and Punt, P.J. (2019). Itaconic acid degradation in *Aspergillus niger*: the role of unexpected bioconversion pathways. *Fungal Biol. Biotechnol.*, 6, 1.
334. Sieker, T., Duwe, A., Poth, S., Tippkötter, N. and Ulber, R. (2012). Itaconsäureherstellung aus Buchenholz-Hydrolysaten. *Chem. Ing. Tech.*, 84, 1300-1300.
335. Itaconix, L. (2009). Development of integrated production of polyitaconic acid from northeast hardwood biomass. National Institute of Food and Agriculture,
336. Mueller, O., Kahmann, R., Aguilar, G., Trejo-Aguilar, B., Wu, A. and de Vries, R.P. (2008). The secretome of the maize pathogen *Ustilago maydis*. *Fungal Genet. Biol.*, 45, S63-S70.
337. Couturier, M., Navarro, D., Olive, C., Chevret, D., Haon, M., Favel, A., Lesage-Meessen, L., Henrissat, B., Coutinho, P.M. and Berrin, J.G. (2012). Post-genomic analyses of fungal lignocellulosic biomass degradation reveal the unexpected potential of the plant pathogen *Ustilago maydis*. *Bmc Genomics*, 13,
338. Doehlemann, G., Wahl, R., Horst, R.J., Voll, L.M., Usadel, B., Poree, F., Stitt, M., Pons-Kuhnemann, J., Sonnewald, U., Kahmann, R. and Kamper, J. (2008). Reprogramming a maize plant: transcriptional and metabolic changes induced by the fungal biotroph *Ustilago maydis*. *Plant J.*, 56, 181-195.
339. Du, C., Lin, S., Koutinas, A., Wang, R. and Webb, C. (2007). Succinic acid production from wheat using a biorefining strategy. *Appl. Microbiol. Biotechnol.*, 76, 1263-1270.

340. Sugiyama, M., Sasano, Y., and Harashima, S. (2015). Mechanism of yeast adaptation to weak organic acid stress. in: Stress biology of yeasts and fungi: Applications for industrial brewing and fermentation. Springer Japan. Tokyo. 107-121. 978-4-431-55248-2.
341. Gao, T. and Ho, K.P. (2013). L-lactic acid production by *Bacillus subtilis* MUR1 in continuous culture. J. Biotechnol., 168, 646-51.
342. Kautola, H., Vassilev, N., and Linko, Y.Y. (1990). Continuous itaconic acid production by immobilized biocatalysts. J. Biotechnol., 13, 315-23.
343. Kaur, G. and Elst, K. (2014). Development of reactive extraction systems for itaconic acid: a step towards *in situ* product recovery for itaconic acid fermentation. RSC Advances, 4, 45029-45039.
344. Datta, D., Kumar, S., and Uslu, H. (2015). Status of the reactive extraction as a method of separation. J. Chem., ID 853789.
345. Aşçi, Y.S. and İnci, İ. (2012). A novel approach for itaconic acid extraction: Mixture of trioctylamine and tridodecylamine in different diluents. J. Ind. Eng. Chem., 18, 1705-1709.
346. Wennersten, R. (1983). The extraction of citric-acid from fermentation broth using a solution of a tertiary amine. J. Chem. Tech. Biot. B., 33, 85-94.
347. Vieux, A.S., Rutagengwa, N., Rulinda, J.B. and Balikungeri, A. (1974). Extraction of some dicarboxylic acids by *tri*-isooctylamine. Anal. Chim. Acta, 68, 415-424.
348. Weinzierl, G. (2001). Dissertation. Isolierung und Charakterisierung von Komponenten der b-vermittelten Regulationskaskade in *Ustilago maydis*. Philipps-Universität Marburg.
349. Bölker, M., Bohnert, H.U., Braun, K.H., Gohl, J. and Kahmann, R. (1995). Tagging pathogenicity genes in *Ustilago maydis* by restriction enzyme-mediated integration (*remi*). Mol. Gen. Genet., 248, 547-552.
350. König, J. (2008). Dissertation. Die Identifikation von Ziel-Transkripten des RNA bindenden Rrm4 aus *Ustilago maydis*. Philipps-Universität Marburg.
351. Brachmann, A. (2001). Dissertation. Die frühe Infektionsphase von *Ustilago maydis*: Genregulation durch das bW/bE-Heterodimer. Ludwig-Maximilians-Universität München.

Curriculum vitae

Personal data

Name: Hamed Hosseinpour Tehrani
Born: December 21, 1983, in Teheran, Iran
Nationality: German

Education

Apr. 2016-Mar. 2019 Doctoral studies at the Institute of Applied Microbiology of the RWTH-Aachen University (Aachen, Germany)
Oct. 2013-Aug. 2015 Master of Science Biology at RWTH-Aachen University (Aachen, Germany)
Oct. 2010-Sep. 2013 Bachelor of Science Biology RWTH-Aachen University (Aachen, Germany)
Oct. 2007-Apr.2008 Internship at surgery for orthodontist by Dr. Thomas Gesche (Düsseldorf/ Germany)
Oct. 2006-Sep. 2007 Study in Metallurgy and materials engineering at RWTH-Aachen University (Aachen, Germany)
May. 2006-Jun. 2006 Internship at Arens Werkzeug- und Maschinenbau GmbH (Trier, Germany)
Jul 2005: Balthasar Neumann Technikum Trier (Trier, Germany) for the acquisition of Abitur (higher education entrance qualification)

Work experience

Since April. 2019 Scientific employee of Bio- and Geosciences (IBG-1: Biotechnology) of Forschungszentrum Jülich (Jülich, Germany)
Sep. 2015-Mar. 2016 Scientific employee at the Institute of Applied Microbiology of the RWTH-Aachen Iniversity (Aachen, Germany)
Apr. 2015-May. 2015 Research assistant at the Institute of Applied Microbiology (Research group Shirawski) at RWTH-Aachen University (Aachen, Germany)
Oct. 2006-Dec. 2010 Barceeper at Café Extrablatt Aachen (Aachen, Germany)
2005-2006 Civilian services at AWO Arbeiterwohlfahrt Aachen (Aachen, Germany,)

Awards and grants

- 2018 ME-12 Junior Researcher Grant to visit the Metabolic Engineering 12 conference in Munich (Munich, Germany)
- 2005 Most dedicated student at the Balthasar Neumann Technikum Trier (Trier, Germany)

Publications

Hamed Hosseinpour Tehrani, Apilaasha Tharmasothirajan, Elia Track, Lars M. Blank and Nick Wierckx. Engineering the morphology and metabolism of pH tolerant *Ustilago cynodontis* for efficient itaconic acid production. *Metabolic Engineering* (2019) 54, 293-300, <https://doi.org/10.1016/j.ymben.2019.05.004>

Hamed Hosseinpour Tehrani, Elena Geiser, Meike Engel, Sandra K. Hartmann, Abeer H. Hossain, Peter J. Punt, Lars M. Blank, Nick Wierckx. (2019). The interplay between transport and metabolism in fungal itaconic acid production. *Fungal Genetics and Biology*, 125, 45-52, <https://doi.org/10.1016/j.fgb.2019.01.011>.

Elena Geiser, **Hamed Hosseinpour Tehrani**, Svenja Meyer, Lars M. Blank and Nick Wierckx. (2018). Evolutionary freedom in the regulation of the conserved itaconate cluster by Ria1 in related Ustilaginaceae. *Fungal Biology and Biotechnology*, 5, 14, <https://doi.org/10.1186/s40694-018-0058-1>

Hamed Hosseinpour Tehrani, Lars M. Blank and Nick Wierckx (2018). Morphologic engineering in basidiomycota. Patent Application: EP 18 176 325.1

Hartmann SK, Stockdreher Y, Wandrey G, **Hosseinpour Tehrani H**, Zambanini T, Meyer AH, Büchs J, Blank LM, Schwarzländer M, Wierckx N. (2018). Online in vivo monitoring of cytosolic NAD redox dynamics in *Ustilago maydis*. *Biochimica et Biophysica Acta (BBA) – Bioenergetics*, 1859, 1015-1024, <https://doi.org/10.1016/j.bbabi.2018.05.012>.

Thiemo Zambanini, **Hamed Hosseinpour Tehrani**, Elena Geiser, Christiane K. Sonntag, Joerg M. Buescher, Guido Meurer, Nick Wierckx, Lars M. Blank. (2017). Metabolic engineering of *Ustilago trichophora* TZ1 for improved malic acid production. *Metabolic engineering communication*, 4, 12-21, <https://doi.org/10.1016/j.meteno.2017.01.002>.

Thiemo Zambanini, Sandra K. Hartmann, Lisa M. Schmitz, Linda Büttner, **Hamed Hosseinpour Tehrani**, Elena Geiser, Melanie Beudels, Dominik Venc, Georg Wandrey, Jochen Büchs, Markus Schwarzländer, Lars M. Blank and Nick Wierckx. (2017). Promoters from the itaconate cluster of *Ustilago maydis* are induced by nitrogen depletion. *Fungal Biology and Biotechnology*, 4, 11, <https://doi.org/10.1186/s40694-017-0040-3>.

Thiemo Zambanini, **Hamed Hosseinpour Tehrani**, Elena Geiser, Dorothee Merker, Sarah Schleese, Judith Krabbe, Joerg M. Buescher, Guido Meurer, Nick Wierckx and Lars M. Blank. (2017). Efficient itaconic acid production from glycerol with *Ustilago vetiveriae* TZ1. *Biotechnology for Biofuels*, 10, 131, <https://doi.org/10.1186/s13068-017-0809-x>.

Hamed Hosseinpour Tehrani, Ulrike Becken, Lars M. Blank, Nick Wierckx. (2016). Transfer of an Itaconate Production Process in *Ustilago maydis* to the BioFlo® 120 Bioprocess Control Station, Application Note Eppendorf No. 309.

Poster presentations

Hamed Hosseinpour Tehrani, Elena Geiser, Apilaasha Tharmasothirajan, Lars M. Blank and Nick Wierckx. Enhanced itaconic acid production in *Ustilago cynodontis* with Metabolic and Morphologic engineering. (March 17-20, 2019). Annual conference 2019 of the Association for general and applied microbiology. Mainz, Germany.

Hamed Hosseinpour Tehrani, Elena Geiser, Apilaasha Tharmasothirajan, Lars M. Blank and Nick Wierckx. Metabolic and Morphologic Engineering for efficient itaconic acid production in *Ustilago*. (February 18-20, 2019). BioProcessingDays 2019. Recklinghausen, Germany.

Hamed Hosseinpour Tehrani, Elena Geiser, Lars M. Blank and Nick Wierckx. (June 24-28, 2018). Metabolic and Morphologic Engineering for efficient itaconic acid production in *Ustilago*. Metabolic Engineering 12. Munich, Germany.

Hamed Hosseinpour Tehrani, Lars M. Blank and Nick Wierckx. (February 19-21, 2018). Itaconic acid production in *Ustilago maydis*. BioProcessingDays 2018. Recklinghausen, Germany.

Elena Geiser, **Hamed Hosseinpour Tehrani**, Svenja Meyer, Lars M. Blank and Nick Wierckx. (September 28-30, 2017). Insights into the itaconate pathway of Ustilaginaceae enable enhanced production. 12th conference of the VAAM special group molecular biology of fungi. Jena, Germany.

Oral presentations

Hamed Hosseinpour Tehrani, Lars M. Blank and Nick Wierckx. (September 10-13, 2018). Morphologische und metabolische Veränderung von *Ustilago cynodontis* optimieren die Herstellung von Itakonsäure bei niedrigem pH-Wert. ProcessNet-Jahrestagung und 33. Dechema-Jahrestagung der Biotechnologen 2018. Aachen, Germany.

Hamed Hosseinpour Tehrani, Elena Geiser, Peter J. Punt, Lars M. Blank and Nick Wierckx. (September 28-30, 2017). Comparative analysis of transporters from *Aspergillus terreus* and *Ustilago maydis* involved in itaconic acid production. 12th conference of the VAAM special group molecular biology of fungi. Jena, Germany.

*“Experience is what you get
when you didn’t get what you wanted.
And experience is often the most valuable
thing you have to offer”*

-Randy Pausch-

